

NUREG/CR-5254
BNL-NUREG-52168

Bias in Peak Clad Temperature Predictions Due to Uncertainties in Modeling of ECC Bypass and Dissolved Non-Condensable Gas Phenomena

Prepared by U. S. Rohatgi, L. Y. Neymotin, J. Jo, W. Wulff

Brookhaven National Laboratory

Prepared for
U.S. Nuclear Regulatory Commission

9010090047 900930
PDR NUREG
CR-5254 R PDR

AVAILABILITY NOTICE

Availability of Reference Materials Cited in NRC Publications

Most documents cited in NRC publications will be available from one of the following sources:

1. The NRC Public Document Room, 2120 L Street, NW, Lower Level, Washington, DC 20555
2. The Superintendent of Documents, U.S. Government Printing Office, P.O. Box 37082, Washington, DC 20013-7082
3. The National Technical Information Service, Springfield, VA 22161

Although the listing that follows represents the majority of documents cited in NRC publications, it is not intended to be exhaustive.

Referenced documents available for inspection and copying for a fee from the NRC Public Document Room include NRC correspondence and internal NRC memoranda; NRC Office of Inspection and Enforcement bulletins, circulars, information notices, inspection and investigation reports; Licensee Event Reports; vendor reports and correspondence; Commission reports; and applicant and licensee documents and correspondence.

The following documents in the NUREG series are available for purchase from the GPO Sales Program: formal NRC staff and contractor reports, NRC-sponsored conference proceedings, and NRC booklets and brochures. Also available are Regulatory Guides, NRC regulations in the *Code of Federal Regulations*, and *Nuclear Regulatory Commission Issuances*.

Documents available from the National Technical Information Service include NUREG series reports and technical reports prepared by other federal agencies and reports prepared by the Atomic Energy Commission, forerunner agency to the Nuclear Regulatory Commission.

Documents available from public and special technical libraries include all open literature items, such as books, journal and periodical articles, and transactions. *Federal Register* notices, federal and state legislation, and congressional reports can usually be obtained from these libraries.

Documents such as theses, dissertations, foreign reports and translations, and non-NRC conference proceedings are available for purchase from the organization sponsoring the publication cited.

Single copies of NRC draft reports are available free, to the extent of supply, upon written request to the Office of Information Resources Management, Distribution Section, U.S. Nuclear Regulatory Commission, Washington, DC 20555.

Copies of industry codes and standards used in a substantive manner in the NRC regulatory process are maintained at the NRC Library, 7920 Norfolk Avenue, Bethesda, Maryland, and are available there for reference use by the public. Codes and standards are usually copyrighted and they be purchased from the originating organization or, if they are American National Standards, from the American National Standards Institute, 1430 Broadway, New York, NY 10018.

DISCLAIMER NOTICE

This report was prepared as an account of work sponsored by an agency of the United States Government. Neither the United States Government nor any agency thereof, or any of their employees, makes any warranty, expressed or implied, or assumes any legal liability of responsibility for any third party's use, or the results of such use, of any information, apparatus, product or process disclosed in this report, or represents that its use by such third party would not infringe privately owned rights.

NUREG/CR-5254
BNL-NUREG-52168
R4

Bias in Peak Clad Temperature Predictions Due to Uncertainties in Modeling of ECC Bypass and Dissolved Non-Condensable Gas Phenomena

Manuscript Completed: April 1990
Date Published: September 1990

Prepared by
U. S. Rohatgi, L. Y. Neymotin, J. Jo, W. Wuiff

Brookhaven National Laboratory
Upton, NY 11973

Prepared for
Division of Systems Research
Office of Nuclear Regulatory Research
U.S. Nuclear Regulatory Commission
Washington, DC 20555
NRC FIN A3952

ABSTRACT

The U.S. Nuclear Regulatory Commission (USNRC), its contractors and consultants have developed a methodology for evaluating Code Scaling, Applicability and Uncertainty (CSAU). The CSAU method is systematic, practical and auditable, and it has been demonstrated by applying it to the TRAC-PF1/MOD1, Version 14.3 code and its analysis of a Large Break Loss of Coolant Accident (LBLOCA) for a Westinghouse four-loop plant. In applying the methodology, the accident course is divided into three different phases, namely: Blowdown, Refill and Reflood. There are two distinct peaks in the clad temperature history, one in the Blowdown Phase and one in the Reflood Phase. The Peak Clad Temperature (PCT) of the Blowdown Phase is governed by fuel characteristics. The peak clad temperature of the Reflood Phase is governed by the phenomena affecting the Refill Phase as the clad temperature continues to rise almost adiabatically during the Refill phase. Specifically, the second PCT is affected by critical break flow, two-phase pump degradation and the phenomena related to Emergency Core Cooling System (ECCS) in the downcomer and lower plenum of the reactor vessel.

This report describes a general method for estimating the effect on the Reflood Phase PCT from systematic errors (biases) associated with the modelling of the ECCS and dissolved nitrogen, and the application of this method in estimating biases in the Reflood Phase PC₂ (second PCT) predicted by the TRAC/PF1/MOD1, Version 14.3. The bias in the second PCT due to the uncertainty in the existing code models for ECCS related phenomena is -19°K (-34°F). The negative bias implies that the code models for this phenomena are conservative. The bias in the second PCT due to the lack of modelling of dissolved N_2 in the code is estimated to be 9.9°K (17.8°F). The positive bias implies that the absence of dissolved N_2 model makes the code prediction of PCT non-conservative.

The bias estimation in this report is a major exception among all other uncertainty and bias assessments performed in conjunction with the CSAU methodology demonstration, because this bias estimation benefitted from using full-scale test data from the full-scale Upper Plenum Test Facility (UPTF). Thus, the bias estimates presented here are unaffected by scale distortions in test facilities. Data from small size facilities were also available and an estimate of bias based on these data will be conservative.

EXECUTIVE SUMMARY

Introduction

The Large Break Loss of Coolant Accident (LBLOCA) is a design basis accident for licensing purposes. The licensee is required to demonstrate that during a hypothetical LBLOCA the emergency core cooling system (ECCS) will provide adequate core cooling to prevent damage to the fuel cladding. In August of 1988, the U.S. Nuclear Regulatory Commission (USNRC) published new guidelines for assessing the adequacy of the ECCS. The revised guidelines allow the licensee to predict LBLOCA events with a best estimate computer code, provided the uncertainty in predicting safety parameters, such as the peak clad temperature, is quantified with a high level of confidence.

The USNRC has developed a methodology [TPG, 1989] for evaluating Code Scaling, Applicability and Uncertainty (CSAU). This method was demonstrated by applying it to the TRAC-PF1/MOD1 Version (14.3) code and by its analysis of LBLOCA for a Westinghouse four-loop plant [TJG, 1989]. In applying the methodology, one divides the accident course into three different phases, namely, Blowdown, Refill, and Reflood. There are two distinct peaks in clad temperature history, one in the Blowdown Phase and one in the Reflood Phase. The Peak Clad Temperature (PCT) of the Blowdown Phase is governed by fuel characteristics [Shaw et al., 1988; Walff, 1987]. The Peak Clad Temperature of the Reflood Phase is governed by the phenomena affecting the Refill Phase, as the clad continues to heat up during the Refill Phase. Specifically, the second PCT is affected by critical break flow, two-phase pump degradation and ECCS-related phenomena in the downcomer and lower plenum of the reactor vessel [Shaw et al., 1988]. This report addresses ECCS- and N₂-related phenomena and also deals with the effect that the modeling of these phenomena has on the PCT of the Reflood Phase.

Objective of the Research Program

The objective of the analysis described in this document is to present a general method for estimating the effects on PCT from systematic errors associated with the modeling of ECCS and dissolved nitrogen, and to apply this method to the TRAC code.

Specifically, as part of a CSAU application, the purpose is to estimate the biases in the TRAC-PF1/MOD1, Version 14.3 prediction of PCT in the Reflood Phase due to:

- 1) uncertainties in modeling ECC bypass phenomena in the downcomer and lower plenum, and
- 2) the lack of a model for dissolved nitrogen N₂.

The biases in PCT to be estimated arise from systematic modeling errors in TRAC causing errors in the prediction of the time at which, after blowdown, the lower plenum is again full of liquid delivered by ECCS. This time occurs at the end of the Refill Phase and the beginning of liquid injection into the core, which, in turn, terminates the rise in clad temperature in and thereby controls PCT. The bias estimates developed in this analysis are used to shift the probability distribution of PCT uncertainty as obtained from the statistical analysis of stochastic uncertainties [TPG, 1989].

Summary of Procedure

During the Refill Phase, the core is voided and the cladding heats up until the lower plenum is full of liquid and some of the liquid begins to enter the core. The bias in the PCT prediction is due to the bias in predicting the duration of the Refill Phase. The longer the Refill Phase lasts, the larger will be the PCT. The Refill Phase is shown to be divided into four phenomenologically distinct periods, namely the Complete Bypass Period, the Delay Period, the Counter Current Flow Period, and the No-Bypass Period. The net bias in predicting the duration of the Refill Phase is obtained from predicting the sum of the four biases. The bias in the PCT is then estimated by multiplying the total bias in the duration predicted for the Refill Phase by the average clad heatup rate during the Refill Phase. The heatup rate is obtained from the reference calculation of the plant, using the TRAC computer code.

Bias Due to ECC Bypass Phenomena Modeling

The bias in the PCT due to ECC bypass phenomena modeling is estimated by using ECC bypass data from the full-scale Upper Plenum Test Facility (UPTF) [Siemens, A. G., 1987; Damarell, 1988a, 1988b, 1988c; Wolfe, 1988a, 1988b], which models the upper plenum and downcomer components of a reactor vessel without scale distortion. We have estimated the three discrepancies in the prediction of (i) the critical steam-flow rate (i.e., the steam flow rate below which there would be liquid delivery to the lower plenum given sufficient time), (ii) the delay in the delivery of liquid to the lower plenum from the time of injection, and (iii) the rate of liquid delivery to the lower plenum, and have converted them into the bias of the Refill Phase time period. The resulting bias in PCT is estimated by multiplying the cladding heatup rate by the bias in the Refill Phase time period, as explained above. No corrections are needed to account for scale distortion in the test data.

Bias Due to the Lack of a Model of Dissolved N_2

The N_2 -related bias in PCT is obtained by developing a separate model of the reactor system, accounting for the effect of the dissolved N_2 . This is accomplished by performing a TRAC calculation for UPTF Test 6 conditions with and without N_2 injection. The biases in the durations of the four periods listed earlier are estimated from the effect of N_2 on the critical steam flow rate, on the delay in delivery of liquid to the lower plenum, and on the rate of liquid delivery to the lower plenum. This bias in the prediction of the duration of the Refill Phase is obtained by summing the four biases. The bias in PCT is estimated by multiplying the cladding heatup rate by the bias in the Refill Phase period. Again, no corrections are needed to account for scale distortion in the test data.

Summary of Results

The bias in the PCT due to the uncertainty in the existing TRAC models for bypass phenomena is -19°K (-34°F). The negative bias implies that the code is conservative in modelling the bypass phenomena and, relative to ECCS effects, predicts PCT too high. This bias will be subtracted from the overall PCT uncertainty.

The Refill Phase was divided into four phenomenologically different periods. The largest contribution to the bias is from the Delay Period (-17.7°K) during which the ECC is accumulating in the cold legs and the downcomer region of the reactor. The Counter Current Flow Period was surprisingly small (0.5 s) and contributed only -1.3°K to the total bias in PCT. The most important parameter during the Delay Period is the critical steam flow rate. Since the data for determining this critical steam flow rate are sparse, more data are needed, particularly at high steam flow rates. Furthermore, additional test data are needed to provide a meaningful statistical analysis.

The bias in PCT due to the lack of modeling effects of dissolved N_2 in the TRAC code is 9.9°K (17.8°F). This bias was computed in part with bounding calculations. The positive value of the bias implies that the inclusion of a dissolved N_2 model would lead to a code prediction of a higher PCT. It is recommended that a model of dissolved N_2 , based on the variation in the solubility of the non-condensable gas (i.e., Henry's model), be included in the code. The code has a model of non-condensable gas, but it does not allow for mass transfer of gas from or to the liquid phase.

TABLE OF CONTENTS

	Page
ABSTRACT	iii
EXECUTIVE SUMMARY	v
LIST OF FIGURES	xi
LIST OF TABLES	xiii
NOMENCLATURE	xv
ACKNOWLEDGEMENTS	xvii
1. INTRODUCTION	1
1.1 Background	1
1.2 The CSAU Methodology	1
1.2.1 Contributions to Uncertainty	2
1.2.2 Description of CSAU Methodology	2
1.2.3 Application of CSAU Methodology to LBLOCA Prediction	4
1.2.3.1 Bias in ECC Bypass Phenomena Prediction	5
1.2.3.2 Bias Due to Lack of Dissolved N ₂ Model	5
1.3 Report Organization	5
2. OBJECTIVES	7
3. BIAS IN PCT FROM THE MODELLING OF ECC BYPASS PHENOMENA	9
3.1 The ECC Bypass Phenomena	9
3.1.1 Four Periods of the Refill Phase	13
3.2 Principle of Bias Estimate	17
3.3 Bias in Timing of Refill Phase	17
3.3.1 Bias in Timing of Bypass Period	18
3.3.1.1 Bias in Timing of Complete Bypass Period	18
3.3.1.2 Bias in Timing of Delay Period	19
3.3.2 Bias in the Timing of the Filling Period	21
3.3.2.1 Bias in the Timing of the Counter- Current Flow Period	22
3.3.2.2 Bias in the Timing of No-Bypass Period	23
3.3.3 Total Bias in the Refill Phase	24
3.3.4 Required Information for Application	24
3.4 Application	25
3.4.1 Experiments for Estimating Bias	25
3.4.1.1 Available Data	25
3.4.1.2 UPTF Experiments	27
3.4.2 Evaluation of Biases	30
3.4.2.1 Bias in the Timing of the Complete Bypass Period	30
3.4.2.2 Bias in the Timing of the Delay Period	37
3.4.2.3 Bias in the Timing of the Counter- Current Flow Period	37
3.4.2.4 Bias in the Timing of the No-Bypass Period	38
3.4.2.5 Total Bias in the Refill Phase	38
3.4.2.6 Bias in PCT	39

	<u>Page</u>
3.5 Conclusions	39
4. LACK OF MODEL FOR DISSOLVED N ₂ AND RESULTING PCT BIAS	41
4.1 Effect of N ₂ on the Refill Phase	41
4.2 Principle of Uncertainty Estimation	42
4.3 Estimation of N ₂ Modeling Bias in Refill Phase	42
4.3.1 Bias in the Timing of the Bypass Period	43
4.3.1.1 Bias in the Timing of the Period of Complete Bypass	43
4.3.1.2 Bias in the Timing of the Delay Period	44
4.3.2 Bias in the Timing for the Filling Period	45
4.3.3 Total Bias in the Timing of the Refill Phase	46
4.4 Application	47
4.4.1 Supporting Analysis	47
4.4.2 Evaluation of the Biases	51
4.4.2.1 Bias in Timing of the Complete Bypass Period	51
4.4.2.2 Bias in the Timing of the Delay Period	53
4.4.2.3 Bias in the Timing of the Filling Period	54
4.4.2.4 Total Bias in the Refill Phase	54
4.4.2.5 Bias in Predicted PCT due to the Omission of Dissolved N ₂ Model	55
4.5 Conclusions	55
5. SUMMARY OF CONCLUSIONS	57
REFERENCES	59
APPENDICES	
Appendix A: UPPER PLENUM TEST FACILITY (UPTF) EXPERIMENTS	63
Appendix B: NODALIZATION FOR SEPARATE EFFECT TESTS, UPTF	71
Appendix C: TRAC-PF1 INPUT DECK FOR UPTF	73
Appendix D: TRAC-PF1 PREDICTION OF UPTF LOWER PLENUM FILLING RATES	131
Appendix E: Estimate of ECCS Flow in Presence of Dissolved N ₂	135
E.1 Introduction	135
E.2 Purpose	135
E.3 Approach	135
E.3.1 Formulation	136
E.3.1.1 Formulation for Reactor System	136
E.3.1.2 Formulation for Accumulator Flows	143
E.3.2 Estimate of Rate of N ₂ Dissolution in the Reactor System	144
E.3.3 Estimation of Condensation in the Presence of N ₂	147
E.4 Results	150
Nomenclature for Appendix E	158

LIST OF FIGURES

Figure	Page
1.1 Code Scaling, Applicability and Uncertainty Evaluation Methodology	3
3.1 Expected Conditions in a PWR System at 9 Seconds After Rupture (Shaw, et al., 1988)	10
3.2 Expected Conditions in a PWR System at 14 Seconds After Rupture (Shaw, et al., 1988)	10
3.3 Expected Conditions in a PWR System at 20 Seconds After Rupture (Shaw, et al., 1988)	11
3.4 Expected Conditions in a PWR System at 24 Seconds After Rupture (Shaw, et al., 1988)	11
3.5 Expected Conditions in a PWR System at 25 Seconds After Rupture (Shaw, et al., 1988)	12
3.6 Expected Conditions in a PWR System at 33 Seconds After Rupture (Shaw, et al., 1988)	14
3.7 Schematic of LBLOCA in NPP	15
3.8 Schematic of Flooding Curve and Critical Steam Velocity	16
3.9 Schematic of Steam Flow Rate From the Lower Plenum to the Downcomer in the NPP	16
3.10 Schematic of Lower Plenum Inventory During LBLOCA	20
3.11 Schematic of Lower Plenum Inventory of Separate Effects Tests	20
3.12 Comparison of Ratios of Predicted and Measured Lower Plenum Fill Rates for Three Subscale Facilities and UPTF Test 6	28
3.13 Identification of t_1 from the Predicted Accumulator Discharge Mass Flow Rate. (Nominal TRAC-PF1/MOD1, Version 14.3 Calculation Performed by INEL in Support of CSAU Methodology Demonstration)	31
3.14 Identification of t_A and t_B from the Predicted Lower Plenum Liquid Inventory. (Nominal TRAC-PF1/MOD1, Version 14.3 Calculation Performed by INEL in Support of CSAU Methodology Demonstration)	32

3.15	Identification of t_D and t_E from the Predicted Steam Flow Rate from the Lower Plenum to the Downcomer. (Nominal TRAC-PF1/MOD1, Version 14.3 Calculation Performed by INEL in Support of CSAU Methodology Demonstration)	33
3.16	Identification of $t_{A'}$, $t_{B'}$, $t_{A''}$, and $t_{B''}$ from the Predicted Rod 9 (Hot Rod) Clad Temperature (Nominal TRAC-PF1/MOD1, Version 14.3 Calculation Performed by INEL in Support of CSAU Methodology Demonstration)	34
4.1	Prediction of Integrated ECC Injection	48
A.1	System Configuration of Test No. 6 (Siemens, 1987)	64
A.2	Contour Plots of Fluid Temperature Distribution in Downcomer (Siemens, 1987)	65
A.3	Contour Plots of Fluid Temperature Distribution in Downcomer (Siemens, 1987)	66
A.4	Lower Plenum Liquid Mass Inventory, UPTF Test 6 (Run 136)	70
B.1	Schematic of the VESSEL Nodalization	72
D.1	UPTF Test 6 Run 132, Vessel, Downcomer, Lower Plenum Liquid Masses	132
D.2	UPTF Test 6 Run 133, Vessel, Downcomer, Lower Plenum Liquid Masses	132
D.3	TRAC-PF1 Prediction, Test 6, Run 136	133
E.1	Schematic of Three Control Volume Representation of NPP	137
E.2	Predicted Steam Flow Rate from Lower Plenum to the Downcomer	149
E.3	System Pressure During Refill Period	156
E.4	Predictions of Integrated ECC Injection	156

LIST OF TABLES

Table	Page
3.1 Geometrical Parameters for Test Facilities (Facilities Scaled on Vessel Dia (CREARE TM 707) & MPR Info. Mtg.)	26
3.2 Summary of UPTF Results (Test 6), Corresponding TRAC Calculations and Their Comparisons	29
3.3 Comparison Between NPP and UPTF (Full-Scale Facility) Conditions	36
4.1 Integrated ECC Mass With and Without N ₂	49
4.2 TRAC Simulation of UPTF Test 6	50
A.1 UPTF Test 6, Run 131 (Steam Flow 400 kg/s)	67
A.2 UPTF Test 6, Run 132 (Steam Flow 300 kg/s)	67
A.3 UPTF Test 6, Run 133 (Steam Flow 200 kg/s)	68
A.4 UPTF Test 6, Run 136 (Steam Flow 100 kg/s)	68
A.5 Summary of UPTF Results (Test 6)	69
D.1 Predicted Lower Plenum Water Inventory and Filling Rates, UPTF Test 6	134
D.2 Summary of UPTF Results (Test 6)	134
E.1 N ₂ Solubilities (Chemical Engineering Handbook, Perry & Chilton) (Tables 3-139 and 3-140)	146
E.2 LBLOCA Flow Parameters From TRAC Calculation	151
E.3 Estimated Condensation Rates in the Nominal NPP Calculation	152
E.4 Estimates of N ₂ Solubility	153
E.5 Estimated Volume Fraction and Rate of Dissolution of N ₂	154
E.6 Integrated ECC With and Without N ₂	157

NOMENCLATURE

CSAU	Code Scalability, Applicability and Uncertainty
DC	Downcomer
ECC	Emergency Core Coolant
ECCS	Emergency Core Cooling System
LP	Lower Plenum
m	Inventory, kg
\dot{m}	Filling rate
$\delta\dot{m}$	Bias in filling rate
PCT	Peak Clad Temperature
δPCT	Bias in Peak Clad Temperature
PWR	Pressurized Water Reactor
R_{ECC}	Ratio of ECC injection rates, without N ₂ and with N ₂
R_{mLP}	Ratio of predicted to observed lower plenum filling rates
R_t	Rates of predicted to observed durations of the Delay Period
$R_{t,th}$	Ratio of durations of Delay Period without N ₂ and with N ₂
T	Temperature
t	Time
t_A	Time at which lower plenum inventory is lowest
t_{AB}	Duration of Filling Period, $t_B - t_A$
t_{AE}	Duration of Counter Current Flow Period, $t_E - t_A$
t_B	Time at which lower plenum is full, end of Refill Phase
t_D	Time at which steam flow to the downcomer is equal to critical steam flow rate
t_{DA}	Duration of Delay Period; $t_A - t_D$
t_E	Time at which the steam flow to downcomer ends
t_{EB}	Duration of No-Bypass Period, $t_B - t_E$

t_I	Time at which ECC injection begins
t_{IA}	Duration of Bypass Period; $t_A - t_I$
t_{IB}	Duration of Refill Phase, $t_B - t_I$
t_{ID}	Duration of Complete Bypass Period, $t_D - t_I$
t_{ij}	Duration, $t_j - t_i$
δt_{ij}	Bias in time period t_{ij}
W_{gc}	Critical steam flow rate

Subscripts

AB	Lower plenum Filling Period
AE	Counter Current Flow Period
A'	Point on clad temperature history curve
act	Actual or expected for PWR
B'	Point on clad temperature history curve
C	Clad
CL	Cold Leg
DA	Delay Period
EB	No-Bypass Period
exp	Experimental
IB	Refill Phase
ID	Complete Bypass Period
LP	Lower Plenum
mLP	Lower Plenum filling rate
N_2	N_2 dissolution considered (Chapter 4 only)
NPP	Nuclear Power Plant
pred	Predicted or calculated
SET	Separate Effects Test
th	Based only on calculation

ACKNOWLEDGEMENTS

The authors would like to thank the members of the Technical Program Group, Dr. B. Boyack of LANL, Dr. R. Duffey of INEL, Professor P. Griffith of MIT, Drs. G. Lellouche and S. Levy of S. Levy, Inc., Mr. G. Wilson of INEL, and Dr. N. Zuber of NRC, for technical discussions, suggestions and support for this effort. Numerous technical suggestions and the advice of Professor I. Catton of UCLA are greatly appreciated. The bulk of the TRAC calculations was done by Dr. H. Stampf of LANL whose expertise in the code contributed greatly to this report. The authors would like to extend their appreciation to Dr. J. Guppy of BNL for continuous support of this project. Finally, the extraordinary patience and fine typing of Mrs. L. Hanlon and Mrs. N. Siemon is highly appreciated.

1. INTRODUCTION

1.1 Background

The Large Break Loss of Coolant Accident (LBLOCA) is a design basis accident that must be analyzed for licensing purposes. The licensee has to demonstrate that during a hypothetical LBLOCA the Emergency Core Cooling System (ECCS) will provide adequate cooling to the core and prevent damage to the fuel cladding. With inadequate core cooling, there is a possibility for core heatup, oxidation of the zirconium fuel rod cladding and cladding rupture, leading eventually to a release of radiation into the reactor vessel.

In 1974, the USNRC set up rules for assessing the performance of ECCS for light water reactors under LBLOCA conditions. These rules consist of acceptance criteria, listed in the Code of Federal Regulation, Title 10, Section 50.46 (10 CFR 50.46); constraints in the method of analyzing the ECCS performance are listed in the accompanying Appendix K. The acceptance criteria focus on maintaining the integrity of the cladding.

Since 1974, there has been extensive research in reactor thermohydraulics and development of Best Estimate (BE) computer codes. The results of these BE codes indicate that the ECCS rules are conservative [Rohatgi, et al., 1986]. To account for the technological advances made in the last 15 years and to use the realistic BE codes for analyzing the ECCS performance, the USNRC approved a revision of 10CFR50.46 and Appendix K in August, 1988 [USNRC, 1988]. The revisions, which lead to the analyses reported here, require that the uncertainties arising from the prediction of ECCS performance and impacting on safety (PCT being the most important parameter for safety), be quantified with a high level of assurance.

1.2 The CSAU Methodology

To provide a technical basis for the revision of the ECCS evaluation methodology, the USNRC, its contractors and consultants developed a general method of quantifying the uncertainty in the code predictions [TPG, 1989]. This method is called Code Scaling, Applicability, and Uncertainty (CSAU) evaluation methodology. It provides a structured, auditable, and traceable method of combining quantitative analysis with expert opinion. The code prediction of the safety parameter (PCT for LBLOCA), along with the uncertainty estimated through the CSAU methodology, are compared with the acceptance criteria to assess the plant's safety margin.

The CSAU evaluation methodology was applied to the LBLOCA analysis of the Westinghouse four-loop Pressurized Water Reactor (PWR), using TRAC-PF1/MOD1, Version 14.3 [TPG, 1989]. The code was used to predict PCT for the accident. The CSAU methodology was used to estimate the uncertainty with a 95% level of confidence for the TRAC code prediction of PCT. The predicted PCT plus its uncertainty must be less than the permissible value of PCT (2200°F). The difference between the permissible value of PCT and the predicted PCT, augmented by its uncertainty, is the safety margin and, thus, an adequacy measure of the ECCS performance.

1.2.1 Contributions to Uncertainty

Computer codes to predict of reactor transients consist of a set of balance equations for two-phase coolant flows, a model for conduction in the neutron fission power and for solids, a set of intrinsic constitutive relationships for material properties of gases, liquids and solids, extrinsic constitutive relationships such as flow regime maps, wall and interfacial heat and momentum transfer coefficients, and numerical procedures. The results depend upon the models in the code, the initial and boundary conditions, the numerical methods and the nodalization scheme used. The uncertainty in the prediction can arise from an inadequate formulation of flow models, inappropriateness of some of the constitutive relationships, insufficient detail in the nodalization, the approximation in the numerical methods, and uncertainty in specifying the boundary conditions and plant parameters.

Among the many relationships in the code, the inappropriate constitutive relationships include correlations which are either based on data from improperly scaled test facilities, or do not cover the range of the flow conditions expected during the reactor transient, or, in some cases, have no verifiable basis. The uncertainty in the reactor's conditions arises from the imprecise knowledge of the reactor's initial conditions, fuel composition and geometry of the plant. Any method for evaluating the uncertainty in the code prediction must account for all the contributors listed here. The CSAU methodology provides a systematic means of quantifying these uncertainties.

1.2.2 Description of CSAU Methodology

The CSAU methodology [TPG, 1989] consists of 14 steps which are organized in three groups (Figure 1.1). The first group (Steps 1-6) is called Requirements and Code Capabilities [Wilson, et al., 1988]; it consists of the specification of the transient (Step 1) and Nuclear Power Plant (NPP) (Step 2), the identification of phenomena and their ranking (Step 3), leading to the Phenomena Identification and Ranking Table (PIRT), and the selection of the code (Step 4) and its documentation (Step 5). The final step in this group is the determination of the code's capability to model the important phenomena identified in Step 3.

The second group, Steps 7 to 10, is called Assessment and Ranging of Parameters [Wulff, et al., 1988]. This part of the methodology consists of selecting a matrix of Separate Effects Tests (SET) and Integral Effect Tests (IET) (Step 7), relevant to the scenario, as well as to the important phenomena and components selected in Step 3. Step 8 requires setting up of the standard nodalization for the nuclear power plant (NPP) representation, thereby accounting for all the important phenomena. Nodalization for the SET and IET calculations must be the same as the nodalization used in the NPP calculation. The identification of the code parameters which model the important phenomena, and the ranging of the parameters on the basis of their uncertainties and stand-alone calculations are performed in Step 9. Finally, in cases where the data base or the separate effects tests used in Step 9 did not cover the fluid conditions expected in the accident nor the full-plant size, the range of the parameter has to be modified to conservatively account for the scale compromises. This modification is performed in Step 10. The IET calculations provide an independent check on the overall uncertainty in the predicted safety parameter (Steps 9 and 10).

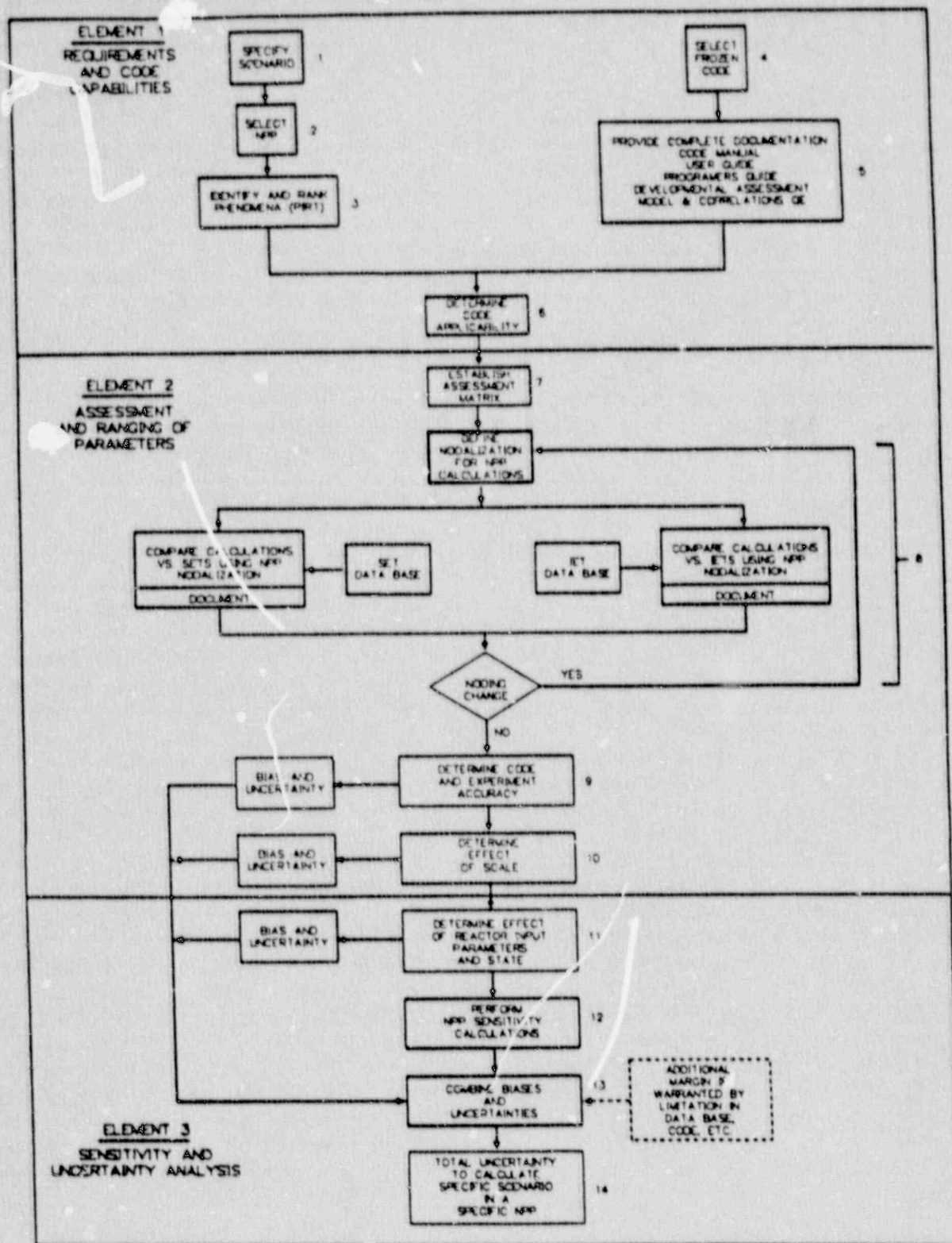


Figure 1.1 Code Scaling, Applicability and Uncertainty Evaluation Methodology

The third group (Steps 11-14) is called Sensitivity and Uncertainty Analysis [Lellouche, et al., 1988]. In Step 11, NPP calculations are performed to predict the sensitivity of the safety parameter to the perturbed value of the modeling parameters. The range of perturbation is determined from the range of the modeling parameter uncertainty (Step 9). A response surface is developed to approximate the relationship between modelling parameters and the safety parameter (PCT). This alleviates the need for expensive code calculation in the statistical analysis, used to compute the uncertainty distribution for the safety parameter (Step 12). When the modelling parameters in the code, governing an important phenomenon, have systematic errors either due to the lack of a data base, or due to artificial constraints, the code is said to have a bias in the prediction of safety parameters. In such cases, a bias is estimated either directly through the code or through a separate calculation. This bias is used to shift the uncertainty probability distribution, and this is accomplished in Step 13. The uncertainty in the safety parameter is documented in the last step.

1.2.3 Application of CSAU Methodology to LBLOCA Prediction

The CSAU methodology [TPG, 1989] described here was applied to the best estimate (BE) analysis of LBLOCA in a Westinghouse four-loop plant using TRAC-FF1/MOD1, Version 14.3. The uncertainty from modeling ECCS phenomena and from omitting the modeling of dissolved nitrogen in the predicted PCT, which is the safety parameter in LBLOCA, is estimated here with this method.

The time span of the transient from the time of the break to the time of the complete clad quenching was divided into three periods, namely Blowdown, Refill, and Reflood Phases. The Blowdown Phase is the period during which the system depressurizes, as it loses coolant through the break. This Blowdown Phase ends when the ECC flow is initiated in the intact loops. The Refill Phase is next, during which the ECC liquid initially bypasses the downcomer, and later, begins to accumulate in the downcomer and lower plenum. The Refill phase ends when the lower plenum is filled. During the third or Reflood Phase, the core begins to fill up. This phase ends when the cladding is quenched. There are two peaks in the clad temperature history: the first is in the Blowdown Phase and the second in the Reflood Phase.

The Phenomena Identification and Ranking Table (PIRT) [Shaw, et al., 1988; Wilson, et al., 1988] was developed as part of the CSAU demonstration for LBLOCA; it showed that the downcomer is an important component, and the ECC bypass phenomena and the effect of non-condensables during the Refill Phase are important. The uncertainty in modelling the downcomer flows leads to uncertainty in predicting the filling rate of the lower plenum and, consequently, the duration of the Refill Phase. During the Refill Phase, the cladding continues to heat up: heat-up ends when the lower plenum is full and the coolant is entrained into the core. Any uncertainty in the prediction of the duration of the Refill Phase will lead to uncertainty in the time available for clad heat-up and, therefore, in PCT. There will be contributions to PCT uncertainty by the uncertainty in modelling the bypass phenomena and the effect of any non-condensable. The estimates of these contributions are the subject of this report.

1.2.3.1 Bias in ECC Bypass Phenomena Prediction

The bypass phenomena are modelled in TRAC by seven sets of code parameters; namely, the parameters defining flow regime maps, interfacial area density, interfacial shear coefficients, interfacial heat transfer coefficients, entrainment, wall friction, and wall heat transfer coefficients. The wall friction and wall heat transfer will have lesser influence on the bypass phenomena than the other five sets of parameters.

The correlations for the important five sets of ECCS model parameters in the TRAC code are not based on data relevant to conditions in Nuclear Power Plants (NPP) and have built-in constraints. Therefore, they have systematic errors and cause biases in the code prediction of PCT. Furthermore, because these systematic modeling errors do not have stochastic distributions and cannot be ranged, their contribution to the uncertainty in predicted PCT cannot be included in the probability distribution of PCT uncertainty.

Instead, the bias in PCT due to the systematic modeling errors will be estimated by first computing the bias in the lower plenum filling rate from the simulation of a full-scale Separate Effects Test (Upper Plenum Test Facility) and then by converting the bias in the filling rate into the bias in the duration of the Refill Phase, and finally, into the bias in PCT. This PCT bias is used to shift the PCT uncertainty distribution.

1.2.3.2 Bias Due to Lack of Model for Dissolved N₂ Model

During the Refill Phase, Emergency Core Coolant (ECC) flows from the accumulators into the cold legs. The ECC liquid in the accumulator is saturated with dissolved N₂. The dissolution of N₂ occurs because of depressurization. The N₂ emerging from the ECC liquid affects the filling rate of the lower plenum by displacing liquid from the cold legs to the downcomer, by reducing the condensation rate, and by causing the reduction in ECC flow. The TRAC code does not have a model for such phenomena, and the predicted PCT will have a bias.

This bias in PCT is estimated by a separate calculation first, to determine the bias in ECC flow rate and then in the duration of the Refill Phase. The bias in the Refill Phase duration is converted to a bias in PCT by multiplying the bias in duration by the clad heat-up rate. The resulting PCT bias is used to shift the PCT uncertainty distribution.

1.3 Report Organization

This report describes the procedure for estimating biases due to the modelling of ECC bypass phenomena and due to the lack of a model for dissolved N₂ when the TRAC code is applied to calculate a LBLOCA for a Westinghouse FWR. The report has five chapters and five appendices. Chapter 2 describes the objective of the task, Chapter 3 describes the procedure and its application in estimating the PCT bias due to deficiencies in the ECC bypass model; Chapter 4 describes a procedure and its application of estimating PCT bias due to the lack of a model for dissolved N₂, and, finally, Chapter 5 provides the summary and conclusions. The five appendices describe the Upper Plenum Test Facility (UPTF) and the method of computing lower plenum filling rate (Appendix A), the nodalization used to model UPTF with TRAC (Appendix B), the input deck for UPTF code simulation (Appendix C), the method of obtaining UPTF lower plenum filling

rate from TRAC predictions (Appendix D) and, lastly, Appendix E describes the procedure of estimating the dissolution rate of N_2 and its effect on the ECC flow rate.

2. OBJECTIVES

The objectives of the work reported here are the following:

1. To demonstrate a method for assessing the uncertainties in Peak Clad Temperature (PCT) predictions by computer code, caused by stochastic modeling uncertainties and systematic modeling errors, associated with predicting
 - (i) ECC bypass hydraulics, and
 - (ii) effects from the release of dissolved nitrogen from the ECCS,
2. To apply the above method to the TRAC-PF1/MOD1, Version 14.3 code, as it is used to analyze an LBLOCA for a Westinghouse four-loop PWR.

Specifically, the purpose is to determine the effects from existing modeling uncertainties and scale distortions on Peak Clad Temperature (PCT), as well as to find PCT uncertainties and biases from stochastic and systematic errors in downcomer modeling. Such biases can be added by statistical methods [TPG, 1999] to the PCT uncertainties arising from modeling errors associated with the code prediction of all other phenomena related to LBLOCA.

3. BIAS IN PCT FROM THE MODELLING OF ECC BYPASS PHENOMENA

The ECC bypass phenomena result from the interaction of downcomer flows, cold leg flows and break flows. These flows are governed by the combination of interfacial momentum transfer, interfacial mass transfer (flashing and condensation), entrainment, wall heat and momentum transfer and critical flow. The TRAC code (documented in Step 5, Figure 1.1) has seven sets of parameters to model these interactions, namely: flow regime transitions, interfacial area density, interfacial shear coefficients, interfacial heat transfer coefficients, entrainment, wall friction, and heat transfer coefficients. Some of the correlations used to model these interactions are not based on experiments relevant to NPP and have non-physical constraints [Liles, et al., 1988]. Therefore, they have systematic errors and the parameters in these correlations have no statistical distributions and, can not be treated by statistical analysis. Furthermore, there is a lack of data to determine standard deviations of individual parameters. There is strong coupling between the interfacial and wall interactions. Therefore, it is not possible to isolate uncertainty distributions or biases of parameters, based on downcomer flow tests. Therefore, the effects from the deficiencies in the code models for the bypass phenomena cannot be accounted for in the generation of a response surface and have to be accounted for through a bias.

The next section describes the important processes taking place during the Refill Phase and the division of this phase into four phenomenologically distinct periods.

3.1 The ECC Bypass Phenomena

During LBLOCA, the system depressurizes because of coolant loss through the break(s). Depressurization causes vapor generation by flashing in the core, the lower plenum, and the downcomer. The core empties quickly while the lower plenum and the downcomer continue to produce steam. Figure 3.1 shows a schematic of plant conditions calculated approximately nine seconds after break. The accumulators, which provide the bulk of the ECC fluids, start injecting cold fluid in the cold legs when the system pressure decreases below 40 bar. However, initially, there is sufficient steam being produced in the lower plenum and in the downcomer such that none of the ECC fluid reaches the lower plenum.

Figure 3.2 shows the schematic of the plant conditions in the early part of the Refill Phase. The accumulator flows have begun, but there is no accumulation in the downcomer nor in the lower plenum since the ECC fluid bypasses through the downcomer and out through the break. The lower plenum inventory continues to deplete for a few seconds. As the rate of depressurization decreases the steam production also decreases which allows some of the ECC fluid to reach the lower plenum.

Figures 3.3, 3.4 and 3.5 show the progression of the transient. The lower plenum and the downcomer liquid inventories are still depleting after 20 seconds from the start of the transient. Around 24 seconds, there is some accumulation in the top of the downcomer. Figure 3.5 shows a rapid accumulation of ECC in the downcomer and the lower plenum as the steam flow in the downcomer decreases. The cold ECC fluid mixes with the steam in the downcomer and in the lower plenum, and causes the steam to condense. As the Refill Phase proceeds, the rate of ECC

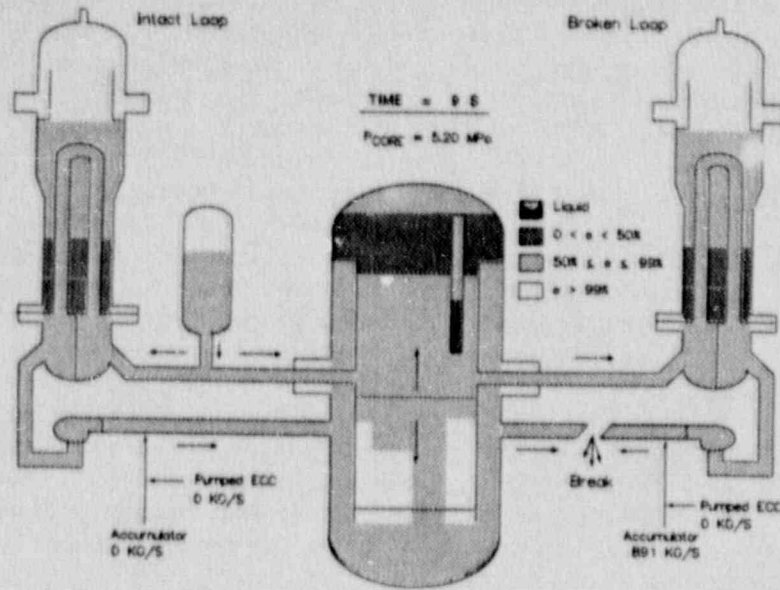


Figure 3.1 Expected Conditions in a PWR System at 9 Seconds After Rupture (Shaw, et. al., 1988) (BNL 1-361-90)

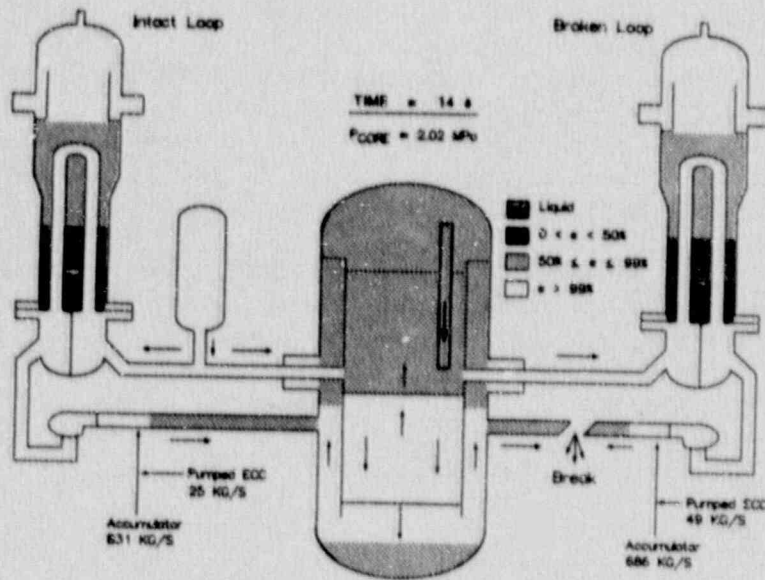


Figure 3.2 Expected Conditions in a PWR System at 14 Seconds After Rupture (Shaw, et. al., 1988) (BNL 3-164-90)

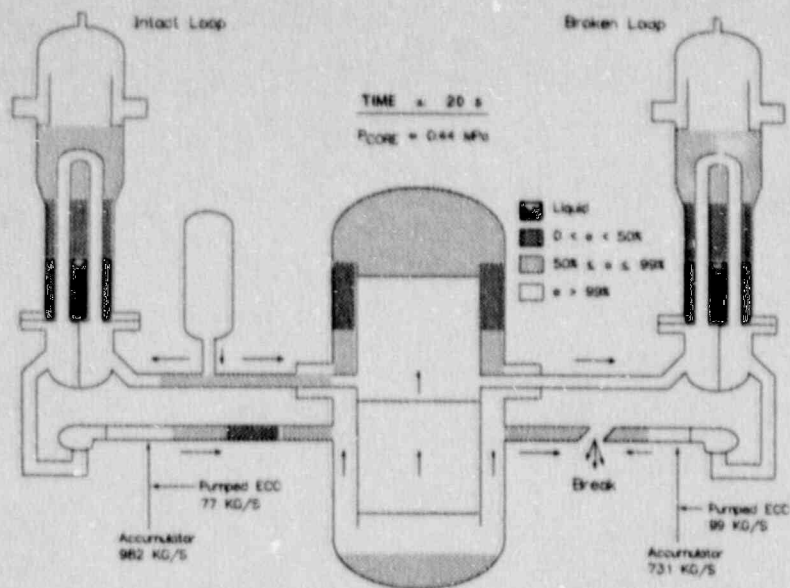


Figure 3.3 Expected Conditions in a PWR System at 20 Seconds After Rupture (Shaw, et al., 1988) (BNL-1-365-90)

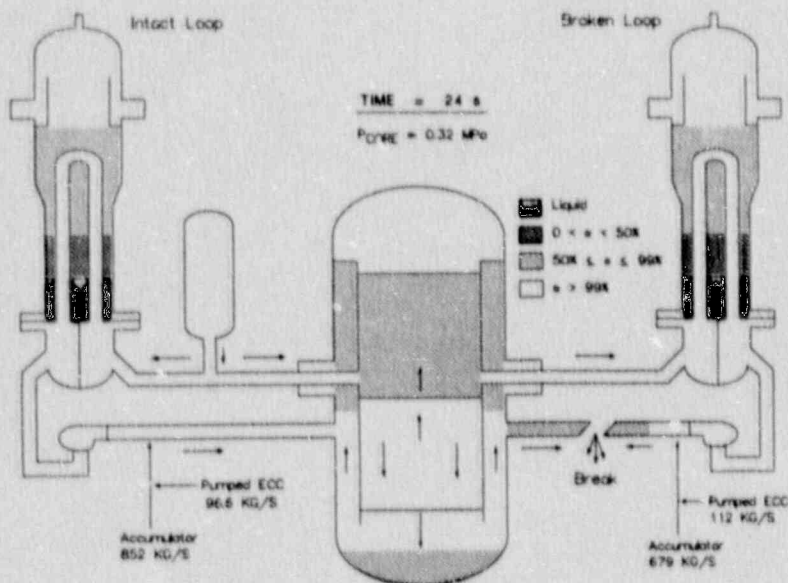


Figure 3.4 Expected Conditions in a PWR System at 24 Seconds After Rupture (Shaw, et al., 1988) (BNL-1-363-90)

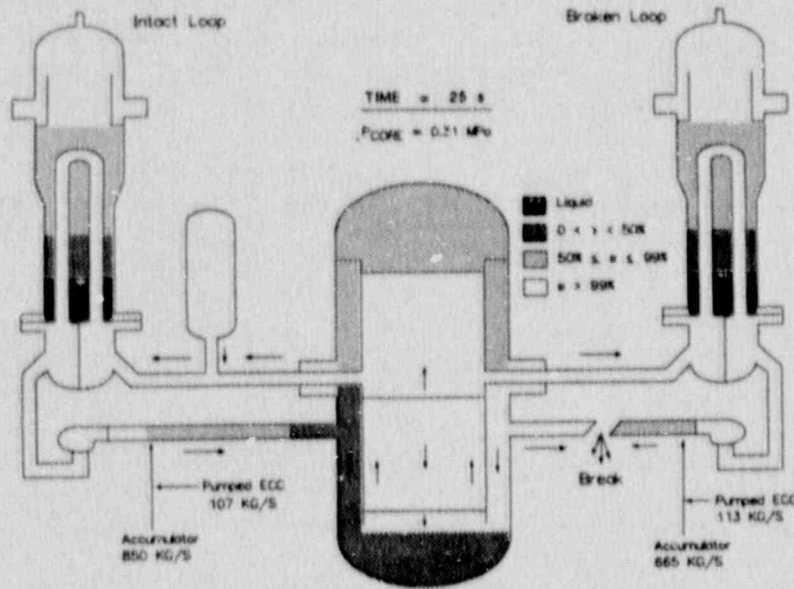


Figure 3.5 Expected Conditions in a PWR System at 25 Seconds After Rupture (Shaw, et al., 1988) (BNL-2-120-90)

delivery increases, eventually becoming equal to the rate of injection, i.e., there is complete delivery.

During this Refill Phase the core is normally empty and the fuel clad is heating up almost adiabatically. However, when the lower plenum is almost full, as shown in Figure 3.6, the liquid enters the core and begins to quench the fuel rods, leading to a peak in the clad temperature history.

3.1.1 Four Periods of the Refill Phase

The LOCA described above is summarized in Figure 3.7 which shows typical time plots of the downcomer inventory, fuel clad temperature, rate of steam flow from the lower plenum to the downcomer, and downcomer inventory during the transient. The Refill Phase of LOCA begins at time t_I , when the accumulator flow starts and ends at time t_B , when the lower plenum is full. The duration of the Refill Phase is t_{IB} . The clad temperature plot (Figure 3.7) shows that during the Refill Phase, the clad heated up almost linearly in time and the temperature turn-around occurred around time t_B .

The Refill Phase is divided into two periods; the Bypass Period and the Filling Period, as shown in Figure 3.7. The Bypass Period begins at time t_I and ends at time t_A , and its duration is t_{IA} . The Filling Period begins at time t_A and ends at time t_B , and its duration is t_{AB} . The Bypass Period is further divided into two subperiods, namely the Period of Complete Bypass and the Delay Period, as shown in Figure 3.7. The Period of Complete Bypass begins at time t_I and ends at time t_D , and its duration is t_{ID} . The Delay Period begins at time t_D and ends at time t_A , and its duration is t_{DA} . The Filling Period is also divided into two subperiods; the Counter Current Flow Period and the No-Bypass Period, as shown in Figure 3.7. The Counter Current Flow Period begins at time t_A and ends at time t_E and its duration is t_{AE} . The No-Bypass Period begins at time t_E and ends at time t_B , and its duration is t_{EB} .

During the Bypass Period, t_{IA} , the steam flow from the lower plenum in the downcomer decreases. This period ends when the lower plenum inventory begins to increase. The boundary between the two subperiods in the Bypass Period is time t_D when the critical steam flow rate (W_{GC}) is reached. The critical steam flow rate is the highest steam flow rate which will permit liquid delivery to the lower plenum, provided the liquid injection is maintained for a long enough time to reach the lower plenum. The critical steam flow rate is estimated from steady state flooding curves for the PWR downcomer. The flooding curves are obtained from either full-scale, or properly scaled, experiments. A schematic of a flooding curve is shown in Figure 3.8. The time t_D corresponding to the critical steam flow rate is obtained from the computed curve for the rate of steam flow from the lower plenum to the downcomer. A schematic of steam flow rate curve is shown in Figure 3.9. During the complete Bypass Period, t_{ID} , the steam flow rate is higher than the critical steam flow rate and, therefore, there is no possibility of liquid delivery to the lower plenum.

During the Delay Period, t_{DA} , the rate of steam flow into the downcomer is low enough to permit liquid delivery to the lower plenum. However, there is a delay in liquid delivery to the lower plenum equal to the time needed by the liquid to flow down through the downcomer. This delay decreases with the decrease in steam flow rate. This subperiod ends at time t_A when the liquid

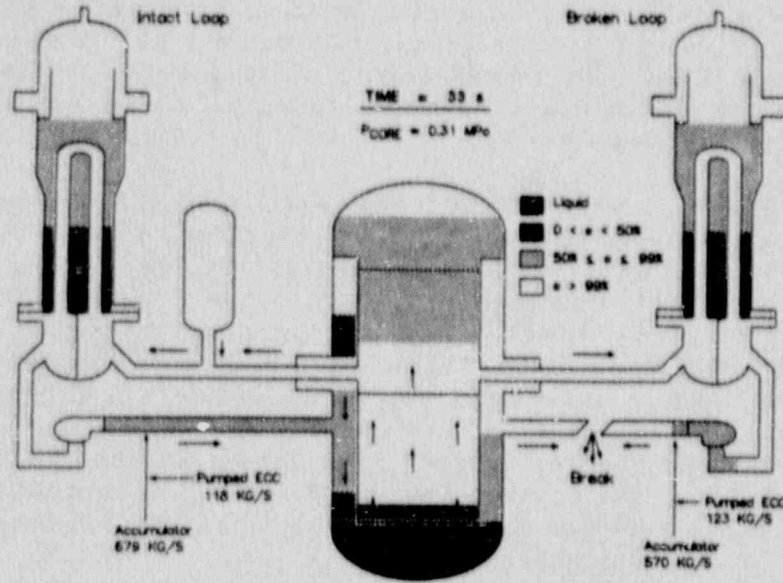


Figure 3.6 Expected Conditions in a PWR System at 33 Seconds after Rupture (Shaw, et al., 1988) (BNL-1-367-90)

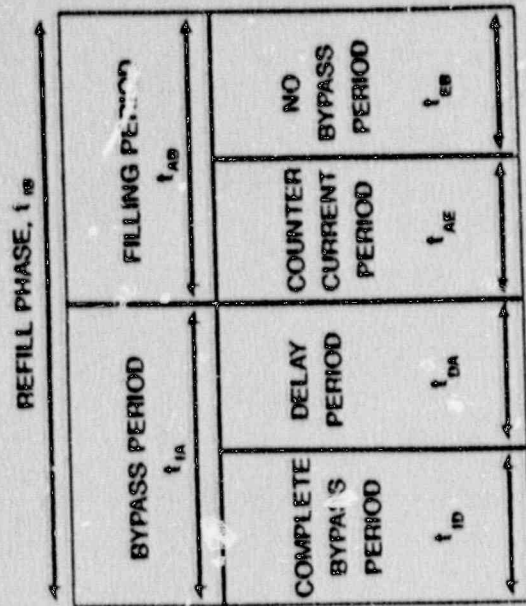
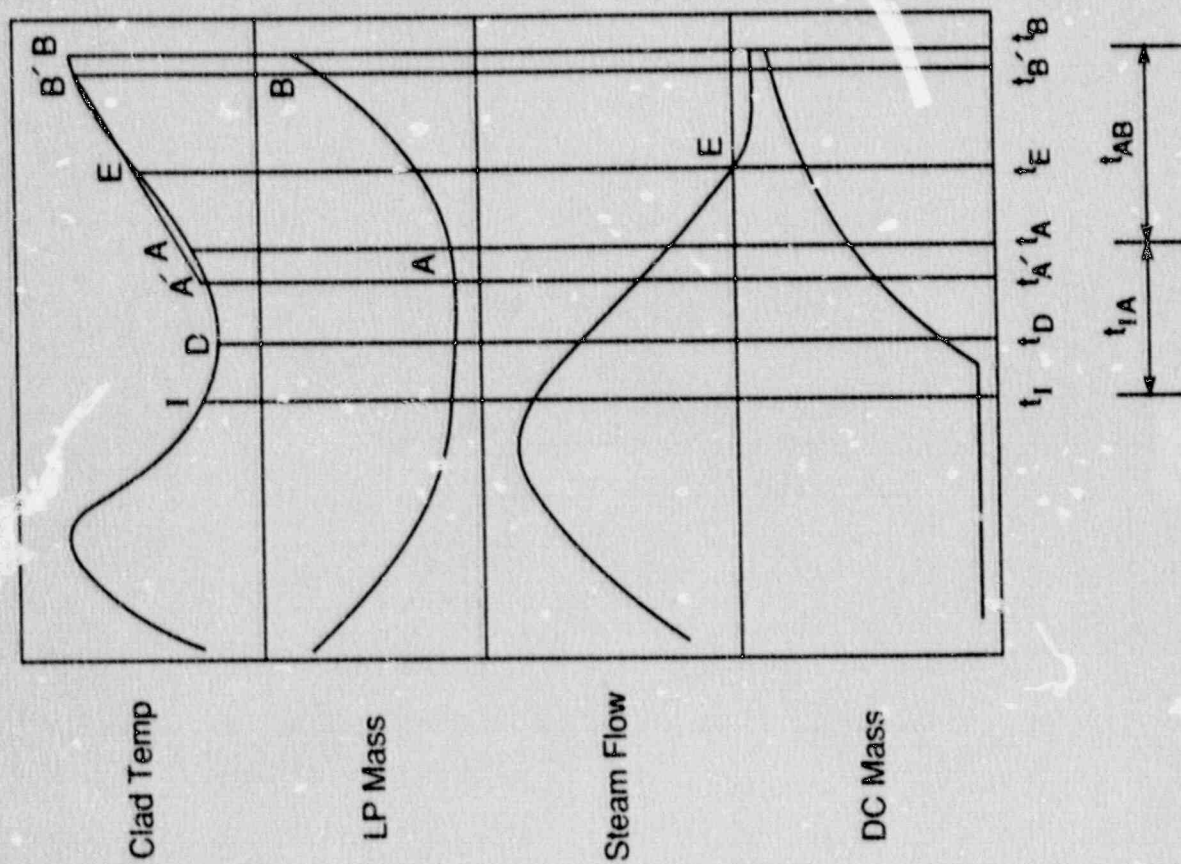


Figure 3.7 Schematic of LBLOCA in NPP

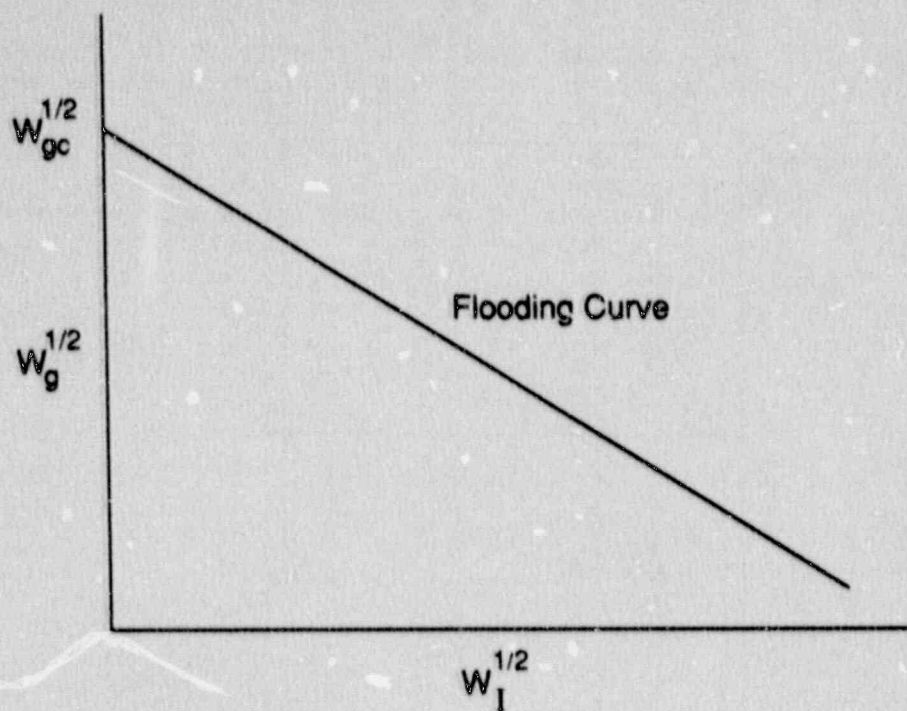


Figure 3.8 Schematic of Flooding Curve and Critical Steam Velocity

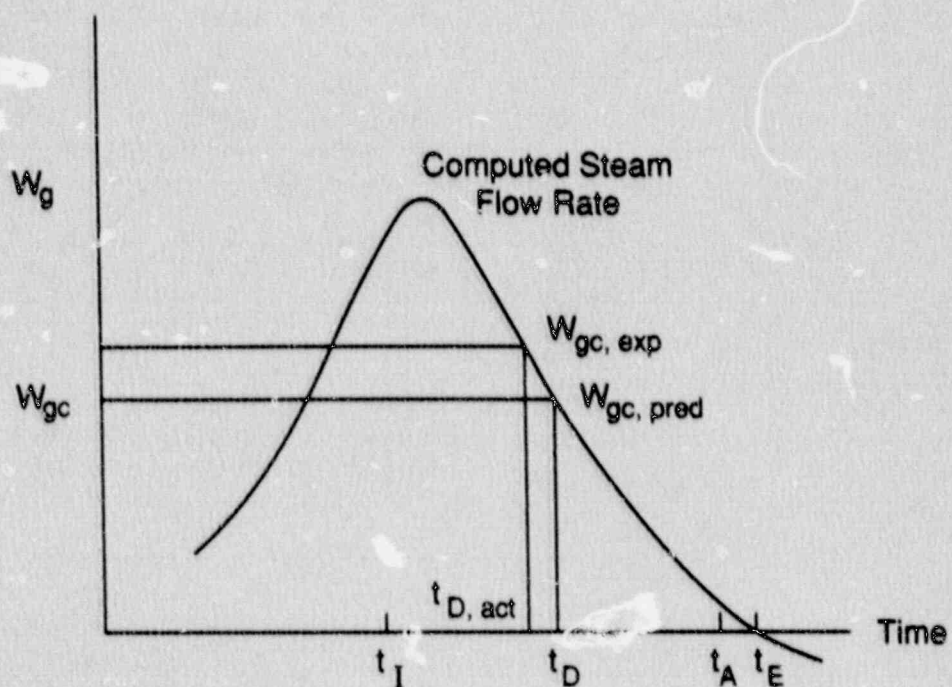


Figure 3.9 Schematic of Steam Flow Rate From the Lower Plenum to the Downcomer in the NPP

delivery to the lower plenum begins. Such a delay was observed in CREARE [Crowley, 1987, 1988] and UPTF [Wolfe, 1988a; Damarell, 1988a] experiments.

The Filling Period, t_{AB} , is the period during which the lower plenum fills up. This period ends at time t_B when the lower plenum is full. The boundary between the two subperiods is the time t_E when there is no steam flow from the lower plenum to the downcomer, as indicated in Figure 3.9. During the first subperiod, i.e. the Counter Current Flow Period, there is liquid down-flow and steam up-flow in the downcomer. During the second or No-Bypass Period, there is no steam flow from the lower plenum to oppose the liquid down-flow and almost all the injected liquid (some may be evaporated due to wall heat transfer) is delivered to the lower plenum.

The next section describes the principles involved in estimating the bias in PCT.

3.2 Principle of Bias Estimate

During the Refill Phase, t_{IB} , the core continues to void and heat transfer from the clad to vapor is small. The clad continues to heat up (almost adiabatically) until the ECC liquid reaches the core as shown in Figure 3.7. Any uncertainty in predicting t_{IB} will result in a bias in the Reflood Phase PCT. The PCT bias δPCT is estimated as follows:

$$\delta PCT = (dT_c/dt) * \delta t_{IB} \quad (3.1)$$

where dT_c/dt and δt_{IB} , are the average rate of clad temperature rise during heatup and the uncertainty in the predicted duration of the Refill Phase, respectively. The average clad temperature rise is obtained from the hot rod clad temperature history predicted by the code for the nominal conditions. The approach is similar to the method suggested by [Damarell, 1988b]. Figure 3.7 also shows the hot rod clad temperature history. The average clad heatup rate during the Refill Phase is computed as follows:

$$dT_c/dt = (T_{B'} - T_{A'}) / (t_{B'} - t_{A'}) \quad (3.2)$$

where $T_{B'}$, $T_{A'}$, $t_{B'}$, and $t_{A'}$ are the clad temperatures and corresponding times as shown in Figure 3.7. The only variable that remains to be determined in Equation 3.1 is δt_{IB} , which is the bias in predicting the Refill Phase duration. Thus, the estimation of PCT bias is reduced to the estimation of bias in the Refill Phase duration.

3.3 Bias in Timing of Refill Phase

The bias in predicting the period of Refill Phase reduces to the biases in predicting the Bypass and Filling Periods as defined in Section 3.1. The Refill Period bias is computed from the biases in the two periods as follows:

$$t_{IB} = t_{IA} + t_{AB} ,$$

(3.3)

$$\delta t_{IB} = \delta t_{IA} + \delta t_{AB} ,$$

where δt_{IA} and δt_{AB} are the biases in the prediction of the Bypass Period and the Filling Period, respectively.

3.3.1 Bias in Timing of Bypass Period

The net bias in the Bypass Period is evaluated from the biases in the subperiods, namely "Complete Bypass Period" and "Delay Period," as follows:

$$t_{IA} = t_{ID} + t_{DA} ,$$

(3.4)

$$\delta t_{IA} = \delta t_{ID} + \delta t_{DA} ,$$

where δt_{ID} and δt_{DA} are the biases in the "Complete Bypass" Period and "Delay Period," respectively.

3.3.1.1 Bias in Timing of Complete Bypass Period

The bias in this period is due to the uncertainty in predicting the critical steam flow rate for the NPP. The evaluation of bias requires the determination of the critical steam flow rate from the data obtained from full-scale, separate effect tests in the Upper Plenum Test Facility (UPTF) under NPP conditions. These separate effects tests are simulated with the code, by using NPP-type nodalization. The predicted critical steam flow rate for this SET will be the critical steam flow rate for the NPP calculation. The measured critical steam flow rate ($W_{gc,exp}$) from the SET will be the actual critical steam flow ($W_{gc,act}$) act for the NPP. Any discrepancy in the predicted and actual critical steam flow rates ($W_{gc,pred}$ and $W_{gc,act}$) will produce a bias in the code prediction of the time, t_D . The times t_D and $t_{D,act}$, corresponding to the critical steam flow rates $W_{gc,pred}$ and $W_{gc,act}$, respectively are estimated from the time plot of the rate of steam flow from the lower plenum to the downcomer obtained from a reference NPP calculation.

The bias δt_{ID} is computed as follows:

$$t_D = t(W_{gc,pred}) ,$$

(3.5)

$$t_{D,act} = t(W_{gc,act}) \quad (3.6)$$

$$\delta t_{ID} = t_{D,act} - t_D \quad (3.7)$$

A schematic of computed steam flow rate curve with critical steam flow rates and corresponding times is shown in Figure 3.9, presented earlier.

3.3.1.2 Bias in Timing of Delay Period

This period spans from the time t_D to time t_A . The time t_A is the time at which the lower plenum inventory is the lowest and begins to increase as shown in Figure 3.10. The time span for this period is estimated from time t_A , read from Figure 3.10 and time t_D obtained from Equation (3.5).

$$t_{DA} = t_A - t_D \quad (3.8)$$

The bias of this period is estimated by modelling with TRAC the full-scale separate effects tests in UPTF with the nodalization corresponding to NPP and simulating the complete transient until steady state is reached for fixed steam and liquid flow rates. Figure 3.11 shows a schematic of the expected lower plenum inventory in the SET and the delay t_{DA} . The measured and predicted delays are compared and the difference between them is the bias in the Delay Period. As it is difficult to simulate the conditions in the NPP during the Delay Period, a ratio, R_t , of predicted $t_{DA,pred}$ to observed $t_{DA,exp}$ for each steam flow rate in the SET is estimated and this ratio is a measure of the deficiency in the code.

$$R_{t,SET} = \left(\frac{t_{DA,pred}}{t_{DA,exp}} \right)_{SET} \quad (3.9)$$

During the Delay Period, t_{DA} , the steam flow rate decreases in the NPP. Therefore, an average of the ratios (R_t) obtained from the many tests for the SET is used for the application to NPP. Since the SET is properly scaled, an average delay ratio $\langle R_t \rangle_{SET}$ estimated for the SET is also applicable to the NPP.

Therefore,

$$\langle R_t \rangle_{NPP} = \langle R_t \rangle_{SET} \quad (3.10)$$

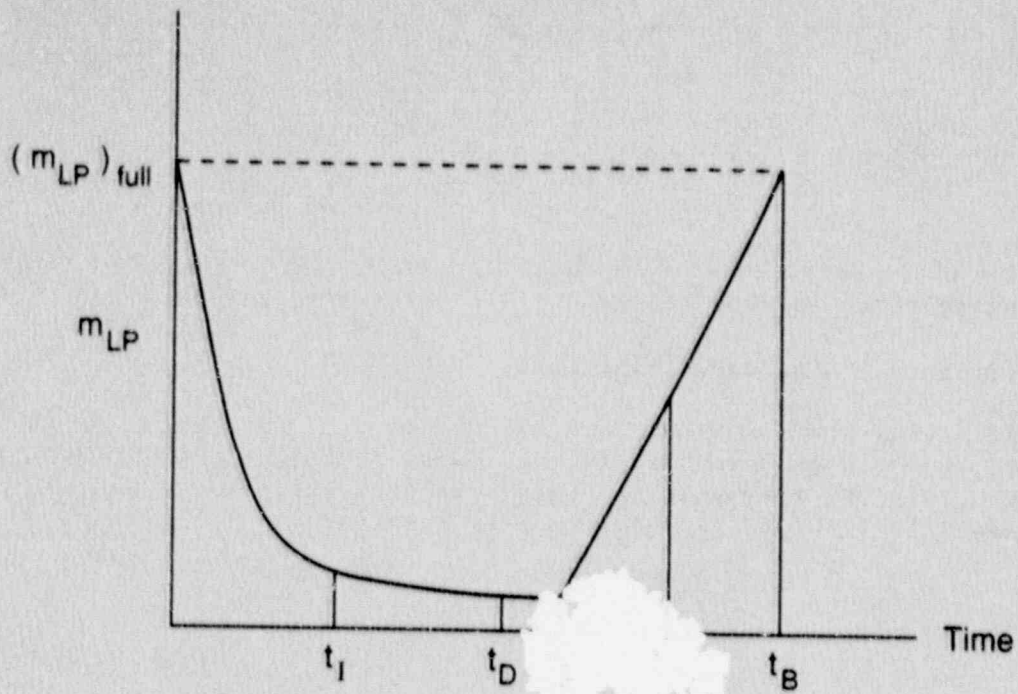


Figure 3.10 Schematic of Lower Plenum Inventory During LBLOCA

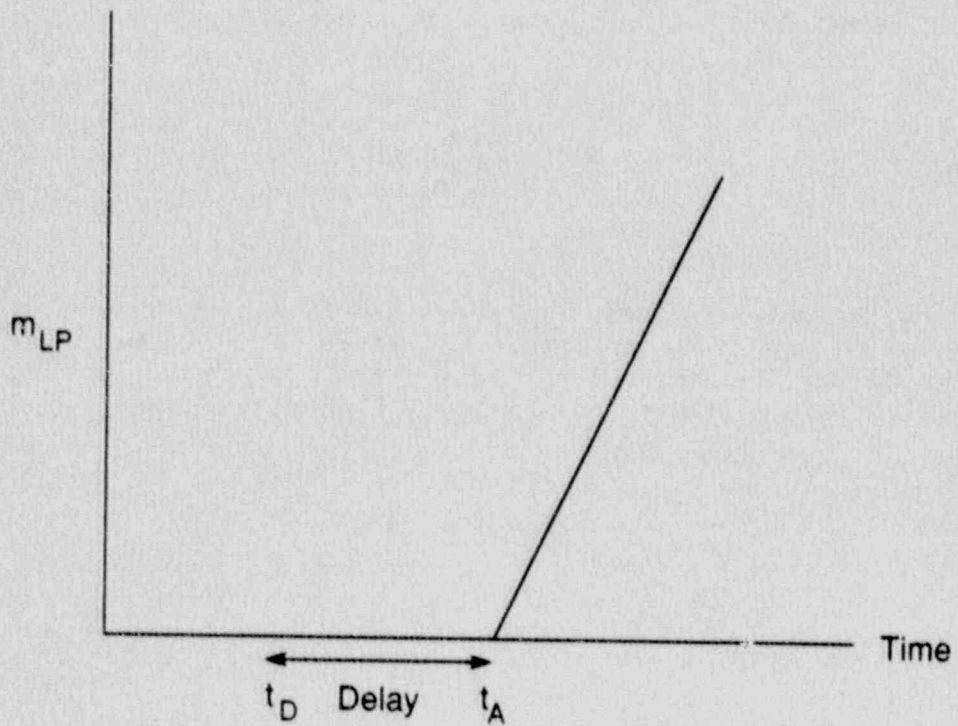


Figure 3.11 Schematic of Lower Plenum Inventory of Separate Effects Tests

The average delay ratio for the NPP is used to estimate the bias in the Delay Period:

By definition for the bias in the Delay Period,

$$\delta t_{DA} = t_{DA,act} - t_{DA,pred} \quad (3.11)$$

By combining Eqs.(3.9) and (3.10), one finds

$$\langle R_t \rangle_{NPP} = \frac{t_{DA,pred}}{t_{DA,act}} \quad (3.12)$$

By eliminating $t_{DA,act}$ from Eqs.(3.11) and (3.12), one gets:

$$\delta t_{DA} = t_{DA,pred} \frac{(1 - \langle R_t \rangle_{NPP})}{\langle R_t \rangle_{NPP}} \quad (3.13)$$

where δt_{DA} is the bias in the Delay Period and $t_{DA,act}$ is the expected actual duration of the Delay Period for the NPP.

3.3.2 Bias in the Timing of the Filling Period

The second part of the Refill Phase is the Filling Period which spans from time t_A to time t_B . During this period, the lower plenum fills up slowly at first and then at the rate of the ECC injection. The time t_A is obtained from Figure 3.11, as explained before in Section 3.3.1.2. The time t_B is reached when the lower plenum is full. The time t_B is read from the lower plenum inventory curve obtained from a reference NPP calculation (cf. Figure 3.10). The time period t_{AB} is obtained as follows:

$$t_{AB} = t_B - t_A \quad (3.14)$$

The steam flow into the downcomer decreases and completely ceases at time t_E . This time, t_E , divides the Filling Period into two phenomenologically different periods, namely the Counter Current Flow Period and the No-Bypass Period. The bias in the Filling Period, therefore, is the sum of the biases in the prediction of two subperiods.

From:

$$t_{AB} = t_{AE} + t_{EB} \quad ,$$

and component biases, the overall bias is computed as follows: (3.15)

$$\delta t_{AB} = \delta t_{AE} + \delta t_{EB} \quad ,$$

where δt_{AE} and δt_{EB} are the subperiod biases for the Counter-Current Flow and No-Bypass Flow Periods, respectively.

3.3.2.1 Bias in the Timing of the Counter-Current Flow Period

This period spans from time t_A to time t_E . The time t_E is obtained from the predicted steam flow rate curve shown in Figure 3.9. The duration of this period is computed as follows:

$$t_{AE} = t_E - t_A \quad (3.16)$$

The bias in the Counter-Current Flow Period is due to the uncertainty in predicting the amount of the ECC delivered to the lower plenum. The more the ECC fluid accumulates during this period, the shorter will be the Filling Period. The downward ECC flow in the downcomer depends upon the steam flow rate from the lower plenum and the interfacial mass and momentum transfer in the downcomer.

The discrepancy between the predicted and measured lower plenum filling rates, $\delta \dot{m}_{LP}$, is defined via the ratio $\langle R_{mLP} \rangle$ of the predicted ($\dot{m}_{LP,pred}$) and actual ($\dot{m}_{LP,act}$) filling rates, as follows:

$$\delta \dot{m}_{LP} = \dot{m}_{LP,act} - \dot{m}_{LP,pred} \quad (3.17)$$

$$\langle R_{mLP} \rangle_{NPP,AE} = \dot{m}_{LP,pred} / (\dot{m}_{LP,pred} + \delta \dot{m}_{LP}) \quad . \quad (3.18)$$

From the discrepancy in the filling rate one computes the bias in the predicted duration t_{AE} ; Figure 3.10 shows the times and the corresponding lower plenum inventories for this period. The filling rate discrepancy will lead to the bias in the time period for the Counter-Current Flow Period to achieve the same inventory in the lower plenum in both the reference NPP calculation and the NPP.

$$m_{LP,E} - m_{LP,A} = \dot{m}_{LP,pred} * t_{AE} \quad (3.19)$$

$$= (\dot{m}_{LP, pred} + \delta \dot{m}_{LP}) * (t_{AE} + \delta t_{AE}) \quad (3.20)$$

where $m_{LP,A}$ and $m_{LP,E}$ are the liquid inventories in the lower plenum at times t_A and t_E , respectively.

The bias δt_{AE} is obtained from Equations (3.16), (3.17), (3.18), and (3.19) and is shown here:

$$\delta t_{AE} = (\langle R_{mLP} \rangle_{NPP,AE} - 1) * t_{AE} \quad (3.21)$$

The prediction of bias in the Counter Current Flow Period is reduced to the estimation of ratio $\langle R_{mLP} \rangle_{NPP,AE}$. This ratio is obtained from the full-scale Separate Effect Test (SET) facilities (UPTF) for the downcomer flows measured under conditions as expected in the NPP during the Counter Current Flow Period. Since there is no scale distortion in UPTF, one gets

$$\langle R_{mLP} \rangle_{NPP,AE} = \langle R_{mLP} \rangle_{SET} \quad (3.22)$$

The ratio $\langle R_{mLP} \rangle_{SET}$ is obtained by modelling with the code the tests previously conducted in the SET facility (UPTF) and by computing a set of ratios of predicted over measured lower plenum filling rates.

$$R_{mLP} = \dot{m}_{LP, pred} / \dot{m}_{LP, meas} \quad (3.23)$$

An average of all the ratios (Equation 3.23) in the set is computed according to Equation (3.22) and this average ratio is applied to compute δt_{AE} according to Equation (3.21).

3.3.2.2 Bias in the Timing of No-Bypass Period

The No-Bypass time Period is the last period (t_{EB}) of the Refill Phase and begins at time t_E at which time the steam flow into the downcomer ceases and ends at time t_B when the lower plenum is full. The time t_B is obtained from Figure 3.10 as the intersection of the TRAC-predicted $m_{LP}(t)$ curve with the horizontal line corresponding to $(m_{LP})_{full}$. The duration of this period is computed as follows:

$$t_{EB} = t_B - t_E \quad (3.24)$$

The bias in this period is due to the bias in predicting the lower plenum filling rate or the error in predicting the distribution of ECC fluid between the lower plenum and the downcomer. The steps to estimate the uncertainty in the duration of this period are the same as in the previous section. A ratio $\langle R_{m,LP} \rangle$ of the

predicted and the actual lower plenum filling rates is computed and it is used to estimate the bias in t_{EB} .

$$\delta t_{EB} = (\langle R_{mLP} \rangle_{NPPEB} - 1) * t_{EB} \quad (3.25)$$

where the ratio $\langle R_{mLP} \rangle_{NPPEB}$ is obtained from properly scaled or full-scale Separate Effects Tests with conditions similar to the conditions expected in NPP for No-Bypass Period.

$$\langle R_{mLP} \rangle_{NPPEB} = \langle R_{mLP} \rangle_{SET} \quad (3.26)$$

3.3.3 Total Bias in the Refill Phase

The biases estimated in the Sections 3.3.1 and 3.3.2 are added to provide the bias in the Refill Phase.

$$\delta t_{IB} = \delta t_{ID} + \delta t_{DA} + \delta t_{AE} + \delta t_{EB} \quad (3.27)$$

The total bias δt_{IB} estimated in Equation (3.27) is used in Equation (3.1) to estimate the bias in PCT.

3.3.4 Required Information for Application

Application of the procedure developed in the previous sections (Sections 3.3.1 to 3.3.3) requires information from the nominal NPP calculation and from SETs for the downcomer flow. The information needed and its source are summarized here:

t_I	Time of ECC Injection	NPP Calculation/Accumulator Flow
$t_D (W_{gc})$	Time of Critical Steam Flow	NPP Calculation/Steam Flow from LP to DC
t_A	Time of Lowest LP Inventory	NPP Calculation/LP Liquid Inventory
t_E	Time of End of Steam Flow DC	NPP Calculation/Steam Flow from LP to DC
t_B	Time When LP Full	NPP Calculation/LP Liquid Inventory
dT_c/dt	Rate of Clad Temp Rise	NPP Calculation/Hot Rod Clad Temperature History
W_{gc}	Critical Steam Flow Rate	Calculation/Stand alone DC with Fixed ECC and Steam Flows
$W_{gc,exp}$	Critical Steam Flow Rate, Exp	SET
$R_{t,SET}$	Ratio of Delays From SET	SET
$R_{mLP,SET}$	Ratio of Filling Rates From SET	SET

The information from the SETs is used for evaluating the bias in the timing of the Refill Phase.

3.4 Application

The methodology developed in the previous section is applied to the TRAC-PF1/MOD1, Version 14.3 calculation of a LBLOCA for a four loop Westinghouse plant. This section describes the numerical evaluation of Equations (3.1), (3.2) and (3.27) to obtain the bias in the predicted PCT due to the uncertainty in the code modelling of the Refill Phase.

3.4.1 Experiments for Estimating Bias

The evaluation of the bias in the Refill Phase timing requires a comparison of the code predictions with the data from well-scaled or full-scale test facilities simulating the downcomer flow during the Refill Phase. These tests are identified in Step 8 of the CSAU Methodology (Section 1.2.2).

There are two types of facilities which simulate the downcomer flow during the Refill Phase. They are: Integral Effects Test (IET) and Separate Effects Test (SET). The IETs, such as LOFT, are scaled with power to volume scaling method [Zuber, et al., 1990]. While preserving the time scales and the mass and energy distributions, such scaling distorts the downcomer flows. The downcomer in the IET has narrow gaps and therefore, does not accurately simulate the flow regimes and counter-current flow.

The SETs are designed to overcome the scale distortion in the downcomer in the IET. The downcomer flow phenomena are affected by geometry such as that of the annular gap, the arrangement of cold legs, and by wall heat transfer, by rate of steam flow from the lower plenum to the downcomer, and the temperature and flow rate of the ECC fluid. These conditions are easily controlled in the SETs. The procedure for bias assessment (described in Section 3.3) needs three empirical parameters $W_{gc,exp}$, $R_{t,SET}$ and $R_{mLP,SET}$ from the steady state tests with constant steam flow and ECC injection rates. These parameters can only be obtained from SETs and therefore, only SETs will be considered. In the next section, the available SETs for the downcomer flow are described.

3.4.1.1 Available Data

A search through the literature indicated that the data from five sub-scale experiments and one full-scale experiment were available. The dimensions of these facilities are listed in Table 3.1. In this table, the first column lists the type of dimension, the second column indicates the size of a typical PWR, and the remaining six pairs of columns list the actual dimension and the ratio of these dimensions to the corresponding dimensions of PWR, for the six SETs used, i.e., the Upper Plenum Test Facility (UPTF), CREARE (1/5), Battelle Columbus Laboratory (BCL) tests (2/15), BCL (1/15), CREARE (1/15), and CREARE (1/30) respectively. All the facilities had four cold legs. Three of the cold legs had injections, and the fourth cold leg represented the break. The UPTF [Siemens/KWU, 1987; Liebert, 1988] is a full-scale test facility. The subscale test facilities [Crowley, et al., 1977, 1979, 1980, 1981; Cudnik, et al., 1977, 1978] covered variations in the steam or air flow rates, ranging from no liquid delivery or complete bypass to full liquid delivery.

Table 3.1 - Geometrical Parameters for Test Facilities***

	PWR	UPTF		CREARE (1/5)		BCL (2/15)		BCL (1/15)		CREARE (1/15)		CREARE (1/30)	
		ACTUAL	SCALE*	ACTUAL	SCALE	ACTUAL	SCALE	ACTUAL	SCALE	ACTUAL	SCALE	ACTUAL	SCALE
VESSEL DIA	4.4m	4.87	1.1	0.89m	0.2	0.618m	0.14	0.307	0.070	0.292m	0.066	0.152m	0.034
DC,GAP	0.26m	0.25m	0.96	0.038m	0.146	0.031m	0.119	0.015	0.058	0.0126m	0.048	0.0064m	0.025
DC,HEIGHT	5.33m	6.64m	1.25	1.37m	0.257	0.82m	0.153	0.521	0.098	0.46m	0.086	0.229m	0.043
LP,DEPTH	1.94m	2.48m	1.28	1.52m	0.783	1.022m	0.526	0.508**	0.262	0.86m	0.443	0.528m	0.272
LP VOL,m ³	29.6	24.9	0.84	0.94	0.032	0.302	0.010	0.038**	0.0013	0.058	0.0019	0.0096	3x10 ⁻⁴
COLD LEG DIA	0.74m	0.75m	1.01	0.152m	0.21	0.102m	0.14	0.053	0.072	0.0476m	0.064	0.076m	0.1
D _{CL} /D	0.168	0.154	-----	0.168	-----	0.165	-----	0.173	-----	0.163	-----	-----	0.5

* Scale is the ratio of the dimension of the facility and the dimension of PWR.

** Dimensions are taken from sketch (Fig. 1, BMI-1941, November 1975).

*** Data obtained from Crowley, et al. (1980).

The subscale facilities were scaled with the linear scaling method [Zuber, et al., 1990]. The gap size, vessel diameter and cold leg diameter were linearly scaled from the PWR as shown in Table 3.1. However, the downcomer height and the lower plenum depth were oversized. These facilities are not similar and do not model the same flow phenomena. Three flow regimes [Richter, 1977; Liebert, 1988] are possible in the downcomer during the counter-current flow; falling films on the wall, bridging of the films with liquid globules and flow of ECC as column below intact cold legs in the downcomer. These flow regimes are dependent on the physical dimensions of the downcomer. The first two flow regimes have been observed in the subscale facilities, but the third flow regime has only been observed in the UPTF [Appendix A]. Use of subscale test data for bias evaluation will introduce uncertainty in the bias due to scale distortion.

The TRAC code does not have constitutive package to represent the flow regimes expected in the downcomer and it is impossible to estimate the uncertainty due to scale distortion in the bias by using the code. As an illustration of the uncertainty due to scale distortion, four of the SETs [Neymotin et al, 1988] were modelled with the TRAC code and the ratios (R_{mLP}) of lower plenum filling rates are shown in Figure 3.12. The TRAC code overpredicts the LP filling rate for smaller facilities and underpredicts for the larger facilities. The code is conservative for the larger facilities. Therefore, an estimate of bias (Equations 3.21, 3.25, 3.27) in the timing of the Refill Phase on the basis of the above smaller facilities can lead to both a small reduction and an increase in the timing. The uncertainty in the bias in the PCT due to scale distortion of the SET could make the bias conservative. However, a definite conclusion could only be reached on the basis of the full-scale UPTF data.

Fortunately the data from a full-scale facility, such as UPTF, are available and the estimate of bias on the basis of this data will not have uncertainties due to scale distortion. UPTF data are used below in estimating the bias.

3.4.1.2 UPTF Experiments

The procedure described in Section 3.3 requires data from Separate Effects Tests. The full-scale data are available from the Upper Plenum Test Facility (UPTF) and the biases are evaluated on the basis of UPTF data only. However, only five UPTF data points are available which precludes any statistical analysis.

Appendix A describes UPTF Test 6 and the procedure for analyzing the data. These tests were modelled with TRAC-PF1/MOD1, Version 14.3 with the same nodalization as for NPP analyses. The description of the nodalization and the input deck listing are given in Appendices B and C, respectively. The results of the TRAC model of the UPTF Test 6 runs have been analyzed in Appendix D. The results from Appendix A and D for five steam flow rates are summarized in Table 3.2. The first column indicates the run numbers, and the second column provides the steam flow rates. The next four columns (3 to 6) list the lower plenum filling rates, the time of injection, the time at which the lower plenum inventory begins to increase, and the delay in the delivery of ECC to the lower plenum. The next four columns (7 to 10) list the predicted values of the lower plenum filling rates, the time of injection, the time at which the lower plenum inventory begins to increase, and the delay in ECC liquid delivery to the

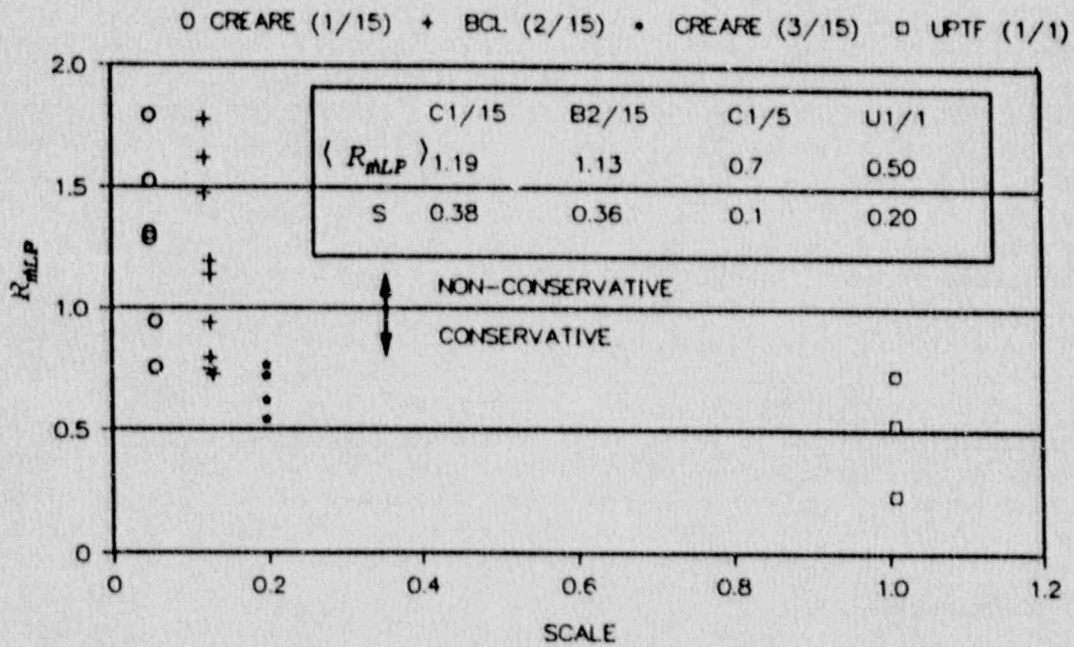


Figure 3.12 Comparison of Ratios of Predicted and Measured Lower Plenum Fill Rates for Three Subscale Facilities and UPTF Test 6

Table 3.2 - Summary of UPTF Results (Test 6)

E X P E R I M E N T						T R A C					
Run	W_g kg/s	\dot{m}_{LP} kg/s	t_I s	t_A s	$t_{IA,UPTF}$ s	\dot{m}_{LP} kg/s	t_I s	t_A s	$t_{IA,UPTF}$ s	R_{mLP}	R_t
131	400	419	43	49(54)	6(11)	0	43	∞	∞	0	∞
132	300	840	43	52	9	199	43	63	20	0.24	2.22
133	200	699	43	50	7	360	43	59	16	0.52	2.29
135	440	> 0	43	-----	-----	0	43	∞	∞	-----	-----
136	100	644	43	45	2	512	43	50	7	0.7	3.50

$\langle R_{mLP} \rangle = 0.5^2$ (Runs 132, 133, 136)

$\langle R_{t,NPP} \rangle = 2.67$ (Runs 132, 133, 136)

lower plenum. The last two columns indicate the ratios of the predicted and the measured lower plenum filling rates and the ratios of the predicted and the measured delay in the delivery of ECC fluid. These ratios will be used to estimate the bias in PCT.

In addition to the experimental data and code predictions for the UPTF tests, one also needs results from the reference NPP calculations, namely accumulator flow rate (Figure 3.13), lower plenum liquid inventory (Figure 3.14), rate of steam flow from the lower plenum to the downcomer (Figure 3.15), and hot rod clad temperature (Figure 3.16). The next section describes the application of the procedure developed in Section 3.3 and the available UPTF data described in this section.

3.4.2 Evaluation of Biases

Figure 3.13 shows the accumulator flows in one of the intact loops from the NPP calculation carried out with TRAC-PF1/MOD1, Version 14.3. The flow begins at 11.5 seconds, which is the beginning of the Refill Phase.

$$t_I = 11.5 \text{ s} \quad (3.28)$$

Times t_A and t_B are read from Figure 3.14 which shows the lower plenum inventory from the NPP calculation.

$$t_A = 22.9 \text{ s} \quad (3.29)$$

and

$$t_B = 33.5 \text{ s} \quad (3.30)$$

The times obtained from the NPP calculation delineate the subperiods in the Refill Phase and will be used to estimate biases in the subperiods.

3.4.2.1 Bias in the Timing of the Complete Bypass Period

The bias in this period is due to the uncertainty in predicting the critical steam flow rate (W_{gc}) and is evaluated from Equation (3.7). Full-scale data are available from UPTF Test 6 as shown in Table 3.2, where Column 2 shows the steam flow rates and the Column 3 lists the lower plenum filling rates. The highest steam flow rate reported is 440 kg/s for Run 135, and there was liquid delivery to the lower plenum for this run. This observation implies that a complete bypass will take place at an even higher steam flow rate. From the available data one can only conclude:

$$W_{gc, UPTF, exp} > 440 \text{ kg/s} \quad (3.31)$$

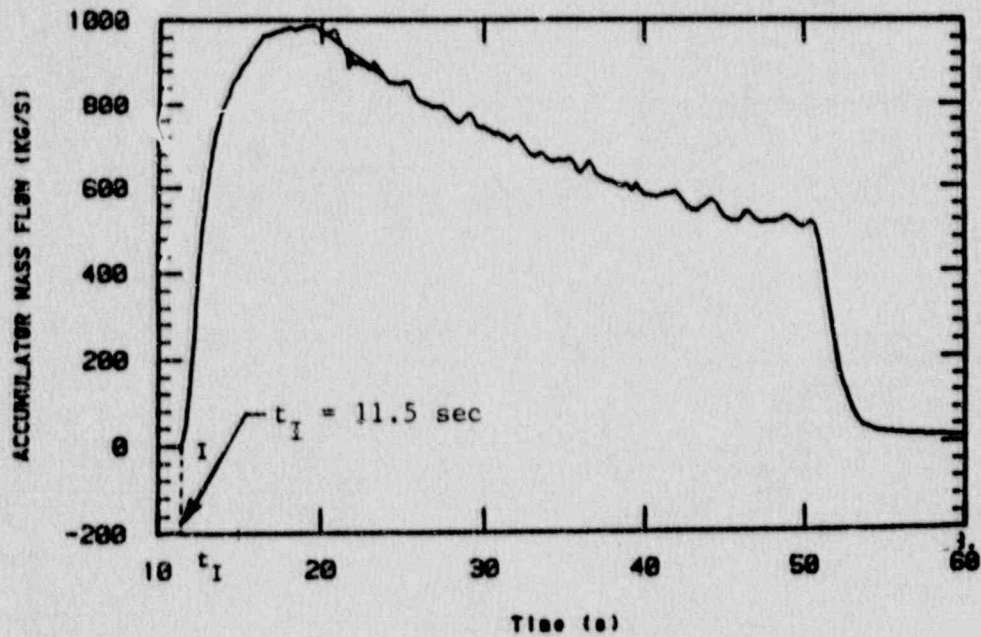


Figure 3.13 Identification of t_I from the Predicted Accumulator Discharge Mass Flow Rate. (Nominal TRAC-PF1/MOD1 Version 14.3 Calculation Performed by INEL in Support of CSAU Methodology Demonstration) (BNL-1-368-90)

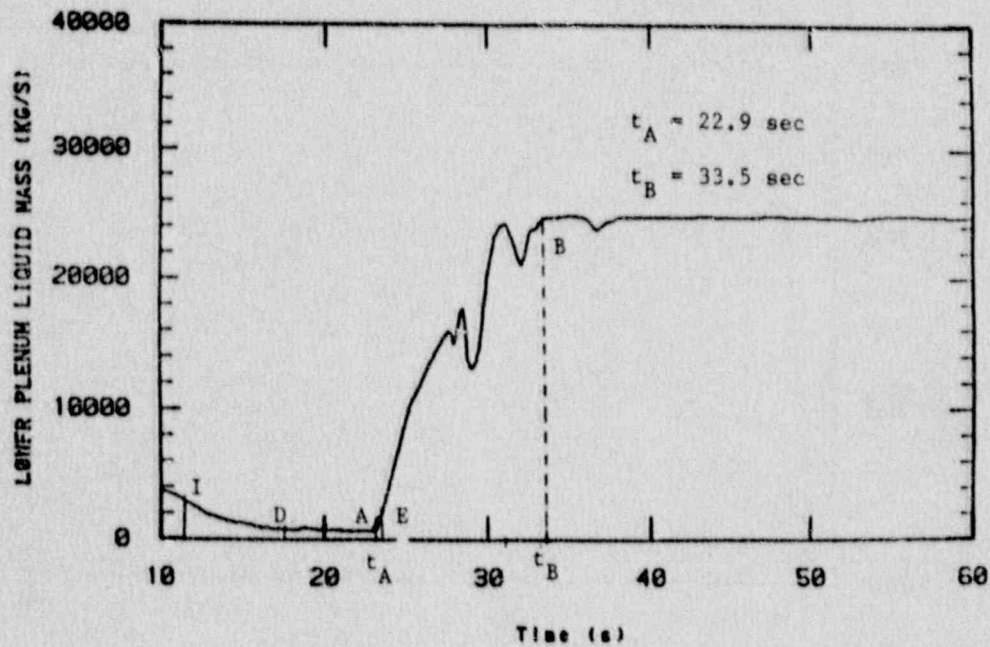


Figure 3.14 Identification of t_A and t_B from the Predicted Lower Plenum Liquid Inventory. (Nominal TRAC-PF1/MOD1 Version 14.3 Calculation Performed by INEL in Support of CSAU Methodology Demonstration) (BNL-1-360-90)

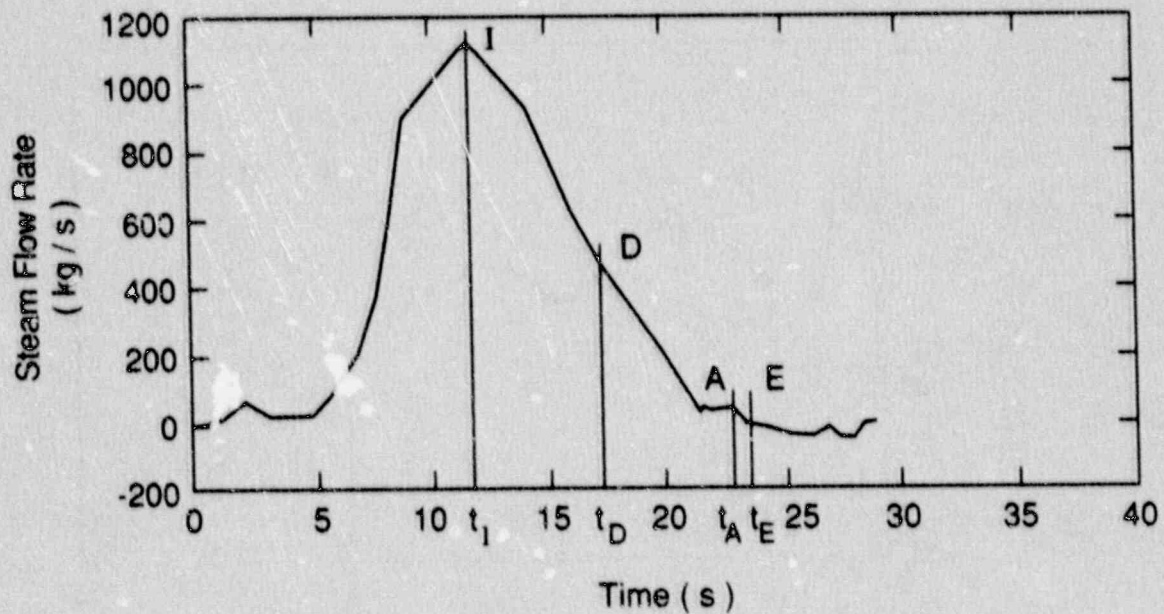


Figure 3.15 Identification of t_I and t_E from the Predicted Steam Flow Rate from the Lower Plenum to the Downcomer. (Nominal TRAC-PF1/MOD1 Version 14.3 Calculation Performed by INEL in Support of CSAU Methodology Demonstration)

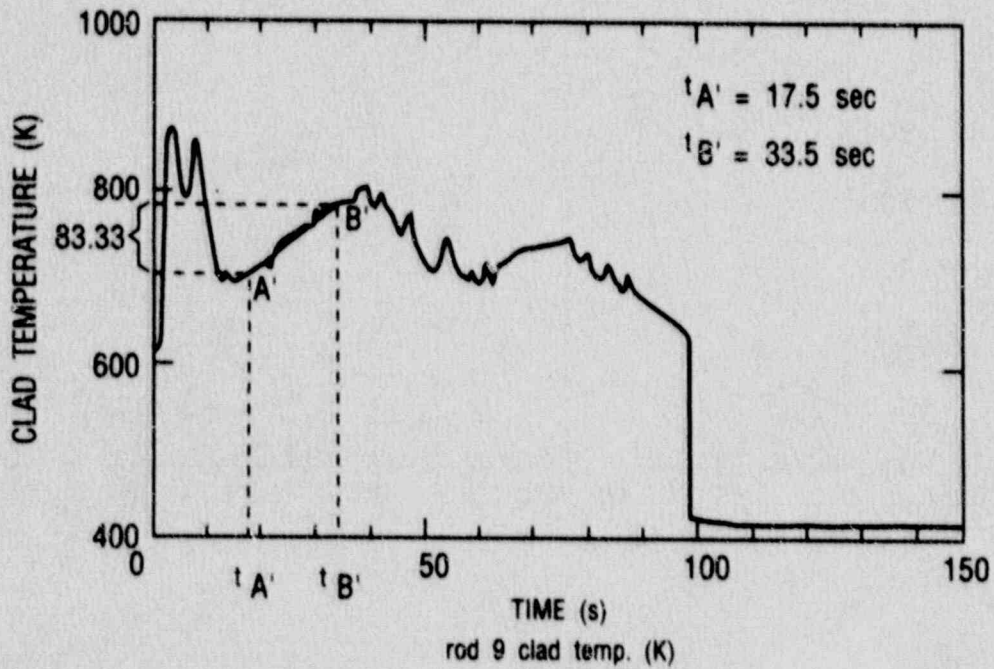


Figure 3.16 Identification of $T_{A'}$, $T_{B'}$, $t_{A'}$, and $t_{B'}$ from the Predicted Rod 9 (Hot Rod) Clad Temperature (Nominal TRAC-PF1/MOD1 Version 14.3 Calculation Performed by INEL in Support of CSAU Methodology Demonstration)

The critical steam flow rate $W_{gc,NPP}$ for the NPP will be larger than for any UPTF run reported in Test 6, because the ECC subcooling and ECC injection rate in UPTF Test 6 were lower than in the NPP prediction as shown in Table 3.3. These differences imply that there is a larger condensation in the NPP, and a larger steam flow rate will be needed for complete bypass in the NPP than in the UPTF Test 6. Therefore,

$$W_{gc,NPP} > W_{gc,UPTF,exp} \quad (3.32)$$

For a conservative estimate of the bias in the PCT, a lower bound for $W_{gc,NPP}$ is chosen from Equations (3.31) and (3.32):

$$W_{gc,NPP} = 440 \text{ kg/s} \quad (3.33)$$

The time t_D corresponding to the critical steam flow rate in Equation (3.32) is obtained from Figure 3.15, which shows the steam flow rate from the lower plenum to the downcomer, as obtained from the NPP calculation.

$$t_D = 17.5 \text{ s} \quad (3.34)$$

The actual value $W_{gc,NPP,act}$ of the critical steam flow rate will be higher than given in Equation (3.33) and, as shown in Figure 3.14, the steam flow rate from the lower plenum to the downcomer decreases monotonically with time. The time, $t_{D,act}$ corresponding to $W_{gc,NPP,act}$ will occur earlier than t_D , i.e.,

$$W_{gc,NPP,act} > W_{gc,NPP} \quad (3.35)$$

Therefore,

$$t_{D,act} < t_D \quad (3.36)$$

The bias in the Bypass Period is obtained from Equation (3.7), which gives

$$\delta t_{ID} = t_{D,act} - t_D < 0.0 \text{ s} \quad (3.37)$$

The bias δt_{ID} is negative because of Equation (3.36) and can only reduce the refill time period t_{IB} , and the PCT. Therefore, a conservative estimate is

Table 3.3 - Comparison Between NPP and UPTF (Full-Scale Facility) Conditions

NO.	CONDITIONS	NPP	UPTF
1	STEAM FLOW LP TO DC	FROM FLASHING IN LP DECREASING WITH TIME	FIXED FLOW RATE
2	SYSTEM PRESSURE	DECREASING	INCREASING
3	BREAK FLOW RATE	DECREASING	INCREASING
4	ECC SUBCOOLING	HIGH (~90°K)	LOW (~50°K)
5	ECC FLOW RATE	HIGH (~2500 kg/s)	LOW (~1500 kg/s)
6	COLD LEGS	OPEN LOOPS	LOOPS CLOSED AT PUMP SIMULATOR
7	NUMBER OF ECC INJECTION	FOUR	THREE, NONE IN BROKEN LOOP

$$\delta t_{ID} = 0.0 \text{ s} \quad (3.38)$$

3.4.2.2 Bias in the Timing of the Delay Period

The duration t_{DA} of the Delay Period is obtained from Equations (3.29) and (3.34)

$$t_{DA} = 22.9 \text{ s} - 17.5 \text{ s} = 5.4 \text{ s} \quad (3.39)$$

The delay ratio ($\langle R_t \rangle_{NPP}$) is obtained from Table 3.2 by averaging the last three values of R_t in the last column.

$$\langle R_t \rangle_{NPP} = 2.67 \quad (3.40)$$

The bias for the Delay Period is estimated by substituting Equations (3.39) and (3.40) into Equation (3.13). The result is

$$\delta t_{DA} = -3.4 \text{ s} \quad (3.41)$$

3.4.2.3 Bias in the Timing of the Counter-Current Flow Period

The Counter-Current Flow Period spans from time t_A to time t_E . The time t_A is obtained from Equation (3.29). The time t_E is read from Figure 3.15 and is:

$$t_E = 23.4 \text{ s} \quad (3.42)$$

The duration of this period is

$$t_{AE} = t_E - t_A = 23.4 \text{ s} - 22.9 \text{ s} = 0.5 \text{ s} \quad (3.43)$$

The filling rate ratio, $\langle R_{mLP} \rangle_{NPP,AE}$, for the NPP is obtained from Table 3.2 by averaging the last three values of $R_{mLP} > LP$ in the eleventh column.

$$\langle R_{mLP} \rangle_{NPP,AE} = 0.52 \quad (3.44)$$

The bias is estimated by substituting Equations (3.43) and (3.44) into Equation (3.21), and the result is

$$\delta t_{AE} = -0.24 \text{ s} \quad (3.45)$$

3.4.2.4 Bias in the Timing of the No-Bypass Period

The No-Bypass Period spans from time t_E to the end of the Refill Phase at time t_B . The times t_E and t_B are obtained from Equations (3.29) and (3.42). The bias in this period is due to the discrepancy in predicting the lower plenum filling rate. There are no data available at low steam flow rate cases and, therefore, an estimate of the bias is made on the basis of UPTF data listed in Table 3.2. The eleventh column shows $R_{m,LP}$, the ratio of the predicted to measured lower plenum filling rates. The trend in this column shows that this ratio increases with the decrease in the steam flow rate. The values of the ratio ($R_{m,LP}$) were extrapolated down to zero steam flow rate and it is assumed that this value is applicable to the NPP. Therefore:

$$\langle R_{m,LP} \rangle_{NPP,EB} = 0.87 \quad (3.46)$$

As the extrapolated value of the $\langle R_{m,LP} \rangle$ is less than 1.0, the code underpredicts the filling rate and therefore, it is conservative. This ratio is substituted into Equation (3.25), and the following estimate of the bias is obtained:

$$\delta t_{EB} < 0.0 \text{ s} \quad (3.47)$$

Therefore, a conservative estimate of the bias for the No-Bypass Period is:

$$\delta t_{EB} = 0.0 \text{ s} \quad (3.48)$$

3.4.2.5 Total Bias in the Refill Phase

The bias in the duration of the Refill Phase (δt_{IB}) is obtained by substituting Equations (3.38), (3.41), (3.45), and (3.48) into Equation (3.27).

$$\delta t_{IB} = -3.64 \text{ s} \quad (3.49)$$

3.4.2.6 Bias in PCT

The Bias in the PCT is obtained from Equation (3.1). The clad heat up rate (dT_c/dt) is estimated from Figure 3.15, which shows the clad temperature history for the hot rod from the reference NPP calculation. The result is as follows:

$$dT_c/dt = (83.3^\circ K)/(33.5 s - 17.5 s) = 5.2^\circ K/s \quad (3.50)$$

The bias in PCT due to the deficiencies in the code in modelling the ECC bypass phenomena is estimated by substituting Equations (3.49) and (3.50) into Equation (3.1). The final result is

$$\delta PCT = -19^\circ K (-34^\circ F) \quad (3.51)$$

3.5 Conclusions

A procedure has been developed to estimate the bias in the PCT due to the deficiencies in the code modelling of the important processes, numerics and nodalization affecting the bypass flow phenomena in the Refill Phase of the LBLOCA. The estimated bias in PCT is $-19^\circ K$ which implies that the code overpredicts the PCT and is conservative with respect to the bypass phenomena.

The Refill Phase was divided into four phenomenologically different periods. The largest contribution to the bias is from the Delay Period ($-17.7^\circ K$) during which the ECC is accumulating in the cold legs and the downcomer region of the reactor. The Counter Current Flow Period was surprisingly small (0.5 s) and contributed only $-1.3^\circ K$ to the total bias in PCT. The most important parameter during the Delay Period is the critical steam flow rate. Since the available data for determining this critical steam flow rate is sparse, more data is needed, particularly at the high and low ends of the steam flow rate range. Furthermore, additional test data are needed to provide a meaningful statistical analysis.

4. LACK OF MODEL FOR DISSOLVED N₂ AND RESULTING PCT BIAS

N₂ is a non-condensable gas which is present in the accumulators in the form of a free gas above the ECC liquid and dissolved in the liquid. During an LBLOCA, as the coolant flows from the accumulators to the low pressure regions of the cold legs and the downcomer, the dissolved N₂ emerges from the solution. This dissolution of the N₂ will affect the hydraulics of the coolant through influences on system pressure, break flow and condensation processes during the Refill Phase and, thus, also influence the reflood PCT. The TRAC-PF1/MOD1, Version 14.3 code, which is being used here to simulate LBLOCA, does not have a model for dissolved N₂ and, therefore, cannot account for its effect on the PCT. The lack of a model for an important phenomenon is a systematic error or deficiency in the code and will bias the code prediction. The bias in the predicted PCT is estimated here through a separate calculation.

The next five sections describe the effect of the emerging N₂ on the thermal hydraulic behavior of the Refill Phase and a procedure for estimating the bias due to the lack of a dissolved N₂ model in the code.

4.1 Effect of N₂ on the Refill Phase

The accumulators have ECC liquid in equilibrium with N₂ in the gas space at a pressure of 40 bar. Therefore, there is dissolved N₂ in the liquid of the accumulators. During an LBLOCA, the system pressure decreases rapidly. When the primary system pressure drops below 40 bar, the ECC liquid begins to flow from the accumulators to the cold legs and eventually to the downcomer and the lower plenum. As the cold leg pressure is lower than the pressure in the accumulators, the solubility of the N₂ in the coolant is lower in the cold leg than in the accumulators. This drop in the solubility will cause some of the N₂ to emerge in the cold legs and in the downcomer. However, the amount of N₂ emerging in the cold legs will decrease as the N₂ solubility in the accumulator decreases during depressurization of the accumulators. The N₂ escaping from the ECC in the accumulators collects above the ECC level in the accumulators.

The presence of the emerging N₂ in the primary system will lower the system depressurization rate by reducing the condensation rate through a decrease in the interfacial heat transfer rate, and by increasing the gas volume. This reduction in the system depressurization rate extends the time the system remains at high pressure and, therefore causes a higher break flow rate, a lower rate of safety injection and lower accumulator flows than in the situation without N₂. The additional volume of N₂ will also cause coolant from the cold legs and upper downcomer to become displaced to the lower downcomer and finally to the lower plenum. There are two competing effects. The reduction of ECC flow and the displacement of the ECC liquid from the cold leg and the downcomer to the lower plenum, and the influence of the N₂ on the PCT will depend on the relative strengths of these two effects. The analysis for predicting the expected amount of N₂ and its effects on condensation and ECC flow rates in the NPP is described in Appendix E.

The remaining four subsections describe the procedure for using the information generated in Appendix E to estimate the bias in PCT.

4.2 Principle of Uncertainty Estimation

The principle here is the same as that described in Section 3.2. The bias in PCT due to the omission of modelling dissolved N_2 effects is estimated by first computing the bias in the predicted duration t_{IB} of the Refill Phase due to dissolved N_2 . Next, the bias in the time period is converted into a bias in PCT, by multiplying the time bias with the average time rate of temperature rise of the hot rod clad during the Refill Phase (Equation 3.1). The refill duration t_{IB} is computed from the time at which the ECC begins to the time at which the lower plenum is full as shown in the Figure 3.7. The clad heatup rate is obtained from the code-predicted clad temperature history:

The PCT bias arising from the omission in TRAC-PF1 of the modeling for N_2 effects is, therefore:

$$\delta PCT_{N_2} = \frac{dT_c}{dt} \delta t_{IB, N_2} \quad (4.1)$$

where $\delta t_{IB, N_2}$ and dT_c/dt are the bias in the Refill Phase duration and the clad heatup rate, respectively.

The approach taken here consists of the following four steps, using the nominal NPP calculation:

1. Estimate the amount of N_2 which would have emerged if the code had a model for dissolved N_2 .
2. Estimate the effect of the N_2 on the condensation process.
3. Set up a separate model for the reactor (vessel, steam generators, pumps and pipes), and the broken and intact loop accumulators to estimate the system pressure and the new ECC flows (accumulator flows and safety injection rates) during the Refill Phase in the presence of N_2 .
4. Compute the effect of new ECC flows on the timing of the Refill Phase.

The bias in the Refill Phase duration is computed via the timings estimated from a separate calculation and obtained from the nominal NPP calculation.

4.3 Estimation of N_2 Modeling Bias in Refill Phase

The procedure is that used in Section 3.3. The Refill Phase is divided into two periods, shown in Figure 3.7. The first period, t_{IA} , is the Bypass Period, and the second period, t_{AB} , is the Filling Period. The effects of N_2 on these periods are summed to yield the bias in the Refill Phase.

$$\delta t_{ID,N_2} = \delta t_{IA,N_2} + \delta t_{AB,N_2} \quad (4.2)$$

4.3.1 Bias in the Timing of the Bypass Period

This period consists of two distinct sub-periods, namely, the Complete Bypass Period and the Delay Period, as described in Section 3.1.

The bias in this period t_{IA} is computed from the estimates of the biases in the sub-periods t_{ID} and t_{DA} .

$$\delta t_{IA,N_2} = \delta t_{ID,N_2} + \delta t_{DA,N_2} \quad (4.3)$$

4.3.1.1 Bias in the Timing of the Period of Complete Bypass

The time (t_I) of the initiation of the accumulator flow is not affected by N_2 dissolved in the ECC. The critical steam flow rate, which is the maximum steam flow rate at which there is ECC delivery to the lower plenum if sufficient time is available, changes in the presence of the N_2 and this affects the time (t_{D,N_2}) at which the Period of Complete Bypass ends.

The time t_{D,N_2} is estimated from the steam flow rate curve obtained from the nominal NPP calculation. This curve is shown in Figure 3.15.

$$t_{D,N_2} = t(W_{gc,N_2}) \quad (4.4)$$

$$t_D = t(W_{gc}) \quad (4.5)$$

where W_{gc} and W_{gc,N_2} are critical steam flow rates without and with N_2 present. The duration of this period with and without the presence of N_2 and the bias are estimated as follows:

$$t_{ID,N_2} = t_{D,N_2} - t_I \quad (4.6)$$

$$t_{ID} = t_D - t_I \quad (4.7)$$

and

$$\delta t_{ID,N_2} = t_{ID,N_2} - t_{ID} \quad (4.8)$$

where $\delta t_{ID,N_2}$ is the bias in the Complete Bypass Period due to the dissolved N_2 effect.

4.3.1.2 Bias in the Timing of the Delay Period

During the Delay Period, t_{DA} , the steam flow rate is less than the critical steam flow rate and there is accumulation of the ECC in the downcomer and the cold legs. There are two opposing effects of N_2 on this period. The emerging N_2 will displace the liquid and will push liquid into the downcomer and also into the lower plenum. This effect will tend to reduce the time span of the Delay Period and therefore, the duration of the Refill Phase and the PCT. The second effect of the N_2 is to slow down the depressurization rate and therefore, reduce the ECC flow rate (accumulator flows and safety injection). A reduction in ECC flow rate will cause an increase in the durations of the Delay Period and Refill Phase, and in PCT. The bias in t_{DA} is the sum of the biases due to these two effects.

$$\delta t_{DA,N_2} = \delta t_{DA,1,N_2} + \delta t_{DA,2,N_2} \quad (4.9)$$

The first of the two biases of the right hand side of Equation (4.9), $\delta t_{DA,1,N_2}$ is due to the effect of N_2 on the accumulation of the ECC in the downcomer for the same ECC flow rates. This bias is estimated from a ratio $\langle R_{t,th} \rangle$ of the code prediction of this time period, with and without the presence of N_2 , for same ECC flow rate and NPP conditions. The ratio is called the delay ratio.

$$\langle R_{t,th} \rangle = \frac{t_{DA,1,N_2}}{t_{DA}} \quad (4.10)$$

The bias, $\delta t_{DA,1,N_2}$ is related to the delay ratio in Equation (4.10) as follows.

$$\delta t_{DA,1,N_2} = t_{DA,1,N_2} - t_{DA} \quad (4.11)$$

$$= t_{DA} * [(R_{v,th}) - 1] \quad (4.12)$$

The second bias $\delta t_{DA,2,N_2}$ of Equation (4.9) is estimated from the ratio R_{ECC} of the ECC flow rates in the NPP calculations with and without N_2 . It is assumed that the ratio of the rates of the ECC accumulation in the cold legs and the downcomer with and without N_2 is equal to the ratio of the rates of ECC flow rates with and without N_2 .

$$R_{ECC} = \frac{\dot{m}_{ECC}}{\dot{m}_{ECC,N_2}} \quad (4.13)$$

$$= \frac{\dot{m}_{(DC+CL)}}{\dot{m}_{(DC+CL),N_2}} \quad (4.14)$$

where \dot{m}_{ECC,N_2} and \dot{m}_{ECC} are the ECC injection rates with and without N_2 , and $\dot{m}_{(DC+CL),N_2}$ and $\dot{m}_{(DC+CL)}$ are the rate of ECC accumulation in the cold leg and the downcomer with and without N_2 .

The second bias is then computed by assuming that the amount of accumulation required in the downcomer and the cold legs, which will lead to the delivery of the ECC to the lower plenum, is the same with or without N_2 . Therefore,

$$\delta t_{DA,2,N_2} = t_{DA} * (R_{ECC} - 1) \quad (4.15)$$

The bias for the Delay Period duration is obtained by adding the biases from Equations 4.12 and 4.15.

4.3.2 Bias in the Timing for the Filling Period

This period begins with the initiation of the recovery of the lower plenum inventory at time t_A and ends at time t_B when the lower plenum is full as shown in Figure 3.7.

The major effect of the N_2 is to slow the depressurization rate and to decrease the rate of ECC flow. Any decrease in the ECC flow rate will extend the duration of the Filling Period. Therefore, the bias in the Filling Period due to the absence of a model for dissolved N_2 will be positive. This bias is estimated from the ratio of the predicted ECC flow rates with and without N_2 . The assumption here is that the ratio of the lower plenum filling rates, with and without N_2 , is equal to the ratio R_{ECC} of the ECC flow rates. The bias in this period is computed from

$$\delta t_{AB, N_2} = t_{AB, N_2} - t_{AB} \quad (4.16)$$

where

$$t_{AB} = \frac{m_{LP, B} - m_{LP, A}}{\dot{m}_{LP}} \quad (4.17)$$

$$t_{AB, N_2} = \frac{m_{LP, B} - m_{LP, A}}{\dot{m}_{LP, N_2}} \quad (4.18)$$

and where $m_{LP, A}$ and $m_{LP, B}$ are the lower plenum inventories at times t_A and t_B , and \dot{m}_{LP, N_2} and \dot{m}_{LP} are the average lower plenum Filling Rates during the Filling Period with and without the presence of N_2 , respectively. The lower plenum filling rates are estimated from the ECC flows as follows:

$$R_{ECC} = \frac{\dot{m}_{ECC}}{\dot{m}_{ECC, N_2}} \quad (4.13)$$

$$= \frac{\dot{m}_{LP}}{\dot{m}_{LP, N_2}} \quad (4.19)$$

The bias in the Filling Period is computed from the ECC flow rate ratio R_{ECC} and the duration of the Filling Period t_{AB} obtained from the NPP calculation. An expression for this bias is obtained from the manipulation of Equations (4.16) to (4.19) and is

$$\delta t_{AB, N_2} = t_{AB} * (R_{ECC} - 1) \quad (4.20)$$

4.3.3 Total Bias in the Timing of the Refill Phase

The total bias in the period of the Refill Phase is obtained by substituting the biases for the three periods as given by Equations (4.8), (4.9), and (4.21) into Equations (4.3) and (4.2). The bias in the PCT due to the lack of N_2 modelling in the code is obtained from Equation (4.1).

4.4 Application

The procedure developed in the previous section is applied to the TRAC-PF1/MOD1, Version 14.3 prediction of PCT for a LBLOCA in Westinghouse four loop plant.

The procedure requires nominal NPP calculation results for accumulator flow rate, lower plenum inventory, rate of steam flow from the lower plenum to the downcomer and the hot rod clad temperature history. These results are shown in Figures 3.13, 3.14, 3.15, and 3.16. Beside the nominal NPP calculation the procedure also needs values of critical steam velocity (W_{gc,N_2}) in the presence of N_2 , of the delay ratio $\langle R_{t,th} \rangle$, and the ECC flow ratio, R_{ECC} . The next section describes the analysis performed to obtain these parameters.

4.4.1 Supporting Analysis

A separate model for the NPP was developed. The model consisted of a single volume representation for the primary side of the reactor excluding the accumulators, two volumes representing the intact loop accumulators and one volume for the broken loop accumulator. The model used the results of the nominal NPP calculation. The details of this model and its results are described in Appendix E.

Figure 4.1 shows the total ECC expected into the NPP from the nominal NPP calculation and from the separate model. The average ECC flow rate prediction with N_2 effects accounted for is lower than the average ECC flow rate predicted in the NPP calculation without accounting for N_2 . Table 4.1 summarizes the integrated ECC flow during the Refill Phase as predicted by the separate calculation and in the reference NPP calculation. In this table, the first column is the time of the transient, the second and third columns show the integrated ECC mass flows from the NPP calculation and from the separate calculation. The ratio of average ECC flows, $\langle R_{ECC} \rangle$, is 1.14.

In addition to developing a separate model, accounting for the N_2 -effect on the NPP response, the UPTF Test 6 was also modelled with the TRAC code, but without N_2 injection. The actual tests had a separate N_2 injection of 1 kg/s, to simulate effects from dissolved N_2 . However, 1 kg/s is only an estimate of the emergence rate of N_2 in the PWR during the Refill Phase. The calculations for UPTF Test 6 with and without N_2 provide information about the effect of N_2 on the critical steam flow rate, the delay in the ECC delivery and the lower plenum filling rate. The results for UPTF Test 6 are summarized in Table 4.2. The first column indicates the run numbers, the second column shows the steam flow rates, and the next two columns indicate the lower plenum filling rates, as obtained from TRAC calculations, with and without the N_2 injection. The last two columns list the time spans of the Delay Period, as predicted from TRAC calculation, with and without N_2 injection.

The next section describes the actual calculation of the bias due to the dissolved N_2 . Results are used as obtained from the nominal NPP calculation and shown in Figures 3.13, 3.14, 3.15, and 3.16, and the results from a calculation with a separate model for the NPP and UPTF Test 6 calculations.

INTEGRATED ECC (INTACT LOOPS) (NPP)

33.5

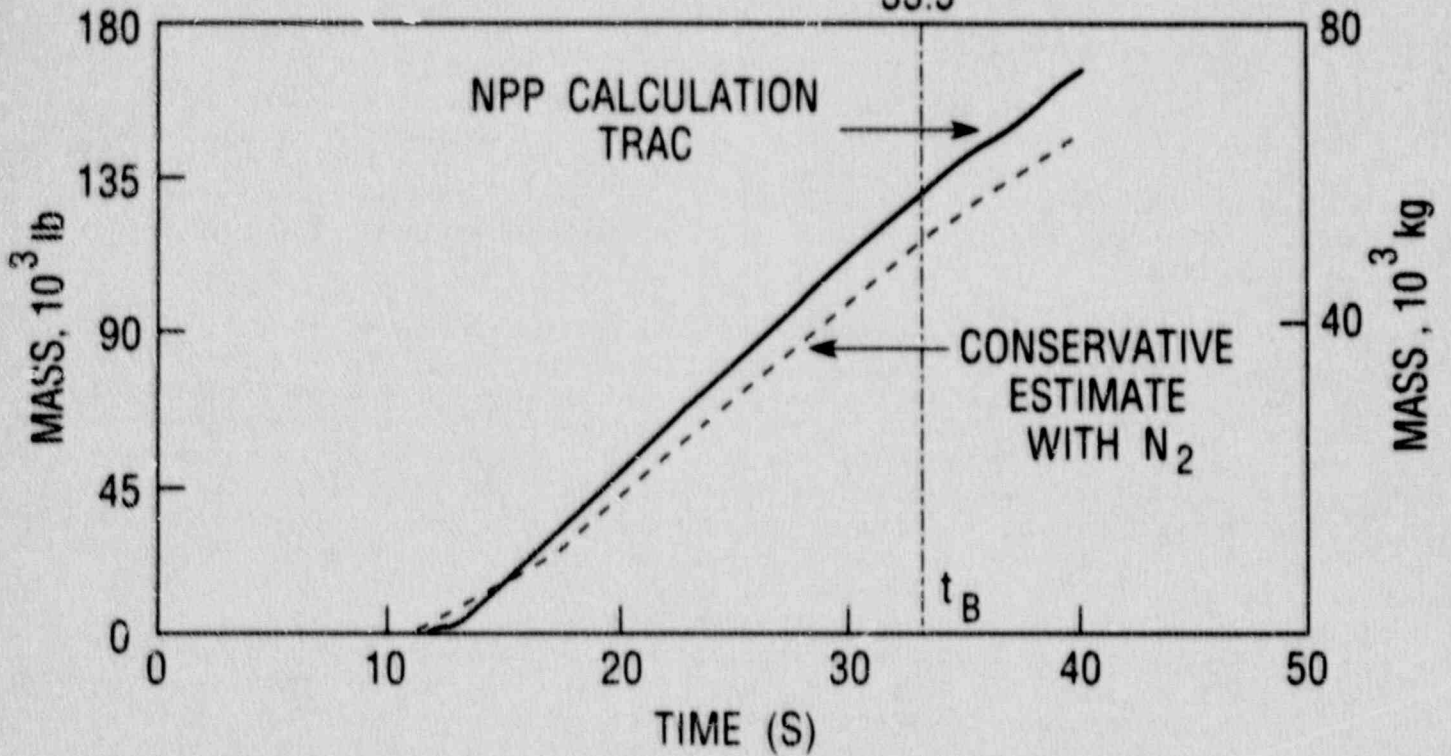


Figure 4.1 Prediction of Integrated ECC Injection

TABLE 4.1 - Integrated ECC Mass With and Without N₂

TIME sec	Δm_{ECC}	$\Delta m_{ECC, N_2}$
	NPP CALC kg	BOUNDING CALC kg
11.5	0.0	0.0
12.1	860	860
18.1	15,900	12,145
22.9	30,670	23,843
23.8	33,490	26,045
26.1	39,940	31,773
29.5	49,070	40,100
33.5	58,800	58,160

$$\Delta m_{ECC} = \int_{11.5}^t \dot{m}_{ECC} dt$$

$$\Delta m_{ECC, N_2} = \int_{11.5}^t \dot{m}_{ECC, N_2} dt$$

$$t_D = 20 \text{ s}$$

$$R_{ECC} = \frac{58,800 \text{ kg} - 21,746 \text{ kg}}{58,160 \text{ kg} - 16,776 \text{ kg}} = 1.14$$

Table 4.2 - TRAC Simulation of UPTF Test 6

RUN	w_g kg/s	PRED. FILLING RATE		PRED. DELAYS	
		\dot{m}_{LP,N_2} kg/s	\dot{m}_{LP} kg/s	$t_{DA,1,N_2}$ S	t_{DA} S
131	400	0	--	∞	∞
132	300	199	0	20	∞
133	250	360	604.6	16	20.6
136	100	512	359.6	7	21.8

\dot{m}_{LP} Lower Plenum Filling rate without N₂
 \dot{m}_{LP,N_2} Lower Plenum Filling rate with N₂
 t_{DA} Delay without N₂
 $t_{DA,1,N_2}$ Delay with N₂ and fixed ECC injection rate
 w_g Steam flow rate

4.4.2 Evaluation of the Biases

In this section, the actual calculations of the biases for the sub-periods defined in the Section 4.3 are performed, using the procedure described in Section 4.3 and the information described in Section 4.4.

4.4.2.1 Bias in Timing of the Complete Bypass Period

This period begins at the time t_I of initiation of the accumulator flows in the intact loops and ends at time t_D , when the steam flow rate decreases to the critical flow rate. The period is obtained from Equation 3.28.

The critical steam flow rate is obtained from UPTF Test 6 calculations. Since the facility is full-scale, the results can be used directly for the NPP. Table 4.2 shows the TRAC prediction for the lower plenum filling rates, with and without accounting for the N_2 injection. There are no deliveries of ECC fluid to the lower plenum at a steam flow rate of 400 kg/s, for the case with N_2 injection, and at a steam flow rate of 300 kg/s for the case with no N_2 injection. The following conclusion is made about the critical steam flow rate,

if N_2 is injected:

$$300 \text{ kg/s} < W_{sc, TRAC, N_2, UPTF} < 400 \text{ kg/s} \quad , \quad (4.21)$$

if no N_2 is injected:

$$200 \text{ kg/s} < W_{sc, TRAC, UPTF} < 300 \text{ kg/s} \quad . \quad (4.22)$$

Therefore, the critical steam flow rate with N_2 will be higher than the critical steam flow rate without N_2 .

$$W_{sc, TRAC, N_2, UPTF} > W_{sc, TRAC, UPTF} \quad . \quad (4.23)$$

Since UPTF is a full-scale facility the conclusion in Equation (4.23) is applied to the NPP.

$$W_{sc, TRAC, N_2, NPP} > W_{sc, TRAC, NPP} \quad . \quad (4.24)$$

Since the steam flow rate from the lower plenum to the downcomer is decreasing during the Refill Phase, the higher steam flow rate will occur earlier as shown in Figure 3.15, and it is concluded that,

$$t_D \approx t_{D,N_2} \quad (4.25)$$

Therefore,

$$t_{ID} \approx t_{ID,N_2} \quad (4.26)$$

The bias $\delta t_{ID,N_2}$ is estimated by substituting Equation (4.26) into Equation (4.4).

$$\delta t_{ID,N_2} \approx 0.0 \quad (4.27)$$

Therefore, a conservative estimate of $\delta t_{ID,N_2}$ is:

$$\delta t_{ID,N_2} = 0.0 \quad (4.28)$$

Furthermore, a conservative limit of the critical steam flow rate for a facility is the lower limit, since the steam flow rate would have to decrease below that limit before any liquid can reach the lower plenum. Therefore, the lower limit is selected from Equation (4.22) for the critical steam flow, which is

$$W_{bc,TRAC,NPP} = 200 \text{ kg/s} \quad (4.29)$$

The time t_2 corresponding to this steam flow rate is obtained from Figure 3.15, and is

$$t_D = 20.0 \text{ s} \quad (4.30)$$

It should be noted that the critical steam flow rate and corresponding time are different from the ones selected in Section 3.4.2.1 (Equations (3.33) and (3.34)). The difference in two critical steam flow rates is due to their application. In Section 3.4.2.1 the bias due to all the model deficiencies in the code, except for the lack of a dissolved- N_2 model, was being estimated. The critical steam flow was obtained from the UPTF data which had N_2 injection to account for dissolved N_2 effect. A lowest possible value of the steam flow rate was selected for the critical flow from the UPTF data. In the current application, the purpose is to estimate the bias due to the lack of a dissolved N_2 model in the code. So, the critical steam flow rate for the NPP with no dissolved N_2 is estimated from a calculation for the UPTF facility with no N_2 injection. A comparison of the results of the two calculations shows the effect of the dissolved N_2 , since the code and the test conditions were the same. The

effect of the N_2 is to increase the critical steam flow rate and therefore, the critical steam flow rate in Equation (3.33) is higher than in Equation (4.29).

4.4.2.2 Bias in the Timing of the Delay Period

The Delay Period begins at time t_D (Equation (3.30)) and ends at time t_A as obtained from Equation (3.29). Therefore, the duration of this period is:

$$t_{DA} = t_A - t_D = 22.9s - 20.0s = 2.9s \quad (4.31)$$

During this period, the N_2 affects the duration of the Delay Period in two ways, each of which contributes to the bias as described in Section 4.3.1.2, and their contributions are estimated using the method described in that section. The computation of the first bias, $\delta t_{DA,1,N_2}$, requires a ratio of delays from the simulation of separate effects tests with and without N_2 . Table 4.2 shows the calculations for UPTF Test 6 with and without the consideration of the N_2 injection. The results in this table indicate that delays are smaller when N_2 injection is considered. This conclusion is applied to Equation (4.10) and the result is,

$$\langle R_{t,th} \rangle < 1.0 \quad (4.32)$$

The first bias for the delay period is computed by substituting Equation (4.32) into Equation (4.12). It follows that

$$\delta t_{DA,1,N_2} < 0.0 \quad (4.33)$$

A conservative estimate of this bias is

$$\delta t_{DA,1,N_2} = 0.0 \quad (4.34)$$

The second bias $\delta t_{DA,2,N_2}$ for this period is due to the decrease in the ECC flow rate. The integrated ECC flow is shown in Table 4.1 from the nominal NPP calculation and from the separate model calculation. The results in this table indicate that there is less ECC flow in the presence of N_2 and a ratio of the average ECC flow rates for the Refill Phase during the time period between t_D and t_B is estimated from this table as defined in Section 4.3.1.2.

$$R_{ECC} = 1.14 \quad . \quad (4.35)$$

The second bias for this period is computed by substituting Equations (4.31) and (4.35) into Equation (4.15).

$$\delta t_{D\lambda, 2, N_2} = 0.41 \text{ s} \quad . \quad (4.36)$$

The total bias for the Delay Period is the sum of the two biases obtained from Equations (4.34) and (4.36).

$$\delta t_{DA, N_2} = 0.41 \text{ s} \quad . \quad (4.37)$$

4.4.2.3 Bias in the Timing of the Filling Period

This period begins at time t_A (Equation (3.29)) and ends at time t_B (Equation (3.30)) when the lower plenum is full. The duration of this period is computed from these times.

$$t_{AB} = (33.5\text{s} - 22.9\text{s}) = 10.6 \text{ s} \quad . \quad (4.38)$$

The bias in this period is estimated by substituting Equations (4.35) and (4.38) into Equation (4.20) and the result is,

$$\delta t_{AB, N_2} = 10.6\text{s}(1.14 - 1) = 1.48 \text{ s} \quad . \quad (4.39)$$

4.4.2.4 Total Bias in the Refill Phase

The total bias $\delta t_{IB, N_2}$ in the Refill Phase is obtained by adding the biases from the Equations (4.28), (4.37) and (4.39).

$$\delta t_{IB, N_2} = (0 + 0.41 + 1.48)s = 1.88 s \quad . \quad (4.40)$$

4.4.2.5 Bias in Predicted PCT due to the Omission of Dissolved N₂ Model

The bias in the PCT due to the lack of a dissolved N₂ model in the code is estimated from Equation (4.1) using the information from Equations (3.50) and (4.40).

$$\delta PCT_{N_2} = 9.9^\circ K \quad (17.8^\circ F) \quad . \quad (4.41)$$

4.5 Conclusions

The bias in the predicted PCT due to the omission of a model for dissolved N₂ in the code is 9.9°K. As this bias is positive, it implies that the inclusion of a model for dissolved N₂ in the code will result in a higher predicted PCT.

The bias in this section was estimated from three independent calculations; a bounding calculation of the NPP during the Refill Phase, the nominal NPP calculation with the TRAC code, and the simulation of UPTF Test 6 with the TRAC code. Since for the bounding calculation it was assumed that no N₂ is dissolved in the cold legs and that N₂ completely terminates the condensation process, and since all the beneficial effects from the dissolved N₂ were neglected, the bias in PCT predictions presented in this section, is conservative.

It is recommended that a model of dissolved N₂ based on the variation in the solubility of the noncondensable gas (i.e., Henry's model) be included in the code. The code has a model of noncondensable gas, but it does not allow for any dissolution of gas. In the absence of such a model, the NPP calculation could be repeated with N₂ injection in the intact loops, such as was done in the UPTF Test 6. The results of the NPP calculations with and without N₂ can estimate the PCT bias. The uncertainty in this approach is in the N₂ injection rate and in the location of the N₂ injection. However, a conservative estimate of the rate of N₂ dissolution, based on equilibrium assumptions, can be made and used to simulate N₂ injection close to the accumulator junction.

5. SUMMARY OF CONCLUSIONS

The peak clad temperature (PCT) predicted by TRAC-PF1/MOD1, Version 14.3 for large break loss of coolant accidents (LBLOCA) has uncertainties arising from (1) ECCS thermohydraulics modelling deficiencies, and (2) lack of a model for dissolved N₂. These uncertainties in PCT are quantified here numerically in terms of biases.

The evaluation of the bias due to modelling deficiencies requires comparisons to data, either from full-scale tests or properly scaled separate effects tests (SETs). A review of available SETs indicated that small-size facilities did not model the flow regimes expected in a nuclear power plant during the Refill Phase of an LBLOCA. Therefore, it was concluded that only full-scale test data, from the Upper Plenum Test Facility (UPTF), could be used for the estimation of this bias. Any bias based on the small scale facilities would be conservative, since the ratio of measured to predicted lower plenum filling rate decreases with size.

The total bias in PCT predicted by the TRAC computer code due to modelling deficiencies is -19°K (-34°F). The negative bias implies that these systematic errors in the code over-predict the PCT. Detailed analysis of the contributions to the total bias indicated that the Counter Current Flow Period (which lasts for 0.5 seconds) leads to only -1.3°K of the bias. The largest contribution (-17.7°K) to the bias results from the prediction of the Delay Period. It is recommended that higher priority be placed on the generation of data at steam flow rate corresponding to the complete bypass region.

The second source of uncertainty (i.e., the lack of a model for dissolved N₂) leads to a bias in PCT of 9.9°K (17.8°F). The positive bias indicates that this systematic error leads to an under-prediction of PCT. Thus, the lack of a model for dissolved N₂ makes the code prediction less conservative. Although the TRAC code has a model for the mass balance of non-condensable gasses, it does not account for mass transfer between the liquid and the gas. It is recommended that a model of mass transfer, based on Henry's model of the solubility of the gasses in the liquid, be included in the code.

REFERENCES

- Beckner, W. D. and Reyes, J. N., Jr., "PWR Lower Plenum Refill Research Results," USNRC Research Information Letter No. 128, December 8, 1981.
- Crowley, C. J., Block, J. A., and Cary, C. N., "Downcomer Effects in a 1/15-Scale PWR Geometry - Experimental Data Report," NUREG-0281, May 1977.
- Crowley, C. J., Block, J. A., and Roth, P. H., "First Quarter FY 1979 Progress Report on Refill Effects Program," NUREG/CR-0719, April 1979.
- Crowley, C. J. and Sam, R. G., "Experimental Facility and Typical Results for Flushing Transients at 1/5-Scale," CREARE/TM-707, July 1980.
- Crowley, C. J., Rothe, P. H., and Sam, R. G., "1/5-Scale Countercurrent Flow Data Presentation and Discussion," NUREG/CR-2106, November 1981.
- Crowley, C. J., "Data Traces for CREARE 1/5 Tests 2.5062, 2.5015, and 2.5017," Letter to J. Jo, BNL, December 1987.
- Crowley, C. J., "Data Traces for CREARE 1/5 Tests 2.5062, 2.5065, 2.5124, 2.5127, and 2.5129," Letter to S. Rohatgi, BNL, July 1988.
- Cudnik, R. A., Flanigan, L. J., Carbiener, W. A., Wooton, R. O., and Denning, R. S., "Penetration Behavior in a 1/15-Scale Model of a Four-Loop Pressurized Water Reactor," BMI-NUREG-1973, June 1977.
- Cudnik, R. A., Flanigan, L. J., Dykhuizen, R. C., Carbiener, W. A., and Liu, J. S., "Baseline Plenum Filling Behavior in a 2/15-Scale Model of a Four Loop Pressurized Water Reactor," NUREG/CR-0069, April 1978.
- Damarell, P. (1988a), "UPTF Test 6 Analysis Results for Run 133," Letter to U.S. Rohatgi, BNL, July 1, 1988.
- Damarell, P. (1988b), "Modification to BNL Evaluation of Effect of UPTF Downcomer Data Uncertainty on Calculation of PWR LOCA Peak Clad Temperature," Letter to N. Zuber, July 14, 1988.
- Damarell, P. and Wolfe, K. A. (1988c), "Mass Balance, UPTF Test 6," 2D/3D Coordinating Meeting, Tokai-Mura, Japan, May 9-13, 1988.
- Delhaye, J. M., Giot, M., and Riethmuller, M. L., "Thermohydraulics of Two-Phase Systems for Industrial Design and Nuclear Engineering," Hemisphere Publishing Corporation, 1981.
- Flanigan, L. J., Cudnik, R. A., and Denning, R. S., "Experimental Studies of ECC Delivery in a 1/15-scale Transparent Vessel Model," BMI-1941, NRC-2, BCL, November 1975.
- Katsma, K., "NPP Calculation Results," INEL, June 23, 1988.
- Lellouche, G. S., et al., "Uncertainty Evaluation of LBLOCA Analysis Based Upon TRAC-PF1/M506," Transaction of sixteenth Water Reactor Safety Information Meeting, NUREG/CP-0096, October, 1988.

Liebert, J., "UPTF-Experiment, Downcomer CCF Test No. 6," 2D/3D Coordination Meeting, Tokai-Mura, Japan, May 9 - 13 1988.

Liles, D., et al., "TRAC-PF1/MOD1 Correlations and Models," NUREG/CR-5069, December 1988.

Neymotin, L. and Rohatgi, U. S., "Scale Effects in ECC Bypass Phenomena," Section 25.2, Safety Research Programs, NUREG/CR-2332, BNL-NUREG-51454, Vol. 8, Nos. 1 and 2, December 1988.

Pushkina, O. L. and Sorokin, Y. L., "Breakdown of Liquid Film Motion in Vertical Tubes," Heat Transfer, Soviet Research, Vol. 1, No. 5, September 1969.

Rohatgi, U. S., Yuelys-Miksis, C., and Saha, P., "Determination of Appendix K Conservatism for Large Break LOCA in a Westinghouse PWR Using TRAC-PD2/MOD1 Code," NUREG/CR-4549, April, 1986.

Richter, H. J., "The Effect of Scale on Two-Phase Countercurrent Flow Flooding in Vertical Tubes," Final Report on Contract No. AT(49-24)-0329, 03755, Thayer School of Engineering, Dartmouth College, Hanover, New Hampshire, 1977.

Rothe, P. H. and Crowley, C. J., "Scaling of Pressure and Subcooling for Countercurrent Flow," NUREG/CR-0464, October 1978.

Sam, R. G. and Crowley, C. J., "Experimental Data Report for Flushing Transients," NUREG/CR-2060 (CREARE TN-330), 1981.

Segev, A., Flanigan, L. J., and Collier, R. P., "Steam-Water Mixing and System Hydrodynamics Program -- Task 4," NUREG/CR-1657, August 1980.

Shaw, R. A., Rouhani, S. Z., Larson, T. K., Dimenna, R. A., "Development of a Phenomena Identification and Ranking Table (PIRT) for Thermal-Hydraulic Phenomena During a PWR Large-Break LOCA", NUREG/CR-5047, EGG-2527, Nov. 1988.

Siemens/KWU, "2D/3D Program, Upper Plenum Test Facility, Test No. 5, Downcomer Separate Effect Test," Quick Look Report, U9316/87/17, Siemens AG, UB KWU, Energy Technology, Mechanical and Process Engineering Laboratories, October, 1987.

Technical Program Group, (TPG), "Quantifying Reactor Safety Margins," NUREG/CR-5249, EGG-2552, Dec. 1989.

USNRC, "Compendium of ECCS Research for Realistic LOCA Analysis," NUREG-1230, August 1988.

Wilson, C. E., et al., "Characterization of Important Contributors To Uncertainty," Transactions of the Sixteenth Water Reactor Safety Information Meeting, NUREG/CP-0096, October, 1988.

Wolfe, K. A. (1988a), "UPTF Test 6 Analysis Results for Runs 131 and 132," Letter to U. S. Rohatgi, BNL June 28, 1988.

Wolfe, K. A. (1988b), "UPTF Test 6 Analysis Results for Run 136," Letter to U. S. Rohatgi, BNL, July 7, 1988.

Wulff, W., "Uncertainties in Modelling and Scaling in Prediction of Fuel Stored Energy and Thermal Response," Proceeding of USNRC 15th Water Reactor Safety Information Meeting, NUREG/CP-0091, Vol 4, October, 1987, p. 23.

Wulff, W., et al., "Assessment and Ranging of Parameters for the Uncertainty Analysis of LBLOCA Codes," Transaction of the Sixteenth Water Reactor Safety Information Meeting, NUREG/CP-0096, October, 1988.

Zuber, N., et al., "Quantifying Reactor Safety Margins Part 5, Evaluation of Scale-up Capabilities of Best Estimate Codes," Nuclear Engineering and Design, Vol. 119, 1990.

APPENDIX A. UPPER PLENUM TEST FACILITY (UPTF) EXPERIMENTS

UPTF [Liebert, 1988] simulates a German four-loop PWR similar to a Westinghouse PWR (Fig. A.1). The facility has a full size vessel, hot and cold legs, ECC injection into the cold legs and the downcomer. The facility also has injection of 1 kg/sec of N₂ in the cold legs to simulate the dissolution of N₂ in the PWR. The main recirculation pumps are simulated by adjustable flow resistances, and the steam generators are represented by four steam/water separators. The core region is simulated by 193 nozzles injecting steam to the lower plenum. The facility's upper plenum internals replicate the actual vessel geometry. The downcomer separate effects tests--ECC bypass in the downcomer--were one of the series of the experiments conducted at the facility.

The clear advantage of using the full-scale facility (UPTF) data is the elimination of the need to extrapolate the results. Also, the question of the flow regimes and their effect on the major parameter of concern, the lower plenum delivery rate, would not arise.

Unfortunately, only 5 runs for UPTF test 6 are available for the investigation which is not a sufficient data base for the statistical analysis.

It is important to note that some of the clearly three-dimensional patterns of the flow ("alternate channeling", for example) developing in the downcomer are considerably different from the classical counter-current flow patterns. The channeling can be observed in the pictures showing the measured liquid temperature in the downcomer region (Figs. A.2 and A.3) [Liebert, 1988].

The runs were performed in two stages. In the first stage the steam was injected in the core and a steady state was achieved. The first stage lasted for 43 seconds. In the second stage, the ECC was injected. The ECC did not immediately reach the lower plenum and there was a delay. The tests were run for 30 seconds after the ECC injection. The lower plenum inventory was estimated from pressure drop measurements.

The next section describes the procedure of evaluating lower plenum filling rates from the UPTF test 6 data.

Lower Plenum Filling Rate in UPTF Tests

The lower plenum and downcomer inventories in five-runs (131, 132, 133, 135 and 136) of test-6 were available [Wolfe, 1988a, 1988b; Damarell, 1988a, 1988c]. The data for Runs 131, 132, 133 and 136 are summarized in Tables A.1 to A.4. In these tables, the first column indicates the time and, the second and third columns show the lower plenum and the downcomer inventories. The lower plenum inventory data for Run 135 were available in the form of lower plenum inventory plot [Damarell, 1988c] which indicated that there was lower plenum filling at 440 kg/S of steam flow. Actual lower plenum filling rate was not needed for current application as TRAC predicted (Appendix D) no ECC delivery for this steam flow rate.

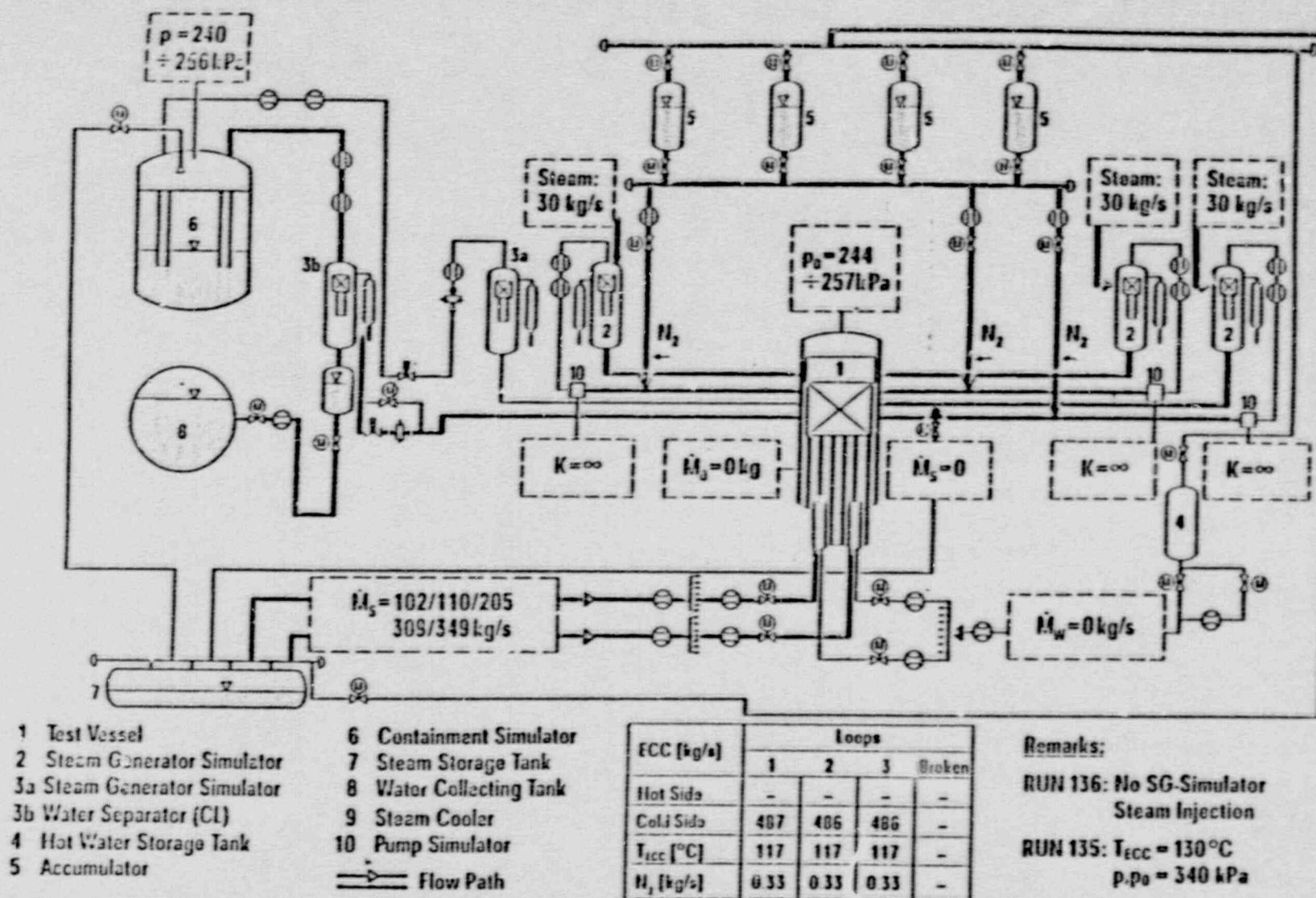
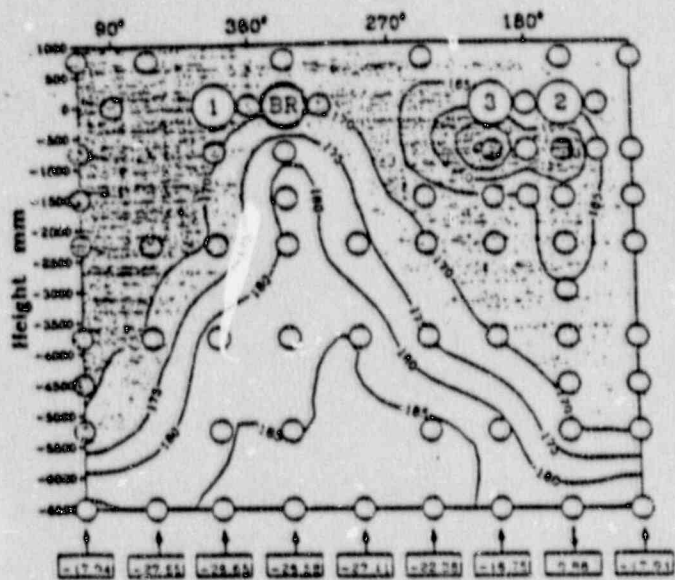


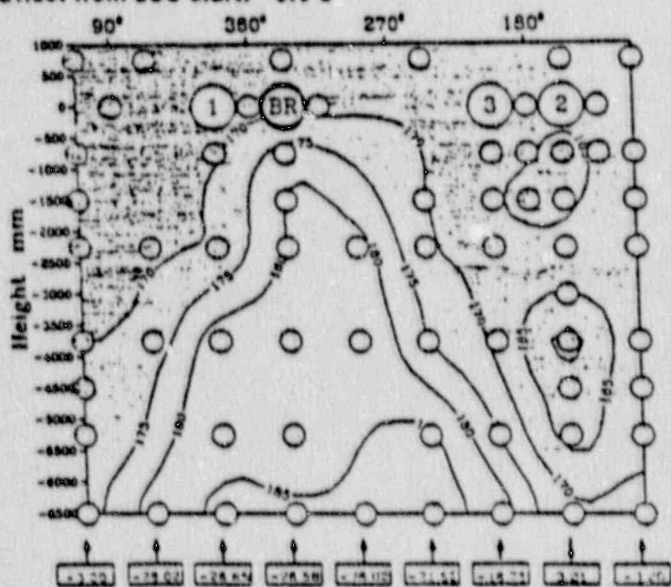
Figure A.1 System Configuration of Test No. 6 (Siemens, 1987)



- ECC delivery from loops 2 and 3
- First water reaches lower plenum
- High steam upflow towards broken cold leg

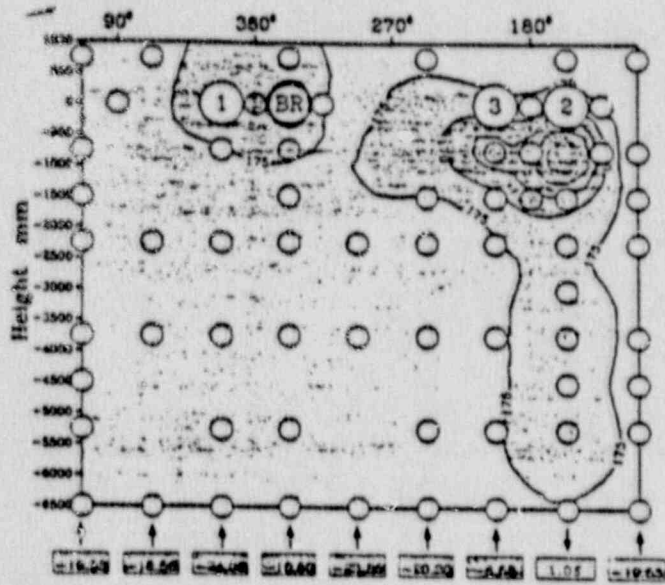
Offset from DAS start: 54.8 s

Offset from ECC start: 9.8 s



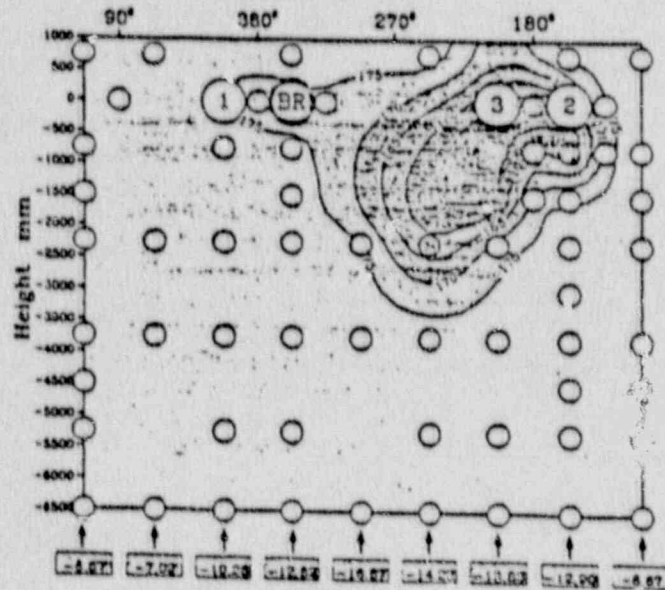
- Water penetrates into lower plenum
- Partial steam condensation by subcooled water

Figure A.2 Contour Plots of Fluid Temperature Distribution in Downcomer (Siemens, 1987)



- ECC bypass, delivery from loops 1, 2 and 3
- Water penetrates into lower plenum
- Massive water breakthrough

Offset from DAS start: 65 s
 Offset from ECC start: 20 s



- ECC bypass, delivery from loops 1, 2 and 3
- No water reaches lower plenum

Figure A.3 Contour Plots of Fluid Temperature Distribution in Downcomer (Siemens, 1987)

Table A.1 - UPTF Test 6, Run 131* (Steam Flow 400 kg/s)

Time s	Lower Plenum Inventory kg	Downcomer Inventory kg
49	0	0
55	(1400)	0
60	2500	(200)
63	(4700)	300
69	9000	(2600)
71	(9700)	3300
72	(10100)	0
80	13000	700

* [Wolfe, 1988a]
() Interpolated Values

Table A.2 - UPTF Test 6, Run 132* (Steam Flow 300 kg/s)

Time s	Lower Plenum Inventory kg	Downcomer Inventory kg
52	0	-----
56	(2800)	0
58	4200	(0)
59	(5100)	0
66	(11700)	0
67	12600	(200)
78	13700	2000

* [Wolfe, 1988a]
() Interpolated Values

Table A.3 - UPTF Test 6, Run 133* (Steam Flow 200 kg/s)

Time s	Lower Plenum Inventory kg	Downcomer Inventory kg
50	0	0
52	1820	0
63	10870	0
70	13980	470
76	14330	3360
80	14670	4090

* [Damarelli, 1988a]

Table A.4 - UPTF Test 6, Run 136* (Steam Flow 100 kg/s)

Time s	Lower Plenum Inventory kg	Downcomer Inventory kg
45	0	0
50	1800	0
60	9820	0
70	16110	1410
80	18190	5010

* [Wolfe, 1998b]

The lower plenum filling rates for four runs were obtained from the inventory data by plotting the data and selecting a window. The windows for Runs 131, 132, 133 and 136 were 49 sec to 80 sec, 52 sec to 67 sec, 50 sec to 70 sec, and 45 sec to 70 sec respectively. As an illustration, the lower plenum inventory for Run 136 is shown in Figure A.4 and steps to calculate filling rate are shown here.

$$\dot{m}_{LP} = \frac{m_2 - m_1}{t_2 - t_1} \quad (A.1)$$

$$\dot{m}_{LP} = \frac{(16110 - 0) \text{ kg}}{(70 - 45) \text{ s}} = 644 \text{ kg/s} \quad (A.2)$$

The lower plenum filling rates and the delays in the initiation of lower plenum filling are summarized in Table A.5. In this table, the first column lists the Run number, the second column lists the steam flow rates, the third column shows the lower plenum filling rates, the fourth column lists the time of ECC injection and the last two columns list the time at which the lower plenum begins to fill up and the delay in the initiation of lower plenum filling.

Table A.5 - Summary of UPTF Results (Test 3)

EXPERIMENT					
Run	W_g kg/s	\dot{m}_{LP} kg/s	t_I s	t_A s	$t_{IA, UPTF}$ s
131	400	419	43	49(54)	6(11)
132	300	840	43	52	9
133	200	699	43	50	7
135	440	> 0	43	-----	-----
136	100	644	43	45	2

UPTF Test 6 (Run 136)
Lower Plenum Liquid Mass Inventory

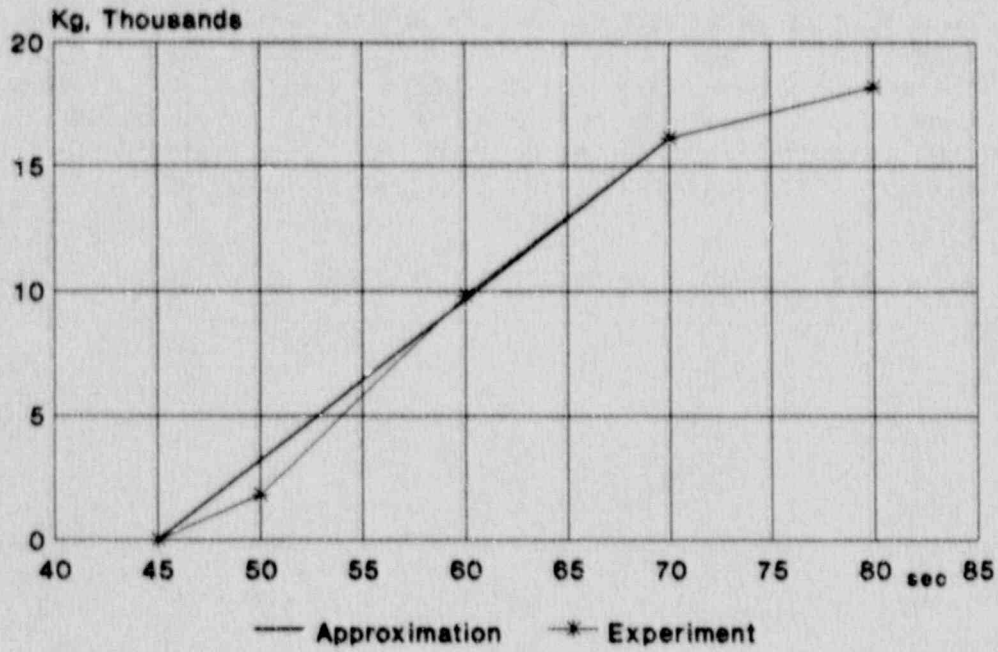


Figure A.4 Lower Plenum Liquid Mass Inventory, UPTF Test 6 (Run 136)

APPENDIX B: NODALIZATION FOR SEPARATE EFFECT TESTS, UPTF

All calculations were performed using same nodalization for the VESSEL component. Figure B.1 shows the schematic of the nodalization for the VESSEL component. The geometrical data for UPTF are provided in Table 3.1. The downcomer was modelled as a two-dimensional region using ten cells in the vertical direction and four cells in the azimuthal direction. The cold and hot leg connections were made at level 11 of the VESSEL. The lower plenum was modelled with two axial levels, and the "core" and upper plenum regions were combined into a cylindrical region represented by eleven axial, two radial, and four azimuthal cells. Steam to the downcomer was supplied through the core region.

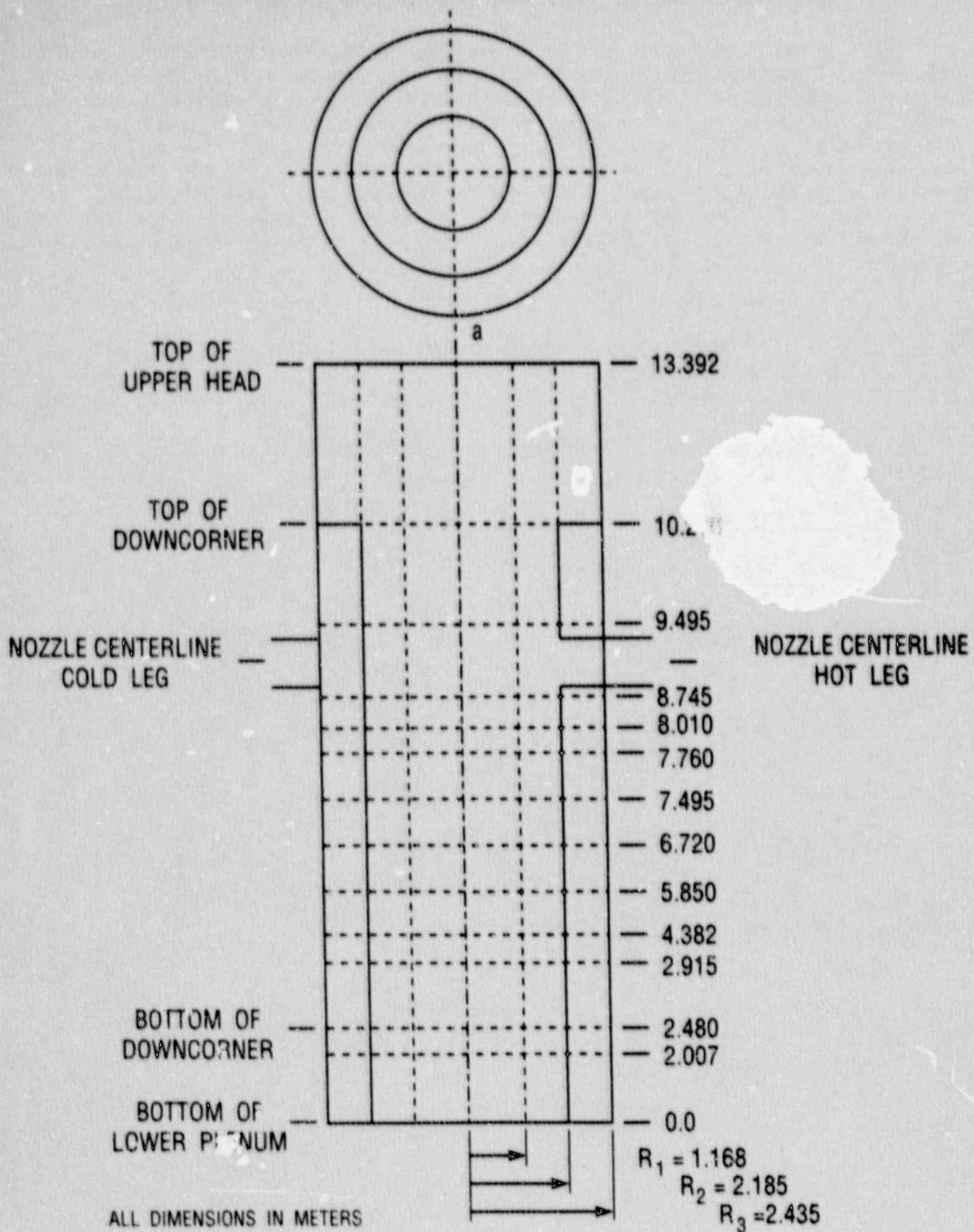


Figure B.1 Schematic of the VESSEL Nodalization

APPENDIX C: TRAC-PF1 INPUT DECK FOR UPTF

This Appendix contains the listing of the input deck used for the UPTF, Test 6 calculations.

UPTD TRAC-PF1 Input Deck

```

FREE
1 0 1 0
BASE CASE: 104 KG/S (U136)
BINOPTS ICFLOW=2,NFRCI=2,NFRC3=1,IADDED=10,NCRG=1,NLT=14,NOAIR=0
SEND 0 0.0 0

```

```

*
*
* 1. MAIN CONTROL DATA
*

```

```

*   STDYST   TRANSI   NCOMP   NJUN   IPAK
*   0         1       78      86     1
*   EPS0     EPSI     EPSS     EPSP
*   001      0001    0001    001
*   OITMAX   IITMAX   SITMAX   SOLUT
*   10       50     10      0
*   NTSV     NTCB     NTCF     NTRP   NTCP
*   22      39     252    31     0

```

```

* COMPONENT LIST CARDS

```

```

* ..... VESSEL AND VESSEL DRAINS
* ..... 101 102 103 107
* ..... CORE SIMULATOR INJECTION TEES
*
* 501 502 503 504 505 S
* 506 507 508 S
* ..... CORE SIMULATOR BASE FILLS
* 601 602 603 604 605 S
* 606 607 608 S
* ..... CORE SIMULATOR FEEDBACK FILLS
* 701 702 703 704 705 S
* 706 707 708 S
* ..... LOOP1
* 10 11 12 13 14 S
* 15 16 18 19 17 S
* ..... LOOP2
* 20 21 22 23 24 S
* 25 26 27 28 29 S
* 229 28
* ..... LOOP3
* 30 31 32 33 34 S
* 35 36 38 39 333 S
* 339 S
* ..... LOOP4
* 40 41 42 45 46 S
* 449 91 S
* ..... NITROGEN INJECTION SYSTEM
* 160 161 260 261 360 S
* 361 E

```

```

* CONTROL-PARAMETER DATA *

```

```

* SIGNAL VARIABLES
*   IDSV   ISVN   ILCN   ICN1   ICN2
*   100    0      0      0      0
*   107    27     101    1      0
*   601    21     1      1010   0
*   480    21     91     1      0
*   99     21     24     21     0

```

```

* SIGNAL VARIABLES FOR THE CORE FEEDBACK SYSTEM

```

```

*   701    32     1     1007   0
*   501    29     501     4     0
*   702    32     1     2007   0
*   502    29     502     4     0
*   703    32     1     3007   0
*   503    29     503     4     0
*   704    32     1     4007   0
*   504    29     504     4     0

```

```

* SIGNAL VARIABLES IN LOOP 1

```

```

*   105    32     10     6     0
*   119    27     12     9     0

```

```

* SIGNAL VARIABLES IN LOOP 2

```

```

*   205    32     20     6     0
*   229    27     22     9     0

```

```

* SIGNAL VARIABLES IN LOOP 3

```

```

*   305    32     30     6     0
*   339    27     32     9     0
*   449    27     41    16     0
*   42     27     18     1     0
*   479    27     47     1     0

```

```

* CONTROL BLOCKS

```

```

*   ICB   ICBN   ICB1   ICB2   ICB3
* CONTROL BLOCKS FOR THE CORE FEEDBACK SYSTEM

```

```

* TIME DELAY CELL 1
  -8001 100 -7001 10 0
  * CBGAIN CBXMIN CBXMAX CBCON1 CBCON2
  1.0000E+00 0.0000E+00 1.0000E+02 1.0000E+00 0.0000E+00
* Z = S X Z CELL 1
  IDCB ICBN ICB1 ICB2 ICB3
  -7001 39 -6001 -5001 0
  * CBGAIN CBXMIN CBXMAX CBCON1 CBCON2
  1.0000E+00 0.0000E+00 1.0000E+02 0.0000E+00 0.0000E+00
* Z TABLE CELL 1
  IDCB ICBN ICB1 ICB2 ICB3
  -5001 101 701 4 0
  * CBGAIN CBXMIN CBXMAX CBCON1 CBCON2
  1.0000E+00 0.0000E+00 1.0000E+02 0.0000E+00 0.0000E+00
* FUNCTION FOR MFRL (KG/S) VS. MFRV (KG/S)
  CBFT * -9.6500E+02 1.0084E+02 -7.2375E+02 9.1675E+01 -4.8250E+02
  CBFTL * 6.7550E+01 -2.4125E+02 0.0000E+00E
* S TABLE CELL 1
  IDCB ICBN ICB1 ICB2 ICB3
  -6001 101 -4001 4 0
  * CBGAIN CBXMIN CBXMAX CBCON1 CBCON2
  1.0000E+00 0.0000E+00 1.0000E+00 0.0000E+00 0.0000E+00
  CBFTB * R02 0.0000E+00 1.2700E+08 6.1000E-01 2.5000E+08 8.2000E-01
  CBFTB * 6.3400E+08 1.0000E+00E
* A - E CELL 1
  IDCB ICBN ICB1 ICB2 ICB3
  -4901 54 -3001 -1001 0
  * CBGAIN CBXMIN CBXMAX CBCON1 CBCON2
  1.0000E+00 0.0000E+00 1.0000E+09 0.0000E+00 0.0000E+00
  A = E0 + ED CELL 1
  IDCB ICBN ICB1 ICB2 ICB3
  -3001 56 -2001 0 0
  * CBGAIN CBXMIN CBXMAX CBCON1 CBCON2
  1.0000E+00 0.0000E+00 1.0000E+09 6.3400E+08 0.0000E+00
  ED = C2 X T CELL 1
  IDCB ICBN ICB1 ICB2 ICB3
  -2001 56 100 0 0
  * CBGAIN CBXMIN CBXMAX CBCON1 CBCON2
  0.0000E+00 0.0000E+00 1.0000E+09 0.0000E+00 0.0000E+00
  E = C1 I WS DT CELL 1
  IDCB ICBN ICB1 ICB2 ICB3
  -1001 73 501 0 0
  * CBGAIN CBXMIN CBXMAX CBCON1 CBCON2
  2.3000E+06 0.0000E+00 1.0000E+09 1.0000E+00 0.0000E+00
  IDCB ICBN ICB1 ICB2 ICB3
  -8002 100 -7002 10 0
  * CBGAIN CBXMIN CBXMAX CBCON1 CBCON2
  1.0000E+00 0.0000E+00 1.0000E+02 1.0000E+00 0.0000E+00
  IDCB ICBN ICB1 ICB2 ICB3
  -7002 39 -6002 -5002 0
  * CBGAIN CBXMIN CBXMAX CBCON1 CBCON2
  1.0000E+00 0.0000E+00 1.0000E+02 0.0000E+00 0.0000E+00
  IDCB ICBN ICB1 ICB2 ICB3
  -5002 101 702 4 0
  * CBGAIN CBXMIN CBXMAX CBCON1 CBCON2
  1.0000E+00 0.0000E+00 1.0000E+02 0.0000E+00 0.0000E+00
  CBFTB * -9.6500E+02 1.0084E+02 -7.2375E+02 9.1675E+01 -4.8250E+02
  CBFTB * 6.7550E+01 -2.4125E+02 0.0000E+00E
  IDCB ICBN ICB1 ICB2 ICB3
  -6002 101 -4002 4 0
  * CBGAIN CBXMIN CBXMAX CBCON1 CBCON2
  1.0000E+00 0.0000E+00 1.0000E+00 0.0000E+00 0.0000E+00
  CBFTB * R02 0.0000E+00 1.2700E+08 6.1000E-01 2.5000E+08 8.2000E-01
  CBFTB * 6.3400E+08 1.0000E+00E
  IDCB ICBN ICB1 ICB2 ICB3
  -4002 54 -3002 -1002 0
  * CBGAIN CBXMIN CBXMAX CBCON1 CBCON2
  1.0000E+00 0.0000E+00 1.0000E+09 0.0000E+00 0.0000E+00
  IDCB ICBN ICB1 ICB2 ICB3
  -3002 56 -2002 0 0
  * CBGAIN CBXMIN CBXMAX CBCON1 CBCON2
  1.0000E+00 0.0000E+00 1.0000E+09 6.3400E+08 0.0000E+00
  IDCB ICBN ICB1 ICB2 ICB3
  -2002 56 100 0 0
  * CBGAIN CBXMIN CBXMAX CBCON1 CBCON2
  0.0000E+00 0.0000E+00 1.0000E+09 0.0000E+00 0.0000E+00
  IDCB ICBN ICB1 ICB2 ICB3
  -1002 23 502 0 0
  * CBGAIN CBXMIN CBXMAX CBCON1 CBCON2
  2.3000E+06 0.0000E+00 1.0000E+09 1.0000E+00 0.0000E+00
  IDCB ICBN ICB1 ICB2 ICB3
  -8003 100 -7003 10 0
  * CBGAIN CBXMIN CBXMAX CBCON1 CBCON2
  1.0000E+00 0.0000E+00 1.0000E+02 1.0000E+00 0.0000E+00
  IDCB ICBN ICB1 ICB2 ICB3
  -7003 39 -6003 -5003 0
  * CBGAIN CBXMIN CBXMAX CBCON1 CBCON2
  1.0000E+00 0.0000E+00 1.0000E+02 0.0000E+00 0.0000E+00
  IDCB ICBN ICB1 ICB2 ICB3

```

```

-5002      101      703      4      0
CBGAIN    CBXMIN    CBXMAX    CBCON1    CBCON2
1.0000E+00 0.0000E+00 1.0000E+02 0.0000E+00 0.0000E+00
* CB1TB *  -9.6500E+02 1.0084E+02 -7.2375E+02 9.1675E+01 -4.8250E+02
* CBFTB *  6.7550E+01 -2.4125E+02 0.0000E+00E
*
IDCB      ICBN      ICB1      ICB2      ICB3
-6003     101      -4003     4      0
CBGAIN    CBXMIN    CBXMAX    CBCON1    CBCON2
1.0000E+00 0.0000E+00 1.0000E+00 0.0000E+00 0.0000E+00
*
CBFTB * R02 0.0000E+00 1.2700E+08 6.1000E-01 2.5000E+08 8.2000E-01
* CBFTB *  6.340E+08 1.0000E+00E
*
IDCB      ICBN      ICB1      ICB2      ICB3
-4003     54      -3003     -1003     0
CBGAIN    CBXMIN    CBXMAX    CBCON1    CBCON2
1.0000E+00 0.0000E+00 1.0000E+09 0.0000E+00 0.0000E+00
*
IDCB      ICBN      ICB1      ICB2      ICB3
-3003     56      -2003     0      0
CBGAIN    CBXMIN    CBXMAX    CBCON1    CBCON2
1.0000E+00 0.0000E+00 1.0000E+09 6.3400E+08 0.0000E+00
*
IDCB      ICBN      ICB1      ICB2      ICB3
-2003     56      100      0      0
CBGAIN    CBXMIN    CBXMAX    CBCON1    CBCON2
0.0000E+00 0.0000E+00 1.0000E+09 0.0000E+00 0.0000E+00
*
IDCB      ICBN      ICB1      ICB2      ICB3
-1003     23      503      0      0
CBGAIN    CBXMIN    CBXMAX    CBCON1    CBCON2
2.5000E+06 0.0000E+00 1.0000E+09 1.0000E+00 0.0000E+00
*
IDCB      ICBN      ICB1      ICB2      ICB3
-8004     100      -7004     10      0
CBGAIN    CBXMIN    CBXMAX    CBCON1    CBCON2
1.3000E+00 0.0000E+00 1.3000E+02 1.0000E+00 0.0000E+00
*
IDCB      ICBN      ICB1      ICB2      ICB3
-7004     39      -6004     -5004     0
CBGAIN    CBXMIN    CBXMAX    CBCON1    CBCON2
1.0000E+00 0.0000E+00 1.0000E+02 0.0000E+00 0.0000E+00
*
IDCB      ICBN      ICB1      ICB2      ICB3
-5004     101      704      4      0
CBGAIN    CBXMIN    CBXMAX    CBCON1    CBCON2
1.0000E+00 0.0000E+00 1.0000E+02 0.0000E+00 0.0000E+00
*
CBFTB *  -9.6500E+02 1.0084E+02 -7.2375E+02 9.1675E+01 -4.8250E+02
* CBFTB *  6.7550E+01 -2.4125E+02 0.0000E+00E
*
IDCB      ICBN      ICB1      ICB2      ICB3
-6004     101      -4004     4      0
CBGAIN    CBXMIN    CBXMAX    CBCON1    CBCON2
1.0000E+00 0.0000E+00 1.0000E+00 0.0000E+00 0.0000E+00
*
CBFTB * R02 0.0000E+00 1.2700E+08 6.1000E-01 2.5000E+08 8.2000E-01
* CBFTB *  6.3400E+08 1.0000E+00E
*
IDCB      ICBN      ICB1      ICB2      ICB3
-4004     54      -3004     -1004     0
CBGAIN    CBXMIN    CBXMAX    CBCON1    CBCON2
1.0000E+09 0.0000E+00 1.0000E+09 0.0000E+00 0.0000E+00
*
IDCB      ICBN      ICB1      ICB2      ICB3
-3004     56      -2004     0      0
CBGAIN    CBXMIN    CBXMAX    CBCON1    CBCON2
1.0000E+00 0.0000E+00 1.0000E+09 6.3400E+08 0.0000E+00
*
IDCB      ICBN      ICB1      ICB2      ICB3
-2004     56      100      0      0
CBGAIN    CBXMIN    CBXMAX    CBCON1    CBCON2
0.0000E+00 0.0000E+00 1.0000E+09 0.0000E+00 0.0000E+00
*
IDCB      ICBN      ICB1      ICB2      ICB3
-1004     23      504      0      0
CBGAIN    CBXMIN    CBXMAX    CBCON1    CBCON2
2.3000E+06 0.0000E+00 1.0000E+09 1.0000E+00 0.0000E+00
*
IDCB      ICBN      ICB1      ICB2      ICB3
-801      101      105      4      0
CBGAIN    CBXMIN    CBXMAX    CBCON1    CBCON2
0.0000E+00 0.0000E+00 3.0000E+01 0.0000E+00 0.0000E+00
*
CBFTB *  -1.0000E+04R03 0.0000E+00 5.0000E+02 2.0000E+01 1.0000E+04
* CBFTB *  2.0000E+01E
*
IDCB      ICBN      ICB1      ICB2      ICB3
-901      100      -801      10      0
CBGAIN    CBXMIN    CBXMAX    CBCON1    CBCON2
1.0000E+00 0.0000E+00 3.0000E+01 1.0000E+00 0.0000E+00
*
IDCB      ICBN      ICB1      ICB2      ICB3
-802      101      205      4      0
CBGAIN    CBXMIN    CBXMAX    CBCON1    CBCON2
0.0000E+00 0.0000E+00 3.0000E+01 0.0000E+00 0.0000E+00
*
CBFTB *  -1.0000E+04R03 0.0000E+00 5.0000E+02 2.0000E+01 1.0000E+04
* CBFTB *  2.0000E+01E
*
IDCB      ICBN      ICB1      ICB2      ICB3
-902      100      -802      10      0
CBGAIN    CBXMIN    CBXMAX    CBCON1    CBCON2
1.0000E+00 0.0000E+00 3.0000E+01 1.0000E+00 0.0000E+00
*
IDCB      ICBN      ICB1      ICB2      ICB3
-803      101      305      4      0
CBGAIN    CBXMIN    CBXMAX    CBCON1    CBCON2
0.0000E+00 0.0000E+00 3.0000E+01 0.0000E+00 0.0000E+00

```

* CBFTB * -1.0000E+04 R03 0.0000E+00 5.0000E+02 2.0000E+01 1.0000E+04
 * CBFTB * 2.0000E+01E

IDCB	ICBN	ICB1	ICB2	ICB3
-903	100	-803	10	0
CBGAIN	CBXMIN	CBXMAX	CBCON1	CBCON2
1.0000E+00	0.0000E+00	3.0000E+01	1.0000E+00	0.0000E+00
IDCB	ICBN	ICB1	ICB2	ICB3
-601	44	601	480	0
CBGAIN	CBXMIN	CBXMAX	CBCON1	CBCON2
1.0000E+00	1.0000E+00	1.0000E+30	1.0000E+00	1.0000E+00

TRIP-DIMENSION VARIABLES CARDS

NTSE	NTCT	NTSF	NTDP	NTSD
0	7	0	1	0
IDTP	ISRT	ISET	ITST	IDSG
701	4	0	1	100
SETP(1)	SETP(2)	SETP(3)	SETP(4)	
1.0000E+29	1.0000E+29	1.0000E+30	1.0000E+30	
DTSP(1)	DTSP(2)	DTSP(3)	DTSP(4)	
0.0000E+00	0.0000E+00	0.0000E+00	0.0000E+00	
IFSP(1)	IFSP(2)	IFSP(3)	IFSP(4)	
0	0	0	0	

IDTP	ISRT	ISET	ITST	ILSG
702	4	0	1	100
SETP(1)	SETP(2)	SETP(3)	SETP(4)	
1.0000E+29	1.0000E+29	1.0000E+30	1.0000E+30	
DTSP(1)	DTSP(2)	DTSP(3)	DTSP(4)	
0.0000E+00	0.0000E+00	0.0000E+00	0.0000E+00	
IFSP(1)	IFSP(2)	IFSP(3)	IFSP(4)	
0	0	0	0	

IDTP	ISRT	ISET	ITST	IDSG
703	4	0	1	100
SETP(1)	SETP(2)	SETP(3)	SETP(4)	
1.0000E+29	1.0000E+29	1.0000E+30	1.0000E+29	
DTSP(1)	DTSP(2)	DTSP(3)	DTSP(4)	
0.0000E+00	0.0000E+00	0.0000E+00	0.0000E+00	
IFSP(1)	IFSP(2)	IFSP(3)	IFSP(4)	
0	0	0	0	

IDTP	ISRT	ISET	ITST	IDSG
704	4	0	1	100
SETP(1)	SETP(2)	SETP(3)	SETP(4)	
1.0000E+29	1.0000E+29	1.0000E+30	1.0000E+30	
DTSP(1)	DTSP(2)	DTSP(3)	DTSP(4)	
0.0000E+00	0.0000E+00	0.0000E+00	0.0000E+00	
IFSP(1)	IFSP(2)	IFSP(3)	IFSP(4)	
0	0	0	0	

TRIP 600, BASE STEAM

IDTP	ISRT	ISET	ITST	IDSG
600	2	0	1	100
SETP(1)	SETP(2)			
0.0	0.0			
DTSP(1)	DTSP(2)			
0.0000E+00	0.0000E+00			
IFSP(1)	IFSP(2)			
0	0			

TRIP 90, BCL CONTAINMENT BREAK

IDTP	ISRT	ISET	ITST	IDSG
90	2	0	1	100
SETP(1)	SETP(2)			
0.0	0.0			
DTSP(1)	DTSP(2)			
0.0000E+00	0.0000E+00			
IFSP(1)	IFSP(2)			
0	0			

TRIP 91, BHL CONTAINMENT BREAK, NOT USED (INACTIVE)

IDTP	ISRT	ISET	ITST	IDSG
91	2	0	1	100
SETP(1)	SETP(2)			
0.0000E+00	0.0000E+00			
DTSP(1)	DTSP(2)			
0.0000E+00	0.0000E+00			
IFSP(1)	IFSP(2)			
0	0			

TRIP 106, VESSEL DRAIN FILL 107, NOT USED (INACTIVE)

IDTP	ISRT	ISET	ITST	IDSG
106	1	0		107
SETP(1)	SETP(2)			
2.0000E-01	8.0000E-01			
DTSP(1)	DTSP(2)			
0.0000E+00	0.0000E+00			
IFSP(1)	IFSP(2)			
0	0			

IDTP	ISRT	ISET	ITST	IDSG
105	2	0	1	100
SETP(1)	SETP(2)			
1.0000E+30	1.0000E+30			
DTSP(1)	DTSP(2)			

```

* 0.0000E+00 0.0000E+00
* IFSP(1) IFSP(2)
* 0 0
* IDTP ISRT ISET ITST IDSG
* 107 2 0 3 -107
* SETP(1) SETP(2)
* 5.0000E-01 5.0000E-01
* DTSP(1) DTSP(2)
* 0.0000E+00 0.0000E+00
* IFSP(1) IFSP(2)
* 0 0

```

* TRIP 220, PRESSURIZER FIL., NOT USED (INACTIVE)

```

* IDTP ISRT ISET ITST IDSG
* 220 2 0 1 100
* SETP(1) SETP(2)
* 1.0000E+30 1.0000E+30
* DTSP(1) DTSP(2)
* 0.0000E+00 0.0000E+00
* IFSP(1) IFSP(2)
* 0 0

```

* HOT LEG ECC. LOOP 1, 2, 3, 4, NOT USED (INACTIVE)

```

* IDTP ISRT ISET ITST IDSG
* 115 2 0 1 100
* SETP(1) SETP(2)
* 1.0000E+30 1.0000E+30
* DTSP(1) DTSP(2)
* 0.0000E+00 0.0000E+00
* IFSP(1) IFSP(2)
* 0 0

```

* COLD LEG ECC. LOOP 1, 2, 3 (COMP 16, 26, 36)

```

* IDTP ISRT ISET ITST IDSG
* 118 2 0 1 100
* SETP(1) SETP(2)
* 30.4 30.4
* DTSP(1) DTSP(2)
* 0.0000E+00 0.0000E+00
* IFSP(1) IFSP(2)
* 0 0

```

* SEPARATOR DRAIN OF LOOP 1 (COMP 119), NOT USED (INACTIVE)

```

* IDTP ISRT ISET ITST IDSG
* 118 1 0 1 119
* SETP(1) SETP(2)
* 2.0000E-01 8.0000E-01
* DTSP(1) DTSP(2)
* 0.0000E+00 0.0000E+00
* IFSP(1) IFSP(2)
* 0 0
* IDTP ISRT ISET ITST IDSG
* 117 2 0 1 100
* SETP(1) SETP(2)
* 1.0000E+30 1.0000E+30
* DTSP(1) DTSP(2)
* 0.0000E+00 0.0000E+00
* IFSP(1) IFSP(2)
* 0 0
* IDTP ISRT ISET ITST IDSG
* 119 2 0 3 -199
* SETP(1) SETP(2)
* 5.0000E-01 5.0000E-01
* DTSP(1) DTSP(2)
* 0.0000E+00 0.0000E+00
* IFSP(1) IFSP(2)
* 0 0

```

* SEPARATOR DRAIN OF LOOP 2 (COMP 229), NOT USED (INACTIVE)

```

* IDTP ISRT ISET ITST IDSG
* 228 1 0 1 229
* SETP(1) SETP(2)
* 2.0000E-01 8.0000E-01
* DTSP(1) DTSP(2)
* 0.0000E+00 0.0000E+00
* IFSP(1) IFSP(2)
* 0 0
* IDTP ISRT ISET ITST IDSG
* 229 2 0 3 -299
* SETP(1) SETP(2)
* 5.0000E-01 5.0000E-01
* DTSP(1) DTSP(2)
* 0.0000E+00 0.0000E+00
* IFSP(1) IFSP(2)
* 0 0

```

* SEPARATOR DRAIN OF LOOP 3 (COMP 339), NOT USED (INACTIVE)

```

* IDTP ISRT ISET ITST IDSG
* 338 1 0 1 339
* SETP(1) SETP(2)
* 2.0000E-01 8.0000E-01
* DTSP(1) DTSP(2)
* 0.0000E+00 0.0000E+00

```



```

*   IFSP(1)   IFSP(2)
*   IDTP      ISRT      ISET      ITST      IDSG
*   839       2         0         3      -399
*   SETP(1)   SETP(2)
* 5.0000E-01 5.0000E-01
* DTSP(1)    DTSP(2)
* 0.0000E+00 0.0000E+00
* IFSP(1)    IFSP(2)
* 0          0

```

TRIP 888, TIME TRIP FOR INACTIVE COMPONENTS

```

*   IDTP      ISRT      ISET      ITST      IDSG
*   888       2         0         1      100
*   SETP(1)   SETP(2)
* 9.9900E+10 9.9900E+10
* DTSP(1)    DTSP(2)
* 0.0000E+00 0.0000E+00
* IFSP(1)    IFSP(2)
* 0          0

```

TRIP 999, END PROBLEM

```

*   IDTP      ISRT      ISET      ITST      IDSG
*   999       1         0         1      100
*   SETP(1)   SETP(2)
* 1.0000E+30 1.0000E+30
* DTSP(1)    DTSP(2)
* 0.0000E+00 0.0000E+00
* IFSP(1)    IFSP(2)
* 0          0

```

TRIP 449, BHL S/W SEPARATOR DRAIN FILL, NOT USED

```

*   IDTP      ISRT      ISET      ITST      IDSG
*   449       1         0         1      100
*   SETP(1)   SETP(2)
* 1.0000E+30 1.0000E+30
* DTSP(1)    DTSP(2)
* 0.0000E+00 0.0000E+00
* IFSP(1)    IFSP(2)
* 0          0

```

BHL BREAK VALVE (COMP 42), NOT USED (CLOSED DURING EXP.)

```

*   IDTP      ISRT      ISET      ITST      IDSG
*   442       2         0         1      100
*   SETP(1)   SETP(2)
* 1.0000E+30 1.0000E+30
* DTSP(1)    DTSP(2)
* 0.0000E+00 0.0000E+00
* IFSP(1)    IFSP(2)
* 0          0

```

BCL SEPARATOR DRAIN FILL (COMP 49)

```

*   IDTP      ISRT      ISET      ITST      IDSG
*   49        2         0         1      100
*   SETP(1)   SETP(2)
* 0.0         0.0
* DTSP(1)    DTSP(2)
* 0.0000E+00 0.0000E+00
* IFSP(1)    IFSP(2)
* 0          0

```

```

*   IDTP      ISRT      ISET      ITST      IDSG
*   498       2         0         3     -498
*   SETP(1)   SETP(2)
* 5.0000E-01 5.0000E-01
* DTSP(1)    DTSP(2)
* 0.0000E+00 0.0000E+00
* IFSP(1)    IFSP(2)
* 0          0

```

BCL BREAK VALVE (COMP 46)

```

*   IDTP      ISRT      ISET      ITST      IDSG
*   446       2         0         1      100
*   SETP(1)   SETP(2)
* 0.0         0.0
* DTSP(1)    DTSP(2)
* 0.0000E+00 0.0000E+00
* IFSP(1)    IFSP(2)
* 0          0

```

TRIP 497, TRIP CONTROLLED TRIP, BHL SEPARATOR DRAIN (COMP 449), NOT USED

```

*   IDTP      ISRT      ISET      ITST      IDSG
*   497       2         0         3     -497
*   SETP(1)   SETP(2)
* 5.0000E-01 5.0000E-01
* DTSP(1)    DTSP(2)
* 0.0000E+00 0.0000E+00
* IFSP(1)    IFSP(2)
* 0          0

```

TRIP 479, TRIP CONTROLLED TRIP, BCL KTA DRAIN (COMP 479)

```

*   IDTP      ISRT      ISET      ITST      IDSG
*   479       2         0         1      100
*   SETP(1)   SETP(2)

```

```

* 0.0      0.0
* DTSP(1) DTSP(2)
* 0.0000E+00 0.0000E+00
* IFSP(1) IFSP(2)
* 0      0
* IDTP      ISRT      ISET      ITST      IDSG
* 601      1      0      1      100
* SETP(1) SETP(2)
* 2.0000E+05 2.0000E+05
* DTSP(1) DTSP(2)
* 0.0000E+00 0.0000E+00
* IFSP(1) IFSP(2)
* 0      0
* IDTP      ISRT      ISET      ITST      IDSG
* 499      2      0      3      -499
* SETP(1) SETP(2)
* 5.0000E-01 5.0000E-01
* DTSP(1) DTSP(2)
* 0.0000E+00 0.0000E+00
* IFSP(1) IFSP(2)
* 0      0

```

TRIP CONTROLLED TRIP CARDS

```

* IDTN      INTN
* -107      3
* ITN(1) ITN(2) ITN(3)
* 105      105      601
* IDTN      INTN
* -199      2
* ITN(1) ITN(2)
* 117      118
* IDTN      INTN
* -299      2
* ITN(1) ITN(2)
* 117      228
* IDTN      INTN
* -399      2
* ITN(1) ITN(2)
* 117      338
* IDTN      INTN
* -497      2
* ITN(1) ITN(2)
* 117      497
* IDTN      INTN
* -498      2
* ITN(1) ITN(2)
* 117      49
* IDTN      INTN
* -499      2
* ITN(1) ITN(2)
* 479      601

```

TRIP INITIATED PROBLEM TERMINATION CARDS

```

* NDMP
* 1
* IDMP()
* -999

```

6. COMPONENT DATA **

COMPONENT NO. 01 VER 1.1 *****

```

VESSEL
* NASX      NRSX      NTSX      MAIN VESSEL
* 13      3      4      NCSR      C 2
* IDCU      IDCL      IDCR      20      ICRU      ICRL      C 3
* 12      2      IUCSP      0      IUHP      ICONC      C 4
* ICRR      ILCSP      7      12      0
* 2 * ICRRG-NOTE USE ONLY WITH VERSION 12.0, TO OBTAIN CORE GLOBAL OUTPUT*
* NFFA      NFFR      NFFT      NVENT      C 5
* IRPWTY      NDGX      NDHX      NRTS      C 6
* 0
* IZPWTR      IZPWSV      NZPWTB      NZPWSV      NZPWRF      C 8
* 0
* RPTR      NMWRX      NFCI      NFCIL      NZMAX      C 9
* 0
* NRDS      NODES      NODHS      INHSMX      C 10
* 0
* RFACT      TNEUT      RPWOF      RRPWMX      RPWSCL      C 11
* 0
* RPWR      ZPWIN      ZPWOF      RZPWMX      C 12
* 0
* SHELV      PLDR      PDRAT      FUCRAC      HGAPO      C 13
* DTXHT(1) DTXHT(2)      DZNHT      C 14
* 0

```

***** VESSEL GEOMETRIE CARDS *****

```

2.007      2.480      2.915      4.3825      5.850 S* Z
6.720      7.495      7.760      8.010 S      * Z
8.745      9.495      10.240      13.3915 E      * Z
1.168      2.185      2.435 E      * RAD
1.570796      3.141593 S      * TH

```

4.712309

6.289186 E

TH

VESSEL SOURCE CARDS

11	6	3	40	* BL4-HL
11	10	3	47	* BL4-CL
11	7	3	10
11	10	3	20
11	11	3	30
11	12	3	17
11	11	3	27
11	11	3	37
6	1	3	501
6	2	3	502
6	3	3	503
6	4	3	504
6	5	3	505
6	6	3	506
6	7	3	507
6	8	3	508
1	5	3	101	* DRAIN L1
1	8	3	102
1	7	3	103
1	6	3	104

LEVEL 1

R 4	7.8042 R 4	9.3428 R 4	2.23572	E	0.013 R 1	0.0158	HSA
1	0.0	0.005	0.01	0.013	0.013	0.0158	HSX-1
1	0.0	0.005	0.01	0.013	0.013	0.0158	HSX-2
1	0.0	0.005	0.01	0.013	0.013	0.0158	HSX-3
1	0.0	0.005	0.01	0.013	0.013	0.0158	HSX-4
1	0.0	0.0094	0.015	0.017	0.017	0.01885	HSX-5
1	0.0	0.0094	0.015	0.017	0.017	0.01885	HSX-6
1	0.0	0.0094	0.015	0.017	0.017	0.01885	HSX-7
1	0.0	0.0094	0.015	0.017	0.017	0.01885	HSX-8
1	0.0	0.025	0.04	0.047	0.047	0.0555	HSX-9
1	0.0	0.025	0.04	0.047	0.047	0.0555	HSX-10
1	0.0	0.025	0.04	0.047	0.047	0.0555	HSX-11
1	0.0	0.025	0.04	0.047	0.047	0.0555	HSX-12
0	0	0	0	0	0	0	
0	0	0	0	0	0	0	
0	0	0	0	0	0	0	
0	0	0	0	0	0	0	
4	0.6178	0.4880	0.1987	E	0.013	0.0158	VOL
4	0.4053	0.3344	0.2017	E	0.013	0.0158	FA-T
4	6.5744	0.55347	1.	E	0.013	0.0158	-Z
4	0.2361	0.3488	0.5	E	0.013	0.0158	-R
4	0.65	1.79	0.54	E	0.013	0.0158	HD-T
4	0.69	1.1414	0.95	E	0.013	0.0158	-Z
4	0.69	1.885	0.0	E	0.013	0.0158	-R
6	416.2						HSTN
6							MATHS
1.000							ALPN
0							VVN-T
0							-Z
0							VLN-T
0							-Z
0							TVN
401.50							TLN
400.65							PN
2.60E+05							PAN
0							

LEVEL 2

R 4	0.8752 R 4	1.8964 R 4	4.1274	E	0.013 R 1	0.0158	HSA
1	0.0	0.005	0.01	0.013	0.013	0.0158	HSX-1
1	0.0	0.005	0.01	0.013	0.013	0.0158	HSX-2
1	0.0	0.005	0.01	0.013	0.013	0.0158	HSX-3
1	0.0	0.005	0.01	0.013	0.013	0.0158	HSX-4
1	0.0	0.0102	0.01634	0.01839	0.01839	0.020435	HSX-5
1	0.0	0.0102	0.01634	0.01839	0.01839	0.020435	HSX-6
1	0.0	0.0102	0.01634	0.01839	0.01839	0.020435	HSX-7
1	0.0	0.0102	0.01634	0.01839	0.01839	0.020435	HSX-8
1	0.0	0.025	0.04	0.047	0.047	0.0555	HSX-9
1	0.0	0.025	0.04	0.047	0.047	0.0555	HSX-10
1	0.0	0.025	0.04	0.047	0.047	0.0555	HSX-11
1	0.0	0.025	0.04	0.047	0.047	0.0555	HSX-12
0	0	0	0	0	0	0	
0	0	0	0	0	0	0	
0	0	0	0	0	0	0	
0	0	0	0	0	0	0	
4	0.4735	0.77815	1.0	E	0.013	0.0158	VOL
4	0.3041	0.40059	1.0	E	0.013	0.0158	FA-T
4	0.4639	0.35834	1.0	E	0.013	0.0158	-Z
4	0.1984	1.0000	0.0	E	0.013	0.0158	-R
4	0.54	2.1754	1.02	E	0.013	0.0158	HD-T
4	0.175	0.16824	0.700	E	0.013	0.0158	-Z
4	0.36	1.49	0.00	E	0.013	0.0158	-R
6	416.2						HSTN
6							MATHS
1							ALPN
0							VVN-T

0.
0.
0.
0.
402.18 E
402.18 E
2.60E+05 E
0. E

VLN-T
TVN
TLN
PAN

LEVEL 3

R 4	5.1750 R 4	9.9450 R 4	2.5394	E	0.013 R 1	0.0155	HSA
R 1	0.0 R 1	0.005 R 1	0.01 R 1	0.013 R 1	0.0155	HSX-1	
R 1	0.0 R 1	0.005 R 1	0.01 R 1	0.013 R 1	0.0155	HSX-2	
R 1	0.0 R 1	0.005 R 1	0.01 R 1	0.013 R 1	0.0155	HSX-3	
R 1	0.0 R 1	0.005 R 1	0.01 R 1	0.013 R 1	0.0155	HSX-4	
R 1	0.0 R 1	0.05829 R 1	0.09326 R 1	0.10492 R 1	0.11658	HSX-5	
R 1	0.0 R 1	0.05829 R 1	0.09326 R 1	0.10492 R 1	0.11658	HSX-6	
R 1	0.0 R 1	0.05829 R 1	0.09326 R 1	0.10492 R 1	0.11658	HSX-7	
R 1	0.0 R 1	0.05829 R 1	0.09326 R 1	0.10492 R 1	0.11658	HSX-8	
R 1	0.0 R 1	0.025 R 1	0.04 R 1	0.047 R 1	0.055	HSX-9	
R 1	0.0 R 1	0.025 R 1	0.04 R 1	0.047 R 1	0.055	HSX-10	
R 1	0.0 R 1	0.025 R 1	0.04 R 1	0.047 R 1	0.055	HSX-11	
R 1	0.0 R 1	0.025 R 1	0.04 R 1	0.047 R 1	0.055	HSX-12	
R 4	8.85 R 4	34.4293 F	0. E			CFZL-T	
R 4	8.85 R 4	34.4293 F	0. E			CFZV-T	
R 4	0.6342 R 4	0.45616 R 4	1.0000			VOL	
R 4	0.0768 R 4	0.28274 R 4	1.0000			FA-T	
R 4	0.1785 R 4	0.10026 R 4	1.0000			-Z	
R 4	0.0652 R 4	0.0000 R 4	0.0			-R	
R 4	0.245 R 4	0.09606 R 4	0.50000			HD-T	
R 4	0.1100 R 4	0.09044 R 4	0.50 E			-Z	
R 4	0.364 R 4	0.01 F	0.01 E			-R	
R 4	416.2 E					HSTN	
R 4	6					MATHS	
R 4	1					ALPN	
R 4	0					VVN-T	
R 4	0					-Z	
R 4	0					-R	
R 4	0					VLN-T	
R 4	0					-Z	
R 4	0					-R	
R 08	432.525 R 04	401.64 E				TVN	
R 08	432.525 R 04	401.64 E				TLN	
R 08	2.60E+05 E					PAN	
R 08	0. E						

LEVEL 4

R 4	7.5000 R 4	20.425 R 4	9.8858	E	0.013 R 1	0.0155	HSA
R 1	0.0 R 1	0.005 R 1	0.01 R 1	0.013 R 1	0.0155	HSX-1	
R 1	0.0 R 1	0.005 R 1	0.01 R 1	0.013 R 1	0.0155	HSX-2	
R 1	0.0 R 1	0.005 R 1	0.01 R 1	0.013 R 1	0.0155	HSX-3	
R 1	0.0 R 1	0.005 R 1	0.01 R 1	0.013 R 1	0.0155	HSX-4	
R 1	0.0 R 1	0.0107 R 1	0.01716 R 1	0.01930 R 1	0.02144	HSX-5	
R 1	0.0 R 1	0.0107 R 1	0.01716 R 1	0.01930 R 1	0.02144	HSX-6	
R 1	0.0 R 1	0.0107 R 1	0.01716 R 1	0.01930 R 1	0.02144	HSX-7	
R 1	0.0 R 1	0.0107 R 1	0.01716 R 1	0.01930 R 1	0.02144	HSX-8	
R 1	0.0 R 1	0.025 R 1	0.04 R 1	0.047 R 1	0.055	HSX-9	
R 1	0.0 R 1	0.025 R 1	0.04 R 1	0.047 R 1	0.055	HSX-10	
R 1	0.0 R 1	0.025 R 1	0.04 R 1	0.047 R 1	0.055	HSX-11	
R 1	0.0 R 1	0.025 R 1	0.04 R 1	0.047 R 1	0.055	HSX-12	
R 4	0.4924 R 4	0.57587 R 4	1.0000			CFZL-T	
R 4	0.0021 R 4	0.28124 R 4	1.0000			-Z	
R 4	53919 R 4	0.29844 R 4	1.0000			CFZV-T	
R 4	0.0027 R 4	0.0 E				-Z	
R 4	0.4182 R 4	0.3227 R 4	0.5000			VOL	
R 4	0.4182 R 4	0.1777 R 4	0.5000			FA-T	
R 4	1.2 F	0.01 E				-Z	
R 4	416.2 E					-R	
R 4	6					HSTN	
R 4	1					MATHS	
R 4	0					ALPN	
R 4	0					VVN-T	
R 4	0					-Z	
R 4	0					-R	
R 4	0					VLN-T	
R 4	0					-Z	
R 4	0					-R	
R 08	432.525 R 04	401.64 E				TVN	
R 08	432.525 R 04	401.64 E				TLN	
R 08	2.60E+05 E					PAN	
R 08	0. E						

LEVEL 5

R 4	7.6755 R 4	20.5750 R 4	9.8851	E	0.013 R 1	0.0155	HSA
R 1	0.0 R 1	0.005 R 1	0.01 R 1	0.013 R 1	0.0155	HSX-1	
R 1	0.0 R 1	0.005 R 1	0.01 R 1	0.013 R 1	0.0155	HSX-2	

R 1	0.09250 S					* HSX-9
R 1	0.000 R 1	.0463 R 1	.074000 R 1	.08330000 S		* HSX-10
R 1	0.09250 S					* HSX-10
R 1	0.000 R 1	.0463 R 1	.074000 R 1	.08330000 S		* HSX-11
R 1	0.09250 S					* HSX-11
R 1	0.000 R 1	.0463 R 1	.074000 R 1	.08330000 S		* HSX-12
R 1	0.09250 E					* HSX-12
R 4	4.687 R 4	1.03911 F	0.0 E			* CFZL-T
R 4	0.0 R 4	137.7815 R 4	0.0 E			* -Z
R 4	2.38 F	0.0 E				* -R
R 4	4.687 R 4	1.03911 F	0.0 E			* -R
R 4	0.0 R 4	137.7815 R 4	0.0 E			* -R
R 4	2.38 F	0.0 E				* -R
R 4	0.5322400 R 4	0.529270 R 4	1.000000			* VOL
R 4	0.3526540 R 4	0.492560 R 4	1.0 E			* FA-T
R 4	0.37 R 4	0.204703 R 4	1.0 E			* -Z
R 4	0.3526540 F	0.0 E				* -R
R 4	0.0127650 R 4	0.157857 R 4	0.200000 E			* HD-T
R 4	0.012765 F	0.016840 R 4	0.200000 E			* -Z
R 4	0.012765 F	0.0 E				* -R
R 40	416.2 F	416.2 E				* HSTN
R 40	0.0 E					* MATHS
R 40	1.00 E					* ALPN
R 40	0.0 E					* VVN-T
R 40	0.0 E					* -Z
R 40	0.0 E					* -R
R 40	0.0 E					* VLN-T
R 40	0.0 E					* -Z
R 40	0.0 E					* -R
R 08	432.525 R04	401.64 E				* TVN
R 08	432.525 R04	401.64 E				* TLN
R 8	2.60E+05 F	2.60E+05 E				* PN
R 8	0.0 E					* PAN

***** LEVEL 8 *****

R 4	21.653000 R 4	33.73010 R 4	1.883960			* HSA
R 1	0.000 R 1	0.0007440 R 1	0.00119000 R 1	.001339000 S		* HSX-1
R 1	0.001488 S					* HSX-1
R 1	0.000 R 1	0.0007440 R 1	0.00119000 R 1	.001339000 S		* HSX-2
R 1	0.001488 S					* HSX-2
R 1	0.000 R 1	0.0007440 R 1	0.00119000 R 1	.001339000 S		* HSX-3
R 1	0.001488 S					* HSX-3
R 1	0.000 R 1	0.0007440 R 1	0.00119000 R 1	.001339000 S		* HSX-4
R 1	0.001488 S					* HSX-4
R 1	0.000 R 1	0.0015700 R 1	0.00251200 R 1	.002825500 S		* HSX-5
R 1	0.0031395 S					* HSX-5
R 1	0.000 R 1	0.0015700 R 1	0.00251200 R 1	.002825500 S		* HSX-6
R 1	0.0031395 S					* HSX-6
R 1	0.000 R 1	0.0015700 R 1	0.00251200 R 1	.002825500 S		* HSX-7
R 1	0.0031395 S					* HSX-7
R 1	0.000 R 1	0.0015700 R 1	0.00251200 R 1	.002825500 S		* HSX-8
R 1	0.0031395 S					* HSX-8
R 1	0.001 R 1	.04630 R 1	.07400 R 1	.0833000 S		* HSX-9
R 1	0.0925 S					* HSX-9
R 1	0.001 R 1	.04630 R 1	.07400 R 1	.0833000 S		* HSX-10
R 1	0.0925 S					* HSX-10
R 1	0.001 R 1	.04630 R 1	.07400 R 1	.0833000 S		* HSX-11
R 1	0.0925 S					* HSX-11
R 1	0.001 R 1	.04630 R 1	.07400 R 1	.0833000 S		* HSX-12
R 1	0.0925 E					* HSX-12
R 4	0.0 E					* CFZL-T
R 4	4.75 R 4	2.79846 F	0.0 E			* -Z
R 4	0.0 E					* -R
R 4	0.0 E					* CFZV-T
R 4	4.75 R 4	2.79846 F	0.0 E			* -Z
R 4	0.0 E					* -R
R 4	0.6934090 R 4	0.658832 R 4	1.000000			* VOL
R 4	0.3386520 R 4	0.352873 R 4	1.0 E			* FA-T
R 4	0.4869400 R 4	0.269400 R 4	1.0000			* -Z
R 4	0.3491100 F	0.0 E				* -R
R 4	0.0567390 R 4	0.113584 R 4	0.157500 E			* HD-T
R 4	0.0751430 R 4	0.087343 R 4	0.266000			* -Z
R 4	0.056739 F	0.00				* -R
R 40	416.2 R20	416.2 F	416.2 E			* HSTN
R 40	0.0 E					* MATHS
R 40	1.00 E					* ALPN
R 40	0.0 E					* VVN-T
R 40	0.0 E					* -Z
R 40	0.0 E					* -R
R 40	0.0 E					* VLN-T
R 40	0.0 E					* -Z
R 40	0.0 E					* -R
R 08	432.525 R04	401.64 E				* TVN
R 08	432.525 R04	401.64 E				* TLN
R 8	2.60E+05 F	2.60E+05 E				* PN
R 8	0.0 E					* PAN

***** LEVEL 9 *****

R 4	5.287820 R 4	7.568010 R 4	1.839787			* HSA
R 1	0.000 R 1	0.007720 R 1	0.0123400 R 1	0.01389 S		* HSX-1
R 1	0.015430 S					* HSX-1
R 1	0.000 R 1	0.007720 R 1	0.0123400 R 1	0.01389 S		* HSX-2
R 1	0.015430 S					* HSX-2
R 1	0.000 R 1	0.007720 R 1	0.0123400 R 1	0.01389 S		* HSX-3
R 1	0.015430 S					* HSX-3
R 1	0.000 R 1	0.009984 R 1	0.0159740 R 1	0.01797 S		* HSX-4
R 1	0.019967 S					* HSX-4

```

1 0.000 R 1 0.009984 R 1 0.0159740 R 1 0.01797 S * HSX- 5
0.019967 S * HSX- 5 * HSX- 6
1 0.000 R 1 0.009984 R 1 0.0159740 R 1 0.01797 S * HSX- 6 * HSX- 6
0.019967 S * HSX- 6 * HSX- 7
1 0.000 R 1 0.009984 R 1 0.0159740 R 1 0.01797 S * HSX- 7 * HSX- 7
0.019967 S * HSX- 7 * HSX- 8
1 0.000 R 1 0.009984 R 1 0.0159740 R 1 0.01797 S * HSX- 8 * HSX- 8
0.019967 S * HSX- 8 * HSX- 9
1 0.000 R 1 .05630 R 1 .0900 R 1 .1013 S * HSX- 9 * HSX- 9
0.11250 S * HSX- 9 * HSX- 10
1 0.000 R 1 .05630 R 1 .0900 R 1 .1013 S * HSX- 10 * HSX- 10
0.11250 S * HSX- 10 * HSX- 11
1 0.000 R 1 .05630 R 1 .0900 R 1 .1013 S * HSX- 11 * HSX- 11
0.11250 S * HSX- 11 * HSX- 12
1 0.000 R 1 .05630 R 1 .0900 R 1 .1013 S * HSX- 12 * HSX- 12
0.11250 E * HSX- 12
0.0 E * CFZL-T
0.0 E * -Z-R
4 2.38 F 0. E * CFZY-T
0.0 E * -Z-R
0.0 E * -R
4 2.38 F 0. E * VOL
4 0.727990 R 4 0.74698100 R 4 1.000000 E * FA-T
4 0.417246 R 4 0.4674220 R 4 1.000000 E * FA-Z
4 0.555720 R 4 0.7076000 R 4 1.000000 E * FA-R
1 0.471050 R 1 0.4086000 R 1 0.47105 R 1 0.4059000 S * HD-T
0.0 E * HD-Z
4 0.95743500 R 4 0.15421700 R 4 0.2500000 E * -R
4 0.23990 F 0.2500000 E * HSTN
1 0.0647500 R 1 0.052107 R 1 0.064750 R 1 0.0521070 S * MATHS
0.0 E * ALPN
40 416.2 R20 416.2 F 416.2 E * VVN-T
0.0 E * -Z-R
1.00 E * -R
0.0 E * VLN-T
0.0 E * -Z-R
0.0 E * -R
0.0 E * TVN
R08 432.525 R01 400.78 R01 403.55 R02 400.78 E * TLN
R08 432.525 R01 423.40 R01 403.55 R02 400.78 E * PN
R 8 2.60E+05 F 2.60E+05 E * PAN
0.0 E

```

***** LEVEL 0 *****

```

R 4 4.698880 R 4 8.580000 R 4 2.599925 E * HSA
1 0.000 R 1 0.007250 R 1 0.0115900 R 1 0.01304 S * HSX- 1
0.014490 S * HSX- 1 * HSX- 2
1 0.000 R 1 0.007250 R 1 0.0115900 R 1 0.01304 S * HSX- 2 * HSX- 2
0.014490 S * HSX- 2 * HSX- 3
1 0.000 R 1 0.007250 R 1 0.0115900 R 1 0.01304 S * HSX- 3 * HSX- 3
0.014490 S * HSX- 3 * HSX- 4
1 0.000 R 1 0.007250 R 1 0.0115900 R 1 0.01304 S * HSX- 4 * HSX- 4
0.014490 S * HSX- 4 * HSX- 5
1 0.000 R 1 0.008340 R 1 0.0133430 R 1 0.01501 S * HSX- 5 * HSX- 5
0.016679 S * HSX- 5 * HSX- 6
1 0.000 R 1 0.008340 R 1 0.0133430 R 1 0.01501 S * HSX- 6 * HSX- 6
0.016679 S * HSX- 6 * HSX- 7
1 0.000 R 1 0.008340 R 1 0.0133430 R 1 0.01501 S * HSX- 7 * HSX- 7
0.016679 S * HSX- 7 * HSX- 8
1 0.000 R 1 0.008340 R 1 0.0133430 R 1 0.01501 S * HSX- 8 * HSX- 8
0.016679 S * HSX- 8 * HSX- 9
1 0.000 R 1 .05630 R 1 .090000 R 1 0.10130 S * HSX- 9 * HSX- 9
0.11250 S * HSX- 9 * HSX- 10
1 0.000 R 1 .05630 R 1 .090000 R 1 .10130 S * HSX- 10 * HSX- 10
0.11250 S * HSX- 10 * HSX- 11
1 0.000 R 1 .05630 R 1 .090000 R 1 .10130 S * HSX- 11 * HSX- 11
0.11250 S * HSX- 11 * HSX- 12
1 0.000 R 1 .05630 R 1 .090000 R 1 .10130 S * HSX- 12 * HSX- 12
0.11250 E * HSX- 12
0.0 E * CFZL-T
0.0 E * -Z-R
4 2.38 F 0. E * CFZY-T
0.0 E * -Z-R
0.0 E * -R
4 2.38 F 0. E * VOL
4 0.913520 R 4 0.86154000 R 4 0.62667 E * FA-T
4 0.404970 R 4 0.5060670 R 1 0.66730 R 1 0.6375000 S * FA-Z
1 0.667300 R 1 0.6375000 E * FA-R
4 0.589280 R 4 0.7246980 R 4 0.683125 E * HD-T
4 0.393900 R 4 0.0 E * HD-Z
4 0.346220 R 4 0.53580000 R 1 0.422780 R 1 0.40631 S * -R
1 0.422780 R 1 0.40631000 E * HSTN
4 0.239900 R 4 0.60509000 R 4 0.339170 E * MATHS
0.181000 F 0.0 E * ALPN
20 416.2 R20 416.2 F 416.2 E * VVN-T
0.0 E * -Z-R
1.00 E * -R
0.0 E * VLN-T
0.0 E * -Z-R
0.0 E * -R
0.0 E * TVN
R08 432.525 R01 400.78 R01 403.55 R02 400.78 E * TLN
R08 432.525 R01 423.40 R01 403.55 R02 400.78 E * PN
R 8 2.60E+05 F 2.60E+05 E

```

```

R 4 4.748920 R 4 8.349300 R 4 3.161260 E * HSA
R 1 0.000 R 1 0.0070100 R 1 0.01122000R 1 .012620000$ HSX-1 * HSX-1
R 1 0.014020 S HSX-1 * HSX-2
R 1 0.000 R 1 0.0070100 R 1 0.01122000R 1 .012620000$ HSX-2 * HSX-2
R 1 0.014020 S HSX-2 * HSX-3
R 1 0.000 R 1 0.0070100 R 1 0.01122000R 1 .012620000$ HSX-3 * HSX-3
R 1 0.014020 S HSX-3 * HSX-4
R 1 0.000 R 1 0.0070100 R 1 0.01122000R 1 .012620000$ HSX-4 * HSX-4
R 1 0.015680 S HSX-4 * HSX-5
R 1 0.000 R 1 0.0078400 R 1 0.01254500R 1 .014113000$ HSX-5 * HSX-5
R 1 0.015680 S HSX-5 * HSX-6
R 1 0.000 R 1 0.0078400 R 1 0.01254500R 1 .014113000$ HSX-6 * HSX-6
R 1 0.015680 S HSX-6 * HSX-7
R 1 0.000 R 1 0.0078400 R 1 0.01254500R 1 .014113000$ HSX-7 * HSX-7
R 1 0.015680 S HSX-7 * HSX-8
R 1 0.000 R 1 0.0078400 R 1 0.01254500R 1 .014113000$ HSX-8 * HSX-8
R 1 0.015680 S HSX-8 * HSX-9
R 1 0.000 R 1 .0614600 R 1 0.0983400 R 1 .11063000 S HSX-9 * HSX-9
R 1 0.122926 S HSX-9 * HSX-10
R 1 0.000 R 1 .0614600 R 1 0.0983400 R 1 .11063000 S HSX-10 * HSX-10
R 1 0.122926 S HSX-10 * HSX-11
R 1 0.000 R 1 0.06146 R 1 0.0983400 R 1 .11063000 S HSX-11 * HSX-11
R 1 0.122926 S HSX-11 * HSX-12
R 1 0.000 R 1 0.06146 R 1 0.0983400 R 1 .11063000 S HSX-12 * HSX-12
R 1 0.122926 E HSX-12
R 1 0.0 E * CFZL-T
R 1 0.0 E * -Z
R 4 2.38 F 0. E * -R
R 1 0.0 E * CFZY-T
R 1 0.0 E * -Z
R 4 2.38 F 0. E * -R
R 4 0.977230 R 4 0.9032550 R 4 0.371325 E * VOL
R 4 0.404970 R 4 0.5060600 R 1 0.84000 R 1 0.5600000 S * FA-T
R 1 0.840000 R 1 0.5600000 E * FA-T
R 4 0.589280 R 4 0.72470 R 4 0.60653 E * FA-Z
R 1 0.393900 F 0.0 E * FA-R
R 4 0.34620 R 4 0.51200 R 1 0.360000 R 1 0.24000 S * HD-T
R 1 0.360000 R 1 0.24000 E * HD-T
R 4 0.239900 R 4 0.610970 R 4 0.38667 E * -Z
R 4 0.184000 F 0.000010 E * -R
R 20 416.2 R20 416.2 F 416.2 E * HSTN
R 1 1.00 E * MATHS
R 1 0.0 E * ALPN
R 1 0.0 E * VVN-T
R 1 0.0 E * -Z
R 1 0.0 E * -R
R 1 0.0 E * VLN-T
R 1 0.0 E * -Z
R 1 0.0 E * -R
R 08 432.525 R04 423.40 E * TVN
R 08 432.525 R04 423.40 E * TLN
R 8 2.60E+05 F 2.60E+05 E * PN
R 1 0.0 E * PAN
  
```

```

R 4 6.905860 R 4 17.60332 R 4 5.32816 E * HSA
R 1 0.000 R 1 0.0077100 R 1 0.01233000R 1 .013880000$ HSX-1 * HSX-1
R 1 0.015420 S HSX-1 * HSX-2
R 1 0.000 R 1 0.0077100 R 1 0.01233000R 1 .013880000$ HSX-2 * HSX-2
R 1 0.015420 S HSX-2 * HSX-3
R 1 0.000 R 1 0.0077100 R 1 0.01233000R 1 .013880000$ HSX-3 * HSX-3
R 1 0.015420 S HSX-3 * HSX-4
R 1 0.000 R 1 0.0077100 R 1 0.01233000R 1 .013880000$ HSX-4 * HSX-4
R 1 0.015420 S HSX-4 * HSX-5
R 1 0.000 R 1 0.0119600 R 1 0.01914000R 1 .021530000$ HSX-5 * HSX-5
R 1 0.023922 S HSX-5 * HSX-6
R 1 0.000 R 1 0.0119600 R 1 0.01914000R 1 .021530000$ HSX-6 * HSX-6
R 1 0.023922 S HSX-6 * HSX-7
R 1 0.000 R 1 0.0119600 R 1 0.01914000R 1 .021530000$ HSX-7 * HSX-7
R 1 0.023922 S HSX-7 * HSX-8
R 1 0.000 R 1 0.0119600 R 1 0.01914000R 1 .021530000$ HSX-8 * HSX-8
R 1 0.023922 S HSX-8 * HSX-9
R 1 0.000 R 1 .056300 R 1 .0900000 R 1 .1080000 S HSX-9 * HSX-9
R 1 0.12 S HSX-9 * HSX-10
R 1 0.000 R 1 .056300 R 1 .0900000 R 1 .1080000 S HSX-10 * HSX-10
R 1 0.12 S HSX-10 * HSX-11
R 1 0.000 R 1 0.0600 R 1 0.0960000 R 1 .1080000 S HSX-11 * HSX-11
R 1 0.12 S HSX-11 * HSX-12
R 1 0.000 R 1 0.0600 R 1 0.0960000 R 1 .1080000 S HSX-12 * HSX-12
R 1 0.12 E * HSX-12
R 1 0.0 E * CFZL-T
R 1 0.0 E * -Z
R 4 2.38 F 0. E * -R
R 1 0.0 E * CFZY-T
R 1 0.0 E * -Z
R 4 2.38 F 0. E * -R
R 4 1.068148 R 4 1.02422000 R 4 0.475235 E * VOL
R 4 0.425200 R 4 0.5602600 R 1 0.475480 R 1 0.44663000 S * FA-T
R 1 0.475480 R 1 0.4466300 E * FA-T
R 4 0.063943 R 4 0.282280 R 4 0.00139258 E * FA-Z
R 1 0.424500 F 0.0 E * FA-R
R 4 0.251160 R 4 0.3027900 R 1 0.271200 R 1 0.25894000 S * HD-T
R 1 0.271200 R 1 0.2589400 E * HD-T
R 8 0.035763 R 4 0.000443 E * -Z
  
```


R 4 0.19458 F 1.0E-12 E
 R30 416.2 R30 416.2 F 416.2 E
 1.00 E
 0.0
 0.0
 0.0
 0.0
 0.0
 0.0
 R08 432.525 R04 423.40 E
 R08 432.525 R04 423.40 E
 R 8 2.60E+05 F 2.60E+05 E
 0.0 E

* -R
 HSTN
 * MATHS
 * ALPN
 * VVN-T
 * -Z
 * -R
 * -R
 * VLN-T
 * -Z
 * -R
 * -R
 * TVN
 * TLN
 * PN
 * PAN

..... LEVEL 13

R 4 30.1816 R 4 41.8896 R 4 9.1754 E * HSA
 R 1 0.000 R 1 0.0070390 R 1 0.01126200R 1 .012670000\$ HSX- 1 * HSX- 1
 R 1 0.014078 S HSX- 2 * HSX- 2
 R 1 0.000 R 1 0.0070390 R 1 0.01126200R 1 .012670000\$ HSX- 3 * HSX- 3
 R 1 0.014078 S HSX- 4 * HSX- 4
 R 1 0.000 R 1 0.0070390 R 1 0.01126200R 1 .012670000\$ HSX- 5 * HSX- 5
 R 1 0.014078 S HSX- 6 * HSX- 6
 R 1 0.000 R 1 0.0108000 R 1 0.01728000R 1 .019440000\$ HSX- 7 * HSX- 7
 R 1 0.021600 S HSX- 8 * HSX- 8
 R 1 0.000 R 1 0.0108000 R 1 0.01728000R 1 .019440000\$ HSX- 9 * HSX- 9
 R 1 0.021600 S HSX- 10 * HSX- 10
 R 1 0.000 R 1 0.06500 R 1 0.10400 R 1 .117000 S * HSX- 11 * HSX- 11
 R 1 0.130 S * HSX- 12 * HSX- 12
 R 1 0.000 R 1 0.06500 R 1 0.10400 R 1 .117000 S * HSX- 13 * HSX- 13
 R 1 0.130 S * CFZL-T
 R 1 0.000 R 1 0.06500 R 1 0.10400 R 1 .117000 S * -Z
 R 1 0.130 S * -R
 R 1 0.000 R 1 0.06500 R 1 0.10400 R 1 .117000 S * CFZV-T
 R 1 0.130 S * -Z
 R 1 0.000 R 1 0.06500 R 1 0.10400 R 1 .117000 S * -R
 R 1 0.130 S * -R
 R 4 0.726035 R 4 0.40182000 R 4 0.208948 E * VOL
 R 4 0.629690 R 4 0.59701000 R 4 0.100010 E * FA-T
 R 4 0.000 E * FA-Z * FA-R
 R 4 0.879560 R 4 0.27527000 R 4 0.0 HD-T
 R 4 0.362360 R 4 0.803075 R 4 0.186210 E * HD-Z * HD-R
 R 4 0.0001 E * HSTN
 R 4 0.491590 R 4 0.9099700 R 4 1.0E-12 * MATHS
 416.2 E * ALPN
 6 E * VVN-T
 1.00 E * -Z
 0.0 E * -R
 0.0 E * -R
 0.0 E * VLN-T
 0.0 E * -Z
 0.0 E * -R
 432.525 E * TVN
 432.525 E * TLN
 2.60E+05 E * PN
 0.0 E * PAN

..... COMPONENT NO. 107

FILL JUN1 107 107 VESSEL KTA DRAIN * C
 107 IFTY IOFF C 2
 * IFTR IFSV 1 NFTB NFSV NFRF C 3
 * 666 100 1
 * TWOLD RFXM CONCIN C 4
 * .00000E+00 240 .00000E+00
 * DXIN VQINN ALPIN VLIN TLIN C 5
 * 1.0 0.2514 0.0 0.0 VVIN TVIN C 6
 * PIN PAIN FLOWIN 0.0 308.15
 * 4.0E+05 0.0 0.0 C 9
 * VMSCL VVSCL
 * 1 1
 * VESSEL DRAIN FILL TABLE PAIRS= 1 *
 * TIME (S) DRAIN FLOW (KG/S)
 * 0.00000E+00 0.00000E+00 E

..... COMPONENT NO. 101

TEE 101 101 VESSEL DRAIN LOOPS 2 3
 JCELL NODES MAT COST ICHF C 2
 * 04 4 6 0 0
 * ICONC1 NCELL1 JUN1 JUN2 IPOW1 C 3
 * 0 06 102 105 0 0
 * IQPTR1 IQPSV1 NQPT1 NQPSV1 NQPRF1 C 5
 * 0 0 0 0 0
 * RADIN1 TH1 HOUTL1 HOUTV1 TOUTL1 C 6
 * 0.1985 .01 0. 30

* TOUTV1	PWIN1	PWOFF1	RPWMX1	PWSCL1	C 7
300	0	0	0		
QPIN1	QPOFF1	RQPMX1	QPSCL1		C 8
0	0	0	0		
ICONC2	NCELL2	JUN3	IPOW2		C 9
0	2	0	0		
IQPTR2	IQPSV2	NQPTB2	NQPSV2	NQPRF2	C 11
0	0	0	0	0	
RADIN2	TH2	HOUTL2	HOUTV2	TOUTL2	C 12
0.1965	.01	0	300	0	
TOUTV2	PWIN2	PWOFF2	RPWMX2	PWSCL2	C 13
300	0	0	0		
QPIN2	QPOFF2	RQPMX2	QPSCL2		C 14
0	0	0	0		

* PRIMARY *

0.396	1.750	4.150	800	4.400 S	* DX
12.350	E				
0.0480	0.2123	0.5034		0.5337 S	* VOL
1.4981	E				
0. F	0.1213 E				* FA
0	8.82E-3	3.21E-3			* S FRIC
0	1.07E-3	E			* FRIC
0	8.82E-3	3.21E-3	2.80E-3		* S REVFRIC
0	1.07E-3	E			* REVFRIC
-1	-0.2731	-0.0093	-0.0086	-0.0100 S	* GRAV
-0.0092	-0.3028	E			* GRAV
7 0.393	E				* HD
0 E					* ICFLAG
1 E					* NFF
1.0 E					* ALP
0.0 E					* VL
0.0 E					* VV
450.00 E					* TV
450.00 E					* P
2.60E+05 E					* PA
0.0 E					* QPPP
0.0 E					* MATID
6 E					* TW
449.00 E					

* SECONDARY *

1.850	0.383	E			* DX
0.2244	0.0465 E				* VOL
R 2 0.1213	0.2				* FA
0	8.47E-3	0 E			* FRIC
0	8.47E-3	0 E			* REVFRIC
0	0.2688	1. E			* GRAV
0.3v3 E					* HD
0 E					* ICFLAG
1 E					* NFF
1.0 E					* ALP
0.0 E					* VL
0.0 E					* VV
450.00 E					* TV
450.00 E					* P
2.60E+05 E					* PA
0.0 E					* QPPP
0.0 E					* MATID
6 E					* TW
449.00 E					

COMPONENT NO. 102

* TEE	JCELL	102	102	VESEL DRAIN LOOPS 1,4	
03	NODES	MAT	COST	ICHF	C 2
ICONC1	NCELL1	JUN1	JUN2	IPOW1	C 3
0	04	104	106	0	
IQPTR1	IQPSV1	NQPTB1	NQPSV1	NQPRF1	C 5
0	0	0	0	0	
RADIN1	TH1	HOUTL1	HOUTV1	TOUTL1	C 6
0.1965	.01	0	300	0	
TOUTV1	PWIN1	PWOFF1	RPWMX1	PWSCL1	C 7
300	0	0	0		
QPIN1	QPOFF1	RQPMX1	QPSCL1		C 8
0	0	0	0		
ICONC2	NCELL2	JUN3	IPOW2		C 9
0	2	101	0		
IQPTR2	IQPSV2	NQPTB2	..QPSV2	NQPRF2	C 11
0	0	0	0	0	
RADIN2	TH2	HOUTL2	HOUTV2	TOUTL2	C 12
0.1965	.01	0	300	0	
TOUTV2	PWIN2	PWOFF2	RPWMX2	PWSCL2	C 13
300	0	0	0		
QPIN2	QPOFF2	RQPMX2	QPSCL2		C 14
0	0	0	0		

* PRIMARY *

0.8960	1.750	3.150	7.350 E		* DX
0.0480	0.2123	0.2893	0.8916 E		* VOL
0. F	0.1213 E				* FA
0	8.82E-3	3.86E-3	0	1.80E-3 E	* FRIC
0	8.82E-3	3.86E-3	0	1.80E-3 E	* REVFRIC
-1.0	-0.1934	-0.0094	-0.0095	-0.3064 E	* GRAV
R 5 0.393	E				* HD
0 E					* ICFLAG
1 E					* NFF
1.0 E					* ALP
0.0 E					* VL

```

0.0 E
450.00 E
450.00 E
2.80E+05 E
0.0
0.0
6
449.00 E
SECONDARY *
1.750 0.391 E
0.2123 0.0474 E
R 2 0.1213 0 E
0. 8.84E-03 0.0
0. 8.84E-03 0.0
0. 0.2032 1. E
0.393 E
0
1
0
0
0
450.00 E
450.00 E
2.80E+05 E
0.0
0.0
6
449.00 E

```

```

VV
TV
P
PA
QPPP
MATID
TW
DX
VOL
FA
FRIC
REVFRIC
GRAV
HD
ICFLG
NFF
ALP
VL
VV
TV
P
PA
QPPP
MATID
TW

```

.....
COMPONENT NO. 103

TEE	JCELL	103 NODES	103 VESSEL DRAIN PART2-TO FILL MAT	COST	ICRF	C 2
*	ICONC1	02	6	JUN1	JUN2	IPOW1 C 3
*	IQPTR1	03	106	NQPTB1	NQPSV1	NQPRF1 C 5
*	RADIN1	01	0	HOUTL1	HOUTV1	TOUTL1 C 6
*	TOUTV1	0	0	PWIN1	PWOFF1	RPWMX1 PWSCL1 C 7
*	QPIN1	0	0	QPOFF1	RQPMX1	QPSCL1 C 8
*	ICONC2	02	6	JUN3	IPOW2	C 9
*	IQPTR2	03	106	NQPTB2	NQPSV2	NQPRF2 C 11
*	RADIN2	01	0	HOUTL2	HOUTV2	TOUTL2 C 12
*	TOUTV2	0	0	PWIN2	PWOFF2	RPWMX2 PWSCL2 C 13
*	QPIN2	0	0	QPOFF2	RQPMX2	QPSCL2 C 14

```

PRIMARY *
5.332 2.461 2.614 E
0.6468 0.2985 0.3049 E
F 0.1213 E
1.07E-03 3.86E-03 0.0
1.07E-03 3.86E-03 0.0
-0.3028 -0.6804 -0.0018 0. E
R 4 0.393 E
0
1
1.0
0.0
0.0
0.0
450.00 E
450.00 E
2.80E+05 E
0.0
0.0
6
449.00 E
SECONDARY *
2.528 3.143 E
0.3066 0.3812 E
F 0.1213 E
1.95E-04 8.56E-04 1.80E-03 E
1.95E-03 8.56E-04 1.80E-03 E
4348 0.9367 0.3064 E
0.393 E
0
1
0
0
0
450.00 E
450.00 E
2.80E+05 E
0.0
0.0
6
449.00 E

```

```

DX
VOL
FA
FRIC
REVFRIC
GRAV
HD
ICFLG
NFF
ALP
VL
VV
TV
P
PA
QPPP
MATID
TW
DX
VOL
FA
FRIC
REVFRIC
GRAV
HD
ICFLG
NFF
ALP
VL
VV
TV
P
PA
QPPP
MATID
TW

```

COMPONENT NO. 501

TEE	JCELL	501 NODES	601 MAT	COST	ICHP	C 1		
ICONC1	0	NCELL1	701	JUN1	501	JUN2	IPOW1	C 3
RADIN1	0	TH1	HOUTL1	HOUTV1	TOUTL1	C 6		
TOUTV1	0	PWIN1	PWOFF1	RPWMX1	PWSCL1	C 7		
ICONC2	0	NCELL2	601	JUN3	IPOW2	C 9		
RADIN2	0	TH2	HOUTL2	HOUTV2	TOUTL2	C 12		
TOUTV2	0	PWIN2	PWOFF2	RPWMX2	PWSCL2	C 13		

PRIMARY

2 0.9 E
 3 0.52 F
 577710 F
 52 E
 577710 E
 1.0E15 E
 0.7184 E
 432.525 E
 432.525 E
 2.60E+05 E
 0. E

DX
 VOL FA
 FRIC
 RVFRIC
 GRAV
 HD
 ICFLG
 NFF
 ALP
 VL
 VV
 TL
 TV
 P
 PA

SECONDARY

0.9 E
 0.52 F
 577710 E
 1.0E15 E
 0.7184 E
 432.525 E
 432.525 E
 2.60E+05 E
 0. E

DX
 VOL FA
 FRIC
 RVFRIC
 GRAV
 HD
 ICFLG
 NFF
 ALP
 VL
 VV
 TL
 TV
 P
 PA

COMPONENT NO. 502

TEE	JCELL	502 NODES	602 MAT	COST	ICHP	C 2		
ICONC1	0	NCELL1	702	JUN1	502	JUN2	IPOW1	C 3
RADIN1	0	TH1	HOUTL1	HOUTV1	TOUTL1	C 6		
TOUTV1	0	PWIN1	PWOFF1	RPWMX1	PWSCL1	C 7		
ICONC2	0	NCELL2	602	JUN3	IPOW2	C 9		
RADIN2	0	TH2	HOUTL2	HOUTV2	TOUTL2	C 12		
TOUTV2	0	PWIN2	PWOFF2	RPWMX2	PWSCL2	C 13		

PRIMARY

2 0.9 E
 3 0.52 F
 577710 F
 52 E
 577710 E
 1.0E15 E
 0.7184 E
 432.525 E
 432.525 E
 2.60E+05 E
 0. E

DX
 VOL FA
 FRIC
 RVFRIC
 GRAV
 HD
 ICFLG
 NFF
 ALP
 VL
 VV
 TL
 TV
 P
 PA

SECONDARY

0.9 E
 0.52 F
 577710 E
 1.0E15 E
 0.7184 E
 432.525 E
 432.525 E
 2.60E+05 E
 0. E

DX
 VOL FA
 FRIC
 RVFRIC
 GRAV
 HD
 ICFLG
 NFF
 ALP
 VL
 VV

432.525 E
 432.525 E
 2.60E+05 E
 0. E

TL
 TV
 P
 PA

COMPONENT NO. 503

TEE	JCELL	503 NODE 1	503 MAT	503 CORE SIMULATOR COST	TEE CELL 3 ICHP	C 2
•	ICONC1	0 NCELL1	6 JUN1	0 JUN2	IPOW1	C 3
•	RADIN1	4 TH1	703 HOUTL1	503 HOUTV1	TOUTL1	C 6
•	TOUTV1	.006 PWIN1	0 PWOFF1	300 RPWMX1	PWSCL1	C 7
•	ICONC2	0 NCELL2	603 JUNS	0 IPOW2		C 9
•	RADIN2	4 TH2	603 HOUTL2	0 HOUTV2	TOUTL2	C 12
•	TOUTV2	.006 PWIN2	0 PWOFF2	300 RPWMX2	PWSCL2	C 13

* PRIMARY *
 0.9 E
 0.52 F
 .577710 F
 0. E
 1.0E15 E
 0. E
 0.7184 E
 0. E
 1. E
 0. E
 0. E
 0. E
 432.525 E
 432.525 E
 2.60E+05 E
 0. E
 * SECONDARY *
 0.9 E
 0.52 F
 .577710 E
 1. E15 E
 0. E
 1. E
 0.7184 E
 0. E
 0. E
 1. E
 0. E
 0. E
 432.525 E
 432.525 E
 2.60E+05 E
 0. E

DX
 VOL
 FA
 • FRIC
 RVFRIC
 GRAV
 HD
 • ICFLG
 NFF
 ALP
 VL
 VV
 • TL
 TV
 P
 PA
 • DX
 VOL
 FA
 • FRIC
 RVFRIC
 GRAV
 HD
 • ICFLG
 NFF
 ALP
 VL
 VV
 • TL
 TV
 P
 PA

COMPONENT NO. 504

TEE	JCELL	504 NODES	504 MAT	504 CORE SIMULATOR COST	TEE CELL 4 ICHP	C 2
•	ICONC1	0 NCELL1	6 JUN1	0 JUN2	IPOW1	C 3
•	RADIN1	4 TH1	704 HOUTL1	504 HOUTV1	TOUTL1	C 6
•	TOUTV1	.006 PWIN1	0 PWOFF1	300 RPWMX1	PWSCL1	C 7
•	ICONC2	0 NCELL2	604 JUNS	0 IPOW2		C 9
•	RADIN2	4 TH2	604 HOUTL2	0 HOUTV2	TOUTL2	C 12
•	TOUTV2	.006 PWIN2	0 PWOFF2	300 RPWMX2	PWSCL2	C 13

* PRIMARY *
 0.9 E
 0.52 F
 .577710 F
 0. E
 1.0E15 E
 0. E
 0.7184 E
 0. E
 1. E
 0. E
 0. E
 0. E
 432.525 E
 432.525 E
 2.60E+05 E
 0. E
 * SECONDARY *
 0.9 E
 0.52 F
 .577710 E
 1. E15 E
 0. E
 1. E
 0.7184 E
 0. E
 0. E

DX
 VOL
 FA
 • FRIC
 RVFRIC
 GRAV
 HD
 • ICFLG
 NFF
 ALP
 VL
 VV
 • TL
 TV
 P
 PA
 • DX
 VOL
 FA
 • FRIC
 RVFRIC
 GRAV
 HD

```

      0
      0
      1.
      0.
      0.
      432.525 E
      432.525 E
      2.60E+05 E
      0. E
  
```

```

      * ICFLG
      * NFF
      * ALP
      * VL
      * VV
      * TL
      * TV
      * P
      * PA
  
```

..... COMPONENT NO. 505

TEE	JCELL	505 NODES	505 MAT	COST	ICHP	C 2
* ICONC1	3	0	6	1.	JUN2	IPOW1 C 3
* RADIN1	4	705	505	0	HOUTV1	TOUTL1 C 6
* TOUTV1	65	.006	0.	0.	RPWMX1	PWSCL1 C 7
* ICONC2	300	0.	0.	0.	IPOW2	C 9
* RADIN2	0	2	605	0	HOUTV2	TOUTL2 C 12
* TOUTV2	65	.006	0.	0.	RPWMX2	PWSCL2 C 13
	300	0.	0.	0.		

```

* PRIMARY *
R 2 0.9 E
R 3 0.719356 F 0.719356 E
R 3 7.999284 F 7.999284 E
      0. E
      1.0E15 E
      0. E
      0.861 E
      0.
      1.
      0.
      0.
      432.525 E
      432.525 E
      2.60E+05 E
      0. E
  
```

```

      * DX
      * VOL
      * FA
      * FRIC
      * RVFRIC
      * GRAV
      * HD
      * ICFLG
      * NFF
      * ALP
      * VL
      * VV
      * TL
      * TV
      * P
      * PA
  
```

..... SECONDARY

```

R 2 0.9 E
R 3 0.7193560 E
R 3 0.7999284 E
      1.E15 E
      0.
      0.
      0.861 E
      0.
      1.
      0.
      0.
      432.525 E
      432.525 E
      2.60E+05 E
      0. E
  
```

```

      * DX
      * VOL
      * FA
      * FRIC
      * RVFRIC
      * GRAV
      * HD
      * ICFLG
      * NFF
      * ALP
      * VL
      * VV
      * TL
      * TV
      * P
      * PA
  
```

..... COMPONENT NO. 506

TEE	JCELL	506 NODES	506 MAT	COST	ICHP	C 2
* ICONC1	3	0	6	1.	JUN2	IPOW1 C 3
* RADIN1	4	706	506	0	HOUTV1	TOUTL1 C 6
* TOUTV1	65	.006	0.	0.	RPWMX1	PWSCL1 C 7
* ICONC2	300	0.	0.	0.	IPOW2	C 9
* RADIN2	0	2	606	0	HOUTV2	TOUTL2 C 12
* TOUTV2	65	.006	0.	0.	RPWMX2	PWSCL2 C 13
	300	0.	0.	0.		

```

* PRIMARY *
R 2 0.9 E
R 3 7.19356 F 7.19356 E
R 3 7.999284 F 7.999284 E
      0. E
      1.0E15 E
      0. E
      0.861 E
      0.
      1.
      0.
      0.
      432.525 E
      432.525 E
      2.60E+05 E
      0. E
  
```

```

      * DX
      * VOL
      * FA
      * FRIC
      * RVFRIC
      * GRAV
      * HD
      * ICFLG
      * NFF
      * ALP
      * VL
      * VV
      * TL
      * TV
      * P
      * PA
  
```

..... SECONDARY

```

R 2 0.9 E
R 3 7.19356 E
  
```

```

      * DX
      * VOL
  
```

0.7999284 E
 1.E15 E
 0. E
 0. E
 0.861 E
 0. E
 432.525 E
 432.525 E
 1.60E+05 E
 0. E

PA
 FRIC
 RVFRIC
 GRAV
 HD
 ICFLG
 NFF
 ALP
 VL
 VV
 TV
 TV
 P
 PA

COMPONENT NO. 507

TEE 507 CORE SIMULATOR TEE CELL 7
 JCELL NODES MAT COST ICHF C 2
 3 0 1 0 0
 * ICONC1 NCELL1 6 JUN1 1 JUN2 0 IPOW1 C 3
 0 4 707 507 0
 * RADIN1 TH1 HOUTL1 HOUTV1 TOUTL1 C 6
 65 .006 0. PWIN1 PWOFF1 RPWMX1 PWSCL1 C 7
 * TOUTV1 300 0. 0. 300
 * ICONC2 NCELL2 6 JUN3 0 IPOW2 C 9
 0 2 607 0
 * RADIN2 TH2 HOUTL2 HOUTV2 TOUTL2 C 12
 65 .006 0. 0. 300
 * TOUTV2 300 0. 0. 0. 300
 PWIN2 PWOFF2 RPWMX2 PWSCL2 C 13

PRIMARY
 R 2 0.9 E
 719356 F 719356 E
 R 3 7999284 F 7999284 E
 0. E
 1.0E15 E
 0. E
 0.861 E
 0. E
 1. E
 0. E
 0. E
 432.525 E
 432.525 E
 2.60E+05 E
 0. E

DX VOL
 FA
 FRIC
 RVFRIC
 GRAV
 HD
 ICFLG
 NFF
 ALP
 VL
 VV
 TV
 TV
 P
 PA

SECONDARY

0.9 E
 719356 E
 7999284 E
 1.E15 E
 0. E
 0. E
 0.861 E
 0. E
 0. E
 1. E
 0. E
 0. E
 432.525 E
 432.525 E
 2.60E+05 E
 0. E

DX VOL
 FA
 FRIC
 RVFRIC
 GRAV
 HD
 ICFLG
 NFF
 ALP
 VL
 VV
 TV
 TV
 P
 PA

COMPONENT NO. 508

TEE 508 CORE SIMULATOR TEE CELL 8
 JCELL NODES MAT COST ICHF C 2
 3 0 1 0 0
 * ICONC1 NCELL1 6 JUN1 1 JUN2 0 IPOW1 C 3
 0 4 708 508 0
 * RADIN1 TH1 HOUTL1 HOUTV1 TOUTL1 C 6
 65 .006 0. PWIN1 PWOFF1 RPWMX1 PWSCL1 C 7
 * TOUTV1 300 0. 0. 300
 * ICONC2 NCELL2 6 JUN3 0 IPOW2 C 9
 0 2 608 0
 * RADIN2 TH2 HOUTL2 HOUTV2 TOUTL2 C 12
 65 .006 0. 0. 300
 * TOUTV2 300 0. 0. 0. 300
 PWIN2 PWOFF2 RPWMX2 PWSCL2 C 13

PRIMARY
 R 2 0.9 E
 719356 F 719356 E
 R 3 7999284 F 7999284 E
 0. E
 1.0E15 E
 0. E
 0.861 E
 0. E
 1. E
 0. E
 0. E
 432.525 E
 432.525 E

DX VOL
 FA
 FRIC
 RVFRIC
 GRAV
 HD
 ICFLG
 NFF
 ALP
 VL
 VV
 TV
 TV
 P
 PA

2.60E+05 E
 0 E
 SECONDARY *
 0 E
 719356 E
 7699284 E
 1.E18 E
 0 E
 0.861 E
 0 E
 0 E
 1 E
 0 E
 0 E
 452.525 E
 432.525 E
 2.60E+05 E
 0 E

* PA P
 * DX
 * VOL
 * FA
 * FRIC
 * RYFRIC
 * GRAV
 * HD
 * ICFLG
 * NFF
 * ALP
 * VL
 * VV
 * TL
 * TV
 * P
 * PA

COMPONENT NO.701

FILL JUN1 701 701 CORE FEEDBACK FILL CELL 01 * C 1
 IFTY IOFF C 2
 IFTR IFSV 1 NFTB NFSV NFRF C 3
 0 0 0 0 0
 TWTOLD 0 RFMX 0 CONCIN C 4
 0 0
 DXIN 30 VOLIN 0 ALPIN VLIN TLIN C 5
 0 52 1 0 461.14
 PIN PAIN FLOWIN VVIN TVIN C 6
 19.8E+05 0 0 0 461.14

COMPONENT NO.702

FILL JUN1 702 702 CORE FEEDBACK FILL CELL 02 * C 1
 IFTY IOFF C 2
 IFTR IFSV 1 NFTB NFSV NFRF C 3
 0 0 0 0 0
 TWTOLD 0 RFMX 0 CONCIN C 4
 0 0
 DXIN 30 VOLIN 0 ALPIN VLIN TLIN C 5
 0 52 1 0 461.14
 PIN PAIN FLOWIN VVIN TVIN C 6
 19.88E+05 0 0 0 461.14

COMPONENT NO.703

FILL JUN1 703 703 CORE FEEDBACK FILL CELL 03 * C 1
 IFTY IOFF C 2
 IFTR IFSV 1 NFTB NFSV NFRF C 3
 0 0 0 0 0
 TWTOLD 0 RFMX 0 CONCIN C 4
 0 0
 DXIN 30 VOLIN 0 ALPIN VLIN TLIN C 5
 0 52 1 0 461.14
 PIN PAIN FLOWIN VVIN TVIN C 6
 19.88E+05 0 0 0 461.14

COMPONENT NO.704

FILL JUN1 704 704 CORE FEEDBACK FILL CELL 04 * C 1
 IFTY IOFF C 2
 IFTR IFSV 1 NFTB NFSV NFRF C 3
 0 0 0 0 0
 TWTOLD 0 RFMX 0 CONCIN C 4
 0 0
 DXIN 30 VOLIN 0 ALPIN VLIN TLIN C 5
 0 52 1 0 461.14
 PIN PAIN FLOWIN VVIN TVIN C 6
 19.88E+05 0 0 0 461.14

COMPONENT NO.705

FILL JUN1 705 705 CORE FEEDBACK FILL CELL 05 * C 1
 IFTY IOFF C 2
 IFTR IFSV 1 NFTB NFSV NFRF C 3
 0 0 0 0 0
 TWTOLD 0 RFMX 0 CONCIN C 4
 0 0
 DXIN 30 VOLIN 0 ALPIN VLIN TLIN C 5
 0 719356 1 0 461.14
 PIN PAIN FLOWIN VVIN TVIN C 6
 19.88E+05 0 0 0 461.14

COMPONENT NO.706

FILL JUN1 706 706 CORE FEEDBACK FILL CELL 06 * C 1
 IFTY IOFF C 2
 IFTR IFSV 1 NFTB NFSV NFRF C 3
 0 0 0 0 0
 TWTOLD 0 RFMX 0 CONCIN C 4
 0 0
 DXIN 30 VOLIN 0 ALPIN VLIN TLIN C 5
 0 719356 1 0 461.14
 PIN PAIN FLOWIN VVIN TVIN C 6
 19.88E+05 0 0 0 461.14

COMPONENT NO.707


```

* FILL 707 707 CORE FEEDBACK FILL CELL 07 * C
JUN1 IFTY IOFF C 2
* 707 2
IFTR IFSV 1 NFTB NFSV NFRF C 3
* 0 0 0 0
TWTOLD RFMX 0 CONCIN C 4
* 0.0 30
DXIN VOLIN 0 ALPIN VLIN TLI C 5
* 9 719356 1 0. 461.14
PIN PAIN FLOWIN 0 VVIN TVIN C 6
* 19.88E+05 0 0 0 461.14
* COMPONENT NO.708

```

```

* FILL 708 708 CORE FEEDBACK FILL CELL 08 * C 1
JUN1 IFTY IOFF C 2
* 708 2
IFTR IFSV 1 NFTB NFSV NFRF C 3
* 0 0 0 0
TWTOLD RFMX 0 CONCIN C 4
* 0.0 50
DXIN VOLIN 0 ALPIN VLIN TLIN C 5
* 9 719356 1 0. 461.14
PIN PAIN FLOWIN 0 VVIN TVIN C 6
* 19.88E+05 0 0 0 461.14
* COMPONENT NO.801

```

```

* FILL 601 601 BASE STEAM-WATER FILL CELL 1
JUN1 IFTY IOFF C 2
* 601 5
IFTR IFSV 1 NFTB NFSV NFRF C 3
* 600 100 0 0
TWTOLD RFMX 0 CONCIN C 4
* 0 100
DXIN VOLIN 0 ALPIN VLIN TLIN C 5
* 9 52 1 0. 484.15
PIN PAIN FLOWIN 0 VVIN TVIN C 6
* 19.4E+05 0 0 0 484.15
VMSCL VVSCL C 9
* 1.0 1.0
T(S) TVSCL PSCL PASCL CONSCL C 10
* 1.0 1.0 1E+05 1.0 1.0
T(S) VLTB(M/S)
* 0.00 0.00
20.00 0.00
30.00 0.00
32.50 0.00
36.00 0.00
40.00 0.00
120.00 0.00
121.00 0.00
140.00 0.00
T(S) VVTB(M/S)
* 0.00 0.00
20.00 0.00
30.00 0.00
32.50 4.09
36.00 2.51
40.00 2.34
120.00 2.57
121.00 0.35
140.00 0.21
T(S) TL
* 0.00 484.15
20.00 484.15
30.00 482.95
32.50 481.15
36.00 481.95
40.00 481.65
120.00 477.15
121.00 477.65
140.00 481.15
T(S) TV
* 0.00 484.15
20.00 484.15
30.00 482.93
32.50 480.15
36.00 481.95
40.00 481.65
120.00 477.15
121.00 477.65
140.00 481.15
T ALPHA
* 0.00 1.0
20.00 1.0
30.00 1.0
32.50 1.0
36.00 1.0
40.00 1.0
120.00 1.0
121.00 1.0
140.00 1.0
T(S) P*BAR
* 0.00 1.64E+01
20.00 1.94E+01
30.00 1.9E+01
32.50 1.79E+01
36.00 1.87E+01
40.00 1.85E+01

```

120.00	1.69E+01	S
121.00	1.71E+01	S
140.00	1.84E+01	S
T(S)	PA(BAR)	
0.00	0.0	S
20.00	0.0	S
30.00	0.0	S
32.50	0.0	S
36.00	0.0	S
40.00	0.0	S
120.00	0.0	S
121.00	0.0	S
140.00	0.0	S

* COMPONENT NO. 603 *

FILL	602	603	BASE STEAM-WATER FILL CELL 2		
JUNI	IFTY	IOFF	C 2		
602	6	0			
IFTR	IFSV	NFTB	NFSV	NFRF	C 3
600	100	0	0	0	
TWXTOLD	RFMX	CONCIN			C 4
0	100	0			
DXIN	VOIN	ALPIN	VLIN	TLIN	C 5
0	0	1.0	484.15		
PIN	PAIN	FLOWIN	VVIN	TVIN	C 6
19.4E+05	0	0	484.15		
VMSCL	VVSCL				C 9
1.0	1.0				
TLSCL	TVSCL	PSCL	PASCL	CONSCL	C 10
1.0	1.0	1E+05	1.0		
T(S)	VLTB(M/S)				
0.00	0.0	S			
20.00	0.0	S			
30.00	0.0	S			
32.50	0.0	S			
36.00	0.0	S			
40.00	0.0	S			
120.00	0.0	S			
121.00	0.0	S			
140.00	0.0	S			
T(S)	VVTB(M/S)				
0.00	0.00	S			
20.00	0.00	S			
30.00	0.00	S			
32.50	4.09	S			
36.00	2.51	S			
40.00	2.34	S			
120.00	2.57	S			
121.00	0.35	S			
140.00	0.21	E			
T	TL				
0.00	484.15	S			
20.00	484.15	S			
30.00	482.95	S			
32.50	480.15	S			
36.00	481.95	S			
40.00	481.65	S			
120.00	477.15	S			
121.00	477.65	S			
140.00	481.15	S			
T(S)	TV				
0.00	484.15	S			
20.00	484.15	S			
30.00	482.95	S			
32.50	480.15	S			
36.00	481.95	S			
40.00	481.65	S			
120.00	477.15	S			
121.00	477.65	S			
140.00	481.15	S			
T	ALPHA				
0.00	1.0	S			
20.00	1.0	S			
30.00	1.0	S			
32.50	1.0	S			
36.00	1.0	S			
40.00	1.0	S			
120.00	1.0	S			
121.00	1.0	S			
140.00	1.0	S			
T(S)	P(BAR)				
0.00	1.94E+01	S			
20.00	1.94E+01	S			
30.00	1.9E+01	S			
32.50	1.79E+01	S			
36.00	1.87E+01	S			
40.00	1.86E+01	S			
120.00	1.69E+01	S			
121.00	1.71E+01	S			
140.00	1.84E+01	S			
T(S)	PA(BAR)				
0.00	0.0	S			
20.00	0.0	S			
30.00	0.0	S			
32.50	0.0	S			
36.00	0.0	S			
40.00	0.0	S			
120.00	0.0	S			
121.00	0.0	S			

140.00 0.0 E

COMPONENT NO. 603

FILL 603 603 BASE STEAM-WATER FILL CELL 3
 IFTY 0 IOFF C 2
 IFTR 603 0 NFTB 0 NFSV 0 NFRF C 3
 600 100 RFMX 0 CONCIN C 4
 TWOLD 0
 DXIN 100 VOLIN 0 ALPIN VLIN TLIN C 5
 9 .52 1.0 FLOWIN C 484.15 TVIN C 6
 PIN PAIN 0. 0. 484.15
 19.4E+05 VMSCV VVSCV C 9
 1.0
 TLSCV TVSCV PSCL PASCL CONSCL C 10
 1.0 1E+05 1.0 1.0
 T(S) VLTB(M/S)

0.00 0.0 S
 20.00 0.0 S
 30.00 0.0 S
 32.50 0.0 S
 36.00 0.0 S
 40.00 0.0 S
 120.00 0.0 S
 121.00 0.0 S
 140.00 0.0 S

T(S) VVTB(M/S)
 0.00 0.00 S
 20.00 0.00 S
 30.00 0.00 S
 32.50 4.09 S
 36.00 2.51 S
 40.00 2.34 S
 120.00 2.57 S
 121.00 .35 S
 140.00 0.21 E

T TL
 0.00 484.15 S
 20.00 484.15 S
 30.00 482.95 S
 32.50 480.15 S
 36.00 481.95 S
 40.00 481.65 S
 120.00 477.15 S
 121.00 477.65 S
 140.00 481.15 S

T TV
 0.00 484.15 S
 20.00 484.15 S
 30.00 482.95 S
 32.50 480.15 S
 36.00 481.95 S
 40.00 481.65 S
 120.00 477.15 S
 121.00 477.65 S
 140.00 481.15 S

T ALPHA
 0.00 1.0 S
 20.00 1.0 S
 30.00 1.0 S
 32.50 1.0 S
 36.00 1.0 S
 40.00 1.0 S
 120.00 1.0 S
 121.00 1.0 S
 140.00 1.0 S

T(S) P(BAR)
 0.00 1.54E+01 S
 20.00 1.94E+01 S
 30.00 1.9E+01 S
 32.50 1.79E+01 S
 36.00 1.87E+01 S
 40.00 1.85E+01 S
 120.00 1.69E+01 S
 121.00 1.71E+01 S
 140.00 1.84E+01 S

T(S) PA(BAR)
 0.00 0.0 S
 20.00 0.0 S
 30.00 0.0 S
 32.50 0.0 S
 36.00 0.0 S
 40.00 0.0 S
 120.00 0.0 S
 121.00 0.0 S
 140.00 0.0 S

COMPONENT NO. 604

FILL 604 604 BASE STEAM-WATER FILL CELL 4
 IFTY 0 IOFF C 2
 IFTR 604 0 NFTB 0 NFSV 0 NFRF C 3
 600 100 RFMX 0 CONCIN C 4
 TWOLD 0

•	DXIN	VOLIN	ALPIN	VLIN	TLIN	C 5
•	9	82	1.0	484.15	TVIN	C 6
•	19.4E+05	PAIN	FLOWIN	VVIN		
•	VMSCL	0.	0.	484.15		C 9
•	1.0	VVSCL				
•	TLSCCL	1.0	PSCL	PASCL	CONSCL	C 10
•	1.0	1.0	1.E+05	1.0		
•	T(S)	VLTB(M/S)				

0.00	0.0 S
20.00	0.0
30.00	0.0
32.50	0.0
36.00	0.0
40.00	0.0
120.00	0.0
121.00	0.0
140.00	0.0
T(S)	VVTB(M/S)
0.00	0.00
20.00	0.00
30.00	0.00
32.50	4.09
36.00	2.51
40.00	2.34
120.00	2.57
121.00	0.36
140.00	0.21
T	TL
0.00	484.15
20.00	484.15
30.00	482.95
32.50	480.15
36.00	481.95
40.00	481.66
120.00	477.15
121.00	477.65
140.00	481.15
T(S)	TV
0.00	484.15
20.00	484.15
30.00	482.95
32.50	480.15
36.00	481.95
40.00	481.66
120.00	477.15
121.00	477.65
140.00	481.15
T	ALPHA
0.00	1.0
20.00	1.0
30.00	1.0
32.50	1.0
36.00	1.0
40.00	1.0
120.00	1.0
121.00	1.0
140.00	1.0
T(S)	P(BAR)
0.00	1.94E+01
20.00	1.94E+01
30.00	1.92E+01
32.50	1.79E+01
36.00	1.87E+01
40.00	1.85E+01
120.00	1.69E+01
121.00	1.71E+01
140.00	1.84E+01
T(S)	PA(BAR)
0.00	0.0
20.00	0.0
30.00	0.0
32.50	0.0
36.00	0.0
40.00	0.0
120.00	0.0
121.00	0.0
140.00	0.0

• COMPONENT NO. 605

FILL	JUN1	605	605	BASE STEAM-WATER	FILL CELL	5
•	605	IFTY	IOFF		C 2	
•	IFTR	IFSV	NFTB	NFSV	NFRF	C 3
•	800	100	9	0	0	
•	TWTOLD	RFMX	CONCIN			C 4
•	0	100	0.			
•	DXIN	VOLIN	ALPIN	VLIN	TLIN	C 5
•	9	719356	1.0	484.15	TVIN	C 6
•	PIN	PAIN	FLOWIN	VVIN		
•	19.4E+05	0.	0.	484.15		C 9
•	VLSCCL	VVSCL				
•	1.0	0.725				
•	TLSCCL	TVSCL	PSCL	PASCL	CONSCL	C 10
•	1.0	1.0	1.E+05	1.0		
•	T(S)	VLTB(M/S)				
•	0.00	0.0 S				

20.00	0.0
30.00	0.0
32.50	0.0
36.00	0.0
40.00	0.0
120.00	0.0
121.00	0.0
140.00	0.0
T(S)	VVT(M/S)
0.00	0.00
20.00	0.00
30.00	0.00
32.50	4.09
36.00	2.81
40.00	2.34
120.00	2.77
121.00	0.35
140.00	0.21
T	TL
0.00	484.15
20.00	484.15
30.00	432.95
32.50	480.15
36.00	481.95
40.00	481.65
120.00	477.15
121.00	477.65
140.00	481.15
T(S)	TV
0.00	484.15
20.00	484.15
30.00	482.95
32.50	480.15
36.00	481.95
40.00	481.65
120.00	477.15
121.00	477.65
140.00	481.15
T	ALPHA
0.00	1.0
20.00	1.0
30.00	1.0
32.50	1.0
36.00	1.0
40.00	1.0
120.00	1.0
121.00	1.0
140.00	1.0
T(S)	P(BAR)
0.00	1.94E+01
20.00	1.94E+01
30.00	1.9E+01
32.50	1.79E+01
36.00	1.87E+01
40.00	1.85E+01
120.00	1.89E+01
121.00	1.71E+01
140.00	1.84E+01
T(S)	PA(BAR)
0.00	0.0
20.00	0.0
30.00	0.0
32.50	0.0
36.00	0.0
40.00	0.0
120.00	0.0
121.00	0.0
140.00	0.0

COMPONENT NO. 606

FILL	JUN1	606	606	BASE	STEAM-WATER	FILL	CELL	6
	606	IFTY	6	IOFF			C	2
	IFTR	IFSV	0	NFTB	NFSV	0	NFRF	C 3
	600	100	9					
	TWTOLD	RFMX	0	CONCIN				C 4
	0	100	0					
	DXIN	VOLIN	ALPIN	VLIN	484.15	TLIN		C 5
	9	.719356	1.0	0				
	PIN	PAIN	FLOWIN	VVIN	484.15	TVIN		C 6
	19.4E+05	0	0	0				
	VLSC	VVSC						C 9
	1.0	0.725						
	TLSC	TVSC	PSCL	PASCL	1.0	CONSC		C 10
	1.0	1.0	1E+05	1	1.0			
	T(S)	VLTB(M/S)						
	0.00	0.0	S					
	20.00	0.0	S					
	30.00	0.0	S					
	32.50	0.0	S					
	36.00	0.0	S					
	40.00	0.0	S					
	120.00	0.0	S					
	121.00	0.0	S					
	140.00	0.0	S					
	T(S)	VVTB(M/S)						
	0.00	0.00	S					
	20.00	0.00	S					

30.00	0.00	S
32.50	4.09	S
36.00	2.51	S
40.00	2.34	S
120.00	2.57	S
121.00	0.35	E
140.00	0.21	E
T	TL	
0.00	484.15	S
20.00	484.15	S
30.00	482.95	S
32.50	480.15	S
36.00	481.95	S
40.00	481.65	S
120.00	477.15	S
121.00	477.65	S
140.00	481.15	S
T(S)	TV	
0.00	484.15	S
20.00	484.15	S
30.00	482.95	S
32.50	480.15	S
36.00	481.95	S
40.00	481.65	S
120.00	477.15	S
121.00	477.65	S
140.00	481.15	S
T	ALPHA	
0.00	1.0	S
20.00	1.0	S
30.00	1.0	S
32.50	1.0	S
36.00	1.0	S
40.00	1.0	S
120.00	1.0	S
121.00	1.0	S
140.00	1.0	S
T(S)	P(BAR)	
0.00	1.94E+01	S
20.00	1.94E+01	S
30.00	1.9E+01	S
32.50	1.79E+01	S
36.00	1.87E+01	S
40.00	1.85E+01	S
120.00	1.69E+01	S
121.00	1.71E+01	S
140.00	1.84E+01	S
T(S)	PA(BAR)	
0.00	0.0	S
20.00	0.0	S
30.00	0.0	S
32.50	0.0	S
36.00	0.0	S
40.00	0.0	S
120.00	0.0	S
121.00	0.0	S
140.00	0.0	S

* COMPONENT NO.607

FILL	JUN1	607	607	BASE STEAM-WATER	FILL	CELL 7
	607	IFTY	IOFF			C 2
	IFTR	IFSV	NFTB	NFSV	NFRF	C 3
	600	100	0	0	0	
	TWTOLD	RFMX	CONCIN			C 4
	0	100	0			
	DXIN	ALIN	ALPIN	VLIN	TLIN	C 5
	9	71	10	0	484.15	
	PIN	PAIN	FLOWIN	VVIN	TVIN	C 6
	19.4E+05	0	0	484.15		
	VLSCCL	VVSCCL				C 9
	10	0.725				
	TLSCCL	TVSCCL	PSCL	PASCL	CONSCL	C 10
	10	1.0	1E+05	1	1.0	
	T(S)	VLTB(M/S)				
	0.00	0.0	S			
	20.00	0.0	S			
	30.00	0.0	S			
	32.50	0.0	S			
	36.00	0.0	S			
	40.00	0.0	S			
	120.00	0.0	S			
	121.00	0.0	S			
	140.00	0.0	S			
	T(S)	VVTB(M/S)				
	0.00	0.00	S			
	20.00	0.00	S			
	30.00	0.00	S			
	32.50	4.09	S			
	36.00	2.51	S			
	40.00	2.34	S			
	120.00	2.57	S			
	121.00	0.35	E			
	140.00	0.21	E			
	T	TL				
	0.00	484.15	S			
	20.00	484.15	S			
	30.00	482.95	S			

32.50	480.15
36.00	481.95
40.00	481.65
120.00	477.15
121.00	477.65
140.00	481.15
T(S)	TV
0.00	484.15
20.00	484.15
30.00	482.95
32.50	480.15
36.00	481.95
40.00	481.65
120.00	477.15
121.00	477.65
140.00	481.15
T	ALPHA
0.00	1.0
20.00	1.0
30.00	1.0
32.50	1.0
36.00	1.0
40.00	1.0
120.00	1.0
121.00	1.0
140.00	1.0
T(S)	P(BAR)
0.00	1.94E+01
20.00	1.94E+01
30.00	1.9E+01
32.50	1.79E+01
36.00	1.87E+01
40.00	1.85E+01
120.00	1.69E+01
121.00	1.71E+01
140.00	1.84E+01
T(S)	PA(BAR)
0.00	0.0
20.00	0.0
30.00	0.0
32.50	0.0
36.00	0.0
40.00	0.0
120.00	0.0
121.00	0.0
140.00	0.0

* COMPONENT NO.608

FILL	JUN1	608	608	BASE STEAM-WATER FILL CELL 8		
	808	IFTY	IOFF	C 2		
	IFTR	IFSV	NFTB	NPSV	NFRF	C 3
	600	100	9	0	0	
	TWTOLD	RFMX	CONCIN			C 4
	0	100	0			
	DXIN	VOLIN	ALPIN	VLIN	TLIN	C 5
	9	719356	1.0	0	484.15	
	PIN	PAIN	FLOWIN	VVIN	TVIN	C 6
	19.4E+05	0	0	484.15		
	VLSC	VVSC				C 9
	1.0	0.725				
	TLSC	TVSC	PSCL	PASCL	CONSC	C 10
	1.0	1.0	1E+05	1.0		
	T(S)	VLTB(M/S)				
	0.00	0.0	S			
	20.00	0.0	S			
	30.00	0.0	S			
	32.50	0.0	S			
	36.00	0.0	S			
	40.00	0.0	S			
	120.00	0.0	S			
	121.00	0.0	S			
	140.00	0.0	S			
	T(S)	VVTB(M/S)				
	0.00	0.00	S			
	20.00	0.00	S			
	30.00	0.00	S			
	32.50	4.09	S			
	36.00	2.51	S			
	40.00	2.34	S			
	120.00	2.57	S			
	121.00	0.35	S			
	140.00	0.21	S			
	T	TL				
	0.00	484.15	S			
	20.00	484.15	S			
	30.00	482.95	S			
	32.50	480.15	S			
	36.00	481.95	S			
	40.00	481.65	S			
	120.00	477.15	S			
	121.00	477.65	S			
	140.00	481.15	S			
	T(S)	TV				
	0.00	484.15	S			
	20.00	484.15	S			
	30.00	482.95	S			
	32.50	480.15	S			

36.00	481.95
40.00	481.65
120.00	477.15
121.00	477.65
140.00	481.15
T	ALPHA
0.00	1.0
20.00	1.0
30.00	1.0
32.50	1.0
36.00	1.0
40.00	1.0
120.00	1.0
121.00	1.0
140.00	1.0
T(S)	P(BAR)
0.00	1.94E+01
20.00	1.94E+01
30.00	1.9E+01
32.50	1.79E+01
36.00	1.87E+01
40.00	1.85E+01
120.00	1.69E+01
121.00	1.71E+01
140.00	1.84E+01
T(S)	PA(BAR)
0.00	0.0
20.00	0.0
30.00	0.0
32.50	0.0
36.00	0.0
40.00	0.0
120.00	0.0
121.00	0.0
140.00	0.0

..... LOOP 1

* COMPONENT NO. 10
 * HOT LEG LOOP 1

TEE	JOELL	10 NODES	10 MAT	HOT-LEG LOOP 1 COST	ICHF	C 2
* ICONC1	4 NCELL1	6 JUN1	11 JUN2	0 IPOW1		C 3
* IQPTR1	0 IQPSV1	0 NQPTB1	0 NQPSV1	0 NQPRF1		C 5
* RADIN1	0 TH1	0 HOUTL1	0 HOUTV1	0 TOUTL1		C 6
* TOUTV1	375 PWIN1	0 PWOFF1	300 RPWMX1	0 PWSCL1		C 7
* QPIN1	0 QPOFF1	0 RQPMX1	0 QPSCL1			C 8
* ICONC2	0 NCELL2	15 JUN3	0 IPOW2			C 9
* IQPTR2	0 IQPSV2	0 NQPTB2	0 NQPSV2	0 NQPRF2		C 11
* RADIN2	0 TH2	0 HOUTL2	0 HOUTV2	0 TOUTL2		C 12
* TOUTV2	11 PWIN2	0 PWOFF2	300 RPWMX2	0 PWSCL2		C 13
* QPIN2	300 QPOFF2	0 RQPMX2	0 QPSCL2			C 14

* PRIMARY *

5107 R 3	1.2867	1.337	1.0420	.6260 E*	DX
2256 R 3	0.5113	.5907	.4603	.2768 E*	VOL
44179 R 3	.3974 R 4	.44179 E			FA
0 R 6	0.016 R 2	0.0 E			FRIC
0 R 6	.016 R 2	0.0 E			RVFRIC
0.0	0.1802	0.5612	0.6803 E		GRAV
.75 R 3	.6388 F	.75 E			HD
0	1 F	0 E			ICFLG
0 F	1 E				NFF
1					ALP
0					VV
0					VV
418.95 E					TL
418.95 E					TV
2.60E+05 E					P
0					PA
0					OPPP
6					MATID
418.95 E					TW

* SECONDARY *

10 E					DX
40660 E					VOL
4066 E					FA
0.0 E					FRIC
0.0 E					RVFRIC
0.0 E					GRAV
.277 E					HL
3 E					ICFLG
1 E					NFF
4.0 E					ALP
0 E					VV
0 E					VV
418.95 E					TL
418.95 E					TV
2.60E+05 E					P
0 E					PA

0. E
 6 E
 418.95 E
 * QPPP
 * MATID
 * TW

 COMPONENT NO. 11
 SEPARATOR BOTTOM LOOP 1

TEE	JCELL	NODES	11	SEPARATOR-BOTTOM LOOP 1	MAT	COST	ICHF	C 2
1	ICONC1	4	NCCELL1	6	JUN1	JUN2	IPOW1	C 3
0	IQPTR1	4	IQPSV1	12	NQPTB1	NQPSV1	NQPRF1	C 5
0	RADIN1	0	TH1	0	HOUTL1	HOUTV1	TOUTL1	C 6
1.25	TOUTV1	.025	PWIN1	0	PWOFF1	RPWMX1	PWSCL1	C 7
300	QPIN1	0	QPOFF1	0	RQPMX1	QPSCL1		C 8
0	ICONC2	0	NCCELL2	0	JUN3	IPOW2		C 9
0	IQPTR2	4	IQPSV2	18	NQPTB2	NQPSV2	NQPRF2	C 11
0	RADIN2	0	TH2	0	HOUTL2	HOUTV2	TOUTL2	C 12
1.25	TOUTV2	.025	PWIN2	0	PWOFF2	RPWMX2	PWSCL2	C 13
300	QPIN2	0	QPOFF2	0	RQPMX2	QPSCL2		C 14

* PRIMARY *
 .95560
 2.597
 0.44179
 R 4 0
 R 4 0.6803 F
 0.75 R 2
 0
 1
 0
 0
 0
 418.95 E
 418.95 E
 2.60E+05 E
 0
 0
 6
 418.95 E

* SECONDARY *
 0.2000 E
 0.0107 E
 0.05326 E
 0.0 E
 0. E
 0.2604 E -4220 E
 0
 1
 0
 0
 0
 418.95 E
 418.95 E
 2.60E+05 E
 0
 0
 6
 418.95 E

* DX
 * VOL FA
 * FRIC
 * RVFRI
 * GRAV
 * HD
 * ICFLG
 * NFF
 * ALP
 * VL
 * VV
 * TL
 * TV
 * P
 * PA
 * QPPP
 * MATID
 * TW
 * DX
 * VOL FA
 * FRIC
 * RVFRI
 * GRAV
 * HD
 * ICFLG
 * NFF
 * ALP
 * VL
 * VV
 * TL
 * TV
 * P
 * PA
 * QPPP
 * MATID
 * TW

.....
 COMPONENT NO. 12
 SEPARATOR MIDDLE LOOP 1

TEE	JCELL	NODES	12	SEPARATOR-MIDDLE LOOP 1	MAT	COST	ICHF	C 2
4	ICONC1	4	NCCELL1	6	JUN1	JUN2	IPOW1	C 3
0	IQPTR1	4	IQPSV1	12	NQPTB1	NQPSV1	NQPRF1	C 5
0	RADIN1	0	TH1	0	HOUTL1	HOUTV1	TOUTL1	C 6
1.25	TOUTV1	.025	PWIN1	0	PWOFF1	RPWMX1	PWSCL1	C 7
300	QPIN1	0	QPOFF1	0	RQPMX1	QPSCL1		C 8
0	ICONC2	0	NCCELL2	0	JUN3	IPOW2		C 9
0	IQPTR2	4	IQPSV2	19	NQPTB2	NQPSV2	NQPRF2	C 11
0	RADIN2	0	TH2	0	HOUTL2	HOUTV2	TOUTL2	C 12
1.25	TOUTV2	.025	PWIN2	0	PWOFF2	RPWMX2	PWSCL2	C 13
300	QPIN2	0	QPOFF2	0	RQPMX2	QPSCL2		C 14

* PRIMARY *
 .188 0.710 0.710 .2 E * DX

```

1574      0.7558      0.7558      0.3129 E
0.8101    1.0645    1.0645 R 2 1.0645 E
.8621     0.      1.E30 E
.9053     0. E
1.0 E
.15880 F  0.2091 E
0
1
1
0
0
0
418.95 E
418.95 E
2.60E+05 E
0
0
0
418.95 E
* SECONDARY *
0.7100      .710      .188      .424 E
2.4617    2.4617    0.7057    1.7130 E
S 3 3.4673 R 2 4.0401 E
0.0 E
0.0 E
-1.0 E
0.44 E
1
1
0
0
0
418.95 F  418.95 E
418.95 F  418.95 E
2.60E+05 E
0
0
0
6
418.95 E

```

```

* VOL
* FA
* FRIC
* RVFRIC
* GRAV
* ICFLG
* NFF
* ALP
* VL
* VV
* TL
* TV
* P
* PA
* OPPP
* MATID
* TW
* DX
* VOL
* FA
* FRIC
* RVFRIC
* GRAV
* HD
* ICFLG
* NFF
* ALP
* VL
* VV
* TL
* TV
* P
* PA
* OPPP
* MATID
* TW

```

***** COMPONENT NO. 13 *****
 ***** SEPARATOR TOP LOOP 1 *****

TEE	JCELL	13 NODES	13 MAT	SEPARATOR-TOP LOOP 1 COST	ICHP	C 2
* ICONC1	3	4	6	0.0	1	C 3
* IQPTR1	0	4	13	0	0	C 5
* RADIN1	0	1	0	0	0	C 6
* TOUTV1	1.25	.025	0	300	300	C 7
* QPIN1	0	0	0	0	0	C 8
* ICONC2	0	1	115	0	0	C 9
* IQPTR2	0	1	0	0	0	C 11
* RADIN2	1.25	.025	0	300	300	C 12
* TOUTV2	0	0	0	0	0	C 13
* QPIN2	0	0	0	0	0	C 14

```

* PRIMARY *
0.2      .285      0.4      0.810 E
R 2 0.2129 1.5732 1.8919 3.0974 E
1.0645 R 2 4.7298 0.44179 E
1.E30 F  0.0 E
1.0 E
R 2 0.2091 R 2 2.454 0.75 E
0
1
1
0
0
0
418.95 E
418.95 E
2.60E+05 E
0
0
0
6
418.95 E
* SECONDARY *
1.0 E
.126 E
.126 E
0.0 E
0.0 E
.4
0
1
1
0
0
418.95 E

```

```

* DX
* VOL
* FA
* FRIC
* RVFRIC
* GRAV
* HD
* ICFLG
* NFF
* ALP
* VL
* VV
* TL
* TV
* P
* PA
* OPPP
* MATID
* TW
* DX
* VOL
* FA
* FRIC
* RVFRIC
* GRAV
* HD
* ICFLG
* NFF
* ALP
* VL
* VV
* TL

```

418.95 E
 2.60E+05 E
 0. E
 0. E
 6 E
 418.95 E

TV
 P
 PA
 QPPP
 MATID
 TW

COMPONENT NO. 14
 LOOP SEAL AND COLD LEG LOOP 1

TEE	JCELL	14 NODES	14 MAT	COST	ICHF	C 2
ICONC1	NCELL1	6	JUN1	JUN2	IPOW1	C 3
IQPTR1	IQPSV1	16	NQPTB1	NQPSV1	NQPRF1	C 5
RADIN1	TH1	0	HOUTL1	HOUTV1	TOUTL1	C 6
TOUTV1	PWIN1	0	PWOFF1	RPWMX1	PWSCL1	C 7
QPIN1	QPOFF1	0	RQPMX1	QPSCL1		C 8
ICONC2	NCELL2	0	JUN3	IPOW2		C 9
IQPTR2	IQPSV2	160	NQPTB2	NQPSV2	NQPRF2	C 11
RADIN2	TH2	0	HOUTL2	HOUTV2	TOUTL2	C 12
TOUTV2	PWIN2	0	PWOFF2	RPWMX2	PWSCL2	C 13
QPIN2	QPOFF2	0	RQPMX2	QPSCL2		C 14

PRIMARY

R 2	1.2 R 2	1.9125	1.2 R 3	2.317	1.514	DX
	1.665 R 2	1.092	.65S			DX
	.800 R 2	1.495	1.5050	1.9110	R ? 1.6825	DX
	0.710 E				DX	
R 2	.5301 R 2	.8449	.5301 R 3	1.0236	.6689	VOL
	.7356 R 2	.4824	.7200	.9480 S		VOL
R 12	0.66048	0.66489	0.40247 R 2	0.74331	0.38058 E	VOL
	.44179	.00000	.6892 R 7	.44179	.6362 E	FA
	0. R 11	.019	10.76 R 8	.008	.0205 E	FRIC
	0. R 11	.016	7.75 R 8	.008	.0205 E	RVFRIC
	1.0	.2313	0.0	-.2313 R 4	-1.0	GRAV
	-.49350	0.0	.7978	1.0	.372	GRAV
	-.7752	1411 R 7	0.0 E			GRAV
21	.75	0.90 E				HD
12	1 E	1 F	0 E			ICFLAG
R07	1. 1.0	1.0	1. 1.0 S			NFF
R10	1.0	E				ALP
	0.0 E					VV
	0.0 E					VV
	411.18					TL
	411.18					TV
	2.60E+05 E					P
	0.0 E					PA
	0.0 E					QPPP
	6 E					MATID
	411.18 E					TW
	0.050 E					DX
	0.019 E					VOL
	3.8010E-02 E					FA
	0. E					FRIC
	0. E					RVFRIC
	+1 E					GRAV
	2.2000E-01 E					HD
	0					ICFLAG
	1					NFF
	0. E					ALP
	0. E					VV
	0. E					VV
	411.18 E					TL
	411.18 E					TV
	2.60E+05 E					P
	0. E					PA
	0. E					QPPP
	6 E					MATID
	411.18 E					TW

COMPONENT NO. 18
 SEPARATOR DRAIN TEE LOOP 1

TEE	JCELL	18 NODES	18 MAT	COST	ICHF	C 2
ICONC1	NCELL1	6	JUN1	JUN2	IPOW1	C 3
IQPTR1	IQPSV1	19	NQPTB1	NQPSV1	NQPRF1	C 5
RADIN1	TH1	0	HOUTL1	HOUTV1	TOUTL1	C 6
TOUTV1	PWIN1	0	PWOFF1	RPWMX1	PWSCL1	C 7
QPIN1	QPOFF1	0	RQPMX1	QPSCL1		C 8
ICONC2	NCELL2	1	JUN3	IPOW2		C 9

```

* IQPTR2      IQPSV2      NQPTB2      NQPSV2      NQPRF2      C 11
* RADIN2      TH2         HOUTL2      HOUTV2      TOUTL2      C 12
* TOUTV2      FWIN2      PWOFF2      RPWMX2      PWSCL2      C 13
* QPIN2       QPOFF2      RQPMX2      QPSCL2      C 14

```

PRIMARY

```

0.9 R 2      0.925 R 3      0.4913 E
0.0283 R 2   0.029 R 3      0.0964 E
4.0401 R 2   0.0314 R 4     0.1963 E
0.0 E
-1.0 E
0.44 R 2     -0.5364 F      0.5 E      -0.3470 R 3
0.0 E
1 R 01      1.0 E
0.0 E
418.95 E   308.15 E
418.95 E   308.15 E
2.60E+05 E
0.0 E
0.6 E
R 20 418.95 F 308.15 E

```

SECONDARY

```

0.5 E
0.0266 E
0.05326 E
0.0 E
0.0 E
0.2604 E
0.0 E
1 E
0.0 E
418.95 E
418.95 E
2.60E+05 E
0.0 E
0.6 E
418.95 E

```

```

* DX VOL
* FA
* FRIC
* RVFRIC
* GRAV
* HD
* ICFLG
* NFF
* ALP
* VL
* VV
* TL
* TV
* P
* PA
* QPPP
* MATID
* TW
* DX VOL
* FA
* FRIC
* RVFRIC
* GRAV
* HD
* ICFLG
* NFF
* ALP
* VL
* VV
* TL
* TV
* P
* PA
* QPPP
* MATID
* TW

```

COMPONENT NO. 10 *****
SEPARATOR DRAIN VALVE LOOP 1 *****

```

VALVE          19          19          SEPARATOR DRAIN VALVE
NCELLS        NODES        JUN1        JUN2        MAT
* ICHF         2          130         IVTY 18     IVPS 6      NVTB2
* IVTR         1          1          NVTB1 2     NVSV 0      NVRF
* IQP3TR       100         2          NQP3TB 0    NQP3SV 0    NQP3RF
* IVTROV       0          0          FMINOV      FMAXOV
* RVMX         1E10       0          HOUTL 1.    HOUTV 300   TOUTL
* RADIN        0.15      .005       HVLVE 0.    FAVLVE 300  XPOS
* TOUTV        300         .03140     RQPSMX 1.   QPSSCL
* QP3IN        0.0          1.0 E      0.0
0.0266        0.05326 E
0.0           1.944 F    0. E
0.0           1.944 F    0. E
2          0.2604 E      .4220 E
0.0 E
1 E
0.0 E
1. E
418.95 E
418.95 E
2.60E+05 E
0.0 E
0.6 E
418.95 E
T(S)          POS(-)
0.0           1. S
300.0        1. E
* VTBI
* VTBI

```

```

* DX VOL
* FA
* FRIC
* RVFRIC
* GRAV
* HD
* ICFLG
* NFF
* ALP
* VL
* VV
* TL
* TV
* P
* PA
* QPPP
* MATID
* TW

```

COMPONENT NO. 113 *****
STEAM SUPPLY FILL LOOP 1 *****

```

FILL      113      113      STEAM SUPPLY LOOP 1
JUN1      IFTY      IOFF      C 2
113
IFTR      IFSV      0      NFTB      NFSV      0      NFRF      C 3
0
TWTOLD    15      RFMX      0      CONCIN      C 4
0
DXIN      VOLIN      ALPIN      0      VLIN      TLIN      C 5
1
PIN      PAIN      FLOWIN      0      VVIN      TVIN      C 6
19.88E+05      0      0      401.88
* COMPONENT NO. 119 .....
* SEPARATOR DRAIN FILL LOOP 1 .....

```

```

FILL      119      119      SEPARATOR DRAIN FILL LOOP 1
JUN1      IFTY      IOFF      C 2
119
IFTR      IFSV      1      NFTB      NFSV      0      NFRF      C 3
666      100      -2
TWTOLD    20.0      RFMX      0      CONCIN      C 4
0
DXIN      VOLIN      ALPIN      0      VLIN      TLIN      C 5
0.4913      0.09640      0      0      308.15
PIN      PAIN      FLOWIN      0      VVIN      TVIN      C 6
2.60E+05      0      0      308.15
VMSCL     VVSCL      C 9
1
TIME (S)  MASS FLOW (KG/S) *
0      0 S
5      -25. E

```

```

* COMPONENT NO. 15 .....
* HOT LEG ECC FILL LOOP 1 .....

```

```

FILL      15      15      HOT-LEG-ECC LOOP 1
JUN1      IFTY      IOFF      C 2
15
IFTR      IFSV      0      NFTB      NFSV      0      NFRF      C 3
666      100      -6
TWTOLD    1.E10      RFMX      0      CONCIN      C 4
0
DXIN      VOLIN      ALPIN      0      VLIN      TLIN      C 5
3.3      134      0      0      303.35
PIN      PAIN      FLOWIN      0      VVIN      TVIN      C 6
19.80E+05      0      0      303.35
VMSCL     VVSCL      C 9
1
TIME (S)  MASS FLOW (KG/S) *
0      0 S
5      0 S
12     500 S
72     400 S
110    300 E

```

```

* COMPONENT NO. 16 .....
* COLD LEG ECC FILL LOOP 1 .....

```

```

FILL      16      16      COLD-LEG-ECC LOOP 1
JUN1      IFTY      IOFF      C 2
16
IFTR      IFSV      0      NFTB      NFSV      0      NFRF      C 3
116      100      12
TWTOLD    1.E10      RFMX      0      CONCIN      C 4
0
DXIN      VOLIN      ALPIN      0      VLIN      TLIN      C 5
3.3      125      0      0      579.65
PIN      PAIN      FLOWIN      0      VVIN      TVIN      C 6
11.0E+05      0      0      457.3
VMSCL     VVSCL      C 9
1
TLSCl     TVSCL      PSCL      PASCL      CONSCL      C 10
1.0      1.0      1.E+05      1.0
T(S)      VLTB(M/S)
0.00      0.00
38.00      0.00
42.00      0.00
45.00      13.72
50.00      13.76
57.80      13.70
80.00      13.83
90.00      13.80
118.00     13.87
120.00     11.66
125.00     0.00
140.00     0.00
T(S)      VVTB(M/S)
0.00      0.0
38.00      0.0
42.00      0.0
45.00      0.0
50.00      0.0
57.80      0.0
80.00      0.0
90.00      0.0
118.00     0.0
120.00     0.0

```

125.00	0.0	TV	
140.00	0.0		
T(S)	TL		
0.00	379.65		
38.00	380.15		
42.00	380.15		
45.00	379.15		
50.00	381.90		
57.80	377.15		
80.00	384.65		
90.00	386.15		
118.00	392.35		
120.00	392.65		
125.00	392.85		
140.00	392.40		
T(S)	TV		
0.00	457.3	ALPHA	
38.00	457.3		
42.00	457.3		
45.00	457.3		
50.00	457.3		
57.80	457.3		
80.00	457.3		
90.00	457.3		
118.00	457.3		
120.00	457.3		
125.00	457.3		
140.00	457.3		
T(S)	ALPHA		
0.00	0.0		P(BARS)
38.00	0.0		
42.00	0.0		
45.00	0.0		
50.00	0.0		
57.80	0.0		
80.00	0.0		
90.00	0.0		
118.00	0.0		
120.00	0.0		
125.00	0.0		
140.00	0.0		
T(S)	P(BARS)		
0.00	11.0	PA(BARS)	
38.00	11.0		
42.00	11.0		
45.00	11.0		
50.00	11.0		
57.80	11.0		
80.00	11.0		
90.00	11.0		
118.00	11.0		
120.00	11.0		
125.00	11.0		
140.00	11.0		
T(S)	PA(BARS)		
0.00	0.0		
38.00	0.0		
42.00	0.0		
45.00	0.0		
50.00	0.0		
57.80	0.0		
80.00	0.0		
90.00	0.0		
118.00	0.0		
120.00	0.0		
125.00	0.0		
140.00	0.0		

..... L O O P 2

* COMPONENT NO. 20 *

TEE	JCELL	20	20	MAT	HOT-LEG LOOP 2	COST	ICHF	C 2
* ICNC1	4	4	4	JUN1	JUN2	1	IPOW1	C 3
* IQPTR1	0	5	20	NQPTB1	NQPSV1	0	NQPRF1	C 5
* RADIN1	0	0	0	HOUTL1	HOUTV1	0	TOUTL1	C 6
* TOUTV1	375	.01	0	PWIN1	PWOFF1	300	RPWMX1	PWSCL1 C 7
* QPIN1	0	0	0	QPOFF1	RQPMX1	0	QPSCL1	C 8
* ICNC2	0	1	0	JUN3	IPOW2	0		C 9
* IQPTR2	0	1	25	NQPTB2	NQPSV2	0	NQPRF2	C 11
* RADIN2	0	0	0	HOUTL2	HOUTV2	0	TOUTL2	C 12
* TOUTV2	11	.01	0	PWIN2	PWOFF2	300	RPWMX2	PWSCL2 C 13
* QPIN2	0	0	0	QPOFF2	RQPMX2	0	QPSCL2	C 14

* PRIMARY *

R 3	.5107	R 2	1.2867	E
R 3	.2256	R 2	.5113	E
R 3	.44179	R 3	.3974	E
R 2	0.	R 4	.016	E
R 2	0.	R 4	.016	E

- * DX
- * VOL
- * FA
- * FRIC
- * RVFRIC

```

0 E
.76 R 3
1 R 3
1 E
0 E
0 E
0 E
422.275 E
422.275 E
2.60E+05 E
0 E
0 E
422.275 E
* SECONDARY *
10 E
40660 E
04066 E
0.0 E
0.0 E
-1.0 E
.2077 E
0 E
1 E
1.0 E
0 E
0 E
422.275 E
422.275 E
2.60E+05 E
0 E
0 E
6 E
422.275 E

```

```

* GRAY
HD
ICFLG
NFF
ALP
VL
VV
TV
TV
P
PA
OPPP
MATID
TW
DX
VOL
FA
FRIC
RVFRIC
GRAY
HD
ICFLG
NFF
ALP
VL
VV
TV
TV
P
PA
OPPP
MATID
TW

```

***** COMPONENT NO. 27 *****

TEE	JCELL	NODES	27	MAT	PRESSURIZER	TEE	ICHF	C
1	ICONC1	NCCELL1	6	JUN1	JUN2	IPOW1		C 2
0	IQPTR1	IQPSV1	227	NQPTB1	NQPSV1	NQPRF1		C 3
0	RADIN1	TH1	0	HOUTL1	HOUTV1	TOUTL1		C 5
375	TOUTV1	PWIN1	0	PWOFF1	RPWMX1	PWSCL1		C 6
300	QPIN1	QPOFF1	0	RQPMX1	QPSCL1			C 7
0	ICONC2	NCCELL2	0	JUN3	IPOW2			C 8
0	IQPTR2	IQPSV2	228	NQPTB2	NQPSV2	NQPRF2		C 9
0	RADIN2	TH2	0	HOUTL2	HOUTV2	TOUTL2		C 11
26	TOUTV2	PWIN2	0	PWOFF2	RPWMX2	PWSCL2		C 12
300	QPIN2	QPOFF2	0	RQPMX2	QPSCL2			C 13
0			0					C 14

```

* PRIMARY *
R 1 1.2867 1.337 1.0420 0.626 E
R 1 0.5113 .5907 .4603 .2766 E
R 1 3974 R 4 .44179 E
R 3 .016 R 2 0 E
R 3 .016 R 2 0 E
R 22 0.0 0.1802 0.5612 0.6803 E
R 22 .6388 F .75 E
0 E
1 E
0 E
0 E
422.275 E
422.275 E
2.60E+05 E
0 E
0 E
6 E
422.275 E
* SECONDARY *
56 .7184 E
.03339 .06833 E
.031416 F .09115 E
0 .0182 0 E
F .7005 .36217 - .97929 E
.2 F .348 E
0 E
1 E
0 E
0 E
422.275 E
422.275 E
2.60E+05 E
0 E
0 E
6 E

```

```

* DX
VOL
FA
FRIC
RVFRIC
GRAY
HD
ICFLG
NFF
ALP
VL
VV
TV
TV
P
PA
OPPP
MATID
TW
DX
VOL
FA
FRIC
RVFRIC
GRAY
HD
ICFLG
NFF
ALP
VL
VV
TV
TV
P
PA
OPPP
MATID
TW

```

COMPONENT NO. 21 SEPARATOR BOTTOM LOOP 2

TEE	JCELL	NODES	21	MAT	COST	ICHF	C 2
•	ICONC1	NCELL1	6	JUN1	JUN2	IPOW1	C 3
•	IQPTR1	IQPSV1	21	NQPTB1	NQPSV1	NQPRF1	C 5
•	RADIN1	TH1	0	HOUTL1	HOUTV1	TOUTL1	C 6
•	TOUTV1	PWIN1	0	PWOFF1	RPWMX1	PWSCL1	C 7
•	QPIN1	QPOFF1	0	RQPMX1	QPSCL1		C 8
•	ICONC2	NCELL2	28	JUN3	IPOW2		C 9
•	IQPTR2	IQPSV2	28	NQPTB2	NQPSV2	NQPRF2	C 11
•	RADIN2	TH2	0	HOUTL2	HOUTV2	TOUTL2	C 12
•	TOUTV2	PWIN2	0	PWOFF2	RPWMX2	PWSCL2	C 13
•	QPIN2	QPOFF2	0	RQPMX2	QPSCL2		C 14

PRIMARY

95560	.3251	.3251	.424 E
2.597	1.5266	1.5253	2587 E
0.44179	4.8584	4.7298 R 2	0.6101 E
0.0	.3621 E		
0.6803 F 2	.9053 E		
0.75 R 2	1.0 E	.1583 E	

- DX
- VOL
- FA
- FRIC
- RVFRI
- GRAV
- HD
- ICFLG
- NFF
- ALP
- VL
- VV
- TL
- TV
- P
- PA
- QPPP
- MATID
- TW
- DX
- VOL
- FA
- FRIC
- RVFRI
- GRAV
- HD
- ICFLG
- NFF
- ALP
- VL
- VV
- TL
- TV
- P
- PA
- QPPP
- MATID
- TW

SECONDARY

0.2000 E			
0.0107 E			
0.05326 E			
0.0 E			
0. E			
0.2604 E		-4220 E	
0. E			
1. E			
0. E			
0. E			
422.275 E			
422.275 E			
2.60E+05 E			
0. E			
0. E			
6. E			
422.275 E			

COMPONENT NO. 22 SEPARATOR MIDDLE LOOP 2

TEE	JCELL	NODES	22	MAT	COST	ICHF	C 2
•	ICONC1	NCELL1	6	JUN1	JUN2	IPOW1	C 3
•	IQPTR1	IQPSV1	22	NQPTB1	NQPSV1	NQPRF1	C 5
•	RADIN1	TH1	0	HOUTL1	HOUTV1	TOUTL1	C 6
•	TOUTV1	PWIN1	0	PWOFF1	RPWMX1	PWSCL1	C 7
•	QPIN1	QPOFF1	0	RQPMX1	QPSCL1		C 8
•	ICONC2	NCELL2	29	JUN3	IPOW2		C 9
•	IQPTR2	IQPSV2	29	NQPTB2	NQPSV2	NQPRF2	C 11
•	RADIN2	TH2	0	HOUTL2	HOUTV2	TOUTL2	C 12
•	TOUTV2	PWIN2	0	PWOFF2	RPWMX2	PWSCL2	C 13
•	QPIN2	QPOFF2	0	RQPMX2	QPSCL2		C 14

PRIMARY

188	0.710	0.710	.2 E
1574	0.7558	0.7558	0.2129 E


```

0.6101      1.0645      1.0645 R 2      1.0645 E
.3621 R 3
.9053 R 4      0. E
1.0 E
.15830 F      0.2091 E
0. E
1. E
0. E
0. E
422.275 E
422.275 E
2.60E+05 E
0. E
0. E
6 E
422.275 E
SECONDARY
0.7100      .710      .188      424 E
2.4617 R 2 4.0401 E 0.7057 1.7130 E
3 3.4673 R 2 4.0401 E
0.0 E
-1.0 E
0.44 E
0. E
1. E
1.00 E
0. E
0. E
422.275 E
422.275 E
2.60E+05 E
0. E
0. E
6 E
422.275 E

```

```

* FA
* FRIC
* RVFRIC
* GRAV
* ICFLG
* NFF
* ALP
* VL
* VV
* TV
* P
* PA
* QPPP
* MATID
* TW
* DX
* VOL
* FA
* FRIC
* RVFRIC
* GRAV
* HD
* ICFLG
* NFF
* ALP
* VL
* VV
* TV
* P
* PA
* QPPP
* MATID
* TW

```

***** COMPONENT NO. 23 *****
 ***** SEPARATOR TOP LOOP 2 *****

TEE	JCELL	NODES	MAT	COST	ICHF	C 2
3	ICONC1	4	JUN1	0.0	JUN2	IPOW1 C 3
0	IQPTR1	4	NQPTB1	24	NQPSV1	NQPRF1 C 5
0	RADIN1	0	TH1	0	HOUTV1	TOUTL1 C 6
1.25	TOUTV1	.025	PWIN1	0	PWOFF1	RPWMX1 PWSCL1 C 7
300	QPIN1	0	QPOFF1	0	RQPMX1	QPSCL1 C 8
0	ICONC2	1	JUN3	0	IPOW2	C 9
0	IQPTR2	4	NQPTB2	223	NQPSV2	NQPRF2 C 11
0	RADIN2	0	TH2	0	HOUTV2	TOUTL2 C 12
1.25	TOUTV2	.025	PWIN2	0	PWOFF2	RPWMX2 PWSCL2 C 13
300	QPIN2	0	QPOFF2	0	RQPMX2	QPSCL2 C 14

```

* PRIMARY *
R 2 0.2129      .285      0.4      0.810 E
1.0645 R 2 4.7298 1.8919 3.0974 E
1.530 F      0.0 E
0. E
1.0 E
0.2091 R 2 2.454 0.75 E
0. E
1. E
0. E
0. E
422.275 E
422.275 E
2.60E+05 E
0. E
0. E
6 E
422.275 E
SECONDARY
1.0 E
.126 E
.126 E
0.0 E
0.0 E
4 E
0. E
1. E
0. E
0. E
422.275 E
422.275 E

```

```

* DX
* VOL
* FA
* FRIC
* RVFRIC
* GRAV
* HD
* ICFLG
* NFF
* ALP
* VL
* VV
* TV
* P
* PA
* QPPP
* MATID
* TW
* DX
* VOL
* FA
* FRIC
* RVFRIC
* GRAV
* HD
* ICFLG
* NFF
* ALP
* VL
* VV
* TV

```

2.60E+05 E
 0.
 0.
 6
 422.275 E

* P
 * PA
 * QPPP
 * MATID
 * TW

 * COMPONENT NO. 24 *****
 * LOOP SEAL AND COLD LEG LOOP 2 *****

TEE	JCELL	24 NODES	24 MAT	24 COST	24 ICHF	C 2
* ICONC1	17 NCELL1	4	6 JUN1	5 JUN2	1 IPOW1	C 3
* IQPTR1	0 IQPSV1	21	24 NQPTB1	27 NQPSV1	0 NQPRF1	C 5
* RADIN1	0 TH1	0	0 HOUTL1	0 HOUTV1	0 TOUTL1	C 6
* TOUTV1	375 PWIN1	.01	0 PWOFF1	300 RPWMX1	0 PWSCL1	C 7
* QPIN1	0 QPOFF1	0	0 RQPMX1	0 QPSCL1	0	C 8
* ICONC2	0 NCELL2	0	0 JUN3	0 IPOW2	0	C 9
* IQPTR2	0 IQPSV2	1	260 NQPTB2	0 NQPSV2	0 NQPRF2	C 11
* RADIN2	0 TH2	0	0 HOUTL2	0 HOUTV2	0 TOUTL2	C 12
* TOUTV2	11 PWIN2	.31	0 PWOFF2	300 RPWMX2	0 PWSCL2	C 13
* QPIN2	0 QPOFF2	0	0 RQPMX2	0 QPSCL2	0	C 14

* PRIMARY *

R 2	1.2 R 2	1.9125	1.2 R 3	2.317	1.514	* DX
	1.665 R 2	1.092	.65S			* DX
	.600 R 2	1.495	1.5050	1.9110 R 2	1.6825	* DX
	0.710 E					* DX
R 2	.5301 R 2	.8449	.5301 R 3	1.0236	.6689	* VOL
R 2	.7356 R 2	.4824	.7200	.9480 S		* VOL
R 12	0.66048	0.66489	0.40247 R 2	0.74331	0.38058 E	* VOL
	.44179	.00000	.6892 R 7	.44179	.6362 E	* FA
	0. R 11	.019	10.76 R 8	.008	.0205 E	* FRIC
	0. R 11	.019	7.75 R 8	.008	.0205 E	* RVFRIC
	1.0	.2313	0.0	-.2313 R 4	-1.0	* GRAV
	-.49350	0.0	.7978	1.0	.372	* GRAV
R 21	-.7752	.1411 R 7	0.0 E			* GRAV
R 12	0	0.90 E	0 E			* HD
R07	1 E	1 F	0 E			* ICFLAG
R10	1.0	1.0	1.0 S			* NFF
	1.0	E				* ALP

0.0 E
 0.0 E
 414.15 E
 414.15 E
 2.60E+05 E
 0.0 E
 0.0 E
 6 E
 414.15 E
 * SECONDARY *
 0.050 E
 0.019 E
 3.8010E-02 E
 0. E
 0. E
 +1.0 E
 2.2000E-01 E
 0. E
 1. E
 0. E
 0. E
 414.15 E
 414.15 E
 2.60E+05 E
 0. E
 0. E
 6 E
 414.15 E
 * PA
 * QPPP
 * MATID
 * TW
 * DX
 * VOL
 * FA
 * FRIC
 * RVFRIC
 * GRAV
 * HD
 * ICFLAG
 * NFF
 * ALP
 * VL
 * VV
 * TL
 * TV
 * P
 * PA
 * QPPP
 * MATID
 * TW

 * COMPONENT NO. 28 *****
 * SEPARATOR DRAIN TEE LOOP 2 *****

TEE	JCELL	28 NODES	28 MAT	28 COST	28 ICHF	C 2
* ICONC1	5 NCELL1	4	6 JUN1	0 JUN2	1 IPOW1	C 3
* IQPTR1	0 IQPSV1	6	29 NQPTB1	229 NQPSV1	0 NQPRF1	C 5
* RADIN1	0 TH1	0	0 HOUTL1	0 HOUTV1	0 TOUTL1	C 6
* TOUTV1	0.1 PWIN1	.025	0 FWOFF1	300 RPWMX1	0 PWSCL1	C 7
* QPIN1	0 QPOFF1	0	0 RQPMX1	0 QPSCL1	0	C 8
* ICONC2	0 NCELL2	0	0 JUN3	0 IPOW2	0	C 9
* IQPTR2	0 IQPSV2	1	230 NQPTB2	0 NQPSV2	0 NQPRF2	C 11

```

0 RADIN2 0 TH2 0 HOUTL2 0 HOUTV2 0 TOUTL2 C 12
0 TOUTV2 0.025 PWIN2 0. PWOFF2 0. RPWMX2 0. PWSCL2 C 13
300 QPIN2 0. QPOFF2 0. RQPMX2 0. QPSCL2 0. C 14
0

```

```

* PRIMARY *
0.9 R 2 0.925 R 3 0.4913 E
0.0285 R 2 0.029 R 3 0.0964 E
4.0401 R 2 0.0814 R 4 0.1963 E
0.
0.
-1.0 -0.5364 0. -0.3470 R 3
0.44 R 2 0.2 F 0.5 E
0.
1.
1.0 E
0.
0.
5 422.75 308.15 E
422.75 E
2.60E+05 E
0.
0.
R 20 422.75 F 308.15 E

```

```

* DX
* VOL
* FA
* FRIC
* RVERIC
* GRAV
* HD
* ICFLG
* NFF
* ALP
* VL
* VV
* TL
* TV
* P
* PA
* QPPP
* MATID

```

```

* SECONDARY *
0.5 E
0.0266 E
0.05326 E
0.0 E
0.0 E
0.2604 E
0.
1.
1.0 E
0.
0.
422.75 E
422.75 E
2.60E+05 E
0.
0.
6
422.75 E

```

```

* DX
* VOL
* FA
* FRIC
* RVERIC
* GRAV
* HD
* ICFLG
* NFF
* ALP
* VL
* VV
* TL
* TV
* P
* PA
* QPPP
* MATID
* TW

```

***** COMPONENT NO. 20 *****
 ***** SEPARATOR DRAIN VALVE LOOP 2 *****

```

VALVE 20 SEPARATOR DRAIN VALVE
NCELLS 20 NODES 230 JUN1 28 JUN2 6 MAT
* ICHF 0 ICONC 4 IVTY 28 IVPS 6 NVTB2
* IVTR 0 IVSV 1 NVTB1 2 NVSV 0 NVRF
* IQPSTR 0 IQPSV 100 2 NQP3TB 0 NQP3SV 0 NQP3RF
* IVTROV 0 IVTVOV 0
* RVMX 0 RVOV 0 FMINOV 0 FMAXOV
1E10 RADIN 0. TH 0 HOUTL 1. HOUTV 0 TOUTL
015 TOUTV 0.005 AVLVE 0. HVLVE 0. FAVLVE 300 XPOS
300 QPSIN 0.3140 20 RQP3MX 1. QP3SCL
0. 0.
0.5 1.0 E
F 0.0266 0.05326 E
0. 1.944 F 0 E
0. 1.944 F 0. E
R 2 0. 4220 E
0.2604 E
0. E
1 E
1. E
0.
0.
422.75 E
422.75 E
2.60E+05 E
0.
0.
6
422.75 E
T(S) POS(-)
0. 1. S
300.0 1. E

```

```

* DX
* VOL
* FA
* FRIC
* RVERIC
* GRAV
* HD
* ICFLG
* NFF
* ALP
* VL
* VV
* TL
* TV
* P
* PA
* QPPP
* MATID
* TW
* VTBI
* VTBI

```

***** COMPONENT NO. 223 *****
 ***** STEAM SUPPLY FILL LOOP 2 *****

```

FILL 223 223 STEAM SUPPLY LOOP 2

```

```

*   JUN1      IFTY      IGFY      C 2
*   229      6
*   IFTR      IFSV      NFTB      NFSV      NFRF      C 3
*   0      902      0      0      0
*   TWTOLD    RFMX      CONCIN      C 4
*   0      15      0
*   DXIN      VOLIN      ALPIN      VLIN      TLIN      C 5
*   1      126      1      0      422.75
*   PIN      PAIN      FLOWIN      VVIN      TVIN      C 6
*   19.88E+05      0      0      422.75
* COMPONENT NO. 229 .....
* SEPARATOR DRAIN FILL LOOP 2 .....

```

```

FILL      229      229 SEPARATOR DRAIN FILL LOOP 2
*   JUN1      IFTY      IOFF      C 2
*   229      8
*   IFTR      IFSV      NFTB      NFSV      NFRF      C 3
*   666      100      -2      0      0
*   TWTOLD    RFMX      CONCIN      C 4
*   0      20.0      0
*   DXIN      VOLIN      ALPIN      VLIN      TLIN      C 5
*   0.4913      0.09640      0      0      308.15
*   PIN      PAIN      FLOWIN      VVIN      TVIN      C 6
*   2.60E+05      0      0      308.15
*   VMSCL      VVSCL      C 9
*   1
*   TIME (S) MASS FLOW (KG/S) *
*   0      0. S
*   5      -25. E

```

```

* COMPONENT NO. 228 .....
* PRESSURIZER FILL .....

```

```

FILL      228      228 PRESSURIZER FILL
*   JUN1      IFTY      IOFF      C 2
*   228      8
*   IFTR      IFSV      NFTB      NFSV      NFRF      C 3
*   666      100      -9      0      0
*   TWTOLD    RFMX      CONCIN      C 4
*   0      1.E10      0
*   DXIN      VOLIN      ALPIN      VLIN      TLIN      C 5
*   .7184      .06833      1      0      422.75
*   PIN      PAIN      FLOWIN      VVIN      TVIN      C 6
*   2.60E+05      0      0      422.75
*   VMSCL      VVSCL      C 9
*   1
*   TIME (S) MASS FLOW (KG/S) *
*   0      0. S
*   2      100. S
*   3      84. S
*   5      56. S
*   7      30. S
*   9      36. S
*   11      30. S
*   13.2      0. S
*   100.      0. E

```

```

* COMPONENT NO. 25 .....
* HOT LEG ECC FILL LOOP 2 .....

```

```

FILL      25      25 HOT-LEG-ECC LOOP 2
*   JUN1      IFTY      IOFF      C 2
*   25      8
*   IFTR      IFSV      NFTB      NFSV      NFRF      C 3
*   666      100      -6      0      0
*   TWTOLD    RFMX      CONCIN      C 4
*   0      1.E10      0
*   DXIN      VOLIN      ALPIN      VLIN      TLIN      C 5
*   3.3      .134      0      0      303.35
*   PIN      PAIN      FLOWIN      VVIN      TVIN      C 6
*   19.80E+05      0      0      303.35
*   VMSCL      VVSCL      C 9
*   1
*   VMTB * R02 0.0000E+00 2.5000E+00 5.0000E+02 1.2500E+01 5.0000E+02
*   VMTB * 1.2500E+01 5.0000E+02 3.2500E+01 4.0000E+02 1.1050E+02
*   VMTB * 3.0000E+02E

```

```

* COMPONENT NO. 26 .....
* COLD LEG ECC FILL LOOP 2 .....

```

```

FILL      26      26 COLD-LEG-ECC LOOP 2
*   JUN1      IFTY      IOFF      C 2
*   26      6
*   IFTR      IFSV      NFTB      NFSV      NFRF      C 3
*   115      100      12      0      0
*   TWTOLD    RFMX      CONCIN      C 4
*   0      1.E10      0
*   DXIN      VOLIN      ALPIN      VLIN      TLIN      C 5
*   3.3      .125      0      0      392.65
*   PIN      PAIN      FLOWIN      VVIN      TVIN      C 6
*   11.00E+05      0      0      394.15
*   VMSCL      VVSCL      C 9
*   1
*   TL SCL      TV SCL      PSCL      PASCL      CONSCL      C 10
*   1.0      1.0      1.E+05      1.0
*   T(S)      VLTB(M/S)
*   0.00      0.00 S

```

38.00	0.00
42.00	0.00
45.00	13.78
50.00	13.92
57.80	13.78
80.00	13.88
90.00	13.82
118.00	13.90
120.00	11.88
125.00	0.00
140.00	0.00
T(S)	VVTB(M/S)
0.00	0.0
38.00	0.0
42.00	0.0
45.00	0.0
50.00	0.0
57.80	0.0
80.00	0.0
90.00	0.0
118.00	0.0
120.00	5.0
125.00	0.0
140.00	0.0
T(S)	TV
0.00	392.65
38.00	392.65
42.00	385.15
45.00	384.15
50.00	385.65
57.80	384.15
80.00	395.45
90.00	394.15
118.00	394.65
120.00	394.85
125.00	394.45
140.00	394.15
T(S)	TL
0.00	457.3
38.00	457.3
42.00	457.3
45.00	457.3
50.00	457.3
57.80	457.3
80.00	457.3
90.00	457.3
118.00	457.3
120.00	457.3
125.00	457.3
140.00	457.3
T(S)	ALPHA
0.00	0.0
38.00	0.0
42.00	0.0
45.00	0.0
50.00	0.0
57.80	0.0
80.00	0.0
90.00	0.0
118.00	0.0
120.00	0.0
125.00	0.0
140.00	0.0
T(S)	P(BARS)
0.00	11.0
38.00	11.0
42.00	11.0
45.00	11.0
50.00	11.0
57.80	11.0
80.00	11.0
90.00	11.0
118.00	11.0
120.00	11.0
125.00	11.0
140.00	11.0
T(S)	PA(BARS)
0.00	0.0
38.00	0.0
42.00	0.0
45.00	0.0
50.00	0.0
57.80	0.0
80.00	0.0
90.00	0.0
118.00	0.0
120.00	0.0
125.00	0.0
140.00	0.0

..... LOOP 3

* COMPONENT NO. 30

* HOT LEG LOOP 3

TEE	JCELL	30 NODES	30 MAT	HOT-LEG LOOP 3 COST	ICHF	C 2
*	ICONC1	4 NCELL1	6 JUN1	1 JUN2	IPOW1	C 3

0	9	30	31	0	
IQPTR1	IQPSV1	NQPTB1	NQPSV1	NQPRF1	C 5
0	0	0	0	0	
RADIN1	TH1	HOUTL1	HOUTV1	TOUTL1	C 6
375	.01	0.	300		
TOUTV1	PWIN1	PWOFF1	RPWMX1	PWSCL1	C 7
0	0	0	0		
QPIN1	QPOFF1	RQPMX1	QPSCL1		C 8
0	0	0			
ICONC2	NCELL2	JUN3	IPOW2		C 9
0	1	35	0		
IQPTR2	IQPSV2	NQPTB2	NQPSV2	NQPRF2	C 11
0	0	0	0		
RADIN2	TH2	HOUTL2	HOUTV2	TOUTL2	C 12
11	.01	0.	300		
TOUTV2	PWIN2	PWOFF2	RPWMX2	PWSCL2	C 13
300	0	0	0		
QPIN2	QPOFF2	RQPMX2	QPSCL2		C 14
0	0	0			

* PRIMARY *

5107 R 3	1.2867	1.337	1.0420	6260 E*	DX
2256 R 3	.5113	.5907	.4603	2766 E*	VOL
44179 R 3	.3974 R 4	44179 E			FA
0 R 6	0.016 R 2	0.0 E			FRIC
0 R 6	0.016 R 2	0.0 E			RVFRIC
0.0	802	0.5612	0.6803 E		GRAV
75 R 4	388 F	.75 E			HD
0	E	0 E			ICFLG
0 F					NFF
1					ALP
0					VL
0					VV
422.75 E					TL
422.75 E					TV
2.60E+05 E					P
0					PA
0					QPPP
6					MATID
422.75 E					TW

* SECONDARY *

10 E					DX
40660 E					VOL
.04066 E					FA
0.0 E					FRIC
0.0 E					RVFRIC
-1.0 E					GRAV
.2077 E					HD
0					ICFLG
1					NFF
1					ALP
0					VL
0					VV
422.75 E					TL
422.75 E					TV
2.60E+05 E					P
0					PA
0					QPPP
6					MATID
422.75 E					TW

.....
 * COMPONENT NO. 31 *
 * SEPARATOR BOTTOM LOOP 3 *

TEE	JCELL	NODES	31	SEPARATOR-BOTTOM LOOP 3	MAT	COST	ICHF	C 2
1	4	6	0.0	1	1	1		
ICONC1	NCELL1	JUN1	JUN2	IPOW1				C 3
0	4	31	32					
IQPTR1	IQPSV1	NQPTB1	NQPSV1	NQPRF1				C 5
0	0	0	0	0				
RADIN1	TH1	HOUTL1	HOUTV1	TOUTL1				C 6
1.25	.025	0.	300					
TOUTV1	PWIN1	PWOFF1	RPWMX1	PWSCL1				C 7
0	0	0	0					
QPIN1	QPOFF1	RQPMX1	QPSCL1					C 8
0	0	0						
ICONC2	NCELL2	JUN3	IPOW2					C 9
0	1	38	0					
IQPTR2	IQPSV2	NQPTB2	NQPSV2	NQPRF2				C 11
0	0	0	0	0				
RADIN2	TH2	HOUTL2	HOUTV2	TOUTL2				C 12
1.25	.025	0.	300					
TOUTV2	PWIN2	PWOFF2	RPWMX2	PWSCL2				C 13
0	0	0	0					
QPIN2	QPOFF2	RQPMX2	QPSCL2					C 14
0	0	0						

* PRIMARY *

.95560	.3251	.3251	.424 E		DX
2.597	1.5266	1.5253	.2587 E		VOL
0.44179	4.5584	4.7298 R 2	0.6101 E		FA
0	.3621 E				FRIC
0	.9053 E				RVFRIC
0.6803 F	1.0 E				GRAV
0.75 R 2	2.30 R 2	.1583 E			HD
0					ICFLG
1					NFF
1					ALP
0					VL
0					VV
422.75 E					TL

```

422.75 E
2.60E+05 E
0.
0.
0.
SECONDARY *
0.2000 E
0.0107 E
0.05326 E
0.0 E
0. E
0. E
0.2604 E - .4220 E
0. E
1.
1.
0.
0.
0.
422.75 E
422.75 E
2.60E+05 E
0.
0.
0.
422.75 E

```

```

* TV
* P
* PA
* QPPP
* MATID
* TW
* DX
* VOL
* FA
* FRIC
* RVFRIC
* GRAV
* HD
* ICFLG
* NFF
* ALP
* VL
* VV
* TL
* TV
* P
* PA
* QPPP
* MATID
* TW

```

COMPONENT NO. 32 *****
SEPARATOR MIDDLE LOOP 3 *****

TEE	JCELL	NODES	32	MAT	COST	ICHF	C 2
4	4	4	6	JUN1	JUN2	IPOW1	C 3
0	0	0	32	NQPTB1	NQPSV1	NQPRF1	C 5
0	0	0	0	HOUTL1	HOUTV1	TOUTL1	C 6
1.25	.025	0.	0.	PWOF1	RPWMX1	PWSCL1	C 7
300.	0.	0.	0.	RQPMX1	QPSCL1		C 8
0	0	0	0	JUN3	IPOW2		C 9
0	0	0	30	NQPTB2	NQPSV2	NQPRF2	C 11
0	0	0	0	HOUTL2	HOUTV2	TOUTL2	C 12
1.25	.025	0.	0.	PWOF2	RPWMX2	PWSCL2	C 13
300.	0.	0.	0.	RQPMX2	QPSCL2		C 14
0	0.	0.	0.				

* PRIMARY *

```

.188 0.710 0.710 .2 E
.1574 0.7558 0.7558 0.2129 E
0.6101 1.0645 1.0645 R 2 1.0645 E
.3621 R 3 0.
.9053 R 4 0. E
1.0 E
.15830 F 0.2091 E
0.
1.
0.
0.
0.
422.75 E
422.75 E
2.60E+05 E
0.
0.
0.
422.75 E

```

```

* DX
* VOL
* FA
* FRIC
* RVFRIC
* GRAV
* ICFLG
* NFF
* ALP
* VL
* VV
* TL
* TV
* P
* PA
* QPPP
* MATID
* TW

```

* SECONDARY *

```

0.7100 .710 .188 .424 E
2.4517 R 2 2.4617 0.7057 1.7130 E
3 3.4673 R 2 4.0401 E
0.0 E
0.0 E
-1.0 E
0.44 E
0. E
1.
1.
0. E
0. E
0. E
422.752 F 422.75 E
422.752 F 422.75 E
2.60E+05 E
0. E
0. E
0. E
422.75 E

```

```

* DX
* VOL
* FA
* FRIC
* RVFRIC
* GRAV
* HD
* ICFLG
* NFF
* ALP
* VL
* VV
* TL
* TV
* P
* PA
* QPPP
* MATID
* TW

```

COMPONENT NO. 33 *****
SEPARATOR TOP LOOP 3 *****

TEE	33	33	SEPARATOR-TOP LOOP 3
-----	----	----	----------------------

JCELL	NODES	MAT	COST	ICHF	C 2
ICONC1	NCELL1	6 JUN1	JUN2	IPOW1	C 3
IQPTR1	IQPSV1	35 NQPTB1	NQPSV1	NQPRF1	C 5
RADIN1	TH1	0 HOUTL1	HOUTV1	TOUTL1	C 6
TOUTV1	PWIN1	0 PWOFF1	RPWMX1	PWSCL1	C 7
QPIN1	QPOFF1	0 RQPMX1	QPSCL1		C 8
ICONC2	NCELL2	35 JUN3	IPOW2		C 9
IQPTR2	IQPSV2	0 NQPTB2	NQPSV2	NQPRF2	C 11
RADIN2	TH2	0 HOUTL2	HOUTV2	TOUTL2	C 12
TOUTV2	PWIN2	0 PWOFF2	RPWMX2	PWSCL2	C 13
QPIN2	QPOFF2	0 RQPMX2	QPSCL2		C 14

* PRIMARY *

0.2	285	0.4	0.810 E		
R 2 0.2129	1.5732	1.8919	3.0974 E		
1.0645 R 2	4.7298	0.44179 E			
1.0 E	0.0 E				

R 2 0.3091	R 2 2.454	0.75 E			
------------	-----------	--------	--	--	--

422.75 E
422.75 E
2.60E+05 E

422.75 E

* SECONDARY *

1.0 E
.126 E
.126 E
0.0 E
0.0 E
4.0 E
1.0 E
1.0 E
0.0 E
0.0 E
422.75 E
422.75 E
2.60E+05 E
0.0 E
0.0 E
422.75 E

DX VOL FA
FRIC
RVFRIC
GRAV HD
ICFLG
NFF
ALP
VV
TV
P
PA
OPPP
MATID
TW
DX VOL FA
FRIC
RVFRIC
GRAV HD
ICFLG
NFF
ALP
VV
TV
P
PA
OPPP
MATID
TW

***** COMPONENT NO. 34 *****
***** LOOP SEAL AND COLD LEG LOOP 3 *****

TEE	JCELL	NODES	34 LOOP-SEAL COLD-LEG LOOP 3	MAT	COST	ICHF	C 2
ICONC1	NCELL1	6 JUN1	JUN2	IPOW1	C 3		
IQPTR1	IQPSV1	34 NQPTB1	NQPSV1	NQPRF1	C 5		
RADIN1	TH1	0 HOUTL1	HOUTV1	TOUTL1	C 6		
TOUTV1	PWIN1	0 PWOFF1	RPWMX1	PWSCL1	C 7		
QPIN1	QPOFF1	0 RQPMX1	QPSCL1		C 8		
ICONC2	NCELL2	360 JUN3	IPOW2		C 9		
IQPTR2	IQPSV2	0 NQPTB2	NQPSV2	NQPRF2	C 11		
RADIN2	TH2	0 HOUTL2	HOUTV2	TOUTL2	C 12		
TOUTV2	PWIN2	0 PWOFF2	RPWMX2	PWSCL2	C 13		
QPIN2	QPOFF2	0 RQPMX2	QPSCL2		C 14		

* PRIMARY *

R 2 1.2 R 2	1.9125	1.2 R 3	2.317	1.514		DX
R 2 1.665 R 2	1.092	.655				DX
600 R 2	1.495	1.5050	1.9110	R 2 1.6825		DX
0.710 E						DX
R 2 .5301 R 2	.8449	.5301 R 3	1.0236	.6689		VOL
R 2 .7356 R 2	.4824	.7200	.9480 S			VOL
R 2 0.66048	0.66489	0.40247 R 2	0.74331	0.38038 E		VOL
R 12 4.4179	.00000	.6892 R 7	.44179	.6362 E		FA
0. R 11	.019	10.76 R 8	.008	.0205 E		FRIC


```

      0. R 11      .019      7.75 R 8      .008      .0205 E* RVFRIC
      1.0      .2513      0.0      -.2313 R 4      .573 GRAV
    -49350      0.0      .7978      1.0      GRAV
    -7762      .1411 R 7      0.0 E      GRAV
R 21      75      0.90 E      0 E      HL
R 12      0      1 F      0 E      ICFLAC
R 07      1 E      1.0      1.0      1.0      1.5      NFF
R 10      0.0      ALP
      0.0      VL
      0.0      VV
      416.78 E      TL
      416.78 E      TV
      2.60E+05 E      PA
      0.0      QPPP
      0.0      MATID
      416.78 E      TW
      0.50 E      DX
      0.019 E      VOL
      .8010E-02 E      FA
      0.0 E      FRIC
      +1.0 E      RVFRIC
      2.2000E-01 E      GRAV
      0      HD
      1      ICFLG
      0.0      NFF
      1.0      ALP
      0.0      VL
      0.0      VV
      416.78 E      TL
      416.78 E      TV
      2.60E+05 E      P
      0.0      PA
      0.0      QPPP
      0.0      MATID
      416.78 E      TW

```

COMPONENT NO. 38
 SEPARATOR DRAIN TEE LOOP 3

TEE	JCELL	NODES	MAT	COST	ICHF	C 2
ICONC1	4	6	JUN1	JUN2	IPOW1	C 3
IQPTR1	6	39	NQPTB1	NQPSV1	NQPRF1	C 5
RADIN1	0	0	HOUTL1	HOUTV1	TOUTL1	C 6
TOUTV1	0.25	0	PWOFF1	RPWMX1	PWSCL1	C 7
QPIN1	0	0	RQPMX1	QPSCL1		C 8
ICONC2	4	6	JUN2	IPOW2		C 9
IQPTR2	6	39	NQPTB2	NQPSV2	NQPRF2	C 11
RADIN2	0	0	HOUTL2	HOUTV2	TOUTL2	C 12
TOUTV2	0.25	0	PWOFF2	RPWMX2	PWSCL2	C 13
QPIN2	0	0	RQPMX2	QPSCL2		C 14

```

* PRIMARY *
0.9 R 2      0.925 R 3      0.4913 E      DX
0.0283 R 2      0.029 R 3      0.0964 E      VOL
4.0401 R 2      0.0314 R 4      0.1963 E      FA
      0.0 E      FRIC
      0.0 E      RVFRIC
      -1.0 E      GRAV
      0.44 R 3      0.2 F      0.5 E      HD
      1 E      ICFLG
      1.0 R01      1. E      NFF
      0.0 E      ALP
      0.0 E      VL
      422.75      308.15 E      VV
      422.75      308.15 E      TL
      2.60E+05 E      P
      0.0      PA
      0.0      QPPP
      0.0      MATID
R 20 422.75 F 308.15 E
* SECONDARY *
      0.5 E      DX
      0.0266 E      VOL
      0.05326 E      FA
      0.0 E      FRIC
      0.0 E      RVFRIC
      0.0 E      GRAV
      0.2604 E      HD
      0.0 E      ICFLG
      1.0 E      NFF
      1.0 E      ALP
      0.0 E      VL
      422.75      308.15 E      VV
      422.75      308.15 E      TL

```

2.60E+05 E
 0.0
 6
 422.75 E

* PA
 * OPP
 * MATID
 * TW

COMPONENT NO. 89 *****
 SEPARATOR DRAIN VALVE LOOP 3 *****

VALVE	NCCELLS	39 NODES	39 JUN1	38 JUN2	SEPARATOR DRAIN VALVE MAT
ICHF	2	4	330	38	IVPS 6 NVTR2
IVTR	1	0	1	2	IVSV 0 NVRF
IQP3TR	0	100	2	0	NQPS3V 0 NQPSRF
IVTROV	0	0	0	0	
RVMX	1.E10	0	0	1.	FMINOV 1. FMAXOV
RADIN	.015	.005	0.	0.	HOUTL 0. HOUTV 300. TOUTL
TOUTV	300	.03140	.20	1.0	HVLVE 0. FAVLVE 0. XPOS
QPSIN	0	0	0.	0.	RQPSMX 0. QPSSCL
F	0.0266	0.05326 E			DX VOL
R	0.05326 E	1.944 F	0. E		FA
	0.	1.944 F	0. E		FRIC
	0.2604 E	.4220 E			RVFRIC
	0.				GRAV
	0.				HD
	1.0	1. E			ICFLG
	0.				NFF
	0.				ALP
	0.				VL
	422.75 E				VV
	422.75 E				TL
	2.60E+05 E				TV
	0.				P
	0.				PA
	6				OPP
	422.75 E				MATID
					TW
T(S)	POS(-)				* VTBI
0	1.0 S				* VTBI
300.0	1.0 E				

COMPONENT NO. 333 *****
 STEAM SUPPLY FILL LOOP 3 *****

FILL	JUN1	333 IFTY	333 IOFF	STEAM SUPPLY LOOP 3 C 2
IFTR	333	5	0	NFTB 0 NFSV 0 NFRF C 3
TWTOLD	0	-0.03	0	CONCIN C 4
DXIN	0	15	0.	ALPIN 0. VLIN 422.75 TLIN C 5
PIN	1	.126	1	FLOWIN 0. VVIN 422.75 TVIN C 6
	19.88E+05	0.	0.	422.75

COMPONENT NO. 339 *****
 SEPARATOR DRAIN FILL LOOP 3 *****

FILL	JUN1	339 IFTY	339 IOFF	SEPARATOR DRAIN FILL LOOP 3 C 2
IFTR	339	6	1	NFTB 0 NFSV 0 NFRF C 3
TWTOLD	666	100	-2	CONCIN C 4
DXIN	0	20.0	0.	ALPIN 0. VLIN 308.15 TLIN C 5
PIN	0.4913	0.09640	0.	FLOWIN 0. VVIN 308.15 TVIN C 6
VMSCL	2.60E+05	0.	0.	308.15 C 9
TIME (S)	1	1		MASS FLOW (KG/S)
0	0.	0. S		
5.	5.	-25. E		

COMPONENT NO. 35 *****
 HOT LEG ECC FILL LOOP 3 *****

FILL	JUN1	35 IFTY	35 IOFF	HOT-LEG-ECC LOOP 3 C 2
IFTR	35	8	7	NFTB 0 NFSV 0 NFRF C 3
TWTOLD	666	100	-6	CONCIN C 4
DXIN	0	1.E10	0.	ALPIN 0. VLIN 303.35 TLIN C 5
	3.3	.134	0.	303.35

PIN	PAIN	FLOWIN	VVIN	TVIN	C 6
2.60E+05	0	0	303.35		
VMSC1	VVSC1			C 9	
TIME (S)	MASS FLOW (KG/S)				
0	0. S				
2.5	500. S				
12.5	500. S				
32.5	500. S				
110.5	300. E				

COMPONENT NO. 36
 COLD LEG ECC FILL LOOP 3

FILL	JUN1	IFTY	IOFF	COLD-LEG-ECC LOOP 3		
	36	6	0			C 2
	IFTR	IFSV	NFTB	NFSV	NFRF	C 3
	116	100	12	0	0	
	TWTFOLD	RPMX	CONCIN			C 4
	0	1.E10	0			
	DXIN	VOLIN	ALPIN	VLIN	TLIN	C 5
	3.3	125	0	381.65		
	PIN	PAIN	FLOWIN	VVIN	TVIN	C 6
	11.0E+05	0	0	386.15		
	VMSC1	VVSC1				C 9
	1	1				
	TL3CL	TVSCL	PSCL	PASCL	CONSCL	C 10
	1.0	1.0	1.E+05	1.0		
	T(S)	VLTB(M/S)				
	0.00	0.00				
	38.00	0.00				
	42.00	0.00				
	45.00	13.76				
	50.00	13.77				
	57.80	13.78				
	80.00	13.86				
	90.00	13.87				
	118.00	13.89				
	120.00	11.87				
	125.00	0.00				
	140.00	0.00				
	T(S)	VVTB(M/S)				
	0.00	0.0				
	38.00	0.0				
	42.00	0.0				
	45.00	0.0				
	50.00	0.0				
	57.80	0.0				
	80.00	0.0				
	90.00	0.0				
	118.00	0.0				
	120.00	0.0				
	125.00	0.0				
	140.00	0.0				
	T(S)	TL				
	0.00	381.65				
	38.00	381.65				
	42.00	381.85				
	45.00	382.15				
	50.00	383.65				
	57.80	384.15				
	80.00	391.65				
	90.00	392.40				
	118.00	393.65				
	120.00	393.65				
	125.00	393.55				
	140.00	393.45				
	T(S)	TV				
	0.00	457.3				
	38.00	457.3				
	42.00	457.3				
	45.00	457.3				
	50.00	457.3				
	57.80	457.3				
	80.00	457.3				
	90.00	457.3				
	118.00	457.3				
	120.00	457.3				
	125.00	457.3				
	140.00	457.3				
	T(S)	ALPHA				
	0.00	0.0				
	38.00	0.0				
	42.00	0.0				
	45.00	0.0				
	50.00	0.0				
	57.80	0.0				
	80.00	0.0				
	90.00	0.0				
	118.00	0.0				
	120.00	0.0				
	125.00	0.0				
	140.00	0.0				
	T(S)	P(BARS)				
	0.00	11.0				

38.00	11.0
42.00	11.0
45.00	11.0
50.00	11.0
57.80	11.0
80.00	11.0
90.00	11.0
118.00	11.0
120.00	11.0
125.00	11.0
140.00	11.0
T(S)	PA(BARS)
0.00	0.0
38.00	0.0
42.00	0.0
45.00	0.0
50.00	0.0
57.80	0.0
80.00	0.0
90.00	0.0
118.00	0.0
120.00	0.0
125.00	0.0
140.00	0.0

COMPONENT NO. 40

TEE	JCELL	40	40	MAT	HOT-LEG LOOP 4	COST	ICHF	C 2
4	ICONC1	4	6	JUN1	JUN2	JUN2	IPOW1	C 3
0	IQPTR1	8	40	NQPTB1	NQPSV1	NQPSV1	NQPRF1	C 5
0	RADIN1	0	0	HOUTL1	HOUTV1	HOUTV1	TOUTL1	C 6
375	TOUTV1	.01	0	PWIN1	PWOFF1	300	RPWMX1	PWSCL1 C 7
0	QPIN1	0	0	RQPMX1	QPSCL1	0	0	C 8
0	ICONC2	0	0	JUN3	IPOW2	0	0	C 9
0	IQPTR2	1	45	NQPTB2	NQPSV2	NQPSV2	NQPRF2	C 11
0	RADIN2	0	0	HOUTL2	HOUTV2	HOUTV2	TOUTL2	C 12
11	TOUTV2	.01	0	PWIN2	PWOFF2	300	RPWMX2	PWSCL2 C 13
0	QPIN2	0	0	RQPMX2	QPSCL2	0	0	C 14

PRIMARY *

5107 R 2	1.8718	2.135	.9817	.6396 E*	DX
2256 R 2	.732	.9432	.4337	.2826 E*	VOL
.44179 R 2	.3913 R 4	.44179 E			FA
0 R 6	0.016 R 2	0.0 E			FRIC
0 R 6	.016 R 2	0.0 E			RVFRIC
0 R 2	.776	0.766 E			GRAV
.75 R 2	.6329 F	.75 E			HD
0 F	1 F	0 E			ICFLG
1 E	1 E				NFF

SECONDARY *

423.15 E					ALP
423.15 E					VL
2.60E+05 E					VV
0 E					TL
0 E					TV
0 E					P
423.15 E					PA
10 E					QPPP
.40660 E					MATID
.04066 E					TW
0.0 E					DX
0.0 E					VOL
-1.0 E					FA
.2077 E					FRIC
0 E					RVFRIC
1 E					GRAV
1.0 E					HD
0 E					ICFLG
0 E					NFF
419.08 E					ALP
419.08 E					VL
2.60E+05 E					VV
0 E					TL
0 E					TV
419.08 E					P
					PA
					QPPP
					MATID
					TW

COMPONENT NO. 45
HOT LEG ECC FILL LOOP 4

FILL	JUN1	45	45	HOT-LEG-ECC LOOP 4	C 2
	45	8	0	IOFF	

* IFTR	IFSV	NFTB	NFSV	NFRF	C 3
666	100	-6	0		
* TWTOLD	RFMX	CONCIN			C 4
0	1.E10	0			
* DXIN	VOLIN	ALPIN	VLIN	TLIN	C 5
3.5	134	0	303.35		
* PIN	PAIN	FLOWIN	VVIN	TVIN	C 6
2.60E+05	0	0	303.35		
* VMSCL	VVSCL				C 9
1	1				
* TIME (S)	MASS FLOW (KG/S)				
0	0 S				
2.5	500 S				
12.5	500 S				
12.5	500 S				
52.5	400 S				
110.5	300 E				

* COMPONENT NO. 41

TEE	JCELL	NODES	MAT	BHL SEPARATOR	ICHF	C 2
8	4	6	JUN1	JUN2	IPOW1	C 3
* ICONC1	NCELL1	41	NQPTB1	NQPSV1	NQPRF1	C 5
0	11	0	0	0		
* IQPTR1	IQPSV1	0	HOUTL1	HOUTV1	TOUTL1	C 6
0	0	0	0	300		
* RADIN1	TH1	0	PWOFF1	RPWMX1	PWSCL1	C 7
1.25	.025	0	0	0		
* TOUTV1	PWIN1	0	RQPMX1	QPSCL1		C 8
300	0	0	0	0		
* QPIN1	QPOFF1	0	JUN3	IPOW2		C 9
0	0	449	0	0		
* ICONC2	NCELL2	0	NQPTB2	NQPSV2	NQPRF2	C 11
0	7	0	0	0		
* IQPTR2	IQPSV2	0	HOUTL2	HOUTV2	TOUTL2	C 12
0	0	0	0	300		
* RADIN2	TH2	0	PWOFF2	RPWMX2	PWSCL2	C 13
1.25	.025	0	0	0		
* TOUTV2	PWIN2	0	RQPMX2	QPSCL2		C 14
300	0	0	0	0		
* QPIN2	QPOFF2	0	0	0		
0	0	0	0	0		

* PRIMARY *

R 2	.9556	0.2814	0.202	0.424	0.188	* DX
	0.710	0.605	0.200	0.346	0.791	* DX
R 2	2.597	1.330	0.9477	0.367	0.223	* VOL
	0.7356	0.644	0.946	1.6365	2.734	* VOL
R 2	.44179	4.5584	4.7298	R 2	0.866	R 4
R 2	4.7298	0.44179	E		1.511	* FA
R 3	0	0.3621	R 4	0.0	0.0	* FRIC
R 3	0	.9053	F	0.0	0.0	* RVFRIC
	.766	1.00	E			* GRAV
	0.75	2.300	R 2	.1583	R 4	0.2091
	0					* ICFLG
	0					* NFF
	0					* ALP
	0					* VL
	0					* VV
	419.08					* TL
	419.08					* TV
	2.60E+05					* P
	0					* PA
	0					* QPPP
	6					* MATID
	419.08					* TW

* SECONDARY *

R 2	0.710	0.188	0.424	0.900	1.850	* DX
R 2	1.474	E	0.701	1.755	0.0283	* DX
R 2	2.359	E	0.701	1.755	0.0283	* VOL
R 3	0.2892	E				* VOL
R 3	3.323	R 2	4.138	R 2	0.0314	.1963
	0	E				* FRIC
	0	E				* RVFRIC
R 5	-1.0	E	-223	-443	-1.0	E
R 4	0.318	R 3	0.200	.40	E	
	0	E				* ICFLG
	1	E				* NFF
	0	E				* ALP
	0	E				* VL
	0	E				* VV
R 4	419.08	F	308.15	E		* TL
R 4	419.08	F	308.15	E		* TV
R 4	2.60E+05	E				* P
	0	E				* PA
	0	E				* QPPP
	6	E				* MATID
R 08	419.08	R20	308.15	E		* TW

* COMPONENT NO. 449

* FILL	JUN1	449	449	BHL SEPARATOR DRAIN	
	8	IFTY	IOFF		C 2
* IFTR	IFSV	NFTB	NFSV	NFRF	C 3
666	100	-2	0		
* TWTOLD	RFMX	CONCIN			C 4
0	20.0	0			

```

*   DXIN      VOLIN      ALPIN      VLIN      TLIN      C 5
*   1.4740    0.28920    0          0.      808.15    TVIN      C 6
*   PIN      PAIN      FLOWIN    VVIN      308.15
*   2.60E+05  0          0          0          C 9
*   VMSCL    VVSCL
*   1        1
*   TIME (S) MASS FLOW (KG/S)
*   0        0
*   5        100. E

```

COMPONENT NO. 42

BROKEN HOT LEG CROSSOVER PIPE, VALVE AND CONTAINMENT PIPING

```

VALVE 42 BHL VALVE
NCELLS 42 JUN1 JUN2 MAT
*   ICHF 0 42 IVTY 91 IVPS 6 NVTB2
*   IVTR 0 4 NVTB1 7 NVSV 0 NVRF
*   666 100 -2 0 0
*   IVTROV 0 IVTYOV
*   RVMX 0 RVOV FMINOV FMAXOV
*   1E10 0 0 1.
*   RADIN 0 TH HOUTL 1. HOUTV 300 TOUTL
*   375 .005 0 0 0
*   TOUTV 0 AVLVE .75 HVLVE 0 FAVLVE XPOS
*   300 .44179 0 0 0
*   QP3IN 0 QP3OFF 1.225 5.077 3.148 S* DX
*   1.080 3.825 1.34 8.3 13.585 S* DX
*   4.181 1.4 0 0 0
*   13.585 4.33 E 0.5413 2.2429 1.3907 S* VOL
*   0.4771 1.6898 1.7786 11.0168 18.0317 S* VOL
*   1.8471 0.6185 0 0 0
*   18.0317 5.7473 E 0 0 0
R 4 0.44179 0.1325 R 2 0.44179 R 6 1.3275 E 0.0555 S* FRIC FA
*   0 0 0.02592 0 0.00 0.02023 0.00891 S* FRIC
*   0 0 0.01088 0.0 E 0.0 0.25 S* RVFRIC
*   0 0 0.02592 0.02515 0.0 0.00891 S* RVFRIC
*   0.01688 0.0 0.0 E 0.02023 0.00891 S* RVFRIC
*   0 0 0.01088 0.0 E -1.0 -1.0 S* GRAV
*   1.0 0.2202 -0.2425 0.0 0.861 0.3793 S* GRAV
*   -0.4295 0.0 -0.2417 -1.0 E 0 0
*   0 0 0.75 R 6 1.3 E 0 1 F 0 E* ICFLG
*   0 0 0 0 0 0
*   1 1 1 1 1 1
*   0 0 0 0 0 0
*   0 0 0 0 0 0
*   6 419.08 F 416.15 E
*   6 419.08 F 416.15 E
*   2.60E+05 E
*   0.0 E
*   * NFF
*   * ALP
*   * VL
*   * VV
*   * TV
*   * PA

```

TIME(S) STEM POS.(-)
0 0 S
4.00 0. E

COMPONENT NO. 46

```

VALVE 46 BCL PIPE AND VALVE
NCELLS 46 JUN1 JUN2 MAT
*   ICHF 4 46 IVTY 46 IVPS 6 NVTB2
*   IVTR 1 4 NVTB1 6 NVSV 0 NVRF
*   446 100 20 0 0
*   IQP3TR 0 IQP3SV 0 NQP3TB 0 NQP3SV NQP3RF
*   IVTROV 0 IVTYOV
*   RVMX 0 RVOV FMINOV FMAXOV
*   1E10 0 0 1.
*   RADIN 0 TH HOUTL 1. HOUTV 300 TOUTL
*   375 .005 0 0 0
*   TOUTV 0 AVLVE .75 HVLVE 0.9753 FAVLVE XPOS
*   300 .44179 0 0 0
*   QP3IN 0 QP3OFF 0 0 0
*   0.67 R 2 1.5475 R 2 1.758 1.945 E 0.4418 E* DX VOL
*   0.3611 R 2 0.6837 2.2867 0.7767 0.4418 E* FA
*   6362 F 44179 E
*   0. E
*   0. E
*   0. E
*   0. E
*   9 F .75 E
*   0 1 F 0 E
*   1 E
*   1.0 0 0 0 0
*   0 0 0 0 0
*   5 412.15 412.15 E
*   5 412.15 412.15 E
*   * NFF
*   * ALP
*   * VL
*   * VV
*   * TV

```

R 5 2.60E+06 2.60E+06 E

PA
OPPP
MATID
TW

R20 412.15 F 412.15 E

T(S)	VTBL(-)
0.0	0.9753 S
22.40	0.9753 S
23.49	0.9753 S
24.49	0.9753 S
99.99	0.9755 S
150.49	0.9756 S
200.49	0.9756 S
250.49	0.9755 S
269.49	0.9755 S
270.99	0.9117 S
72.49	0.7423 S
73.99	0.6781 S
75.99	0.5682 S
77.99	0.1473 S
270.99	0.03359 S
281.49	0.01548 S
282.99	0.00736 S
283.99	0.00676 S
284.99	0.00671 S
299.99	0.00651 S

COMPONENT NO. 90

BREAK	JUN1	ITBY	90 ISAT	90 ISAT	BCL CONTAINMENT BREAK	IOFF	C 2
IBTR	46	1	3	1	1.DV	0	
DXIN	90	100	10	0	NBSV	0	NBRF C 3
PAIN	5	25	1	434.00	TIN	2.28E+05	PIN C 4
PSCL	0	CONCIN	1.E10	2.28E+05	POFF	0	BELV C 5
	1	TLSCl	1	1	PASCL	1	CONSCl C 6

T(S)	P(PA)
0.00	2.28E+05 S
20.00	2.28E+05 S
35.90	2.70E+05 S
46.70	2.30E+05 S
50.00	2.55E+05 S
53.30	2.38E+05 S
79.00	2.38E+05 S
120.00	2.98E+05 S
126.70	2.50E+05 S
140.00	2.41E+05 S

COMPONENT NO. 91

BREAK	JUN1	ITBY	91 ISAT	91 ISAT	BHL CONTAINMENT BREAK	IOFF	C 2
IBTR	91	1	3	1	IVDV	0	
DXIN	91	100	61	0	NBSV	0	NBRF C 3
PAIN	5	25	1	416.15	TIN	2.592E+05	PIN C 4
PSCL	0	CONCIN	1.E10	2.592E+05	POFF	0	BELV C 5
	1	TLSCl	1	1	PASCL	1	CONSCl C 6

T(S)	P(PA)
0.0	2.592E+05 S
4.8010E-01	2.592E+05 S
5.4801E+00	2.598E+05 S
1.0480E+01	2.599E+05 S
1.5480E+01	2.593E+05 S
2.0480E+01	2.572E+05 S
2.5480E+01	2.585E+05 S
3.0480E+01	2.568E+05 S
3.5480E+01	2.514E+05 S
4.0480E+01	2.489E+05 S
4.5480E+01	2.462E+05 S
5.0480E+01	2.458E+05 S
5.5480E+01	2.467E+05 S
6.0480E+01	2.466E+05 S
6.5480E+01	2.463E+05 S
7.0480E+01	2.472E+05 S
7.5480E+01	2.469E+05 S
8.0480E+01	2.482E+05 S
8.5480E+01	2.508E+05 S
9.0480E+01	2.512E+05 S
9.5480E+01	2.519E+05 S
1.0048E+02	2.527E+05 S
1.0548E+02	2.536E+05 S
1.1048E+02	2.550E+05 S
1.1548E+02	2.554E+05 S
1.2048E+02	2.555E+05 S
1.2548E+02	2.545E+05 S
1.3048E+02	2.540E+05 S
1.3548E+02	2.540E+05 S

1.4048E+02	2.528E+05
1.4548E+02	2.528E+05
1.5048E+02	2.519E+05
1.5548E+02	2.520E+05
1.6048E+02	2.530E+05
1.6548E+02	2.539E+05
1.7048E+02	2.551E+05
1.7548E+02	2.560E+05
1.8048E+02	2.551E+05
1.8548E+02	2.561E+05
1.9048E+02	2.565E+05
1.9548E+02	2.563E+05
2.0048E+02	2.555E+05
2.0548E+02	2.554E+05
2.1048E+02	2.550E+05
2.1548E+02	2.546E+05
2.2048E+02	2.546E+05
2.2548E+02	2.538E+05
2.3048E+02	2.512E+05
2.3548E+02	2.519E+05
2.4048E+02	2.578E+05
2.4548E+02	2.581E+05
2.5048E+02	2.529E+05
2.5548E+02	2.538E+05
2.6048E+02	2.554E+05
2.6548E+02	2.560E+05
2.7048E+02	2.565E+05
2.7548E+02	2.570E+05
2.8048E+02	2.572E+05
2.8548E+02	2.571E+05
2.9048E+02	2.572E+05
2.9548E+02	2.573E+05

ARAYA THE FOLLOWING COMPONENT DATA WERE ADDED FOR MODELLING THE NITROGEN INJECTION SYSTEM. THE GEOMETRICAL DATA MAY NOT BE CORRECT BECAUSE OF NO KNOWLEDGE ON DIMENSIONS OF THE SYSTEM. THIS SHOULD BE CORRECTED AFTER GETTING THE DATA.

NEW COMPONENT DATA FOR THE NITROGEN INJECTION SYSTEM

COMP. 160 FOR THE COLD LEG ECC PIPE AND N2 INJ. PIPE, LOOP 1, TEE

*****	TYPE	NUM	ID	CTITLE
TEE	JCELL	160	160 ECC & N2 INJ. PIPES LOOP 1	
	JCELL	NODES	MAT	COST
	2	4	6	0
	ICONC1	NCELL1	JUN1	JUN2
	0	3	160	0
	IQPTR1	IQPSV1	NQPTB1	NQPSV1
	0	0	0	0
	RADIN1	TH1	HOUTL1	HOUTV1
	1.1000E-01	1.0000E-02	0.0000E+00	0.0000E+00
	TOUTV1	PWIN1	PWOFF1	RPWMX1
	3.0000E+02	0	0	0
	QPIN1	QPOFF1	RQPMX1	QPSCL1
	0.0000E+00	0.0000E+00	0.0000E+00	0.0000E+00
	ICONC2	NCELL2	JUN3	IPOW2
	0	1	161	0
	IQPTR2	IQPSV2	NQPTB2	NQPSV2
	0	0	0	0
	RADIN2	TH2	HOUTL2	HOUTV2
	1.1000E-01	1.0000E-02	0.0000E+00	0.0000E+00
	TOUTV2	PWIN2	PWOFF2	RPWMX2
	3.0000E+02	0	0	0
	QPIN2	QPOFF2	RQPMX2	QPSCL2
	0.0000E+00	0.0000E+00	0.0000E+00	0.0000E+00

DX * R6 0.5 E
VOL * R03 1.7000E-02 E
FA * F 3.8010E-02 E
FRIC * F 0.0000E+00 E
RV FRI * F 0.0000E+00 E
GRAV * R03 0.0000E+00 R01 -1.0 E
HD * F 2.2000E-01 E
ICFLG * F 0E
NFF * F 1E
ALP * F 1.0000E+00E
VL * F 0.0000E+00E
VV * F 0.0000E+00E
TL * F 4.1118E+02E
TV * F 4.1118E+02E
P * F 2.6000E+05E
PA * F 0.0000E+00E
QPPP * F 0.0000E+00E
MATID * F 6E
TW * F 4.1118E+02E

DX * 0.5 E
VOL * 1.7000E-02 E
FA * F 3.8010E-02E
FRIC * F 0.0000E+00 E
RV FRI * F 0.0000E+00 E
GRAV * F 1.0000E+00 E
HD * F 2.2000E-01E
ICFLG * F 0E
NFF * F 1E


```

*ALP * F 1.0000E+00E
*VL * F 0.0000E+00E
*VV * F 0.0000E+00E
*TL * F 4.1118E+02E
*TV * F 4.1118E+02E
*P * F 2.6000E+05E
*PA * F 0.0000E+00E
*QPPP * F 0.0000E+00E
*MATID * F 6E
*TW * F 4.1118E+02E

```

COMPONENT 161 FOR THE NITROGEN INJECTION FILL, LOOP 1, FILL

```

***** TYPE NUM ID CTITLE
FILL 161 161 161 N2 INJ. FILL LOOP 1
JUN1 IFTY 10FF
161 8 0
* IFTR IFSV 6 NFTB NFSV NFRF
90 130 0
* TWTOLD RFXM CONCIN F LV
0.0000E+00 1.0000E+10 0.0000E+00 0.0000E+00
* DXIN VOLIN ALFIN VLIN TLIN
5.0000E-01 1.7000E-32 1.0000E+00 0.0000E+00 $10.0
* FIN FAIN FLOWIN VVIN TVIN
2.215E+06 2.215E+06 0.0000E+00 0.0000E+00 $10.0
* VMSCV VVSCV
1.0000E+00 1.0000E+00

```

NITROGEN INJECTION MASS FLOW RATE TABLE

```

T(S) VMTB(KG/S)
0.0 0.0 S
38.00 0.0 S
40.0000 0.340000 S
120.0000 0.340000 S
122.5000 0.0 S
1.E+06 0.0 E

```

COMP. 260 FOR THE COLD LEG ECC PIPE AND N2 INJ. PIPE, LOOP 2, TEE

```

***** TYPE NUM ID CTITLE
TEE 260 260 ECC & N2 INJ. PIPES LOOP 2
JCELL NODES MAT COST ICHF
2 4 0 0
* ICONC1 NCELL1 JUN1 JUN2 IPOW1
0 3 260 0
* IQPTR1 IQPSV1 NQPTB1 NQPSV1 NQPRF1
0 0 0 0
* RADIN1 TH1 HOUTL1 HOUTV1 TOUTL1
1.1000E-01 1.0000E-02 0.0000E+00 0.0000E+00 $0.0000E+02
* TOUTV1 PWIN1 PWOFF1 RPWMX1 PWSCL1
3.0000E+02 0 0 0
* QPIN1 QPOFF1 RQPMX1 QPSCL1
0.0000E+00 0.0000E+00 0.0000E+00 0.0000E+00
* ICONC2 NCELL2 JUNS IPOW2
0 0 0 0
* IQPTR2 IQPSV2 261 NQPTB2 NQPSV2 NQPRF2
0 0 0 0
* RADIN2 TH2 HOUTL2 HOUTV2 TOUTL2
1.1000E-01 1.0000E-02 0.0000E+00 0.0000E+00 $0.0000E+02
* QPIN2 QPOFF2 RQPMX2 QPSCL2
0.0000E+00 0.0000E+00 0.0000E+00 0.0000E+00
* QPIN2 QPOFF2 RQPMX2 QPSCL2
0.0000E+00 0.0000E+00 0.0000E+00 0.0000E+00

```

```

DX * R05 0.5 E
VOL * R03 1.7000E-02 E
FA * F 3.8010E-02 E
FRIC * F 0.0000E+00 E
RV FRI * F 0.0000E+00 E
GRAV * R05 0.0000E+00 R01 -1.0 E
HD * F 2.2000E-01 E
ICPLG * F 0E
NFF * F 1E
ALP * F 1.0000E+00E
VL * F 0.0000E+00E
VV * F 0.0000E+00E
TL * F 4.1415E+02E
TV * F 4.1415E+02E
P * F 2.6000E+05E
PA * F 0.0000E+00E
QPPP * F 0.0000E+00E
MATID * F 6E
TW * F 4.1415E+02E

```

```

DX * 0.5 E
VOL * 1.7000E-02 E
FA * F 3.8010E-02E
FRIC * F 0.0000E+00 E
RV FRI * F 0.0000E+00 E
GRAV * F 1.0000E+00 E
HD * F 2.3000E-01E
ICPLG * F 0E
NFF * F 1E
ALP * F 1.0000E+00E
VL * F 0.0000E+00E
VV * F 0.0000E+00E
TL * F 4.1415E+02E
TV * F 4.1415E+02E
P * 2.6000E+05E

```

* PA * 0.0000E+00E
 * QPPP * F 0.0000E+00E
 * MATID * F 6E
 * TW * F 4.1418E+02E

COMPONENT 261 FOR THE NITROGEN INJECTION FILL, LOOP 2, FILL

```

***** TYPE      NUM      ID      CTITLE
FILL            261      261 N2 INJ. FILL LOOP 2
  UN1           IFTY      IOFF
  TR            IFSV      NFTB      NFSV      NFRF
  TWOLD        RFMX      CONCIN      FELV
0.0000E+00    1.0000E+10  0.0000E+00  0.0000E+00
  DXIN         VOLIN      ALPIN      VLIN      TLIN
5.0000E-01    1.7000E-02    1.0000E+00  0.0000E+00  $10.0
  PIN          PAIN      FLOWIN     VVIN      TVIN
2.215E+06    2.215E+06    0.0000E+00  0.0000E+00  $10.0
  VMSCL        VVSCL
1.0000E+00    1.0000E+00
  
```

NITROGEN INJECTION MASS FLOW RATE TABLE

T(S)	VMTB(KG/S)
0.0	0.0 S
58.00	0.0 S
40.0000	0.340000 S
120.0000	0.340000 S
122.5000	0.0 S
1.E+05	0.0 E

COMP. 360 FOR THE COLD LEG ECC PIPE AND N2 INJ. PIPE, LOOP 3, TEE

```

***** TYPE      NUM      ID      CTITLE
TEE            360      360 ECC & N2 INJ PIPES LOOP 3
  JCELL        NODES      MAT      COST      ICHF
  ICONC1       NCELL1     JUN1     JUN2     IPOW1
  IQPTR1       IQPSV1     NQPTB1   NQPSV1   NQPRF1
  RADIN1       TH1        HOUTL1   HOUTV1   TOUTL1
1.1000E-01    1.0000E-02    0.0000E+00  0.0000E+00  3.0000E+02
  TOUTV1       PWIN1      PWOFF1   RPWMX1   PWSCL1
3.0000E+02    0.0000E+00  0.0000E+00  0.0000E+00  0.0000E+00
  QPIN1        QPOFF1     RQPMX1   QPSCL1
0.0000E+00    0.0000E+00  0.0000E+00  0.0000E+00
  ICONC2       NCELL2     JUN3     IPOW2
  IQPTR2       IQPSV2     NQPTB2   NQPSV2   NQPRF2
  RADIN2       TH2        HOUTL2   HOUTV2   TOUTL2
1.1000E-01    1.0000E-02    0.0000E+00  0.0000E+00  3.0000E+02
  QPIN2        QPOFF2     RQPMX2   QPSCL2
0.0000E+00    0.0000E+00  0.0000E+00  0.0000E+00
  QPIN2        QPOFF2     RQPMX2   QPSCL2
0.0000E+00    0.0000E+00  0.0000E+00  0.0000E+00
  
```

DX * R03 0.5 E
 VOL * R03 1.7000E-02 E
 FA * F 3.8010E-02 E
 FRIC * F 0.0000E+00 E
 RV FRI * F 0.0000E+00 E
 GRAV * R03 0.0000E+00 R01 -1.0 E
 HD * F 2.2000E-01 E
 ICFLG * F 0E
 NFF * F 1E
 ALP * F 1.0000E+00E
 VL * F 0.0000E+00E
 VV * F 0.0000E+00E
 TL * F 4.1678E+02E
 TV * F 4.1678E+02E
 P * F 2.6000E+05E
 PA * F 0.0000E+00E
 QPPP * F 0.0000E+00E
 MATID * F 6E
 TW * F 4.1678E+02E

DX * 0.5 E
 VOL * 1.7000E-02 E
 FA * F 3.8010E-02E
 FRIC * F 0.0000E+00 E
 RV FRI * F 0.0000E+00 E
 GRAV * F 1.0000E+00 E
 HD * F 2.2000E-01E
 ICFLG * F 0E
 NFF * F 1E
 ALP * F 1.0000E+00E
 VL * F 0.0000E+00E
 VV * F 0.0000E+00E
 TL * F 4.1678E+02E
 TV * F 4.1678E+02E
 P * F 2.6000E+05E
 PA * F 0.0000E+00E
 QPPP * F 0.0000E+00E
 MATID * F 6E
 TW * F 4.1678E+02E

*COMPONENT 361 FOR THE NITROGEN INJECTION FILL, LOOP 3, FILL

```

***** TYPE      NUM      ID      CTITLE
FILL  JUN1      361      361 N2 INJ. FILL LOOP 3
      361      IFTY      IOFF
      90      IFSV      NFTB      NFSV      NFRF
      100      RFMX      CONCIN      FELV
* 0.0000E+00  1.0000E+10  0.0000E+00  0.0000E+00
* DXIN      VOLIN      ALPIN      VLIN      TLIN
* 5.0000E-01  1.7000E-02  1.0000E+00  3.0000E+00  $10.0
* PIN      PAIN      FLOWIN      VVIN      TVIN
* 2.215E+06  2.215E+06  0.0000E+00  0.0000E+00  $10.0
* VMSCL      VVSCL
* 1.0000E+00  1.0000E+00
  
```

*NITROGEN INJECTION MASS FLOW RATE TABLE

```

T(S)      VMTB(KG/S)
0.0        0.0 S
38.00     0.0 S
40.0000   0.340000 S
120.0000  0.340000 S
122.5000  0.0 S
1.E+05    0.0 E
  
```

8. TIME-STEP DATA

```

DTMIN      DTMAX      TEND      TRWFP      RELX
.00001      5.000E-01  22.0      1.00E+00
EDINT      GFINT      DMPINT      SEDINT
2.0        1.000E-01  5.00      1.00E+00

DTMIN      DTMAX      TEND      TRWFP      RELX
0.50E-05   0.005     35.0      1.00E+00
EDINT      GFINT      DMPINT      SEDINT
1.00E+00   1.000E-01  2.00      1.00E+00

DTMIN      DTMAX      TEND      TRWFP      RELX
0.50E-05   0.010     150.0     1.00E+00
EDINT      GFINT      DMPINT      SEDINT
1.00E+00   1.000E-01  2.00      1.00E+00

-1.00E+00
  
```

APPENDIX D: TRAC-PF1 PREDICTION OF UPTF LOWER PLENUM FILLING RATES

UPTF Test 6 Runs 131, 132, 133, and 136 have been simulated with TRAC code by Dr. Henry J. Stumpf at LANL. The computation times on the CRAY computer varied from 2 to 5 hours. Figures D.1 - D.3 show the predicted lower plenum liquid inventory curves for Tests 132, 133 and 136; no liquid penetration was predicted for Test 131 ($W_g = 400$ kg/s). The lower plenum fill-up rates were obtained graphically using Figures D.1-D.3. The starting point of the straight line on each graph corresponds to beginning of the lower plenum fill-up and the end point of the line corresponds to the "quasi" steady lower plenum inventory. Table D.1 lists readings from the graphs used for predicting the lower plenum filling rates. The first column is the test number; the second and third columns are the starting time of lower plenum fill-up and the liquid inventory of the lower plenum at that time, respectively; the fourth and fifth columns show the time and the liquid inventory when the "quasi" steady lower plenum liquid inventory was first reached. The last column is the lower plenum fill-up rate. Table D.2 summarizes the experimental and calculational data for the UPTF tests.

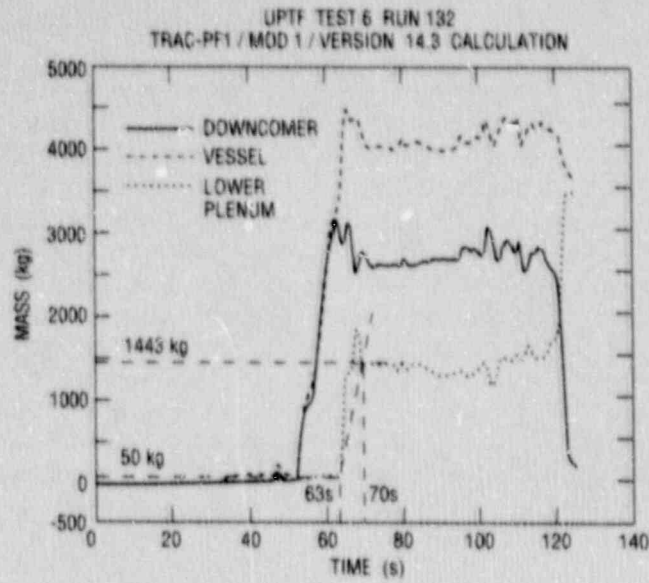


Figure D.1 UPTF Test 6 Run 132, Vessel, Downcomer, Lower Plenum Liquid Masses

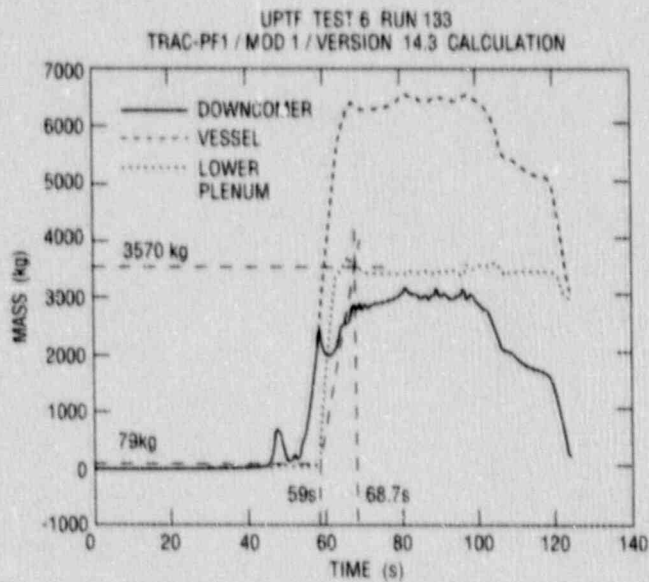


Figure D.2 UPTF Test 6 Run 133, Vessel, Downcomer, Lower Plenum Liquid Masses

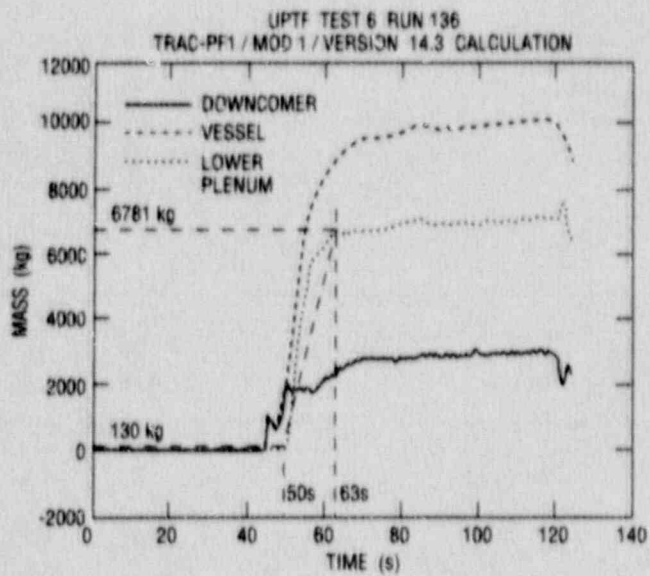


Figure D.3 TRAC-PF1 Prediction, Test 6, Run 136

Table D.1 - Predicted Lower Plenum Water Inventory and Filling Rates, UPTF Test 6

Run	t_1 (s)	$m_{LP,1}$ (kg)	t_2 (s)	$m_{LP,2}$ (kg)	\dot{m}_{LP} (kg/s)
132	63	50	70	1443	199
133	59	79	68.7	3570	360
136	50	130	63	6781	512

Table D.2 - Summary of UPTF Results (Test 6)

EXPERIMENT						TRAC			
Run	W_g (kg/s)	\dot{m}_{LP} (kg/s)	t_I (s)	t_A (s)	$T_{IA,UPTF}$ (s)	\dot{m}_{LP} (kg/s)	t_I (s)	t_A (s)	$t_{IA,UPTF}$ (s)
131	400	419	43	49(54)	6(11)	0	43	∞	∞
132	300	840	43	52	9	199	43	63	20
133	200	699	43	50	7	360	43	59	16
135	440	> 0	43	-----	-----	0	43	∞	∞
136	100	644	43	45	2	512	43	50	7

APPENDIX E

Estimate of ECCS Flow in the Presence of Dissolved N_2

E.1 Introduction

The nitrogen (N_2) gas in the system occupies the top portion of the accumulators, and is also dissolved in the coolant in the accumulators. The coolant in the accumulator is in equilibrium with the nitrogen in the gas space. The amount of the dissolved nitrogen (N_2) is only 57.6 kg and about half of it will emerge from the coolant as it flows from the accumulators to the cold legs and the downcomer where the pressure is lower than in the accumulators.

The N_2 in the cold legs and in the downcomer will mix with the steam. This will affect the thermohydraulics of the coolant in two ways. First, N_2 will occupy volume and displace the coolant into the lower parts of the downcomer and, second, N_2 will reduce the interfacial mass transfer process (condensation) by decreasing the rate of interfacial heat transfer.

E.2 Purpose

The objective of the task described in this appendix is to estimate the amount of ECC flow during LBLOCA in a Westinghouse PWR in the presence of N_2 . The ECC injection rate depends upon system pressure which is affected by the emerging N_2 from the ECC. Therefore, this task will require estimation of the amount of N_2 emerging from ECC and its effect on the system pressure.

The time to fill the lower plenum depends upon the ECC injection rate. Any delay in filling the lower plenum due to the dissolved N_2 will allow the clad to heat up for the duration of delay and contribute to bias in the predicted PCT.

E.3 Approach

The effect of N_2 on the ECC flow rate is estimated by computing a correction to the system pressure obtained from the nominal TRAC calculation. A separate model predicts the ECC flow rate based on corrected system pressure. The method of estimating the correction to TRAC-predicted system pressure consists of the following steps:

- 1) Formulate single volume models of the reactor system (excluding accumulators) and of intact and of broken loop accumulators. The system pressure will be evaluated in this step based on the information obtained from the next two steps.
- 2) Estimate the amount of N_2 emerging in the reactor system from the ECC flow,
- 3) Estimate the effect of the N_2 on prediction of condensation in the reference NPP calculation with TRAC.

E.3.1 Formulation

The emerging N_2 from the ECC reduces condensation which leads to accumulation of steam in the system. This steam along with N_2 will slow down the rate of system depressurization. Furthermore, unlike in the current reference NPP calculation, where the system pressure was at times below the containment pressure due to condensation leading to the flow from the containment to the system, the system pressure in the presence of N_2 will always be higher than the containment pressure and there will be no flow from the containment to the system.

Three control volumes with liquid and gas spaces are used to model three sections of NPP; the NPP primary side (excluding the accumulators), intact loop accumulators and broken loop accumulator, as shown in Figure E-1. The control volume for the primary side receives ECC from the safety injection system and the accumulators. It is conservatively assumed that all the dissolved N_2 emerges from the ECC before it enters the volume and flows to the gas space. The three intact loop accumulators are represented by a single volume and the broken loop accumulator is represented by another single volume. Special care is taken to model steam generator side break, as the break flow consists of flow from accumulator and from the remaining broken loop. The pipe section at which the accumulator joins the broken loop is designated as junction volume, as shown in Figure E-1.

E.3.1.1 Formulation for Reactor System

It is assumed that the N_2 and steam are in thermal and mechanical equilibrium. Furthermore, the gas space is divided into separate sections for steam and N_2 . The phasic densities in each section will be a function of system pressure. The system volume is modelled with phasic mass balances as given here:

$$\frac{dm_l}{dt} = W_{i,l} - W_{o,l} + \dot{m}_{vl,N_2} \quad (E-1)$$

$$\frac{dm_v}{dt} = W_{i,v} - W_{o,v} - \dot{m}_{vl,N_2} \quad (E-2)$$

$$\frac{dm_{N_2}}{dt} = W_{i,N_2} - W_{o,N_2} \quad (E-3)$$

Where, m_l , m_v , m_{N_2} are masses of liquid, steam and nitrogen, and \dot{m}_{vl,N_2} is net condensation rate in the presence of nitrogen at the interface of liquid/vapor regions. The remaining six variables $W_{i,l}$, $W_{o,l}$, $W_{i,v}$, $W_{o,v}$, W_{i,N_2} , W_{o,N_2} represent the mass flow rates at the inlet and outlet for the liquid, steam and N_2 , respectively.

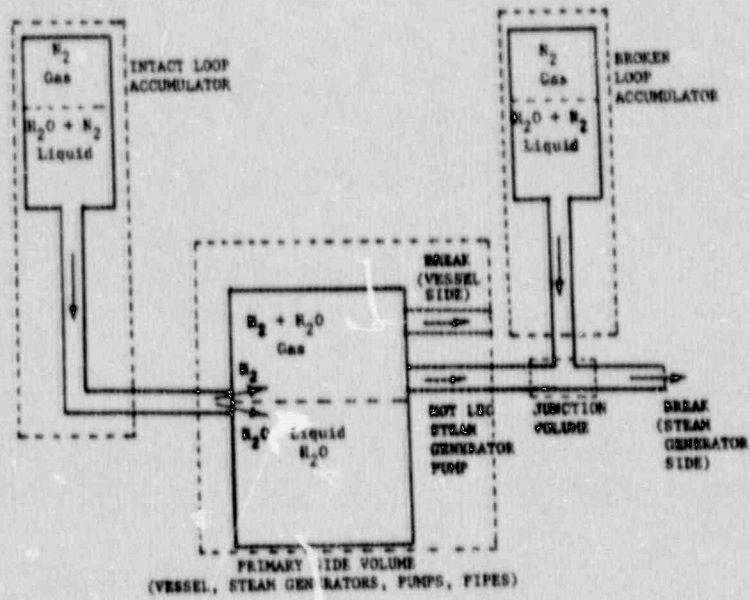


Figure E.1 Schematic of Three Control Volume Representation of NPP (BNL-3-178-90)

The phasic masses are defined as:

$$m_l = V_l \rho_l \quad (E-4)$$

$$m_v = V_v \rho_v \quad (E-5)$$

$$m_{N_2} = V_{N_2} \rho_{N_2} \quad (E-6)$$

The system volume, V , is the sum of phasic volumes, V_l , V_v and V_{N_2} .

$$V = V_l + V_v + V_{N_2} \quad (E-7)$$

We define a system void fraction α and phasic volume fractions α_v and α_{N_2} as:

$$\alpha_v = V_v / V$$

$$\alpha_{N_2} = V_{N_2} / V$$

$$\alpha = \alpha_v + \alpha_{N_2} \quad (E-8)$$

The nitrogen volume fraction α_{N_2} of the reactor system is expected to be small during the Refill Phase and it is estimated from the nitrogen volume fraction in the downcomer.

$$\alpha_{N_2} = \alpha_{N_2,DC} * V_{DC} / V \quad (E-9)$$

where V_{DC} and V are the downcomer and system volumes, and obtained from the reference NPP calculation. The formulation is based on separate regions of steam, nitrogen and the liquid in equilibrium and so the phasic density can be obtained from the system pressure instead of partial pressures as shown here.

$$\rho_v = \rho_v(P) = \frac{m_v}{V_v} = \frac{m_v}{\alpha V} \quad (E-10)$$

$$\rho_{N_2} = \rho_{N_2}(P, T)$$

The fraction of N_2 in the gas space is very small, so the steam partial pressure is close to the system pressure, and the steam and N_2 temperatures are obtained as

$$T = T_{sat}(P)$$

Also,

$$\rho_l = \rho_l(P, u_l)$$

We will also need the liquid energy balance as the liquid density is a function of internal energy. The viscous effects and mechanical energy effects (kinetic energy and work due to interface movements) have been neglected.

$$\frac{d(m_{\ell} u_{\ell})}{dt} = W_{i,\ell} h_{i,\ell} - W_{o,\ell} h_{o,\ell} + \dot{m}_{v\ell,N_2} h_v + q_{w\ell} \quad (E-11)$$

where u_{ℓ} , $h_{i\ell}$, $h_{o\ell}$, h_v , $\dot{m}_{v\ell,N_2}$ and $q_{w\ell}$ are the internal energy of the bulk liquid, liquid enthalpies at the inlet and the outlet of the volume, enthalpy of the steam, condensation rate in the presence of N_2 and net wall heat transfer to the liquid phase.

Equations (E-4) to (E-7) and (E-10) to (E-11) are substituted in Equations (E-1) to (E-3) and the derivatives of the volume fractions are eliminated and gas phase expansion ($d\rho_g/dP$) has been approximated by the vapor term as the amount of N_2 is small; the equation for the system pressure is obtained, as given here.

$$\begin{aligned} \dot{P}_{NPP,N_2} \left\{ \frac{1-\alpha}{\rho_{\ell}} \frac{d\rho_{\ell}}{dP} + \frac{\alpha}{\rho_v} \frac{d\rho_v}{dP} \right\} = & - \frac{1-\alpha}{\rho_{\ell} m_{\ell}} \left(\frac{\partial \rho_{\ell}}{\partial u_{\ell}} \right) \{ W_{i,\ell,N_2} (h_{i,\ell} - u_{\ell}) - W_{o,\ell,N_2} (h_{o,\ell} - u_{\ell}) \\ & + \dot{m}_{v\ell,N_2} (h_v - u_{\ell}) + q_{w\ell} \} - \frac{\dot{m}_{v\ell,N_2}}{V} \left(\frac{\rho_{\ell} - \rho_v}{\rho_{\ell} \rho_v} \right) \\ & + \frac{W_{i,\ell,N_2} - W_{o,\ell,N_2}}{V \rho_{\ell}} + \frac{W_{i,v,N_2} - W_{o,v,N_2}}{V \rho_v} \\ & + \frac{W_{i,N_2} - W_{o,N_2}}{V \rho_{N_2}} \end{aligned} \quad (E-12)$$

This equation represents the system behavior in the presence of N_2 injection into the system. The nominal NPP calculation also accounts for all the effects except N_2 shown in Equation (E-12) during the Refill Phase. There are additional differences in the system behavior due to the N_2 that are not accounted for in the NPP calculation, such as reduced condensation in the downcomer, and no backflow from the containment. In order to estimate the system pressure P_{NPP,N_2} , we will represent the results of the NPP calculations in a form similar to Equation (E-12).

$$\begin{aligned} \dot{P}_{NPP} \left\{ \frac{1-\alpha}{\rho_{\ell}} \frac{d\rho_{\ell}}{dP} + \frac{\alpha}{\rho_v} \frac{d\rho_v}{dP} \right\} = & - \frac{1-\alpha}{\rho_{\ell} m_{\ell}} \left(\frac{\partial \rho_{\ell}}{\partial u_{\ell}} \right) \{ W_{i,\ell} (h_{i,\ell} - u_{\ell}) - W_{o,\ell} (h_{o,\ell} - u_{\ell}) \\ & + \dot{m}_{v\ell} (h_v - u_{\ell}) + q_{w\ell} \} - \frac{\dot{m}_{v\ell}}{V} \left(\frac{\rho_{\ell} - \rho_v}{\rho_{\ell} \rho_v} \right) \end{aligned}$$

$$+ \frac{W_{i,l} - W_{o,l}}{V\rho_l} + \frac{W_{i,v} - W_{o,v}}{V\rho_v} \quad (E-13)$$

Equations (E-12) and (E-13) are combined; the terms in the coefficients of \dot{P}_{NPP, N_2} and \dot{P}_{NPP} representing the compressibility of the liquid are smaller than the terms representing the compressibility of the vapor and are neglected. It is further assumed that the internal energy of the bulk liquid, inlet and outlet and the net wall heat transfer to the liquid phase are the same in two equations. Furthermore, terms representing the differences in the phasic relative velocity have been neglected. The phasic flow rates have been combined to form mixture flow rates. The terms with \dot{m}_{vl} have been compared and the first \dot{m}_{vl} term containing $(h_v - u_l)$ is two orders of magnitude smaller than the second \dot{m}_{vl} term containing $(\rho_l - \rho_v)$ and so the first \dot{m}_{vl} term is neglected.

As we are looking for conservative estimate, it is assumed that no N_2 leaves the system.

$$W_{O, N_2} = 0.0 \quad (E-14)$$

The resulting equation is:

$$\begin{aligned} \dot{P}_{NPP, N_2} = & \dot{P}_{NPP} + \frac{1}{V} \left\{ \frac{W_{i, N_2}}{\rho_{N_2}} + \left(\frac{W_{i, m}}{\rho_m} \right)_{N_2} - \left(\frac{W_{i, m}}{\rho_m} \right) \right. \\ & \left. + \left(\frac{W_{o, m}}{\rho_m} \right) - \left(\frac{W_{o, m}}{\rho_m} \right)_{N_2} + \frac{(\dot{m}_{vl} - \dot{m}_{vl, N_2})}{V} \left[\frac{\rho_l - \rho_v}{\rho_l \rho_v} \right] \right\} / \left(\frac{\alpha}{\rho_v} \frac{d\rho_v}{dP} \right) \end{aligned} \quad (E-15)$$

where $W_{i, m}$ and $W_{o, m}$ are the flow rates of mixture of steam and water going into and out of the volume, and \dot{m}_{vl} and \dot{m}_{vl, N_2} are condensation rates with and without the presence of N_2 . Equation (E-15) indicates that the primary effect of N_2 will be to modify fluid flows at the boundary and the condensation rates.

The condensation term, \dot{m}_{vl} , in Equation (E-15) is estimated from the results from NPP calculation. The rate of condensation due to subcooled ECC is estimated from ECC flow rate and subcooling. The sensible heat released by the condensate in order to reach DC conditions is neglected in comparison to the latent heat.

$$\dot{m}_{v\ell} = \frac{\dot{m}_{ECC,NPP} (T_{DC} - T_A) C_P}{h_{fg}} \quad (E-16)$$

where $\dot{m}_{ECC,NPP}$, T_{DC} , and T_A are the rate of ECC injection, downcomer and accumulator fluid temperatures.

Steps to evaluate $\dot{m}_{v\ell}$ from the NPP calculations are listed here for any time period from t_1 to t_2 during the Refill Phase (t_1 to t_B). The times t_1 and t_2 are times at which the NPP calculation results are available.

$$\Delta m_{CON,NPP} = \Delta m_{ECC,NPP} \frac{C_P}{h_{fg}} \left[\frac{(T_{DC} - T_A) t_1 + (T_{DC} - T_A) t_2}{2} \right] \quad (E-17)$$

$$\dot{m}_{v\ell} = \frac{\Delta m_{CON,NPP}}{t_2 - t_1} \quad (E-18)$$

where $\Delta m_{CON,NPP}$ and $\Delta m_{ECC,NPP}$ are the amounts of steam condensed and ECC injected between t_1 and t_2 .

The condensation rate, $\dot{m}_{v\ell,N_2}$ in Equation (E-15) will be less than $\dot{m}_{v\ell}$. For conservative estimate of system pressure, the condensation rate in the presence of N_2 is neglected.

$$\dot{m}_{v\ell,N_2} = 0 \quad (E-18a)$$

A procedure of estimating $\dot{m}_{v\ell,N_2}$ is described in Section E.3.3. It is shown in Section E.3.4 that condensation reduces by 80% in the presence of N_2 for the conditions expected during the Refill Phase.

The remaining four terms on the right side of Equation (E-15) represent the injection flow rates and break flow rates for NPP with and without including the N_2 effect. The NPP break flow rate and injection rate without N_2 effects were obtained from the reference NPP calculation. The break flow rate for the N_2 case is estimated from the information available from the reference NPP calculation. The pressure difference between the system pressure and break pressure is related to the break flow rate.

$$W_{o,m} = K \sqrt{(P_s - P_B) \rho_m} \quad (E-19)$$

K is estimated at times during the Refill Phase at which the reference NPP calculation results are available. The lowest value of K is selected for the conservative estimate of system pressure. The system has two breaks: one on the vessel side and the other on the steam generator side. The flow coefficient K will be different for two sides. The vessel side break flow is:

$$w_{o,m,VE} = K_{VE} \sqrt{(P_V - P_B) \rho_m} \quad (E-20)$$

where K_{VE} , P_V and P_B are the flow coefficient for the flow path from the vessel to the break, the vessel and break pressures, respectively.

The steam generator side break flow is a combination of flow from the accumulator and from the broken loop.

$$W_{BR,SG} = W_{o,m,SG} + W_{BR,A} \quad (E-21)$$

where $W_{BR,SG}$, $W_{o,m,SG}$ and $W_{BR,A}$ are the flow rates at the steam generator side break, and flow rates from the vessel and the accumulator to the junction volume (Figure E-1), respectively. These flows are related to the pressures as follows:

$$W_{BR,SG} = K_{JB} \sqrt{(P_J - P_B) \rho_J} \quad (E-22)$$

$$W_{o,m,SG} = K_{VJ} \sqrt{(P_V - P_J) \rho_V} \quad (E-23)$$

$$W_{BR,A} = K_{AJ} \sqrt{(P_A - P_J) \rho_\ell} \quad (E-24)$$

$$\rho_J = \alpha_J \rho_g + (1 - \alpha_J) \rho_\ell \quad (E-25)$$

where K_{JB} , K_{VJ} and K_{AJ} are the flow coefficients for the flow paths from the junction volume to the break, from the vessel and the accumulator to the junction volume. Additionally, P_J , P_B and P_A are the pressures at the junction volume, the break, and in the accumulator, respectively. Furthermore, ρ_J and α_J are the mixture density and void fraction in the junction volume. The flow coefficients in the Equations (E-22) through (E-24) are obtained from the nominal NPP calculation with the TRAC code. The void fraction α_J for the volume is estimated from the volume flow rates to this volume. It is assumed that the flow leaving the junction is homogeneous, the flow coming from the reactor is all steam, and the flow from the accumulator is all liquid.

$$\alpha_J = \frac{(W_{o,m,SG}/\rho_g)}{((W_{o,m,SG}/\rho_g) + (W_{BR,A}/\rho_\ell))} \quad (E-26)$$

The solution of Equation (E-15) requires the amount of N_2 injected into the system (W_{i,N_2}), and the procedure of evaluating W_{i,N_2} is described in Section E.3.2.

The ECC flow rate or injection rate (accumulator flows and safety injection) in the presence of N_2 is estimated from the system pressure and a model for the accumulator. The next section, E.3.1.2, describes the accumulator model.

E.3.1.2 Formulation for Accumulator Flows

The rate of accumulator flow is estimated from a model of accumulator and the pipe connecting it to the cold leg. The accumulator has a gas space filled with N_2 and a liquid space filled with subcooled water with dissolved N_2 . It has been observed in the reference NPP calculation that the liquid temperature changes by less than $1^\circ K$ during the Refill Phase, but there has been temperature change in the gas phase of the order of $30^\circ K$. Therefore, the nitrogen expansion is not isothermal, and we can assume an adiabatic expansion for the nitrogen. The adiabatic expansion will predict lower accumulator pressure and lower ECC flow rate than the isothermal conditions. The gas space pressure will also be affected by the N_2 which will emerge from the liquid as the accumulator pressure decreases. The system of equations which govern this model is given here:

Mass balances for N_2 :

$$\frac{d(\rho_{N_2} V_{A,N_2})}{dt} = \dot{m}_{N_2} \quad (E-27)$$

where \dot{m}_{N_2} is the rate of nitrogen emerging from the liquid and V_{A,N_2} is the volume of the accumulator occupied by N_2 . A mass balance for N_2 in the liquid phase is also needed.

$$\frac{d}{dt} (\rho_l V_{A,l} X_{N_2} \frac{M_{N_2}}{M_{H_2O}}) = -\dot{m}_{N_2} \quad (E-28)$$

where M_{N_2} and M_{H_2O} are the molecular weights of nitrogen and water, and X is the solubility (mole of N_2 in a mole of solution) of N_2 in water. X_{N_2} is related to the accumulator pressure P_A , through Henry's law,

$$X_{N_2} = P_A / H \quad (E-29)$$

where H is Henry's constant.

The N_2 will follow an adiabatic expansion:

$$P_A \rho_{N_2}^{-\gamma} = \text{constant} = K \quad (E-30)$$

It is also assumed that N_2 behaves as perfect gas:

$$P_A V_{A,N_2} = n R T_A \quad (E-31)$$

As the accumulator volume is fixed, there is an additional constraint on the V_{A,N_2} :

$$V_A = V_{A,N_2} + V_{A,l} \quad (E-32)$$

In addition to the N_2 balance equations, mass and momentum balances are also needed for the liquid phase (water):

$$\frac{dV_{A,\ell}}{dt} = -Q_\ell \quad (E-33)$$

$$\rho_\ell = K_A \sqrt{(P_A - P_S) \rho_\ell} \quad (E-34)$$

where Q_ℓ is the volume flow rate from the accumulator, P_A and P_S are the pressures in the accumulator and the rest of the NPP system.

After combining Equations (E-27) to (E-34), an equation for dP_A/dt is obtained.

$$\frac{dP_A}{dt} = \frac{Q_\ell \left[\frac{\rho_\ell}{H} \frac{M_{N_2}}{M_{H_2O}} \frac{P_A}{\rho_g} - 1 \right]}{\left[\frac{V_{A,\ell}}{H} \frac{M_{N_2}}{M_{H_2O}} \frac{\rho_\ell}{\rho_g} + \frac{V_{A,g}}{\gamma P_A} \right]} \quad (E-35)$$

It should be noted that for PWR application, the terms containing H in the above equation are three orders of magnitude smaller than the terms they are added to, implying that the effect of N_2 dissolution on the accumulator pressure is small and could be neglected.

The flow coefficient K_A is obtained from the reference NPP calculation. The accumulator pressure is obtained from Equation (E-35). The liquid flow rate in Equation (E-35) is related to $W_{1,m}$ in Equation (E-15).

$$W_{1,m} = W_{SI} + \dot{m}_A \quad (E-36)$$

$$\dot{m}_A = Q_\ell \rho_\ell \quad (E-37)$$

where \dot{m}_A and W_{SI} are the accumulator and safety injection flow rates.

E.3.2 Estimate of Rate of N_2 Dissolution in the Reactor System

It is assumed that the N_2 and steam are in equilibrium with the water. As the fluid particle moves from the accumulator to the cold leg, the N_2 solubility decreases and this difference in the solubility leads to the emergence of N_2 in the cold legs.

The amount of N_2 emerging from ECC into the cold leg can be estimated as follows:

$$W_{1,N_2} = \dot{m}_A (c_{N_2,A} - c_{N_2,CL}) \quad (E-38)$$

where $c_{N_2,A}$ and $c_{N_2,CL}$ are the concentration of N_2 in the water in the accumulator and the cold leg. The other variables appearing in the above equation are defined below.

\dot{m}_A Rate of ECC injection into cold legs from accumulators,

W_{1,N_2} Rate of N_2 emerging into cold legs,

c_{N_2} Concentration of N_2 in solution; kg of N_2 per kg of the solution.

The concentration of N_2 in the solution is related to its solubility as follows,

$$c_{N_2} = \frac{X_{N_2}}{1-X_{N_2}} \frac{M_{N_2}}{M_{H_2O}} = X_{N_2} \frac{M_{N_2}}{M_{H_2O}} \quad \text{for } X_{N_2} \ll 1 \quad (E-39)$$

The solubility of N_2 in the water varies with the pressure and temperature. The partial pressure of N_2 in the gas phase is related to the solubility by Henry's law:

$$P_{N_2} = H X_{N_2} \quad (E-40)$$

where P_{N_2} is the partial pressure of N_2 in the gas phase, X_{N_2} is the solubility of N_2 in water (moles of N_2 per mole of solution) and H is Henry's constant. Henry's constant, H , is listed in Table E-1 (Chemical Engineering Handbook, Perry & Chilton, Pages 3-98). H is not very sensitive to the partial pressure of N_2 but does vary with the temperature.

The partial pressure of N_2 in Equation (E-40) is computed as follows:

$$P_{N_2} = P_{NPP} - P_{\text{sat},H_2O} \quad (E-41)$$

where P_{NPP} is the fluid pressure obtained from the NPP calculation and P_{sat,H_2O} is the saturation pressure for water corresponding to the water temperature in the NPP calculation.

The average rate of N_2 injection (W_{1,N_2}) into the reactor system during any time period t_1 to t_2 in the Refill Phase of the accident is computed from Δm_{N_2} (the amount of N_2 emerged during this period) as follows:

$$W_{1,N_2} = \frac{\Delta m_{N_2}}{t_2 - t_1} \quad (E-42)$$

Δm_{N_2} is estimated by integrating Equation (E-38) after substituting Equation (E-39).

TABLE E-1

N₂ Solubilities (Chemical Engineering Handbook, Perry & Chilton)
(Tables 3-139 and 3-140)

T, °C	0	5	10	15	20	25	30	35
10 ⁻⁴ x H	5.29	5.97	6.68	7.38	8.04	8.65	9.24	9.85

t, °C	40	45	50	60	70	80	90	100
10 ⁻⁴ x H	10.4	10.9	11.3	12.0	12.5	12.6	12.6	12.6

Partial Pressure of N ₂ , mm, Hg	10 ⁻⁴ x H	
	19.4°C	24.9°C
900	8.24	9.08
2000	8.32	9.15
3000	8.41	9.25
4000	8.49	9.38
5000	8.59	9.49
6000	8.74	9.62
7000	8.86	9.62
8100	9.04	
8200		9.91

$$\Delta m_{N_2} = \int_{t_1}^{t_2} \dot{m}_A dt \left(\frac{X_{N_2;A,t_1} - X_{N_2,CL,t_1}}{2} + \frac{X_{N_2;A,t_2} - X_{N_2,CL,t_2}}{2} \right) \frac{M_{N_2}}{M_{H_2O}} \quad (E-43)$$

$$\Delta m_{N_2} = \Delta m_A \left(\frac{X_{N_2;A,t_1} - X_{N_2,CL,t_1}}{2} + \frac{X_{N_2;A,t_2} - X_{N_2,CL,t_2}}{2} \right) \frac{M_{N_2}}{M_{H_2O}} \quad (E-44)$$

Where Δm_A and Δm_{N_2} are the total ECC injected from the accumulators and the total dissolution of N_2 during t_1 to t_2 . Δm_A is obtained from the reference NPP calculation.

The N_2 injection rate W_{i,N_2} Equation (E-42) is needed in Equation (E-15). The rate of N_2 dissolution is based on ECC flow rate from the reference NPP calculation and will be an overestimation as the ECC flow is expected to be lower in the presence of N_2 .

E.3.3 Estimation of Condensation in the Presence of N_2

During the Refill Phase, the steam is close to saturation while the ECC is subcooled. The condensation rate will be dominated by the interfacial heat transfer on the liquid side.

$$\dot{m}_{vl,N_2} = K_{con} (CHMOD) q_{il} / h_{fg} \quad (E-45)$$

where K_{con} , $CHMOD$, q_{il} and h_{fg} are the constant of proportionality, a multiplier to account for N_2 effect, interfacial heat transfer in the absence of N_2 and the heat of vaporization. The multiplier $CHMOD$ is obtained from the correlation described in TRAC-PF1/MOD1 Correlation and Models document [Liles, 1988, Page 4-26].

$$CHMOD = 0.168 \left[\frac{\alpha(\rho_v - \rho_{N_2})^2}{(1-\alpha)\rho_l \rho_{N_2}} \right] \quad (E-46)$$

where

α Gas void fraction ($\alpha_v + \alpha_{N_2}$)

ρ_v Gas density

ρ_{N_2} Density of nitrogen at its partial pressure, P_{N_2}

The gas volume fraction α and the density of N_2 at its partial pressure are evaluated as follows:

$$\alpha = \alpha_v \left(\frac{1}{1-n_{N_2}} \right) \quad (E-47)$$

$$\rho_{N_2} = \rho_{N_2} (P_{N_2})$$

$$P_{N_2} = P_{NPP} n_{N_2} \quad (E-48)$$

where n_{N_2} is the mole fraction of N_2 in the gas mixture and α_v is the vapor volume fraction in the downcomer as obtained from the reference NPP calculation results.

An estimate of n_{N_2} , mole fraction of N_2 in the gas space of the downcomer at a given time has been made from the information obtained from the reference NPP calculation. The net steam flow into the downcomer during a time period (t_1 to t_2) is computed from Figure E-2, which was plotted from the information obtained from the reference NPP calculation. The assumption in this procedure is that during the period of interest, all the steam flow from the lower plenum to the downcomer and all the N_2 emerging from the ECC, mixes with the existing gas phase in the downcomer and the part of this mixture (vapor + N_2) leaves through the break. It is further assumed that steam and N_2 densities are constant.

$$n_{N_2}(t_2) = \frac{V_{N_2,DC,t_1} + V_{N_2,i,t_1,t_2}}{V_{g,DC,t_1} + V_{N_2,i,t_1,t_2} + V_{H_2O,i,t_1,t_2}} \quad (E-49)$$

n_{N_2} in the above equation is the mole fraction of N_2 in the gas mixture as the volume per kg-mole for each gas is the same at the same temperature and pressure conditions.

The other variables used in Equation (E-49) are defined below:

V_{N_2,DC,t_1} Volume of DC occupied by N_2 at t_1 at system pressure

V_{g,DC,t_1} Gas space volume in DC at t_1 at system pressure

V_{N_2,i,t_1,t_2} Total volume of N_2 emerged during t_1 and t_2 at system pressure

V_{H_2O,i,t_1,t_2} Total volume of steam injected from LP during t_1 to t_2 at system pressure

n_{N_2} Mole fraction of N_2 in the DC gas space

V_{g,DC,t_1} $V_{H_2O,DC,t_1} + V_{N_2,DC,t_1} = V_{H_2O,DC,t_1} \left(\frac{1}{1-n_{N_2}(t_1)} \right)$

where

V_{H_2O,DC,t_1} Volume of DC occupied by steam at t_1 at system pressure, obtained from NPP calculation

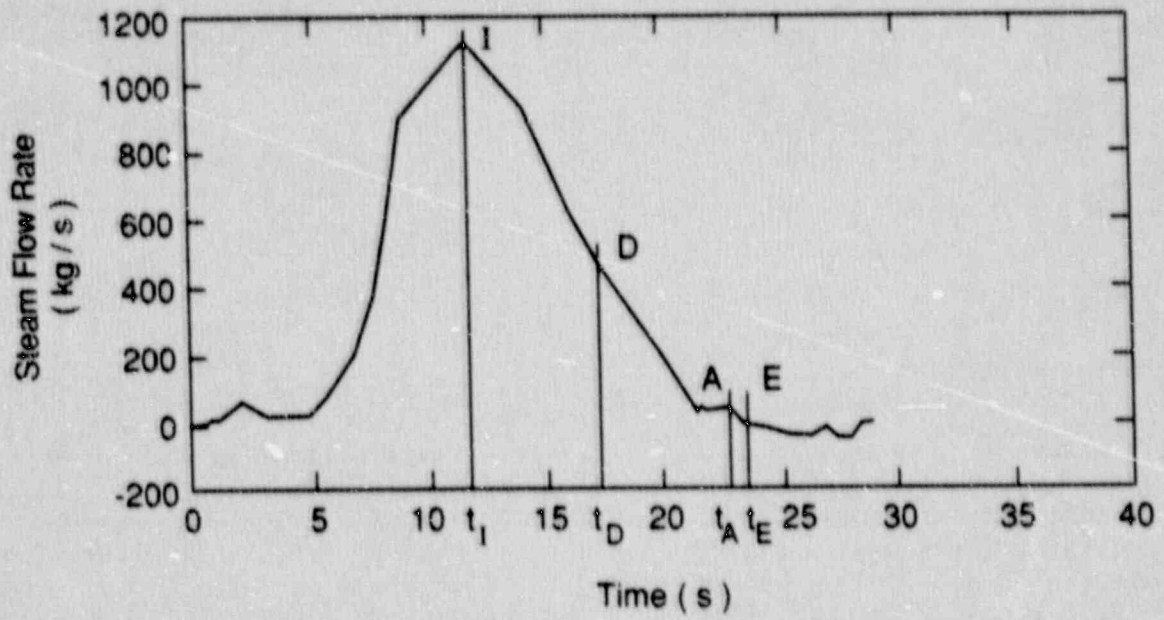


Figure E.2 Predicted Steam Flow Rate from Lower Plenum to the Downcomer

E.4 Results

The model described in Section E.3 requires the results of a nominal NPP calculation. Some of the values used in the estimate are listed in Table E-2. Columns 1 through 8 list the number, time of the transient, downcomer pressure, vessel and steam generator side break flow rates, and the liquid temperatures in the downcomer and in the accumulator, and average void fraction for the vessel, respectively. The Equations (E-15) and (E-35) have been integrated by Euler's method.

The flow coefficients K_{VE} , K_{JB} , K_{VJ} and K_{AJ} in Equations (E-20), (E-22), (E-23) and (E-24) are estimated from the nominal NPP calculation results during the Refill Phase. The values of these coefficients varied during the Refill Phase and conservative values - ones which will lead to smaller loss of the inventory and larger system pressure - were selected.

$$K_{VE} = 0.32 \text{ m}^2 \quad (\text{E-50})$$

$$K_{JB} = 0.41 \text{ m}^2 \quad (\text{E-51})$$

$$K_{VJ} = 0.22 \text{ m}^2 \quad (\text{E-52})$$

$$K_{AJ} = 0.02 \text{ m}^2 \quad (\text{E-53})$$

The rate of condensation \dot{m}_{vf} is computed by substituting downcomer liquid temperature, accumulator liquid temperature, integrated safety injection rate and integrated accumulator flows (originated from the loss of accumulator inventory) obtained from the nominal NPP calculation, into Equations (E-17) and (E-18). These values are summarized in Table E-3. In this table, Columns 1 through 6 list the time periods, integrated ECC flow consisting of safety injection and accumulator flows for the three intact loops, latent heat of vaporization, net condensation, and rates of condensation and ECC injection.

The rate of N_2 dissolution is obtained by substituting the NPP conditions obtained from the nominal NPP calculation in the Equation (E-44). These values are shown in Table E-4. The first column in this table shows the time of the transient. The next five columns (2 through 6) show the accumulator conditions: pressure, liquid temperature, saturation pressure, Henry's constant and solubility of nitrogen in the liquid, respectively. Similarly, the last five columns (7 through 11) represent the fluid conditions in the cold legs: pressure, liquid temperature, saturation pressure, Henry's constant and nitrogen solubility in the liquid. The fluid conditions listed in Table 4, along with the equations in Section E.3.2, are used to compute the rate of dissolution of N_2 . The rate of N_2 emergence has been computed for six intervals. The void fraction in the downcomer will change slightly and is computed from Equation (E-47). Table E-5 summarizes the results. There are ten columns: the time of the transient, net accumulator flow, net emergence of N_2 , net steam supplied to the downcomer, steam volume in the downcomer, densities of the steam and the nitrogen, mole fraction of nitrogen in the gas space, new void fraction in the presence of N_2 , and the rate of N_2 dissolution.

TABLE E-2

LBLOCA Flow Parameters from TRAC Calculation

No.	Time Sec	$P_{DC,NPP}$ bar	$W_{o,m,v}$ kg/s	$W_{o,m,sg}$ kg/s	T_{DC} K	T_A K	$\sum \Delta w_A$ kg	$\sum \Delta m_{SI}$ kg	$\sum \Delta m_{ECC}$ kg
1	11.5					305	0.0		
2	12.1	34.5	3612	1127	515	305	780	76	860
3	18.1	7.35	3599	74.6	394	305	15360	544	15900
4	22.9	3.15	-5.0	295.8	362	305	28980	1666	30670
5	23.8	3.29	-43.6	58.5	354	305	31530	1960	33490
6	26.1	3.07	-84	-14.0	348	305	37290	2646	39940
7	29.5	2.72	-113	-788.2	355	305	45300	3771	49070
8	33.5	2.91	-66.7	5.50	348	305	53670	5130	58800
9	37.6	3.04	-42.9	-676.3	352.4	305	61920	5540	68560
10	39.6	3.54	35.9	81.6	342	305	65550	7365	72920

$$\sum \Delta \dot{m}_A = \sum \int_{11.5}^t \dot{m}_A dt$$

$$\sum \Delta \dot{m}_{SI} = \sum \int_{11.5}^t \dot{m}_{SI} dt$$

$$\sum \dot{m}_{ECC} = \sum \dot{m}_{ACC} + \sum \dot{m}_{SI}$$

TABLE E-3

Estimated Condensation Rates in the Nominal NPP Calculation

Time Period <u>s</u>	$\Delta m_{ECC}(t_1-t_2)$ <u>kg</u>	h_{fg} <u>KJ/kg</u>	Δm_{vl} <u>kg</u>	$\dot{\Delta m}_{vl}$ <u>kg/s</u>	\dot{m}_{ECC} <u>kg/s</u>
12.1-18.1	15040	1955.5	1376	229	2480
18.1-22.9	14770	2154	500	104	3110
22.9-26.1	9270	2154	216	67	2900
26.1-29.5	9130	2154	197	58	2685
29.5-33.5	9730	2154	210	53	2430
33.5-37.6	9760	2154	205	50	2380

TABLE E-4

Estimates of N₂ Solubility

TIME SEC	ACCUMULATOR					COLD LEG				
	P bar	T _K	P _{sat,H₂O} bar	H* atm	X _{N2}	P bar	T _K	P _{sat,H₂O} bar	H atm	X _{N2}
12.1	41.2	305.5	0.047	9.55x10 ⁴	4.3x10 ⁻⁴	34.7	484.5	19.5	12.6x10 ⁴	1.2x10 ⁻⁴
18.1	27.33	305.5	0.047	9.55x10 ⁴	2.8x10 ⁻⁴	7.27	336.3		12.2x10 ⁴	5.9x10 ⁻⁵
22.9	21.25	305.4	0.047	9.55x10 ⁴	2.2x10 ⁻⁴	3.33	324.6	0.13	11.4x10 ⁴	2.8x10 ⁻⁵
23.8	20.37	305.4	0.047	9.55x10 ⁴	2.1x10 ⁻⁴	3.20	319.3	0.10	11.0x10 ⁴	2.8x10 ⁻⁵
26.1	18.48	305.4	0.047	9.55x10 ⁴	1.9x10 ⁻⁴	2.73	314		10.4x10 ⁴	2.6x10 ⁻⁵
29.5	16.5	305.3	0.047	9.55x10 ⁴	1.7x10 ⁻⁴	2.6	322.6		11.2x10 ⁴	2.3x10 ⁻⁵
33.53	15.08	305.2	0.047	9.55x10 ⁴	1.6x10 ⁻⁴	1.66	332	0.19	12x10 ⁴	1.2x10 ⁻⁵
37.6	13.6	305.1	0.047	9.55x10 ⁴	1.4x10 ⁻⁴	2.85	321	0.11	11.2x10 ⁴	2.5x10 ⁻⁵
39.6	13.05	305.1	0.047	9.55x10 ⁴	1.4x10 ⁻⁴	3.49	330.2	0.17	11.8x10 ⁴	2.8x10 ⁻⁵

* P = HX Henry's Law

TABLE E-5

Estimated Volume Fraction and Rate of Dissolution of N₂

TIME SEC	Δm_A^{**} kg	Δm_{N_2} kg	Δm_{steam} kg	$V_{v,DC}^{**}$ m ³	ρ_{steam}^* kg/m ³	$\rho_{N_2}^*$ kg/m ³	$n_{N_2,DC}$	α_g	W_{1,N_2} kg/s
11.5	-----	-----	-----	-----	17.4	27.1	0.0	0.97	-----
12.1	787	0.25	667.5	25.66	17.4	27.1	0.00014	0.97	0.42
22.9	28,980	12.2	5057.5	16.0	1.57	2.44	0.0017	0.60	1.1
23.8	31,530	13.1	5070	14.83	1.57	2.44	0.016	0.57	1.0
33.5	53,670	19.4	5070	10.22	1.5	2.33	0.163	0.46	0.65
39.6	65,550	22.2	5070	2.0	2.16	3.36	0.22	0.097	0.46

$$\Delta m_A = \int_{11.5}^t m_A dt \quad = \text{Total ECC Injection, Accumulators Only}$$

$$\Delta m_{N_2} = \int_{11.5}^t m_{N_2} dt \quad = \text{Total N}_2 \text{ Emerged}$$

$$\Delta m_{\text{steam}} = \int_{11.5}^t m_{\text{steam}} dt \quad = \text{Total steam flow into DC from LP}$$

$$n_{N_2,DC} = \text{mole fraction} = \text{Vol } N_2 / (\text{Vol } N_2 + \text{Vol Steam})$$

$$V_{DC} = 26.48 \text{ m}^3$$

$$W_{1,N_2} = \frac{\Delta M_{N_2}(t_2) - \Delta M_{N_2}(t_1)}{t_2 - t_1}$$

* Densities are obtained at the system pressure
 ** Obtained from NPP calculation

The effect of N_2 on the condensation rate is computed from Equation (E-46). The multiplier CHMOD is computed for the following conditions:

$$P = 3.0 \text{ bar}, n_{N_2} = 0.001, P_{\text{steam}} = 2.997 \text{ bar}, P_{N_2} = 0.003 \text{ bar}$$

$$\rho_v - \rho_{N_2} = \rho_{\text{steam}} = 1.65 \text{ kg/m}^3,$$

$$\rho_l = 1000 \text{ kg/m}^3$$

$$\rho_{N_2} = 0.00257 \text{ kg/m}^3,$$

$$\text{CHMOD} = 0.17 \left[\frac{\alpha}{1-\alpha} \right]^{0.1}$$

$$\text{CHMOD} = 0.14, \alpha = 0.1$$

$$\text{CHMOD} = 0.21, \alpha = .9$$

$$\text{and at } P = 3.0, n_{N_2} = 0.01, P_{\text{steam}} = 2.7 \text{ bar}, P_{N_2} = 0.3 \text{ bar}$$

$$\rho_{\text{steam}} = 1.496 \text{ kg/m}^3$$

$$\rho_l = 1000 \text{ kg/m}^3$$

$$\rho_{N_2} = 0.034 \text{ kg/m}^3$$

$$\text{CHMOD} = 0.128 \left[\frac{\alpha}{1-\alpha} \right]^{0.1}$$

$$\text{CHMOD} = 0.1, \alpha = 0.9$$

$$\text{CHMOD} = 0.16, \alpha = 0.9$$

The above calculations indicate that there will be a large reduction in the condensation rate (~80%). For the purpose of a conservative estimate of the N_2 effect, it is assumed that there will be no condensation in the presence of N_2 .

$$\dot{m}_{v\ell, N_2} = 0.0$$

(E-52)

The Equations (E-15) and (E-35) are integrated by a first order Euler's method and the predicted system pressure is shown in Figure E-3. The system pressure in the presence of N_2 is higher. Figure E-4 compares the total ECC flows in the NPP calculation with the ECC flow predicted by the bounding calculation. As expected, the ECC flows in the presence of N_2 are smaller. The results are summarized in Table E-6. The first column in this table is time, Columns 2 and 3 show the system pressures from the TRAC calculation and from the bounding calculation, and the last two columns are the total ECC flow in the intact loops as obtained from the nominal NPP calculation (TRAC) and from the bounding calculation. The ECC flow rates are used in Chapter 4 to estimate the bias in the time period of the Refill Phase and in the PCT.

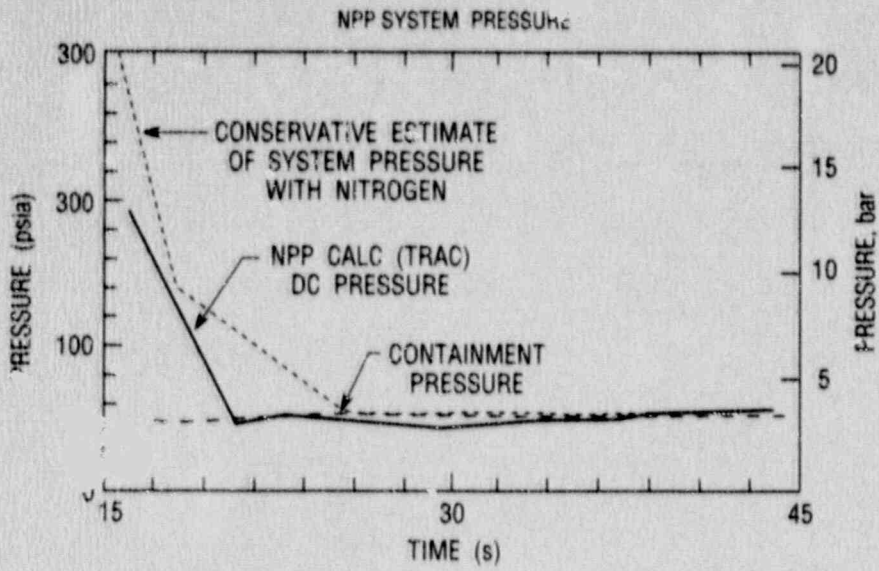


Figure E.3 System Pressure during Refill Period

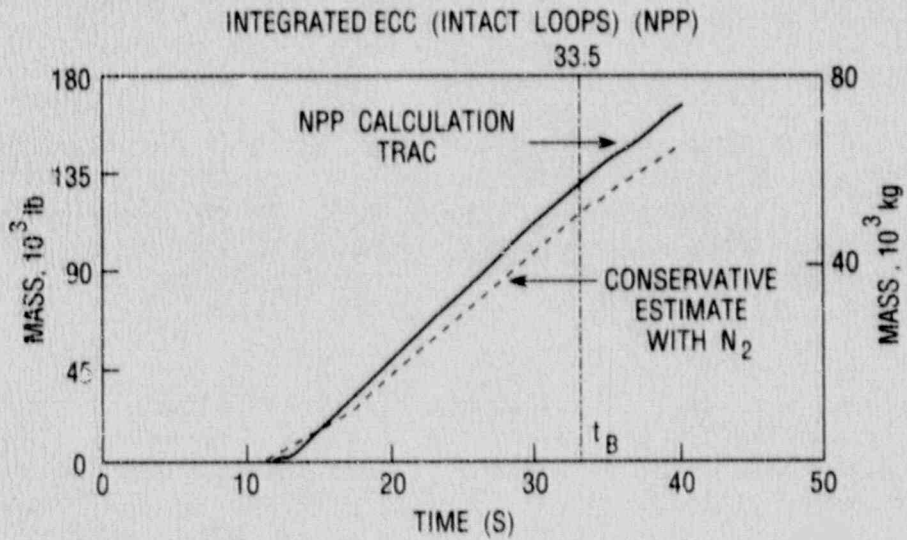


Figure E.4 Predictions of Integrated ECC Injection

TABLE E-6

Integrated ECC with and without N₂

Time	P _{NPP1} bar	P _{NPP, N₂} bar	Δm _{ECC} kg	Δm _{ECC, N₂} kg
12.1	34.5	34.5	860	860
18.1	17.35	11.23	15,900	12,145
22.9	3.28	7.29	30,670	23,843
23.8	3.07	6.38	33,490	24,145
26.1	3.07	4.61	39,940	31,773
29.5	2.72	3.51	49,070	40,100
33.5	2.92	3.61	58,800	49,310
37.6	3.04	3.28	68,560	58,610

$$R_{ECC} = \frac{\Delta m_{ECC} (33.5s) - \Delta m_{ECC} (t_D)}{\Delta m_{ECC, N_2} (33.5 s) - \Delta m_{ECC} (t_D)}$$

$$\Delta m_{ECC} = \int_{11.5}^t \dot{m}_{ECC} dt$$

$$P_{NPP} = \text{System Pressure}$$

NOMENCLATURE FOR APPENDIX E

C	Concentration, kg per kg of solution
CHMOD	Multiplier for N ₂ effect on condensation
h	Enthalpy
h _{fg}	Latent heat of vaporization
H	Henry's constant
K	Flow coefficient
\dot{m}_{cond}	Rate of condensation
m	Mass
M	Molecular weight
n	Mole fraction
P	Pressure
q _{wf}	Reactor power
Q	Volume flow rate
R _{ECC}	Ratio of the amounts of ECC delivered with no N ₂ and with N ₂
t	Time
T	Temperature
V	Volume
W	Mass flow rate
X	Solubility, mole per mole of solution

Greek

α	Volume fraction
ρ	Density
γ	Ratio of specific heats

Subscripts

A	Accumulator
B	Break
BR	Break
CL	Cold Leg
CON	Condensation
DC	Downcomer
ECC	Emergency Core Coolant
H ₂ O	Water
i	Inlet
J	Junction Volume (Figure E-1)
l	Liquid
N ₂	Nitrogen
NPP	Nuclear Power Plant
O	Outlet
S	System
SG	Steam Generator
SI	Safety Injection
v	Vapor
V	Vessel

BIBLIOGRAPHIC DATA SHEET

(See instructions on the reverse)

1. REPORT NUMBER
 (Assigned by NRC, Add Vol., Supp. Rev.,
 and Addendum Numbers, if any.)

NUREG/CR-5254
 BNL/NUREG-52168

2. TITLE AND SUBTITLE

Bias in Peak Clad Temperature Predictions Due to
 Uncertainties in Modeling of ECC Bypass and
 Dissolved Non-Condensable Gas Phenomena

3. DATE REPORT PUBLISHED

MONTH YEAR

September 1990

4. FIN OR GRANT NUMBER

A3952

5. AUTHOR(S)

U. S. Rohatgi, L. Y. Neymotin, J. Jo and W. Wulff

6. TYPE OF REPORT

7. PERIOD COVERED (Inclusive Dates)

8. PERFORMING ORGANIZATION -- NAME AND ADDRESS (If NRC, provide Division, Office or Region, U.S. Nuclear Regulatory Commission, and mailing address; if contractor, provide name and mailing address.)

Brookhaven National Laboratory
 Upton, NY 11973

9. SPONSORING ORGANIZATION -- NAME AND ADDRESS (If NRC, type "Same as above"; if contractor, provide NRC Division, Office or Region, U.S. Nuclear Regulatory Commission, and mailing address.)

Division of Systems Research
 Office of Nuclear Regulatory Research
 U.S. Nuclear Regulatory Commission
 Washington, DC 20555

10. SUPPLEMENTARY NOTES

11. ABSTRACT (200 words or less) The U.S. Nuclear Regulatory Commission (USNRC), its contractors and consultants have developed a methodology for evaluating Code Scaling, Applicability and Uncertainty (CSAU). The CSAU method has been demonstrated by applying it to the TRAC-PH1/MOD1, Version 14.3 code and its analysis of a Large Break Loss of Coolant Accident (LBLOCA) for a Westinghouse four-loop plant. In applying the methodology, the accident course is divided into three different phases, namely: Blowdown, Refill and Reflood. There are two distinct peak clad temperatures (PCT), one in the Blowdown Phase and one in the Reflood Phase. The Reflood Phase PCT is affected by the phenomena related to Emergency Core Cooling System (ECCS) in the downcomer and lower plenum of the reactor vessel.

This report describes a general method for estimating the biases in the Reflood Phase PCT from systematic errors (biases) associated with the modelling of the ECCS and dissolved nitrogen, and the application of this method. The bias in the Reflood Phase PCT due to the uncertainty in the existing code models for ECCS related phenomena is -19°K (-34°F). The bias in the PCT due to the lack of modelling of dissolved N_2 in the code is estimated to be 9.9°K (17.8°F). The code prediction for PCT is conservative if the bias is negative, and nonconservative if the bias is positive. The bias estimated here is based on full scale data from the Upper Plenum Test facility and is unaffected by the scale distortions

12. KEY WORDS/DESCRIPTORS (List words or phrases that will assist researchers in locating the report.)

Reactor Accidents--Mathematical Models; PWR Type Reactors--Reactor Accidents; PWR Type Reactors--Reactor Safety; Loss of Coolant--T Codes; PWR Type Reactors--Loss of Coolant; Blowdown; Cladding; Computerized Simulation; ECCS; Parametric Analysis; Test Facility; Heat Transfer; Computer Codes

13. AVAILABILITY STATEMENT

Unlimited

14. SECURITY CLASSIFICATION

(This Page)

Unclassified

(This Report)

Unclassified

15. NUMBER OF PAGES

16. PRICE

THIS DOCUMENT WAS PRINTED USING RECYCLED PAPER.

UNITED STATES
NUCLEAR REGULATORY COMMISSION
WASHINGTON, D.C. 20555

OFFICIAL BUSINESS
PENALTY FOR PRIVATE USE, \$300

SPECIAL FOURTH CLASS RATE
POSTAGE & FEE PAID
USNRC
PERMIT No. 6-57

120555139531
US NRC-OADM 1 1A1R4
DIV FOIA & PUBLICATIONS SVCS
TPS PDR-NUREG
P-223
WASHINGTON DC 20555